



NTNU – Trondheim
Norwegian University of
Science and Technology

Reconsolidation of Clay Pre-strained in Shear Mode

Alexei S Borchtchev

Geotechnics and Geohazards

Submission date: June 2015

Supervisor: Gudmund Reidar Eiksund, BAT

Co-supervisor: Arnfinn Emdal, BAT

Norwegian University of Science and Technology
Department of Civil and Transport Engineering

MSc Student Alexei S. Borchtchev

Reconsolidation of Clay Pre-Strained in Shear Mode

Impact of Various Levels of Pre-Straining on Shear
Strength and Compressibility Characteristics of Clay

Master's Thesis TBA4900

Trondheim, June 2015

Main supervisor: Professor Gudmund Reidar Eiksund

Co-supervisor: Assistant Professor Arnfinn Emdal

Department of Civil and Transport Engineering
Norwegian University of Science and Technology (NTNU)



NTNU – Trondheim
Norwegian University of
Science and Technology



Report Title: Reconsolidation of Clay Pre-strained in Shear Mode Master's Thesis	Date:10.06.2015 Number of pages (incl. appendices): 323 Master's Thesis x Project Work
Name: MSc student Alexei S. Borchtchev	
Professor in charge/supervisor: Professor Gudmund Reidar Eiksund	
Other external professional contacts/supervisors: Einar John Lande, NGI	

<p>Abstract:</p> <p>Through the past years unexpectedly large settlements of the existing structures have been registered as a result of geotechnical site works, and especially, due to the boring and installation of steel core piles. One of the recognized effects related to the bored piles which may lead to the settlements, is remoulding and reconsolidation of soft clay in a limited zone around the pile shaft during installation phase.</p> <p>The radial extent of the remoulded clay around the bored shaft remains unknown, but the pore pressure measurements from recent projects indicate that installation of bored shafts may have larger impact on the surrounding soft soil than what is known for the driven piles.</p> <p>During the past decades, large amount of research has been done on the effects of pile driving and axial capacity of driven piles. The research has resulted in several analytical and numerical methods for prediction of strains, stress changes and consolidation times due to the installation of driven piles. Contrary to the driven piles, there is fairly limited amount of research dealing with the effects of bored shaft installation.</p> <p>Through an extensive laboratory test programme, the thesis investigates how installation of bored shafts may affect strength and compressibility properties of the surrounding soft soils. The simulation of pile installation effects is achieved by subjecting different clay types to different levels of pre-straining through extrusion. The strength and compressibility properties of pre-strained samples are respectively evaluated by falling cone and oedometer testing. The same tests are also carried out on manually remoulded material. Furthermore, an attempt is made to identify the correlation between different levels of reconsolidation stresses and increase in shear strength of pre-strained reconsolidated samples, as well as volume changes due to the reconsolidation. The laboratory test programme also includes index and oedometer tests on undisturbed samples of the same clay types.</p>
--

Keywords:

1. Reconsolidation
2. Shear strain
3. Pile installation
4. Volume change

Alexei Borchtchev

Preface

The work presented below is a master's thesis TBA4900 in geotechnical engineering at Norwegian University of Science and Technology (NTNU). The master's thesis has been carried out during spring semester 2015, and is a part of MSc programme Geotechnics and Geohazards taught at NTNU. The thesis is based on previously completed geotechnical specialization project TBA4510 (literature study) carried out during autumn semester 2014.

The main objective of this master's thesis was an investigation of how various levels of pre-straining and subsequent reconsolidation may affect stress-strain and strength parameters of soft soils. The thesis consists of a series of laboratory tests, among them falling cone and oedometer test, on the clay samples subjected to known levels of pre-straining in shear mode. The laboratory investigations are aimed to provide a better understanding of the behaviour of disturbed clay around a pile after the installation phase.

The thesis has been carried out in cooperation with Norwegian Geotechnical Institute (NGI). It was NGI staff who were kind to suggest the topic and provided this excellent opportunity to execute this project. The topic was proposed by Einar John Lande from NGI during one of NTNU's Ph.D. courses. It is planned that author's thesis on reconsolidation of clay subjected to the pre-straining might be used in further research carried out by E. J. Lande for his doctoral thesis.

Trondheim, 2015-06-10

Alexei S. Borchtchev

Acknowledgment

I would like express my gratitude to my supervisor, Professor Gudmund Reidar Eiksund at NTNU's Department of Civil and Transport Engineering, for the invaluable advice and help he provided during preparation of this thesis.

I would also like to thank the rest of academic staff at the Department, especially Assistant Professor Arnfinn Emdal, Professor Steinar Nordal and Professor Gustav Grimstad, for their motivating lecturing throughout MSc programme Geotechnics and Geohazards. Their introduction of the world of geotechnical engineering to me was highly appreciated and inspiring.

The execution of laboratory test programme would not be possible without the equipment constructed at the workshop of Geotechnical Division, Department of Civil and Transport Engineering, NTNU. I am grateful to Senior Engineer Jan Jønland, Staff Engineer Gunnar Winther and Staff Engineer Per Asbjørn Østensen who have been involved in sampling and fabrication of necessary equipment for the test programme of this thesis.

I highly appreciate the contributions and suggestions provided by the staff at NGI. Special thanks go to Ph.D. Senior Engineer Kjell Karlsrud for his impressive research which has made it possible for me to carry out the literature study prior to this thesis, and to Einar John Lande who has proposed the idea of this thesis to me.

Finally, I would like to thank Research Assistant Ashenafi Lulseged Yifru who has found time to demonstrate user interface of the laboratory equipment, despite his busy schedule.

A.B.

Summary and Conclusions

The thesis focuses on reconsolidation of clay pre-strained in shear mode. Two main variables investigated in the study were various levels of pre-straining and different clay types with respect to overconsolidation ratio, water content and sensitivity. Various levels of pre-straining were achieved by extrusion of undisturbed clay samples through the tapered cylinders with different diameters. The main objectives of the study were to evaluate following aspects:

- Impact of various levels of pre-straining on strength and compressibility properties of different types of clay.
- Impact of reconsolidation on strength and volume changes of pre-strained specimens.

To meet the objectives, an extensive laboratory test programme has been carried out on two different clay types from central Norway. The laboratory tests were executed on undisturbed, pre-strained and manually remoulded clay samples. Undisturbed clay samples were subjected to index testing and CRS oedometer testing. Pre-strained clay samples were subjected to water content measurements, CRS oedometer testing, fall cone testing and reconsolidation in the oedometer at different stress levels. Additional measurements of shear strength and water content have been carried out after reconsolidation. Manually remoulded clay specimens were subjected to CRS oedometer tests, water content measurements and fall cone testing.

The main conclusions of the study are as following:

- Increase in level of pre-straining leads to decrease in residual shear strength of the material. The shear strength of manually remoulded clay represents the lowest strength limit.
- Reconsolidation of the material pre-strained to remoulding leads to significant gain in shear strength. The magnitude of shear strength after reconsolidation is depending on the clay type and reconsolidation stress. The largest gain in shear strength after reconsolidation has been observed for the clay with lowest water content. For this clay, peak shear strength after reconsolidation has been measured to 3.6 times undrained shear strength of intact material.
- Shear strength of moderately and severely pre-strained clay specimens appears to drop below the undrained shear strength of intact material when reconsolidation is carried

out at the stresses smaller than approximately 80 kPa. With respect to pile problems, this implies that moderately and severely strained soft soil around the pile shaft is likely to experience reduction of strength properties at shallow depths. For reconsolidation stresses in range 100-200 kPa, the moderately and severely pre-strained specimens demonstrate gain in shear strength. The gain in shear strength is larger for moderately pre-strained clay than for severely pre-strained clay.

- Substantial loss of volume and reduction in water content has been observed for clays subjected to remoulding by pre-straining and subsequent reconsolidation at stresses in range 42-200 kPa. Depending on the type of the clay and reconsolidation stress level, the material reconsolidates to a water content 5.3-9.4 % less than initial water content. The lower and upper limit for corresponding volume changes are 8.5 % and 16.6 %.
- Moderately and severely pre-strained material also demonstrates significant volume reduction at reconsolidation stress levels exceeding approximately 100 kPa. The values of this volume reduction are close to the volume changes encountered by the remoulded clay reconsolidated at the same stress levels. The observation indicates that the zone of moderately and severely pre-strained soft soil around a long pile will undergo large settlements at moderate and large depths.
- CRS oedometer tests show that stress-strain curves for pre-strained specimens are unambiguously located between the curves for undisturbed and manually remoulded test specimens. Increasing level of pre-straining leads to increasing volumetric strain at the same stress level. The undisturbed and pre-strained stress-strain curves meet at sufficiently large volume reductions. Stress-strain curve for manually remoulded material represents maximum volumetric strain, which is typically in range of 17-23 % at 800 kPa. Even the material remoulded by pre-straining is not capable of capturing these volume changes.
- The impact of pre-straining and remoulding on stiffness properties is such that oedometer modulus of pre-strained and remoulded clay is decreasing in OC stress range and increasing in NC stress range of the intact material.
- Pre-straining and remoulding leads to reduction of coefficient of consolidation in OC stress range of intact material. In NC stress range of intact material, coefficient of consolidation of pre-strained and remoulded clay shows contradictory trends due to the dependency on both oedometer modulus and coefficient of permeability.

Content

Preface	v
Acknowledgment.....	vii
Summary and Conclusions	ix
List of Figures	xxi
List of Tables	xxxiii
CHAPTER 1 Introduction and Background.....	1
1.1 Background.....	1
1.2 Objectives of the Thesis	2
1.3 Limitations of the Thesis	2
1.4 Approach to the Study.....	3
1.5 Structure of the Report	4
CHAPTER 2 Test Sites, Key Soil Parameters and Samples	5
2.1 Introduction.....	5
2.2 Tiller	5
2.2.1 General Overview	5
2.2.2 Key Soil Parameters	6
2.3 Stjørdal.....	12
2.3.1 General Overview	12
2.3.2 Key Soil Parameters	12
2.4 Samples Used in This Study	18
CHAPTER 3 Test Programme, Equipment and Method	19
3.1 Introduction.....	19
3.2 Pre-Straining Through Extrusion	21
3.2.1 Purpose	21

3.2.2	Test Equipment	21
3.2.3	Test Procedure.....	21
3.3	Density Measurements	24
3.3.1	Purpose	24
3.3.2	Test Equipment	24
3.3.3	Test Procedure.....	25
3.3.3.1	Average Density.....	25
3.3.3.2	Density Determined with Small Ring	25
3.3.3.3	Grain Density (Density of Solids).....	26
3.4	Natural Water Content.....	27
3.4.1	Purpose	27
3.4.2	Test Equipment	27
3.4.3	Test Procedure.....	27
3.5	Plastic and Liquid Limit	28
3.5.1	Purpose	28
3.5.2	Test Equipment	28
3.5.3	Test Procedure.....	29
3.5.3.1	Liquid Limit.....	29
3.5.3.2	Plastic Limit.....	30
3.5.3.3	Plasticity and Liquidity Index. Classification.....	30
3.6	Degree of Saturation, Void Ratio and Porosity.....	31
3.6.1	Purpose	31
3.6.2	Determination Procedure.....	31
3.7	Grain Size Distribution and Hydrometer Analysis	32
3.7.1	Purpose	32
3.7.2	Test Equipment	32
3.7.3	Test Procedure.....	33

3.8	Measurement of Undrained Shear Strength by UCT	38
3.8.1	Purpose	38
3.8.2	Test Equipment	38
3.8.3	Test Procedure.....	38
3.9	Measurement of Undrained and Remoulded Shear Strength by Fall Cone.....	41
3.9.1	Purpose	41
3.9.2	Test Equipment	41
3.9.3	Test Procedure.....	41
3.10	Reconsolidation in the Oedometer Cell.....	43
3.10.1	Purpose	43
3.10.2	Test Equipment	44
3.10.3	Test Procedure.....	44
3.11	Oedometer Test	47
3.11.1	Purpose	47
3.11.2	Test Equipment	47
3.11.3	Test Procedure.....	49
CHAPTER 4	Observations and Results	53
4.1	Introduction.....	53
4.2	Test Results for Sample T1-H12.....	53
4.2.1	Extrusion of the Sample	53
4.2.2	Density Measurements	57
4.2.2.1	Average Density.....	57
4.2.2.2	Density by Small Ring	58
4.2.2.3	Grain Density by Pycnometer.....	59
4.2.3	Water Content Measurements.....	59
4.2.4	Plastic and Liquid Limit	60

4.2.5	Degree of Saturation, Void Ratio and Porosity	61
4.2.6	Grain Size Distribution.....	61
4.2.7	Undrained Shear Strength by UCT	64
4.2.8	Undrained and Remoulded Shear Strength by Fall Cone.....	65
4.2.9	Shear Strength of Pre-Strained, Non-Reconsolidated Sample by Fall Cone.....	66
4.2.10	Reconsolidation of Pre-Strained Specimen in the Oedometer at In-Situ Vertical Effective Stress 42.2 kPa	67
4.2.11	Reconsolidation of Pre-Strained Specimen in the Oedometer at 100 kPa	68
4.2.12	Reconsolidation of Pre-Strained Specimen in the Oedometer at 150 kPa	70
4.2.13	Reconsolidation of Pre-Strained Specimen in the Oedometer at 200 kPa	71
4.2.14	CRS Oedometer Test on Undisturbed Clay.....	73
4.2.15	CRS Oedometer Test on Pre-Strained Clay.....	77
4.2.16	CRS Oedometer Test on Remoulded Clay	80
4.3	Test Results for Sample T2-H15.....	83
4.3.1	Extrusion of the Sample	83
4.3.2	Density Measurements	85
4.3.2.1	Average Density.....	85
4.3.2.2	Density by Small Ring	86
4.3.2.3	Grain Density by Pycnometer.....	87
4.3.3	Water Content Measurements.....	87
4.3.4	Plastic and Liquid Limit	88
4.3.5	Degree of Saturation, Void Ratio and Porosity	89
4.3.6	Grain Size Distribution.....	89
4.3.7	Undrained Shear Strength by UCT	92
4.3.8	Undrained and Remoulded Shear Strength by Fall Cone.....	94
4.3.9	Shear Strength of Pre-Strained, Non-Reconsolidated Sample by Fall Cone.....	94

4.3.10	Reconsolidation of Pre-Strained Specimen in the Oedometer at In-Situ Vertical Effective Stress 35.6 kPa.....	95
4.3.11	Reconsolidation of Pre-Strained Specimen in the Oedometer at 100 kPa	96
4.3.12	Reconsolidation of Pre-Strained Specimen in the Oedometer at 150 kPa	98
4.3.13	Reconsolidation of Pre-Strained Specimen in the Oedometer at 200 kPa	99
4.3.14	CRS Oedometer Test on Undisturbed Clay.....	100
4.3.15	CRS Oedometer Test on Pre-Strained Clay.....	104
4.3.16	CRS Oedometer Test on Remoulded Clay.....	107
4.4	Test Results for Sample T3-H14.....	109
4.4.1	Extrusion of the Sample	109
4.4.2	Density Measurements	111
4.4.2.1	Average Density.....	111
4.4.2.2	Density by Small Ring	112
4.4.2.3	Grain Density by Pycnometer.....	113
4.4.3	Water Content Measurements.....	113
4.4.4	Plastic and Liquid Limit	114
4.4.5	Degree of Saturation, Void Ratio and Porosity	115
4.4.6	Grain Size Distribution.....	115
4.4.7	Undrained Shear Strength by UCT	117
4.4.8	Undrained and Remoulded Shear Strength by Fall Cone.....	119
4.4.9	Shear Strength of Pre-Strained, Non-Reconsolidated Sample by Fall Cone....	120
4.4.10	Reconsolidation of Pre-Strained Specimen in the Oedometer at In-Situ Vertical Effective Stress 36.1 kPa.....	121
4.4.11	Reconsolidation of Pre-Strained Specimen in the Oedometer at 100 kPa	122
4.4.12	Reconsolidation of Pre-Strained Specimen in the Oedometer at 150 kPa	124
4.4.13	Reconsolidation of Pre-Strained Specimen in the Oedometer at 200 kPa	125

4.4.14	CRS Oedometer Test on Undisturbed Clay.....	126
4.4.15	CRS Oedometer Test on Pre-Strained Clay.....	130
4.4.16	CRS Oedometer Test on Remoulded Clay.....	132
4.5	Test Results for Sample S1-H1	135
4.5.1	Extrusion of the Sample	135
4.5.2	Density Measurements	138
4.5.2.1	Average Density.....	138
4.5.2.2	Density by Small Ring	139
4.5.2.3	Grain Density by Pycnometer.....	140
4.5.3	Water Content Measurements.....	140
4.5.4	Plastic and Liquid Limit	141
4.5.5	Degree of Saturation, Void Ratio and Porosity	142
4.5.6	Grain Size Distribution.....	142
4.5.7	Undrained Shear Strength by UCT	145
4.5.8	Undrained and Remoulded Shear Strength by Fall Cone.....	146
4.5.9	Shear Strength of Pre-Strained, Non-Reconsolidated Sample by Fall Cone....	147
4.5.10	Reconsolidation of Pre-Strained Specimen in the Oedometer at In-Situ Vertical Effective Stress 89.5 kPa	148
4.5.11	Reconsolidation of Pre-Strained Specimen in the Oedometer at 100 kPa	149
4.5.12	Reconsolidation of Pre-Strained Specimen in the Oedometer at 150 kPa	151
4.5.13	Reconsolidation of Pre-Strained Specimen in the Oedometer at 200 kPa	152
4.5.14	CRS Oedometer Test on Undisturbed Clay.....	153
4.5.15	CRS Oedometer Test on Pre-Strained Clay.....	157
4.5.16	CRS Oedometer Test on Remoulded Clay	159
4.6	Test Results for Sample S2-H1	162
4.6.1	Extrusion of the Sample	162
4.6.2	Density Measurements	165

4.6.2.1	Average Density.....	165
4.6.2.2	Density by Small Ring	166
4.6.2.3	Grain Density by Pycnometer.....	167
4.6.3	Water Content Measurements.....	167
4.6.4	Plastic and Liquid Limit	168
4.6.5	Degree of Saturation, Void Ratio and Porosity	169
4.6.6	Grain Size Distribution.....	169
4.6.7	Undrained Shear Strength by UCT	172
4.6.8	Undrained and Remoulded Shear Strength by Fall Cone.....	174
4.6.9	Shear Strength of Pre-Strained, Non-Reconsolidated Sample by Fall Cone....	174
4.6.10	Reconsolidation of Pre-Strained Specimen in the Oedometer at In-Situ Vertical Effective Stress 75.1 kPa.....	175
4.6.11	Reconsolidation of Pre-Strained Specimen in the Oedometer at 100 kPa	176
4.6.12	Reconsolidation of Pre-Strained Specimen in the Oedometer at 150 kPa	178
4.6.13	Reconsolidation of Pre-Strained Specimen in the Oedometer at 200 kPa	179
4.6.14	CRS Oedometer Test on Undisturbed Clay.....	180
4.6.15	CRS Oedometer Test on Pre-Strained Clay.....	184
4.6.16	CRS Oedometer Test on Remoulded Clay	186
4.7	Test Results for Sample S3-H1	189
4.7.1	Extrusion of the Sample	189
4.7.2	Density Measurements	191
4.7.2.1	Average Density.....	191
4.7.2.2	Density by Small Ring	192
4.7.2.3	Grain Density by Pycnometer.....	193
4.7.3	Water Content Measurements.....	193
4.7.4	Plastic and Liquid Limit	194

XVIII

4.7.5	Degree of Saturation, Void Ratio and Porosity	195
4.7.6	Grain Size Distribution.....	195
4.7.7	Undrained Shear Strength by UCT	198
4.7.8	Undrained and Remoulded Shear Strength by Fall Cone.....	199
4.7.9	Shear Strength of Pre-Strained, Non-Reconsolidated Sample by Fall Cone....	200
4.7.10	Reconsolidation of Pre-Strained Specimen in the Oedometer at In-Situ Vertical Effective Stress 79.2 kPa	201
4.7.11	Reconsolidation of Pre-Strained Specimen in the Oedometer at 100 kPa	202
4.7.12	Reconsolidation of Pre-Strained Specimen in the Oedometer at 150 kPa	204
4.7.13	Reconsolidation of Pre-Strained Specimen in the Oedometer at 200 kPa	205
4.7.14	CRS Oedometer Test on Undisturbed Clay.....	206
4.7.15	CRS Oedometer Test on Pre-Strained Clay.....	210
4.7.16	CRS Oedometer Test on Remoulded Clay	212
CHAPTER 5	Evaluation of Results. Discussion	217
5.1	Introduction.....	217
5.2	Key Soil Parameters	217
5.2.1	Tiller Clay.....	217
5.2.2	Stjørdal Clay	223
5.3	Pre-Straining Through Extrusion	228
5.4	Impact of Pre-Straining on Shear Strength.....	229
5.5	Impact of Pre-Straining and Reconsolidation on Shear Strength	232
5.6	Impact of Pre-Straining and Reconsolidation on Water Content and Volume.....	240
5.7	Behaviour in the Oedometer	246
CHAPTER 6	Summary, Conclusions and Recommendations	265
6.1	Summary of Work Undertaken	265
6.2	Overall Conclusions	267
6.2.1	Pre-Straining Through Extrusion	267

6.2.2	Impact of Pre-Straining on Strength Properties	267
6.2.3	Impact of Pre-Straining and Reconsolidation on Strength Properties.....	268
6.2.4	Impact of Pre-Straining and Reconsolidation on Water Content and Volume.	270
6.2.5	Behaviour in the Oedometer	271
6.3	Needs for Improvement and Recommendations for Further Research	272
Appendix A: References.....		275
Appendix B: Nomenclature Used in the Text.....		279
Appendix C: Abbreviations		283

List of Figures

Figure 2.2.1: Tiller site: (a) Site Location, (b) Section of Quaternary geological map (after Gylland et al., 2013).	6
Figure 2.2.2: Tiller clay: (a) Fall cone sensitivity, (b) Remoulded shear strength (after Gylland et al., 2013).	7
Figure 2.2.3: Tiller clay: (a) Preconsolidation stress, (b) Overconsolidation ratio (after Gylland et al., 2013).	8
Figure 2.2.4: Tiller clay: (a) Natural water content, (b) Bulk density, (c) Particle density (after Gylland et al., 2013).	8
Figure 2.2.5: Tiller clay: (a) Plasticity index, (b) Liquidity index (after Gylland et al., 2013).	9
Figure 2.2.6: Summary of oedometer test results for Tiller clay: (a) $\Delta e/e_0$, (b) M_o , (c) M_n , (d) m (after Gylland et al., 2013).	10
Figure 2.2.7: Summary of oedometer test results for Tiller clay: (a) c_{vo} , (b) c_{vn} (after Gylland et al., 2013).	10
Figure 2.2.8: Undrained shear strength of Tiller clay, from: (a) Field vane test, (b) Fall cone test, (c) UCT (after Gylland et al., 2013).	11
Figure 2.3.1: Location of Stjørdal site Leira.	12
Figure 2.3.2: Stjørdal site Leira: soil profile, natural water content, unit weight of soil, undrained shear strength and sensitivity (after Kummeneje, 2003).	14
Figure 2.3.3: Stjørdal site Leira: Undrained and remoulded shear strength at depth 14.0-14.8 m.	15
Figure 2.3.4: CRS oedometer test results for Stjørdal clay at depth 14.5 m: (a) Stress-strain plot, (b) Stress-modulus plot, (c) Stress-coefficient of consolidation, (d) Stress-pore pressure at sample base.	17
Figure 2.4.1: Designation methodology for sample cylinders used in the study.	18
Figure 3.2.1: Pre-straining of clay samples through extrusion.	21
Figure 3.5.1: Casagrande apparatus with grooving tool.	29
Figure 3.7.1: Chart for determination of constant K in hydrometer analysis.	34

Figure 3.7.2: Chart for determination of effective depth Z_r in hydrometer analysis.....	35
Figure 3.7.3: Chart for determination of coefficient a in hydrometer analysis.....	36
Figure 3.8.1: Unconfined compression test rig used in the study.	38
Figure 3.8.2: Graphical representation of Tresca failure criterion during UCT.	40
Figure 3.9.1: Falling cone test apparatus with mounted cone and undisturbed sample.	42
Figure 3.11.1: Cross-section of typical oedometer cell.	48
Figure 3.11.2: Oedometer device developed and built at Geotechnical Division, NTNU.	48
Figure 4.2.1: Sample T1-H12: Extrusion and subdivision.	54
Figure 4.2.2: Variation of strains in the cross-section of pre-strained sample T1-H12: (a) Material from depth 4.326-4.388 m pre-strained in the beginning of extrusion process, (b) Material from depth 4.078-4.140 m pre-strained in the end of extrusion process.	55
Figure 4.2.3: Effects of reconsolidation of pre-strained sample T1-H12 in the atmospheric pressure.	56
Figure 4.2.4: Sample T1-H12: Grain size distribution curve.....	63
Figure 4.2.5: Sample T1-H12: Recorded deformation curve from UCT.	64
Figure 4.2.6: Sample T1-H12: Specimen at failure during UCT.....	65
Figure 4.2.7: Sample T1-H12: Shape of specimen at failure during UCT.....	65
Figure 4.2.8: Sample T1-H12: Stress vs. strain from CRS oedometer test on undisturbed specimen.	75
Figure 4.2.9: Sample T1-H12: Stress vs. pore pressure from CRS oedometer test on undisturbed specimen.	75
Figure 4.2.10: Sample T1-H12: Stress vs. oedometer modulus from CRS oedometer test on undisturbed specimen.	76
Figure 4.2.11: Sample T1-H12: Modulus number from CRS oedometer test on undisturbed specimen.	76
Figure 4.2.12: Sample T1-H12: Stress vs. coefficient of consolidation from CRS oedometer test on undisturbed specimen.	76
Figure 4.2.13: Sample T1-H12: Stress vs. strain from CRS oedometer test on specimen pre-strained to $\gamma_s = 117\%$	78

Figure 4.2.14: Sample T1-H12: Stress vs. pore pressure from CRS oedometer test on specimen pre-strained to $\gamma_s = 117\%$.	78
Figure 4.2.15: Sample T1-H12: Stress vs. oedometer modulus from CRS oedometer test on specimen pre-strained to $\gamma_s = 117\%$.	79
Figure 4.2.16: Sample T1-H12: Modulus number from CRS oedometer test on specimen pre-strained to $\gamma_s = 117\%$.	79
Figure 4.2.17: Sample T1-H12: Stress vs. coefficient of consolidation from CRS oedometer test on specimen pre-strained to $\gamma_s = 117\%$.	80
Figure 4.2.18: Sample T1-H12: Stress vs. strain from CRS oedometer test on remoulded specimen.	81
Figure 4.2.19: Sample T1-H12: Stress vs. pore pressure from CRS oedometer test on remoulded specimen.	82
Figure 4.2.20: Sample T1-H12: Stress vs. oedometer modulus from CRS oedometer test on remoulded specimen.	82
Figure 4.2.21: Sample T1-H12: Stress vs. coefficient of consolidation from CRS oedometer test on remoulded specimen.	82
Figure 4.3.1: Sample T2-H15: Extrusion and subdivision.	84
Figure 4.3.2: Sample T2-H15: Grain size distribution curve.	91
Figure 4.3.3: Sample T2-H15: Recorded deformation curve from UCT.	92
Figure 4.3.4: Sample T2-H15: Specimen at the end of UCT.	93
Figure 4.3.5: Sample T2-H15: Shape of specimen at the end of UCT.	93
Figure 4.3.6: Sample T2-H15: Stress vs. strain from CRS oedometer test on undisturbed specimen.	102
Figure 4.3.7: Sample T2-H15: Stress vs. pore pressure from CRS oedometer test on undisturbed specimen.	102
Figure 4.3.8: Sample T2-H15: Stress vs. oedometer modulus from CRS oedometer test on undisturbed specimen.	103

Figure 4.3.9: Sample T2-H15: Modulus number from CRS oedometer test on undisturbed specimen.	103
Figure 4.3.10: Sample T2-H15: Stress vs. coefficient of consolidation from CRS oedometer test on undisturbed specimen.	104
Figure 4.3.11: Sample T2-H15: Stress vs. strain from CRS oedometer test on specimen pre-strained to $\gamma_s = 66\%$	105
Figure 4.3.12: Sample T2-H15: Stress vs. pore pressure from CRS oedometer test on specimen pre-strained to $\gamma_s = 66\%$	106
Figure 4.3.13: Sample T2-H15: Stress vs. oedometer modulus from CRS oedometer test on specimen pre-strained to $\gamma_s = 66\%$	106
Figure 4.3.14: Sample T2-H15: Stress vs. coefficient of consolidation from CRS oedometer test on specimen pre-strained to $\gamma_s = 66\%$	106
Figure 4.3.15: Sample T2-H15: Stress vs. strain from CRS oedometer test on remoulded specimen.	108
Figure 4.3.16: Sample T2-H15: Stress vs. pore pressure from CRS oedometer test on remoulded specimen.	108
Figure 4.3.17: Sample T2-H15: Stress vs. oedometer modulus from CRS oedometer test on remoulded specimen.	108
Figure 4.3.18: Sample T2-H15: Stress vs. coefficient of consolidation from CRS oedometer test on remoulded specimen.	109
Figure 4.4.1: Sample T3-H14: Extrusion and subdivision.	110
Figure 4.4.2: Sample T3-H14: Grain size distribution curve.	117
Figure 4.4.3: Sample T3-H14: Recorded deformation curve from UCT.	118
Figure 4.4.4: Sample T3-H14: Specimen at failure during UCT.	119
Figure 4.4.5: Sample T3-H14: Shape of specimen at failure during UCT.	119
Figure 4.4.6: Sample T3-H14: Stress vs. strain from CRS oedometer test on undisturbed specimen.	128
Figure 4.4.7: Sample T3-H14: Stress vs. pore pressure from CRS oedometer test on undisturbed specimen.	128

Figure 4.4.8: Sample T3-H14: Stress vs. oedometer modulus from CRS oedometer test on undisturbed specimen.	129
Figure 4.4.9: Sample T3-H14: Modulus number from CRS oedometer test on undisturbed specimen.	129
Figure 4.4.10: Sample T3-H14: Stress vs. coefficient of consolidation from CRS oedometer test on undisturbed specimen.	130
Figure 4.4.11: Sample T3-H14: Stress vs. strain from CRS oedometer test on specimen pre-strained to $\gamma_s = 18\%$	131
Figure 4.4.12: Sample T3-H14: Stress vs. pore pressure from CRS oedometer test on specimen pre-strained to $\gamma_s = 18\%$	131
Figure 4.4.13: Sample T3-H14: Stress vs. oedometer modulus from CRS oedometer test on specimen pre-strained to $\gamma_s = 18\%$	132
Figure 4.4.14: Sample T3-H14: Stress vs. coefficient of consolidation from CRS oedometer test on specimen pre-strained to $\gamma_s = 18\%$	132
Figure 4.4.15: Sample T3-H14: Stress vs. strain from CRS oedometer test on remoulded specimen.	134
Figure 4.4.16: Sample T3-H14: Stress vs. pore pressure from CRS oedometer test on remoulded specimen.	134
Figure 4.4.17: Sample T3-H14: Stress vs. oedometer modulus from CRS oedometer test on remoulded specimen.	134
Figure 4.4.18: Sample T3-H14: Stress vs. coefficient of consolidation from CRS oedometer test on remoulded specimen.	135
Figure 4.5.1: Sample S1-H1: Extrusion and subdivision.	136
Figure 4.5.2: Variation of strains in the cross-section of pre-strained sample S1-H1: (a) Material from depth 8.376-8.440 m pre-strained in the beginning of extrusion process, (b) Material from depth 8.069-8.120 m pre-strained in the end of extrusion process.	137
Figure 4.5.3: Sample S1-H1: Grain size distribution curve.	144
Figure 4.5.4: Sample S1-H1: Recorded deformation curve from UCT.	145

Figure 4.5.5: Sample S1-H1: Specimen at failure during UCT.	146
Figure 4.5.6: Sample S1-H1: Shape of specimen at failure during UCT.	146
Figure 4.5.7: Sample S1-H1: Stress vs. strain from CRS oedometer test on undisturbed specimen.	155
Figure 4.5.8: Sample S1-H1: Stress vs. pore pressure from CRS oedometer test on undisturbed specimen.	155
Figure 4.5.9: Sample S1-H1: Stress vs. oedometer modulus from CRS oedometer test on undisturbed specimen.	156
Figure 4.5.10: Sample S1-H1: Modulus number from CRS oedometer test on undisturbed specimen.	156
Figure 4.5.11: Sample S1-H1: Stress vs. coefficient of consolidation from CRS oedometer test on undisturbed specimen.	156
Figure 4.5.12: Sample S1-H1: Stress vs. strain from CRS oedometer test on specimen pre-strained to $\gamma_s = 117\%$	158
Figure 4.5.13: Sample S1-H1: Stress vs. pore pressure from CRS oedometer test on specimen pre-strained to $\gamma_s = 117\%$	158
Figure 4.5.14: Sample S1-H1: Stress vs. oedometer modulus from CRS oedometer test on specimen pre-strained to $\gamma_s = 117\%$	158
Figure 4.5.15: Sample S1-H1: Stress vs. coefficient of consolidation from CRS oedometer test on specimen pre-strained to $\gamma_s = 117\%$	159
Figure 4.5.16: Sample S1-H1: Stress vs. strain from CRS oedometer test on remoulded specimen.	160
Figure 4.5.17: Sample S1-H1: Stress vs. pore pressure from CRS oedometer test on remoulded specimen.	161
Figure 4.5.18: Sample S1-H1: Stress vs. oedometer modulus from CRS oedometer test on remoulded specimen.	161
Figure 4.5.19: Sample S1-H1: Stress vs. coefficient of consolidation from CRS oedometer test on remoulded specimen.	162
Figure 4.6.1: Sample S2-H1: Extrusion and subdivision.	163

Figure 4.6.2: Variation of strains in the cross-section of pre-strained sample S2-H1: (a) Material from depth 6.339-6.420 m pre-strained in the beginning of pre-straining process, (b) Material from depth 6.064-6.096 m pre-strained in the end of pre-straining process.....	164
Figure 4.6.3: Sample S2-H1: Grain size distribution curve.....	171
Figure 4.6.4: Sample S2-H1: Recorded deformation curve from UCT.....	172
Figure 4.6.5: Sample S2-H1: Specimen at failure during UCT.....	173
Figure 4.6.6: Sample S2-H1: Shape of specimen at failure during UCT.....	173
Figure 4.6.7: Sample S2-H1: Stress vs. strain from CRS oedometer test on undisturbed specimen.	182
Figure 4.6.8: Sample S2-H1: Stress vs. pore pressure from CRS oedometer test on undisturbed specimen.	182
Figure 4.6.9: Sample S2-H1: Stress vs. oedometer modulus from CRS oedometer test on undisturbed specimen.	182
Figure 4.6.10: Sample S2-H1: Modulus number from CRS oedometer test on undisturbed specimen.	183
Figure 4.6.11: Sample S2-H1: Stress vs. coefficient of consolidation from CRS oedometer test on undisturbed specimen.	183
Figure 4.6.12: Sample S2-H1: Stress vs. strain from CRS oedometer test on specimen pre-strained to $\gamma_s = 66\%$	185
Figure 4.6.13: Sample S2-H1: Stress vs. pore pressure from CRS oedometer test on specimen pre-strained to $\gamma_s = 66\%$	185
Figure 4.6.14: Sample S2-H1: Stress vs. oedometer modulus from CRS oedometer test on specimen pre-strained to $\gamma_s = 66\%$	186
Figure 4.6.15: Sample S2-H1: Stress vs. coefficient of consolidation from CRS oedometer test on specimen pre-strained to $\gamma_s = 66\%$	186
Figure 4.6.16: Sample S2-H1: Stress vs. strain from CRS oedometer test on remoulded specimen.	187

Figure 4.6.17: Sample S2-H1: Stress vs. pore pressure from CRS oedometer test on remoulded specimen.	188
Figure 4.6.18: Sample S2-H1: Stress vs. oedometer modulus from CRS oedometer test on remoulded specimen.	188
Figure 4.6.19: Sample S2-H1: Stress vs. coefficient of consolidation from CRS oedometer test on remoulded specimen.	188
Figure 4.7.1: Sample S3-H1: Extrusion and subdivision.	190
Figure 4.7.2: Sample S3-H1: Grain size distribution curve.	197
Figure 4.7.3: Sample S3-H1: Recorded deformation curve from UCT.	198
Figure 4.7.4: Sample S3-H1: Specimen at failure during UCT.	199
Figure 4.7.5: Sample S3-H1: Shape of specimen at failure during UCT.	199
Figure 4.7.6: Sample S3-H1: Stress vs. strain from CRS oedometer test on undisturbed specimen.	208
Figure 4.7.7: Sample S3-H1: Stress vs. pore pressure from CRS oedometer test on undisturbed specimen.	208
Figure 4.7.8: Sample S3-H1: Stress vs. oedometer modulus from CRS oedometer test on undisturbed specimen.	208
Figure 4.7.9: Sample S3-H1: Modulus number from CRS oedometer test on undisturbed specimen.	209
Figure 4.7.10: Sample S3-H1: Stress vs. coefficient of consolidation from CRS oedometer test on undisturbed specimen.	209
Figure 4.7.11: Sample S3-H1: Stress vs. strain from CRS oedometer test on specimen pre-strained to $\gamma_s = 18\%$	211
Figure 4.7.12: Sample S3-H1: Stress vs. pore pressure from CRS oedometer test on specimen pre-strained to $\gamma_s = 18\%$	211
Figure 4.7.13: Sample S3-H1: Stress vs. oedometer modulus from CRS oedometer test on specimen pre-strained to $\gamma_s = 18\%$	212
Figure 4.7.14: Sample S3-H1: Stress vs. coefficient of consolidation from CRS oedometer test on specimen pre-strained to $\gamma_s = 18\%$	212

Figure 4.7.15: Sample S3-H1: Stress vs. strain from CRS oedometer test on remoulded specimen.	214
Figure 4.7.16: Sample S3-H1: Stress vs. pore pressure from CRS oedometer test on remoulded specimen.	214
Figure 4.7.17: Sample S3-H1: Stress vs. oedometer modulus from CRS oedometer test on remoulded specimen.	214
Figure 4.7.18: Sample S3-H1: Stress vs. coefficient of consolidation from CRS oedometer test on remoulded specimen.	215
Figure 5.2.1: Tiller clay: (a) Percentage of clay particles (measured by weight), (b) Ratio d_{75}/d_{50}	218
Figure 5.2.2: Tiller clay: (a) Average unit weight, (b) Small ring density, (c) Density of solids.	218
Figure 5.2.3: Tiller clay: (a) Natural water content, (b) Liquidity index, (c) Plasticity index.	219
Figure 5.2.4: Tiller clay: (a) Fall cone undrained and remoulded shear strength, (b) UCT undrained shear strength, (c) Fall cone sensitivity.	221
Figure 5.2.5: Tiller clay: (a) OCR, (b) Preconsolidation stress.	221
Figure 5.2.6: Tiller clay: (a) Constrained modulus in the overconsolidated range (M_o) and at the preconsolidation stress (M_n), (b) Modulus number (m).	222
Figure 5.2.7: Tiller clay: Coefficient of consolidation in the overconsolidated range (c_{vo}) and at the preconsolidation stress (c_{vn}).	223
Figure 5.2.8: Stjørdal clay: Percentage of clay particles (measured by weight).	224
Figure 5.2.9: Stjørdal clay: (a) Average unit weight, (b) Small ring density, (c) Density of solids.	224
Figure 5.2.10: Stjørdal clay: (a) Natural water content, (b) Liquidity index, (c) Plasticity index.	225
Figure 5.2.11: Stjørdal clay: (a) Fall cone undrained and remoulded shear strength, (b) UCT undrained shear strength, (c) Fall cone sensitivity.	226

Figure 5.2.12: Stjørdal clay: (a) OCR, (b) Preconsolidation stress.....	227
Figure 5.2.13: Stjørdal clay: (a) Constrained modulus in the overconsolidated range (M_o) and at the preconsolidation stress (M_n), (b) Modulus number (m).....	227
Figure 5.2.14: Stjørdal clay: Coefficient of consolidation in the overconsolidated range (c_{vo}) and at the preconsolidation stress (c_{vn}).	228
Figure 5.4.1: Tiller clay: Undrained, residual and remoulded shear strength.....	231
Figure 5.4.2: Stjørdal clay: Undrained, residual and remoulded shear strength.....	231
Figure 5.4.3: Tiller clay: Normalised undrained, residual and remoulded shear strength.....	232
Figure 5.4.4: Stjørdal clay: Normalised undrained, residual and remoulded shear strength. .	232
Figure 5.5.1: Tiller clay: Normalised change in shear strength vs. reconsolidation stress.....	235
Figure 5.5.2: Stjørdal clay: Normalised change in shear strength vs. reconsolidation stress. .	235
Figure 5.5.3: Softening of pre-strained reconsolidated soil around pile shaft.	237
Figure 5.5.4: Haga test site: Shear distortion, water content and fall cone strength vs. radial distance from the pile wall (after Karlsrud and Haugen, 1984).....	238
Figure 5.5.5: Tiller clay: Normalised shear strength vs. reconsolidation stress.	239
Figure 5.5.6: Stjørdal clay: Normalised shear strength vs. reconsolidation stress.....	240
Figure 5.6.1: Tiller clay: Change in water content vs. reconsolidation stress.	243
Figure 5.6.2: Stjørdal clay: Change in water content vs. reconsolidation stress.....	243
Figure 5.6.3: Tiller clay: Volume change vs. reconsolidation stress.	244
Figure 5.6.4: Stjørdal clay: Volume change vs. reconsolidation stress.....	244
Figure 5.7.1: Stress-strain plot for all Tiller clay samples, water content 30-35 %. Linear scale.	248
Figure 5.7.2: Stress-strain plot for all Tiller clay samples, water content 30-35 %. Semi-log scale.	249
Figure 5.7.3: Stress-moduli plot for all Tiller clay samples, water content 30-35 %.....	250
Figure 5.7.4: Stress-coefficient of consolidation plot for Tiller clay samples T2-H15 and T3-H14, water content 30-35 %.	251

Figure 5.7.5: Stress-coefficient of consolidation plot for Tiller clay sample T1-H12, water content 31-34 %.	252
Figure 5.7.6: Stress-strain plot for Stjørdal clay samples S1-H1 and S3-H1, water content 42-46 %. Linear scale.	253
Figure 5.7.7: Stress-strain plot for Stjørdal clay samples S1-H1 and S3-H1, water content 42-46 %. Semi-log scale.	254
Figure 5.7.8: Stress-moduli plot for Stjørdal clay samples S1-H1 and S3-H1, water content 42-46 %.	255
Figure 5.7.9: Stress-coefficient of consolidation plot for Stjørdal clay samples S1-H1 and S3-H1, water content 42-46 %.	256
Figure 5.7.10: Stress-strain plot for Stjørdal clay sample S2-H1, water content 30-33 %. Linear scale.	257
Figure 5.7.11: Stress-strain plot for Stjørdal clay sample S2-H1, water content 30-33 %. Semi-log scale.	258
Figure 5.7.12: Stress-moduli plot for Stjørdal clay sample S2-H1, water content 30-33 %.	259
Figure 5.7.13: Stress-coefficient of consolidation plot for Stjørdal clay sample S2-H1, water content 30-33 %.	260

List of Tables

Table 3.1.1: Summary of extruder cone diameters used in the study.....	19
Table 3.1.2: Summary of laboratory test programme for each sample cylinder.....	20
Table 3.2.1: Summary of diameters of extruder cones and corresponding degrees of pre-straining.	23
Table 3.2.2: Summary of theoretical displacement ratios during clay extrusion.....	24
Table 3.5.1: Classification of clay after plasticity (after NGF, 1982).....	31
Table 3.7.1: Classification of gradation (after NGF, 1982).....	37
Table 3.7.2: Denotation of soil type (after NGF, 1982).	37
Table 3.9.1: Classification of clay after undrained shear strength determined by falling cone test and UCT (after NGF, 1982).....	43
Table 3.9.2: Sensitivity classification chart (after NGF, 1982).	43
Table 3.10.1: Reconsolidation stresses equal to in-situ vertical effective stresses σ'_{v0} , for reconsolidation in the oedometer.	45
Table 3.11.1: Classification of clay after modulus number (after Janbu, 1970).....	51
Table 4.2.1: Sample T1-H12: Calculation of mean density.	57
Table 4.2.2: Sample T1-H12: Calculation of density and dry density with small ring.....	58
Table 4.2.3: Sample T1-H12: Calculation of grain density and unit weight of solids.....	59
Table 4.2.4: Sample T1-H12: Determination of water content.....	60
Table 4.2.5: Sample T1-H12: Calculation of plastic and liquid limit.	60
Table 4.2.6: Sample T1-H12: Observations from hydrometer test.....	62
Table 4.2.7: Sample T1-H12: Results of falling cone test on undisturbed clay.	66
Table 4.2.8: Sample T1-H12: Results of falling cone test on remoulded clay.	66
Table 4.2.9: Sample T1-H12: Results of falling cone test on pre-strained non-reconsolidated clay.	67
Table 4.2.10: Sample T1-H12: Calculation of water content prior to and after reconsolidation at in-situ vertical effective stress 42.2 kPa.	67

Table 4.2.11: Sample T1-H12: Results of falling cone test on pre-strained clay reconsolidated at in-situ vertical effective stress 42.2 kPa.	68
Table 4.2.12: Sample T1-H12: Calculation of water content prior to and after reconsolidation at 100 kPa.....	69
Table 4.2.13: Sample T1-H12: Results of falling cone test on pre-strained clay reconsolidated at 100 kPa.....	70
Table 4.2.14: Sample T1-H12: Calculation of water content prior to and after reconsolidation at 150 kPa.....	70
Table 4.2.15: Sample T1-H12: Results of falling cone test on pre-strained clay reconsolidated at 150 kPa.....	71
Table 4.2.16: Sample T1-H12: Calculation of water content prior to and after reconsolidation at 200 kPa.....	72
Table 4.2.17: Sample T1-H12: Results of falling cone test on pre-strained clay reconsolidated at 200 kPa.....	72
Table 4.2.18: Sample T1-H12: Calculation of index parameters for undisturbed specimen subjected to CRS oedometer test.....	74
Table 4.2.19: Sample T1-H12: Calculation of water content for pre-strained specimen subjected to CRS oedometer test.....	77
Table 4.2.20: Sample T1-H12: Calculation of water content for remoulded specimen subjected to CRS oedometer test.....	80
Table 4.3.1: Sample T2-H15: Calculation of mean density.	85
Table 4.3.2: Sample T2-H15: Calculation of density and dry density with small ring.....	86
Table 4.3.3: Sample T2-H15: Calculation of grain density and unit weight of solids.	87
Table 4.3.4: Sample T2-H15: Determination of water content.....	88
Table 4.3.5: Sample T2-H15: Calculation of plastic and liquid limit.	89
Table 4.3.6: Sample T2-H15: Observations from hydrometer test.....	90
Table 4.3.7: Sample T2-H15: Results of falling cone test on undisturbed clay.	94
Table 4.3.8: Sample T2-H15: Results of falling cone test on remoulded clay.	94

Table 4.3.9: Sample T2-H15: Results of falling cone test on pre-strained non-reconsolidated clay.	95
Table 4.3.10: Sample T2-H15: Calculation of water content prior to and after reconsolidation at in-situ vertical effective stress 35.6 kPa.	95
Table 4.3.11: Sample T2-H15: Results of falling cone test on pre-strained clay reconsolidated at in-situ vertical effective stress 35.6 kPa.	96
Table 4.3.12: Sample T2-H15: Calculation of water content prior to and after reconsolidation at 100 kPa.....	97
Table 4.3.13: Sample T2-H15: Results of falling cone test on pre-strained clay reconsolidated at 100 kPa.....	97
Table 4.3.14: Sample T2-H15: Calculation of water content prior to and after reconsolidation at 150 kPa.....	98
Table 4.3.15: Sample T2-H15: Results of falling cone test on pre-strained clay reconsolidated at 150 kPa.....	99
Table 4.3.16: Sample T2-H15: Calculation of water content prior to and after reconsolidation at 200 kPa.....	99
Table 4.3.17: Sample T2-H15: Results of falling cone test on pre-strained clay reconsolidated at 200 kPa.....	100
Table 4.3.18: Sample T2-H15: Calculation of index parameters for undisturbed specimen subjected to CRS oedometer test.....	101
Table 4.3.19: Sample T2-H15: Calculation of water content for pre-strained specimen subjected to CRS oedometer test.....	104
Table 4.3.20: Sample T2-H15: Calculation of water content for remoulded specimen subjected to CRS oedometer test.....	107
Table 4.4.1: Sample T3-H14: Calculation of mean density.	111
Table 4.4.2: Sample T3-H14: Calculation of density and dry density with small ring.....	112
Table 4.4.3: Sample T3-H14: Calculation of grain density and unit weight of solids.....	113
Table 4.4.4: Sample T3-H14: Determination of water content.....	114

Table 4.4.5: Sample T3-H14: Calculation of plastic and liquid limit.	114
Table 4.4.6: Sample T3-H14: Observations from hydrometer test.	116
Table 4.4.7: Sample T3-H14: Results of falling cone test on undisturbed clay.	120
Table 4.4.8: Sample T3-H14: Results of falling cone test on remoulded clay.	120
Table 4.4.9: Sample T3-H14: Results of falling cone test on pre-strained non-reconsolidated clay.	121
Table 4.4.10: Sample T3-H14: Calculation of water content prior to and after reconsolidation at in-situ vertical effective stress 36.1 kPa.	121
Table 4.4.11: Sample T3-H14: Results of falling cone test on pre-strained clay reconsolidated at in-situ vertical effective stress 36.1 kPa.	122
Table 4.4.12: Sample T3-H14: Calculation of water content prior to and after reconsolidation at 100 kPa.	123
Table 4.4.13: Sample T3-H14: Results of falling cone test on pre-strained clay reconsolidated at 100 kPa.	123
Table 4.4.14: Sample T3-H14: Calculation of water content prior to and after reconsolidation at 150 kPa.	124
Table 4.4.15: Sample T3-H14: Results of falling cone test on pre-strained clay reconsolidated at 150 kPa.	125
Table 4.4.16: Sample T3-H14: Calculation of water content prior to and after reconsolidation at 200 kPa.	125
Table 4.4.17: Sample T3-H14: Results of falling cone test on pre-strained clay reconsolidated at 200 kPa.	126
Table 4.4.18: Sample T3-H14: Calculation of index parameters for undisturbed specimen subjected to CRS oedometer test.	127
Table 4.4.19: Sample T3-H14: Calculation of water content for pre-strained specimen subjected to CRS oedometer test.	130
Table 4.4.20: Sample T3-H14: Calculation of water content for remoulded specimen subjected to CRS oedometer test.	133
Table 4.5.1: Sample S1-H1: Calculation of mean density.	138

Table 4.5.2: Sample S1-H1: Calculation of density and dry density with small ring.....	139
Table 4.5.3: Sample S1-H1: Calculation of grain density and unit weight of solids.....	140
Table 4.5.4: Sample S1-H1: Determination of water content.....	141
Table 4.5.5: Sample S1-H1: Calculation of plastic and liquid limit.....	141
Table 4.5.6: Sample S1-H1: Observations from hydrometer test.....	143
Table 4.5.7: Sample S1-H1: Results of falling cone test on undisturbed clay.....	147
Table 4.5.8: Sample S1-H1: Results of falling cone test on remoulded clay.....	147
Table 4.5.9: Sample S1-H1: Results of falling cone test on pre-strained non-reconsolidated clay.....	148
Table 4.5.10: Sample S1-H1: Calculation of water content prior to and after reconsolidation at in-situ vertical effective stress 89.5 kPa.....	148
Table 4.5.11: Sample S1-H1: Results of falling cone test on pre-strained clay reconsolidated at in-situ vertical effective stress 89.5 kPa.....	149
Table 4.5.12: Sample S1-H1: Calculation of water content prior to and after reconsolidation at 100 kPa.....	150
Table 4.5.13: Sample S1-H1: Results of falling cone test on pre-strained clay reconsolidated at 100 kPa.....	150
Table 4.5.14: Sample S1-H1: Calculation of water content prior to and after reconsolidation at 150 kPa.....	151
Table 4.5.15: Sample S1-H1: Results of falling cone test on pre-strained clay reconsolidated at 150 kPa.....	152
Table 4.5.16: Sample S1-H1: Calculation of water content prior to and after reconsolidation at 200 kPa.....	152
Table 4.5.17: Sample S1-H1: Results of falling cone test on pre-strained clay reconsolidated at 200 kPa.....	153
Table 4.5.18: Sample S1-H1: Calculation of index parameters for undisturbed specimen subjected to CRS oedometer test.....	154

XXXVIII

Table 4.5.19: Sample S1-H1: Calculation of water content for pre-strained specimen subjected to CRS oedometer test.....	157
Table 4.5.20: Sample S1-H1: Calculation of water content for remoulded specimen subjected to CRS oedometer test.....	160
Table 4.6.1: Sample S2-H1: Calculation of mean density.....	165
Table 4.6.2: Sample S2-H1: Calculation of density and dry density with small ring.....	166
Table 4.6.3: Sample S2-H1: Calculation of grain density and unit weight of solids.....	167
Table 4.6.4: Sample S2-H1: Determination of water content.....	168
Table 4.6.5: Sample S2-H1: Calculation of plastic and liquid limit.....	169
Table 4.6.6: Sample S2-H1: Observations from hydrometer test.....	170
Table 4.6.7: Sample S2-H1: Results of falling cone test on undisturbed clay.....	174
Table 4.6.8: Sample S2-H1: Results of falling cone test on remoulded clay.....	174
Table 4.6.9: Sample S2-H1: Results of falling cone test on pre-strained non-reconsolidated clay.....	175
Table 4.6.10: Sample S2-H1: Calculation of water content prior to and after reconsolidation at in-situ vertical effective stress 75.1 kPa.....	175
Table 4.6.11: Sample S2-H1: Results of falling cone test on pre-strained clay reconsolidated at in-situ vertical effective stress 75.1 kPa.....	176
Table 4.6.12: Sample S2-H1: Calculation of water content prior to and after reconsolidation at 100 kPa.....	177
Table 4.6.13: Sample S2-H1: Results of falling cone test on pre-strained clay reconsolidated at 100 kPa.....	177
Table 4.6.14: Sample S2-H1: Calculation of water content prior to and after reconsolidation at 150 kPa.....	178
Table 4.6.15: Sample S2-H1: Results of falling cone test on pre-strained clay reconsolidated at 150 kPa.....	179
Table 4.6.16: Sample S2-H1: Calculation of water content prior to and after reconsolidation at 200 kPa.....	179

Table 4.6.17: Sample S2-H1: Results of falling cone test on pre-strained clay reconsolidated at 200 kPa.....	180
Table 4.6.18: Sample S2-H1: Calculation of index parameters for undisturbed specimen subjected to CRS oedometer test.....	181
Table 4.6.19: Sample S2-H1: Calculation of water content for pre-strained specimen subjected to CRS oedometer test.....	184
Table 4.6.20: Sample S2-H1: Calculation of water content for remoulded specimen subjected to CRS oedometer test.....	187
Table 4.7.1: Sample S3-H1: Calculation of mean density.....	191
Table 4.7.2: Sample S3-H1: Calculation of density and dry density with small ring.....	192
Table 4.7.3: Sample S3-H1: Calculation of grain density and unit weight of solids.....	193
Table 4.7.4: Sample S3-H1: Determination of water content.....	194
Table 4.7.5: Sample S3-H1: Calculation of plastic and liquid limit.....	195
Table 4.7.6: Sample S3-H1: Observations from hydrometer test.....	196
Table 4.7.7: Sample S3-H1: Results of falling cone test on undisturbed clay.....	200
Table 4.7.8: Sample S3-H1: Results of falling cone test on remoulded clay.....	200
Table 4.7.9: Sample S3-H1: Results of falling cone test on pre-strained non-reconsolidated clay.....	201
Table 4.7.10: Sample S3-H1: Calculation of water content prior to and after reconsolidation at in-situ vertical effective stress 79.2 kPa.....	201
Table 4.7.11: Sample S3-H1: Results of falling cone test on pre-strained clay reconsolidated at in-situ vertical effective stress 79.2 kPa.....	202
Table 4.7.12: Sample S3-H1: Calculation of water content prior to and after reconsolidation at 100 kPa.....	203
Table 4.7.13: Sample S3-H1: Results of falling cone test on pre-strained clay reconsolidated at 100 kPa.....	203
Table 4.7.14: Sample S3-H1: Calculation of water content prior to and after reconsolidation at 150 kPa.....	204

Table 4.7.15: Sample S3-H1: Results of falling cone test on pre-strained clay reconsolidated at 150 kPa.....	205
Table 4.7.16: Sample S3-H1: Calculation of water content prior to and after reconsolidation at 200 kPa.	205
Table 4.7.17: Sample S3-H1: Results of falling cone test on pre-strained clay reconsolidated at 200 kPa.....	206
Table 4.7.18: Sample S3-H1: Calculation of index parameters for undisturbed specimen subjected to CRS oedometer test.....	207
Table 4.7.19: Sample S3-H1: Calculation of water content for pre-strained specimen subjected to CRS oedometer test.....	210
Table 4.7.20: Sample S3-H1: Calculation of water content for remoulded specimen subjected to CRS oedometer test.	213
Table 5.4.1: Impact of pre-straining on strength properties, all samples.	230
Table 5.5.1: Tiller clay: Impact of pre-straining and reconsolidation on strength properties.	233
Table 5.5.2: Stjørdal clay: Impact of pre-straining and reconsolidation on strength properties.	234
Table 5.6.1: Tiller clay: Impact of pre-straining and reconsolidation on water content and volume.	241
Table 5.6.2: Stjørdal clay: Impact of pre-straining and reconsolidation on water content and volume.	242
Table 5.7.1: Volume reduction corresponding to void ratio $0.4 \cdot e_0$ for intact and disturbed oedometer curves.....	262

CHAPTER 1 Introduction and Background

1.1 Background

There is currently an ongoing large research project on limiting damages which have occurred due to the geotechnical works, *BegrensSkade*. The research project is executed in Norway by a large team of totally 23 partners, among them Norwegian University of Science and Technology (NTNU), Norwegian Geotechnical Institute (NGI), consulting companies and contractors.

The need for research programme *BegrensSkade* had arisen from the observations made during several construction projects. During these projects, it has been observed that geotechnical site works, and especially boring and installation of steel core piles, have led to structural damages due to the unexpectedly large settlements.

At the time of writing, Norwegian Geotechnical Institute is preparing a report (Lande et al., expected to be released in 2015) on the observations from the projects and field tests considering the impact of bored shaft installation. The report supports the hypothesis that installation of casing and bored shafts leads to large shear strains and subsequent reconsolidation of the surrounding clay. The size of the zone of remoulded clay remains unknown, but the pore pressure measurements indicate that installation of bored piles may have larger impact on the surrounding soils than what is known for driven piles.

There are three recognized effects related to bored piles which may lead to the settlements:

- Remoulding or severe straining, and subsequent reconsolidation, of soft clay in a limited zone around the pile shaft during installation phase.
- Erosion and flushing of the soils masses around the drill bit and casing.
- Reduced pore pressure close to the rock masses due to the drainage along and/or into the casing during boring from an elevation below groundwater level.

During last decades, numerous research programmes have been carried out to investigate the effects of driven pile installation. These research programmes included full scale driven and jacked pile tests, among them the tests at West Delta (NGI, 1989^{a, b, c, d}), Onsøy (NGI, 1985), Haga (Karlsrud and Haugen, 1984) and other test sites. As a part of some pile test programmes, NGI has carried out laboratory investigations on intact and remoulded clays

from the test sites. The laboratory investigations included index testing (natural water content, falling cone) and oedometer tests. The laboratory test results have shown that remoulded and reconsolidated clay demonstrates a substantial reduction of volume (15-17 %) accompanied by a significant increase in undrained shear strength (fall cone) when compared to intact clay (see for instance Karlsrud and Haugen, 1984). In addition to the driven pile test programmes, several analytical models describing the impact of driven pile installation exist.

Although the effects of driven pile installation are well-researched, there is only limited amount of research related to the impact of installation of bored shafts. Currently, little is known about the effects of remoulding and reconsolidation of soft soil surrounding the shaft of a bored pile, as well as how these effects may affect the settlements.

As a part of *BegrensSkade* programme, NGI was kind to propose a combined project thesis and master's thesis to be carried out at the Department of Civil and Transport Engineering, NTNU, during autumn 2014 and spring 2015, respectively. The project thesis, completed by author prior to this master's thesis, consisted of a comprehensive literature study on the effects of driven pile installation.

The master's thesis presented below is aimed to promote further understanding of the behaviour of pre-strained and reconsolidated clay, similar to the effects observed in the zone around bored shafts. The results from this author's thesis are planned to be used for further research as a part of Einar John Lande's Ph.D. thesis related to *BegrensSkade* programme.

1.2 Objectives of the Thesis

The objective of the study is to achieve understanding of two main aspects:

- What impact various levels of pre-straining may have on shear strength (measured by falling cone) and compressibility characteristics (measured in the oedometer).
- How the reconsolidation of pre-strained clay at different stress levels is correlated with increase in shear strength (measured by falling cone), decrease in water content and loss of volume.

1.3 Limitations of the Thesis

The study has following limitations:

- The thesis deals with slightly overconsolidated clays commonly found in Trondheim area. The effect of pre-straining and reconsolidation has not been studied for normally consolidated and heavily overconsolidated clays due to the lacking access to such clays.
- Due to the longitudinal effects of the study, the applied pre-straining has been limited to three different magnitudes.
- The creep and ageing effects after primary reconsolidation have not been studied.
- Limitations imposed by lack of equipment. Initially, one of the thesis' objectives included investigations of the correlation between work (force and displacement) applied during the pre-straining, and shear strength of pre-strained non-reconsolidated material. These investigations had to be omitted due to the lack of appropriate equipment capable to measure the force with required accuracy.

1.4 Approach to the Study

The study on reconsolidation of clay pre-strained in shear mode has been approached in two steps. At the first step, a project thesis has been prepared by the author during autumn semester 2014, e.g. prior to the master's thesis presented below. The project thesis consisted of literature study on the topic, and has been carried out as subject TBA4510 at Department of Civil and Transport Engineering, NTNU. The literature study has been carried out by quantitative and analytical research approach based on collection, critical review and analysis of known relevant facts and data on the topic.

This master's thesis, prepared during spring semester 2015, represents the second step in the study. The master's thesis has been carried out by quantitative and empirical research approach. The approach is based on empirical observations gained through a reproducible laboratory test programme. As part of the test programme, the correlation between variables was investigated by changing the value of main variables under controlled conditions and observing their effect on other variables. The main variables investigated in the study fall into two distinct groups:

- Different magnitudes of shear strain, γ_s .
- Different clay types with respect to overconsolidation ratio (OCR), natural water content (w) and sensitivity (S_t).

The pre-straining has been achieved by extrusion of slightly overconsolidated intact clay samples through a tapered cylinder (extruder cone) with known opening diameter. Applied shear strain, γ_s , was found from the relation between diameters prior to and after extrusion. Different diameters of the extruder cones have been used to achieve different magnitudes of shear strain.

Testing of clays with different OCR, natural water content (w) and sensitivity (S_t) has been achieved by using clay samples from two different sites, both located in central Norway.

The laboratory tests have been carried out on undisturbed, pre-strained and manually remoulded clay samples. Undisturbed clay samples were subjected to CRS oedometer tests and index testing. Pre-strained samples were subjected to water content measurements, CRS oedometer tests, fall cone tests and reconsolidation in the oedometer at different stress levels. Additional measurements of water content and fall cone strength have been executed after reconsolidation. Manually remoulded samples were subjected to water content measurements, CRS oedometer tests and fall cone tests.

1.5 Structure of the Report

The rest of the report is structured as follows. Chapter 2 gives general description of the sites and site conditions where sampling has been carried out. The information about site conditions was obtained through a desk study on existing publications. The chapter also provides an overview of the samples used in this study.

Chapter 3 contains detailed description of the laboratory test programme, test methodology and equipment.

The results of laboratory test programme are presented in Chapter 4. Discussion and comparison of test results is given in Chapter 5.

Summary, conclusions of the study and recommendations for further research are given in Chapter 6.

CHAPTER 2 Test Sites, Key Soil Parameters and Samples

2.1 Introduction

The chapter is aimed to provide a general description of the test sites where the samples used in this study were obtained from. A desk study on the available technical and academic sources has been carried out for each site. In the following, a brief summary of the relevant information obtained from the desk study is presented. In addition to the general overview of the sites, the key soil parameters are briefly described. In this way some of the results from laboratory test programme may be compared to the data from the desk study.

The chapter also contains a brief description of the samples involved in the study. The description includes borehole numbers, depths, sample diameters and other details. In addition, each of the samples is assigned a unique designation number for easy identification in the further.

2.2 Tiller

2.2.1 General Overview

Tiller site is a test site in direct proximity to the city of Trondheim, Sør-Trøndelag County, Norway. The site is located at elev. +125 m above sea level (a.s.l.), approximately 10 km south-east of Trondheim centre. Figure 2.2.1 shows site location.

Due to the presence of highly sensitive marine clay deposits at Tiller site, the site conditions have been extensively documented and analysed in a series of reports from Geotechnical Division of the Norwegian University of Science and Technology, as the Division has conducted research programmes on quick clays for many years. One of the most recent reports among these publications is Gylland et al. (2013). The site and soil conditions provided below are extracted from Gylland et al. (2013) unless noted otherwise.

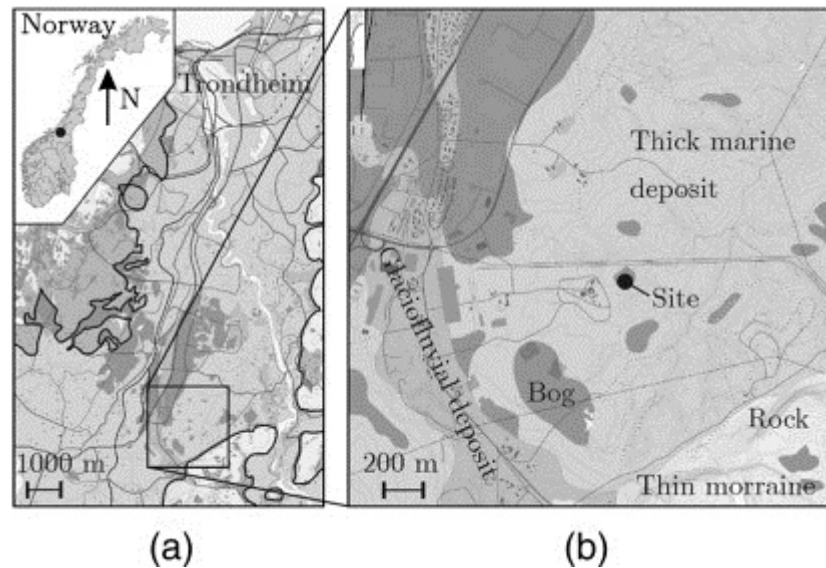


Figure 2.2.1: Tiller site: (a) Site Location, (b) Section of Quaternary geological map (after Gylland et al., 2013).

2.2.2 Key Soil Parameters

Gylland et al. (2013) specifies that groundwater table at the site has been observed approximately 0.5 m below ground level, elev. +124.5 m a.s.l (the figures extracted from the same source, however, show groundwater table at approximately 1.5 m depth). The in-situ pore pressure is hydrostatic (Sandven, 1990). The upper 2 m of soil consist of dry crust layer. The material below dry crust (e.g. below 2 m depth) is fully saturated.

Below dry crust layer, the soil consists of two main strata. A deposit of non-sensitive clay is found between the bottom of dry crust layer and 8 m depth. Below 8 m depth there is a strata of quick clay. NGF (1982) defines clay as "quick" if sensitivity (S_i) is greater than 30 and the remoulded shear strength (s_r) is less than 0.5 kPa. Figure 2.2.2 shows values of fall cone sensitivity and remoulded shear strength obtained from several tests on clay from the test site.

As follows from Figure 2.2.2, the clay between 2 m and 8 m depth has a typical fall cone sensitivity values in range of 10-15 and remoulded shear strength in range of 2-4 kPa. The clay in this layer is homogeneous with a clay content of 30-40 %. The clay is soft but not particularly sensitive.

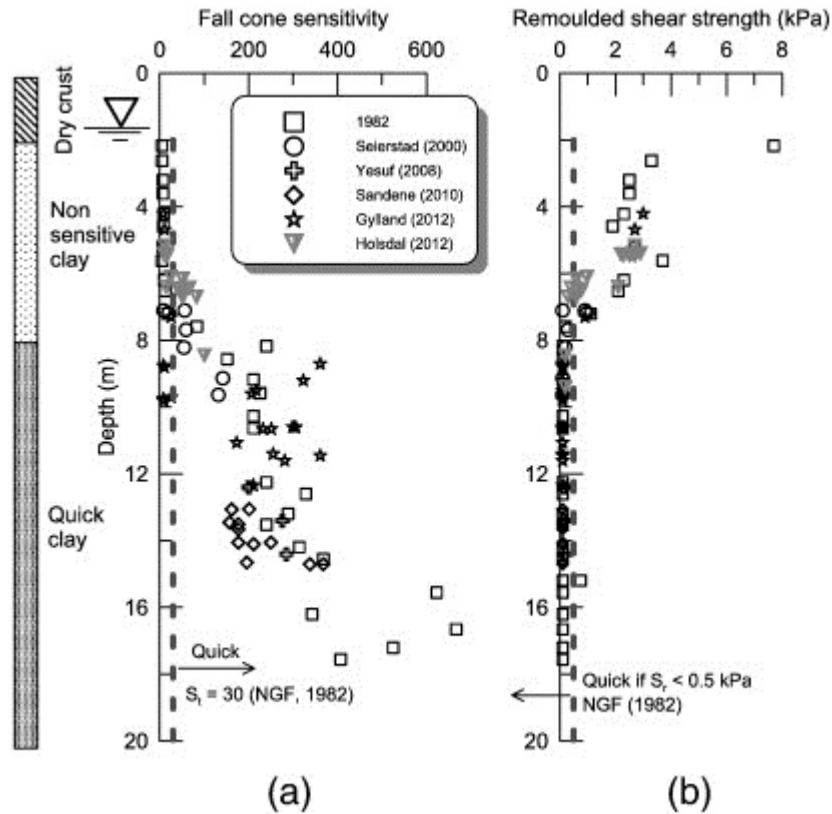


Figure 2.2.2: Tiller clay: (a) Fall cone sensitivity, (b) Remoulded shear strength (after Gylland et al., 2013).

Because the specimens from Tiller site used in this study originate from non-sensitive clay layer between 2 m and 8 m depth, only the properties of this layer are treated in the following. The non-sensitive clay is slightly overconsolidated, with preconsolidation stress varying between approximately 100 and 250 kPa. The overconsolidation ratio (OCR) is consistent throughout the layer with values in range 2.5-3. The OCR is slightly decreasing with depth. Figure 2.2.3 shows preconsolidation stress values, in-situ vertical effective stress values and values of OCR.

The values of natural water content w for the clay layer between 2 and 8 m depth are in range of 25-40 % with an average value of 37.8 % for both strata. The bulk density of clay in this layer lies in range of 18-19.5 kN/m³. Figure 2.2.4 shows natural water content, bulk density and particle density of the clay at Tiller.

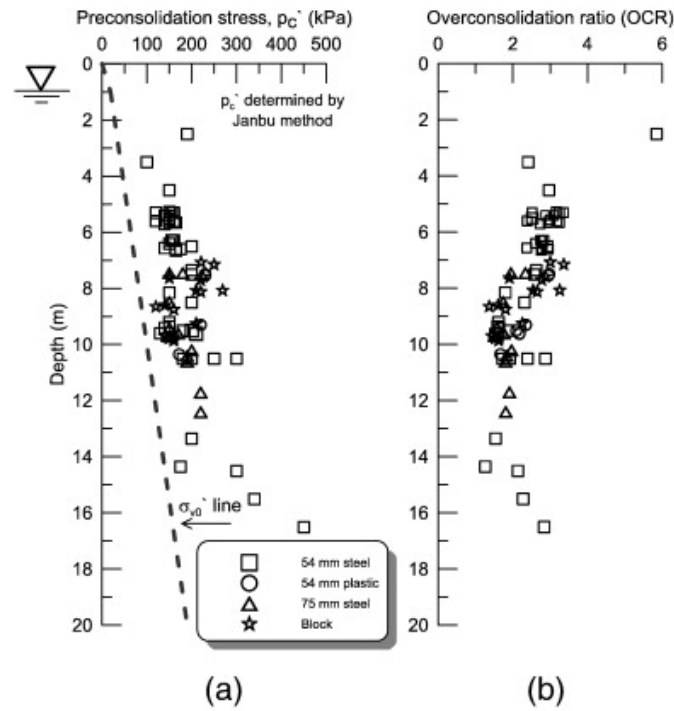


Figure 2.2.3: Tiller clay: (a) Preconsolidation stress, (b) Overconsolidation ratio (after Gylland et al., 2013).

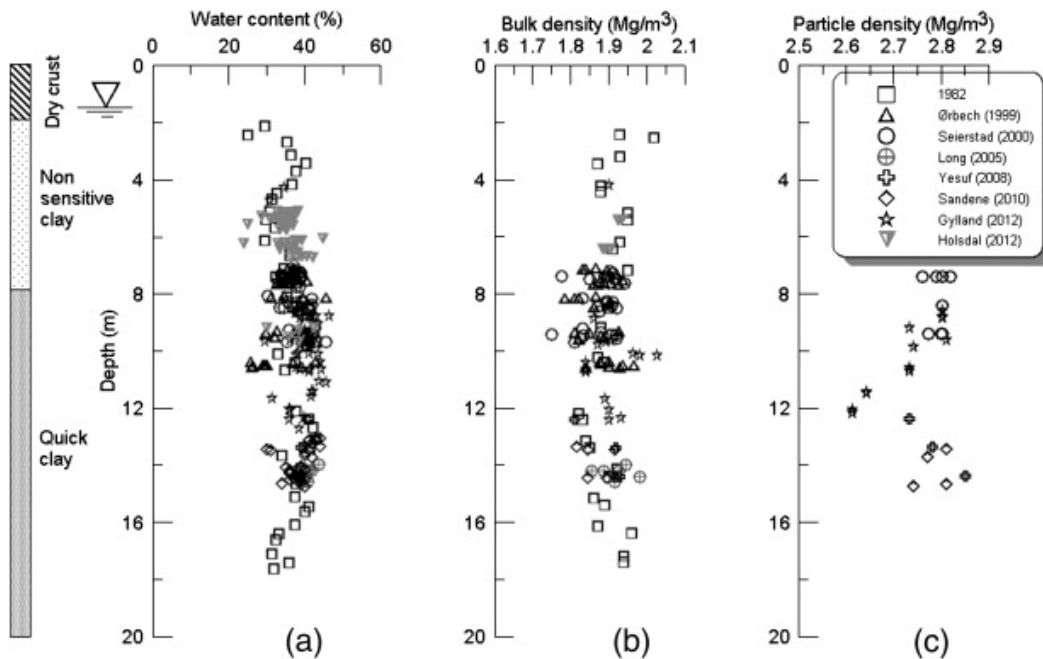


Figure 2.2.4: Tiller clay: (a) Natural water content, (b) Bulk density, (c) Particle density (after Gylland et al., 2013).

The plasticity index (I_p) of non-sensitive clay at Tiller is varying between 4 and 10 %, with an average value of 6.3 %. The clay can be characterised as low plastic in accordance with NGF (1982). Figure 2.2.5 shows plasticity index together with liquidity index values.

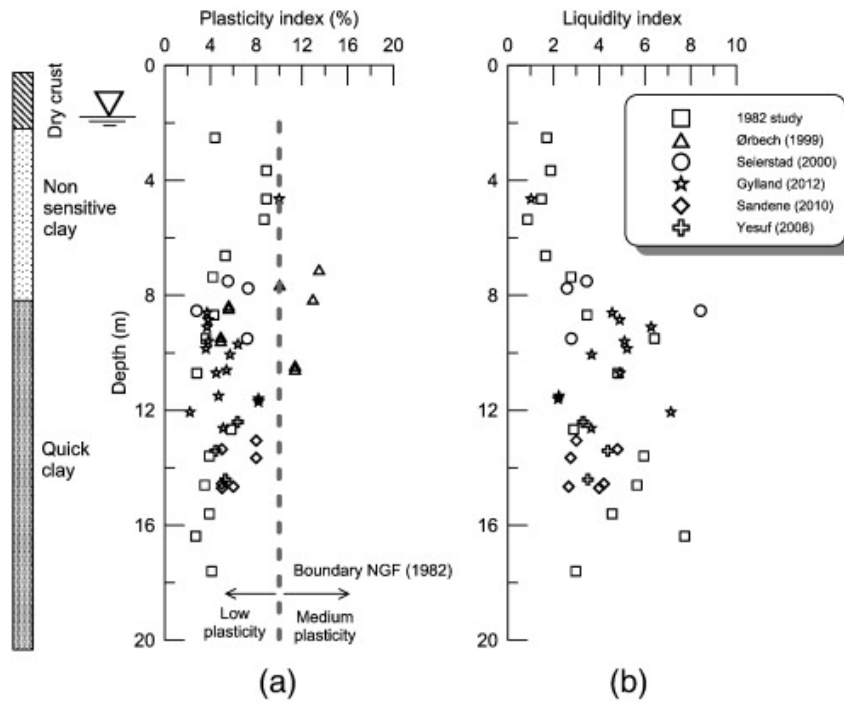


Figure 2.2.5: Tiller clay: (a) Plasticity index, (b) Liquidity index (after Gylland et al., 2013).

Figure 2.2.6 shows summary of IL and CRS oedometer test results. The constrained modulus in overconsolidated range (M_o) is typically 4 MPa. The constrained modulus at preconsolidation stress (M_n) for the non-sensitive clay lies in range of 1-4 MPa. In the normally consolidated range, the non-sensitive clay layer demonstrates fairly homogeneous values of modulus number, m , which are between 17 and 23.

The values of coefficient of consolidation of non-sensitive clay are somewhat inconsistent and show significant scatter. Figure 2.2.7 a and b show values of coefficient of consolidation in overconsolidation range (c_{vo}) and at preconsolidation stress p_c' (c_{vn}), respectively. The average value of c_{vn} is approximately 5 m²/yr. The figure also includes values of coefficient of consolidation (c_h) obtained from the results of piezocone (CPTU) dissipation tests (Bihs et al, 2012). These values vary between 5 m²/yr and 9.5 m²/yr.

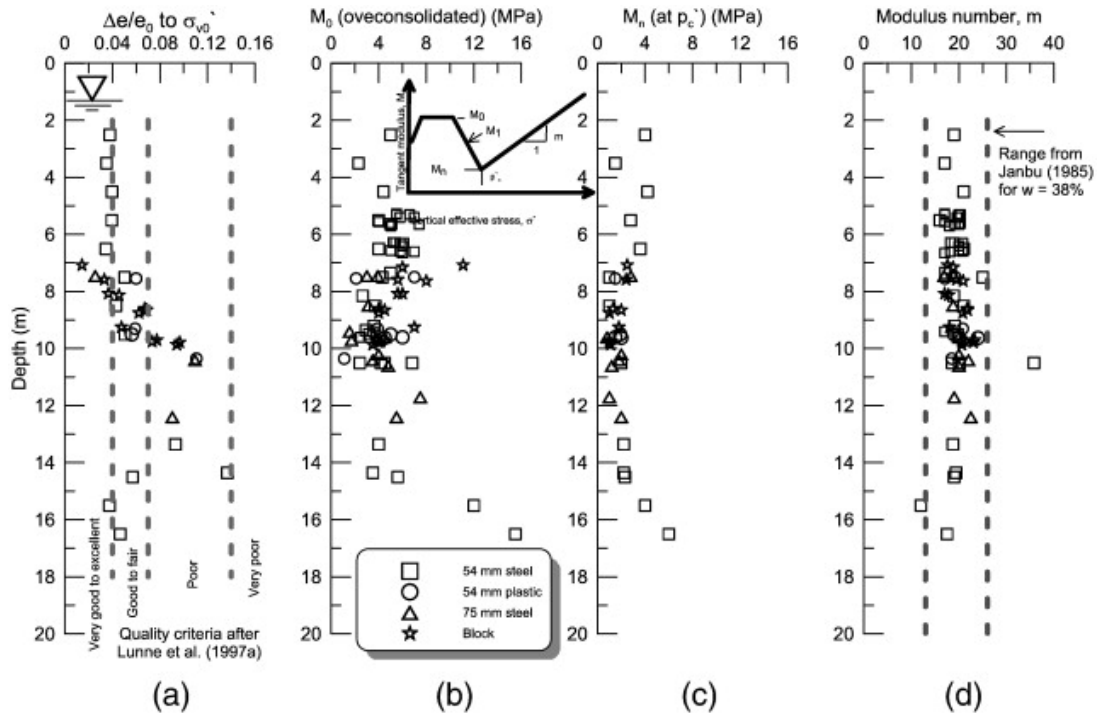


Figure 2.2.6: Summary of oedometer test results for Tiller clay: (a) $\Delta e/e_0$, (b) M_0 , (c) M_n , (d) m (after Gylland et al., 2013).

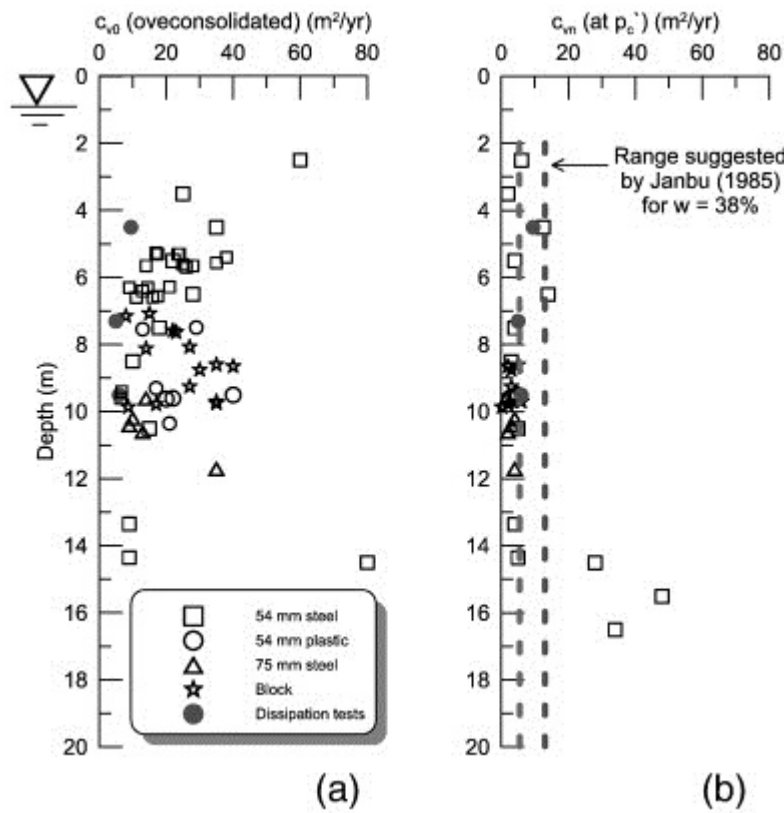


Figure 2.2.7: Summary of oedometer test results for Tiller clay: (a) c_{v0} , (b) c_{vn} (after Gylland et al., 2013).

Figure 2.2.8 shows the fall cone strength values together with field vane strength and unconfined compressive strength values as reported by Gylland et al. (2013). There is large scatter in the values of fall cone strength at the same depths. For the layer of non-sensitive clay (2 to 8 m depth) these fall cone strength values vary between approx. 20 and 40 kPa. The field vane and unconfined compressive strength values suggest that undrained shear strength is in the range of 20 to 30 kPa. However, the results of unconfined compression test (UCT) and vane test may often have low accuracy and should preferably be used together with results from more accurate tests.

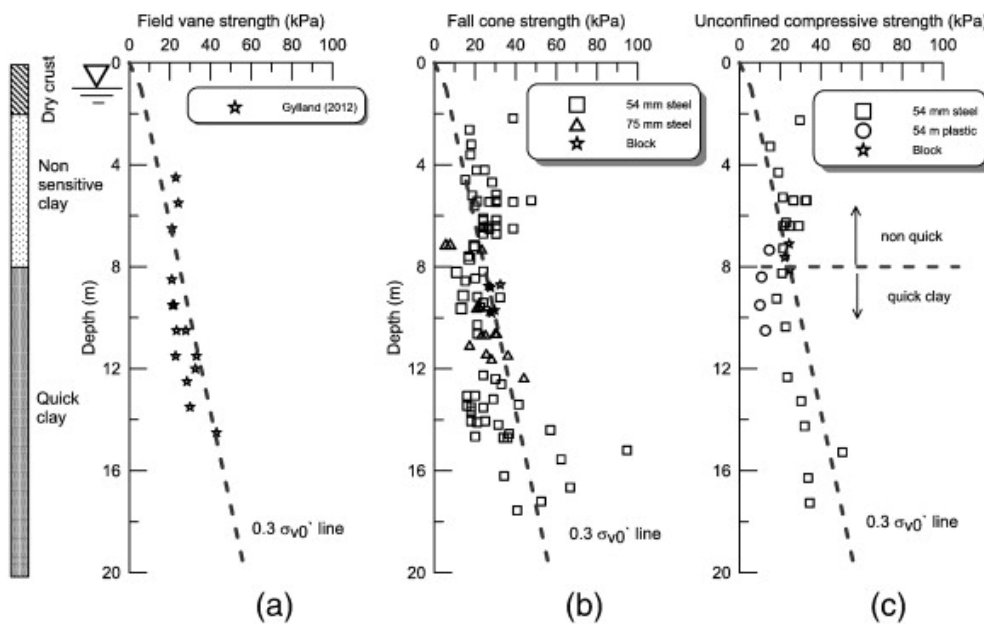


Figure 2.2.8: Undrained shear strength of Tiller clay, from: (a) Field vane test, (b) Fall cone test, (c) UCT (after Gylland et al., 2013).

Gylland et al. (2013) also report test results from CIUC (isotropically consolidated compression test) and CAUC (anisotropically consolidated compression test) triaxial tests. CIUC test results suggest that non-sensitive clay at Tiller demonstrates an undrained shear strength in range 20-40 kPa at depth between 4 and 8 m. These values agree closely with fall cone strength reported in the same publication.

The same publication reports that internal friction angle for Tiller clay is $\phi' = 29^\circ$ and cohesion is $c' = 6$ kPa regardless of sample type and triaxial test type. The clay demonstrates a dilatancy close to zero in the pre-peak regime. When the peak strength is approached, the material dilates slightly before contracting.

2.3 Stjørdal

2.3.1 General Overview

Stjørdal site Leira is located in Nord-Trøndelag County in central Norway, approximately 40 km west of Trondheim city. The elevation of the site is approximately in range +1 to +5 m above sea level (a.s.l.). Figure 2.3.1 shows site location.

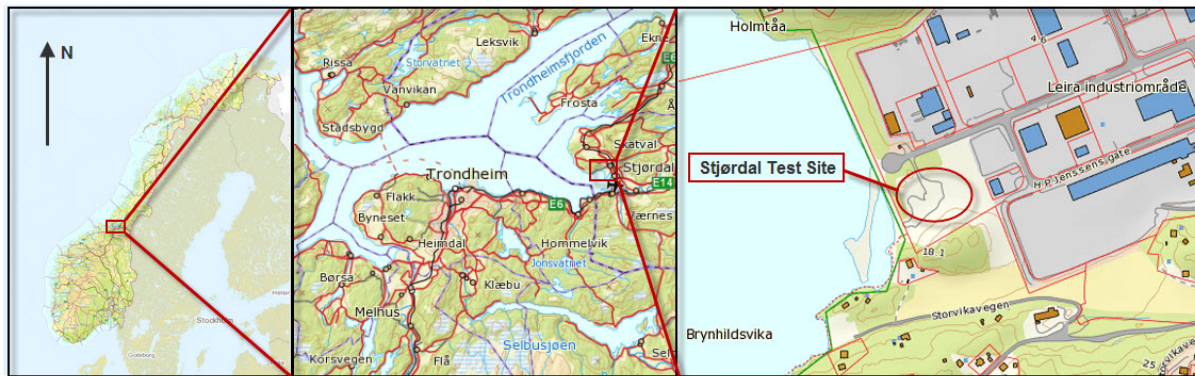


Figure 2.3.1: Location of Stjørdal site Leira.

The land area of Leira is located inside a small berm and has been reclaimed by pumping masses from the seabed. The test site has been extensively explored at several occasions. During 70s and 80s, the shores of Leira were investigated by the company Scandiaconsult (Kummeneje) due to the plans for building of a dry dock for construction of offshore oil platforms. After the area has been reclaimed, geotechnical investigations have been made at the industrial area nearby, to accommodate the industrial facilities. In addition, NTNU has had several extensive geotechnical field investigations at Leira site as a part of the course TBA4110 "Geotechnics: Field and Laboratory Investigations". Unless noted otherwise, the summary of site conditions given below is extracted from the field and laboratory work at which author has participated during the course TBA4110 "Geotechnics: Field and Laboratory Investigations", autumn semester 2013.

2.3.2 Key Soil Parameters

The piezometer measurements indicate that groundwater table at Stjørdal site Leira is located at depth 2.25 m below ground surface. The in-situ pore pressure below groundwater table is hydrostatic.

The results of CPTU sounding show that the soil at Stjørdal consists of two main strata. The top layer is located at depth 0-3.6 m and consists of sand and/or gravel. Below the depth of 3.6 m there is a layer of clay. Total sounding suggests that the bedrock is found at approximate depth of 22.5 m. In the following, the main focus is directed towards the clay layer since the layer is the most relevant for the study.

The clay below groundwater table is fully saturated. Based on the bulk density of the whole sample cylinder, the degree of saturation is estimated as 98 %. Based on the density obtained from small ring test, the degree of saturation is 100 %.

The natural water content (w) of clay estimated by Scandiaconsult (Kummeneje, 2003) lies in range 25-39 % with an average value of approximately 33 %. The unit weight (γ) of sand varies between 17.4 and 20.4 kN/m³ at the boundary of clay layer. The unit weight of clay is consistent throughout the layer and is in range of 18.5-19.5 kN/m³. Figure 2.3.2 (available in Norwegian only) shows data for natural water content and unit weight of the soil, together with undrained and remoulded shear strength and sensitivity, down to a depth of 12 m. The results originate from one of the boreholes Scandiaconsult has investigated due to the construction of an industrial building in the area. Similar values of natural water content and unit weight have been reported during site explorations aimed to assess the building of the dry dock (Kummeneje, 1981).

As seen from Figure 2.3.2, there is some scatter in the values of undrained shear strength (s_u) of the clay close to the boundary of sand layer. Below the layer boundary, the values of undrained shear strength are consistent and there is good agreement between the results of falling cone tests and UCT. Most of the measurements show an undrained shear strength (s_u) and remoulded shear strength (s_r) of approximately 30 kPa and 5 kPa, respectively. Except for the boundary between the soil layers, the sensitivity values are homogeneous and are in range of 6-9. The clay can be characterised as medium stiff, low sensitive.

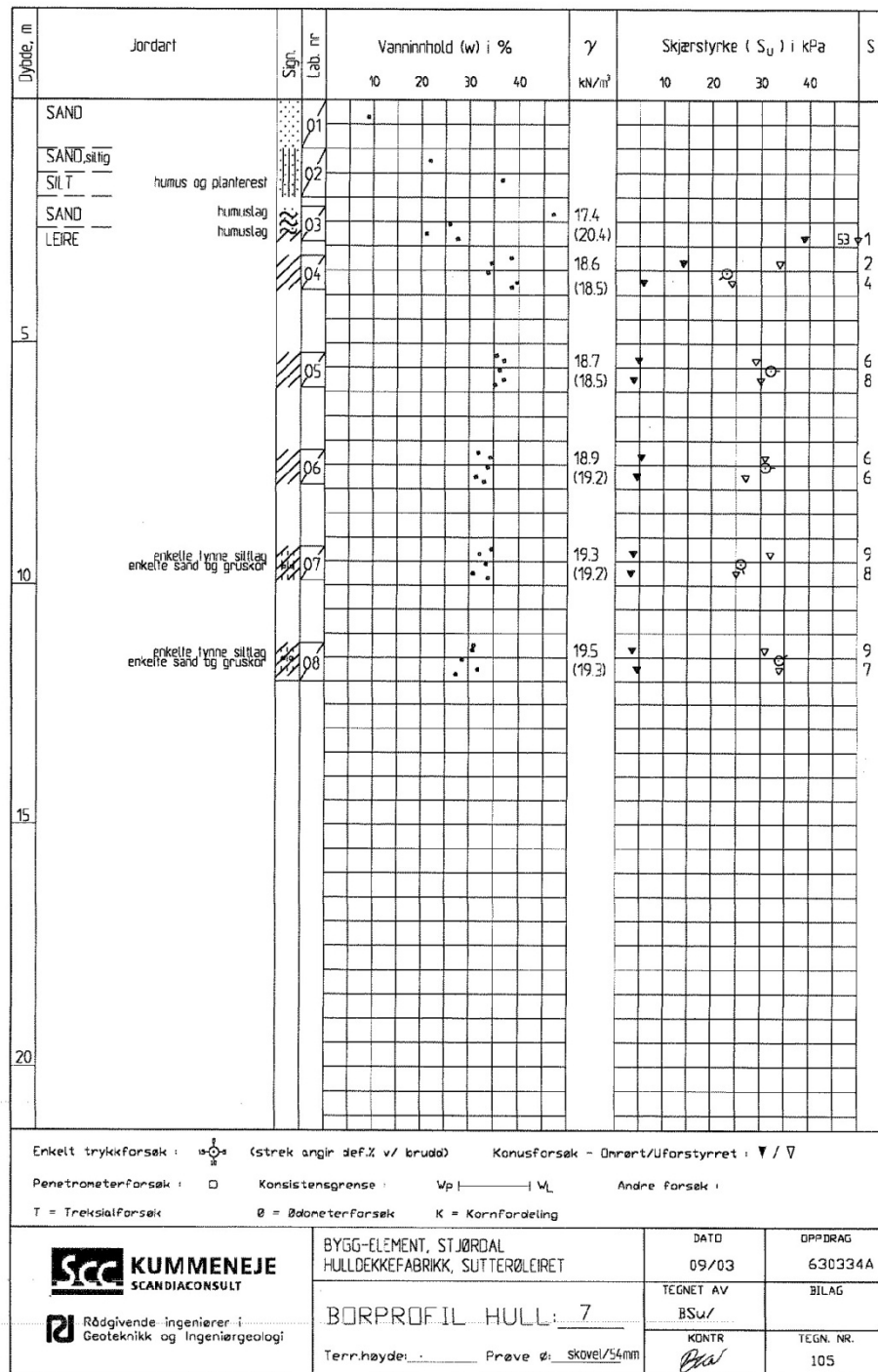


Figure 2.3.2: Stjørdal site Leira: soil profile, natural water content, unit weight of soil, undrained shear strength and sensitivity (after Kummeneje, 2003).

As a part of the course TBA4110 "Geotechnics: Field and Laboratory Investigations" taught during autumn semester 2013, a laboratory test programme has been carried out on ø54 mm sample extracted from 14.0-14.8 m depth. The results indicate some increase in undrained

shear strength at this depth. The undrained shear strength measured by falling cone varies between 38 and 58 kPa while unconfined compression test (UCT) suggests undrained shear strength of 50 kPa. Remoulded shear strength values are similar to those reported by Kummeneje (2003). Figure 2.3.3 shows values of undrained shear strength s_u from falling cone test and UCT, as well as remoulded shear strength s_r at depth 14.0-14.8 m.

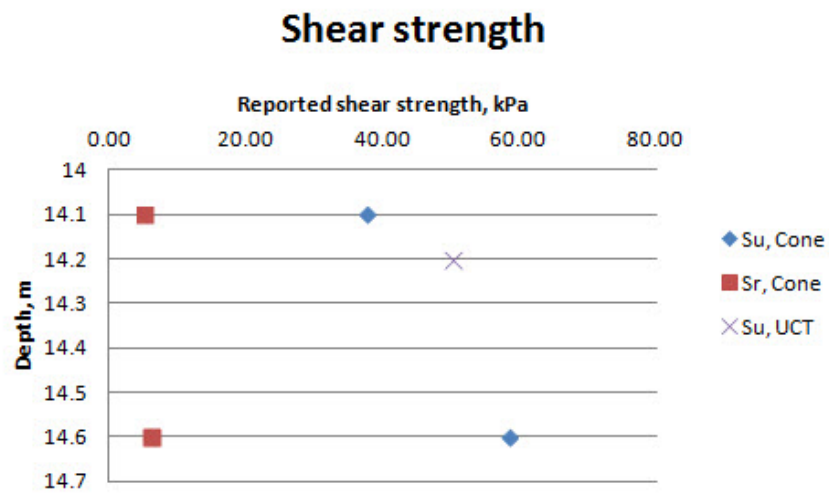


Figure 2.3.3: Stjørdal site Leira: Undrained and remoulded shear strength at depth 14.0-14.8 m.

Other index parameters for Stjørdal clay at depth 14.0-14.8 m are as following:

- Clay content approximately 35 %, the remaining 65 % is silt fraction.
- Average and small ring densities (ρ) are 1.25 gr./cm³ and 1.41 gr./cm³, respectively.
- Grain density (ρ_s) is 2.63 gr./cm³.
- Water content (w) is in range 33-35 %.
- Liquid limit (w_L) and plastic limit (w_p) are 24 % and 35 %, respectively.
- Liquidity index and plasticity index are 0.9 and 12 %, respectively.
- Porosity values (n) determined from average and small ring densities are 52 % and 46 %, respectively.

Following results have been found from CRS oedometer test on Stjørdal clay from depth 14.5 m:

- Preconsolidation stress (p'_c) is 230 kPa.
- Modulus number (m) is 14.4.

- Constrained moduli in the overconsolidated range (M_o) and at the preconsolidation stress (M_n) are 7.0 MPa and 6.0 MPa, respectively.
- Coefficients of consolidation in the overconsolidated zone (c_{v0}) and at about p'_c (c_{vn}) are 8.0 m²/yr and 6.0 m²/yr, respectively .

Figure 2.3.4 shows the results from CRS oedometer test on Stjørdal clay.

A rough estimate of OCR at depth 14.5 m is made by assuming that mean values of unit weights of sand and clay are both 19.0 kN/m³, groundwater table is at depth of 2.3 m and preconsolidation stress of the specimen is 230 kPa:

$$OCR = \frac{p'_c}{\sigma'_{v0}} = \frac{230}{19 \cdot 14.5 - (14.5 - 2.3) \cdot 9.81} = \frac{230}{156} = 1.5 \quad (\text{Eq. 2.1})$$

where

p'_c = preconsolidation stress

σ'_{v0} = in-situ vertical effective stress

In addition to the index and oedometer testing, two CIUC triaxial tests have been carried out on Stjørdal clay sample from depth 14.25-14.35 m and 14.47-14.57 m. Test results suggest an attraction of 55 kPa, a friction angle of 20.5⁰ and zero dilatancy.

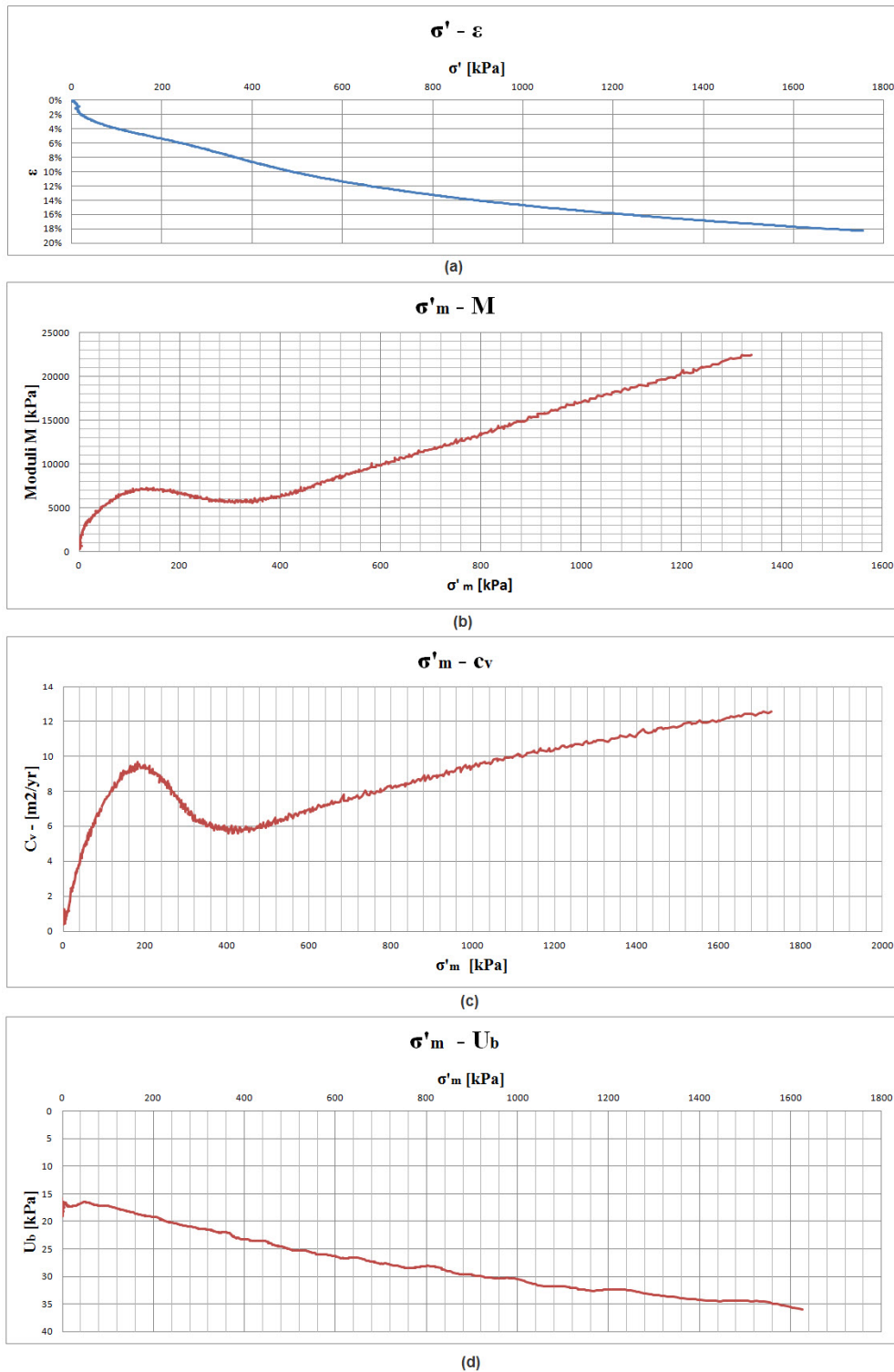


Figure 2.3.4: CRS oedometer test results for Stjørdal clay at depth 14.5 m: (a) Stress-strain plot, (b) Stress-modulus plot, (c) Stress-coefficient of consolidation, (d) Stress-pore pressure at sample base.

2.4 Samples Used in This Study

To distinguish the samples more easily in further, each sample cylinder is assigned a unique designation number. The designation number includes information about site of origin, diameter of extruder cone and borehole number. Figure 2.4.1 shows designation methodology for the sample cylinders used in the study.

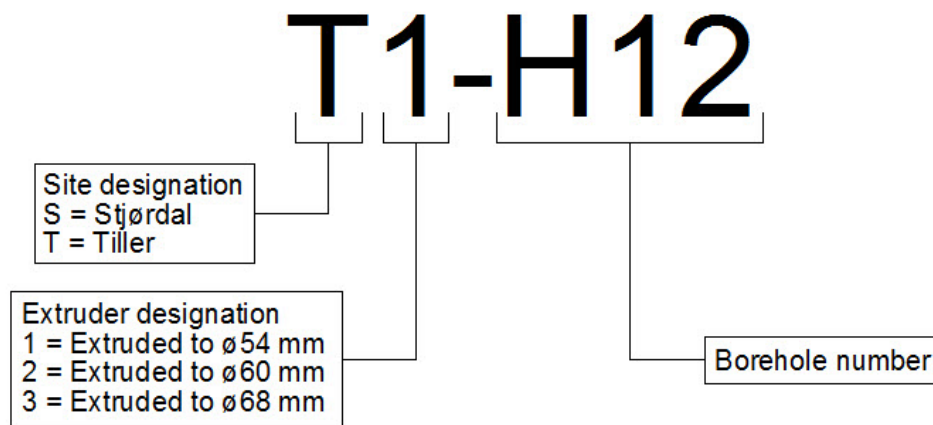


Figure 2.4.1: Designation methodology for sample cylinders used in the study.

There are totally six sample cylinders used in this study. All samples were obtained with standard $\varnothing 72.3$ mm steel cylinders with 9.5° taper angle of the cutting edge. The origin of the samples is as following (with designation referring to Figure 2.4.1):

- Sample cylinder obtained at Tiller site at 10th of February 2015, borehole H12, depth 4.045-4.800 m (hereafter called T1-H12)
- Sample cylinder obtained at Tiller site at 16th of March 2015, borehole H15, depth 3.052-3.800 m (hereafter called T2-H15)
- Sample cylinder obtained at Tiller site at 16th of March 2015, borehole H14, depth 3.043-3.800 m (hereafter called T3-H14)
- Sample cylinder obtained at Stjørdal site at 5th of March 2015, borehole H1, depth 8.043-8.800 m (hereafter called S1-H1)
- Sample cylinder obtained at Stjørdal site at 5th of March 2015, borehole H1, depth 6.041-6.800 m (hereafter called S2-H1)
- Sample cylinder obtained at Stjørdal site at 5th of March 2015, borehole H1, depth 7.040-7.800 m (hereafter called S3-H1).

CHAPTER 3 Test Programme, Equipment and Method

3.1 Introduction

The laboratory test program has been carried out on six $\phi 72.3$ mm sample cylinders. For more details on the origin of the samples and sample designation numbering, refer to Chapter 2.

Approximately half of the length of each cylinder has been extruded undisturbed (intact), while the other half has been pre-strained through an extruder cone (tapered cylinder) with a given diameter. The extruder cone diameters used on each sample are summarized in Table 3.1.1.

Table 3.1.1: Summary of extruder cone diameters used in the study.

Sample designation number	Diameter of applied extruder cone (tapered cylinder), mm
T1-H12	54
T2-H15	60
T3-H14	68
S1-H1	54
S2-H1	60
S3-H1	68

Summary of laboratory test programme for each sample cylinder is given in Table 3.1.2.

Table 3.1.2: Summary of laboratory test programme for each sample cylinder.

Type of clay material	Executed tests and calculations
Intact (undisturbed)	<ul style="list-style-type: none"> • Average density calculation • Density determined with small ring • Grain density determined with pycnometer • Water content measurements • Liquid limit by Casagrande's method • Plastic limit • Determination of degree of saturation, void ratio and porosity • Grain size distribution determined by wet sieving and hydrometer analysis • Unconfined compression test (UCT) • Falling cone test • CRS oedometer test up to 800 kPa
Pre-strained by extrusion through tapered cylinder with a given diameter	<ul style="list-style-type: none"> • Measurement of piston displacement during the pre-straining • Water content measurements • Falling cone test prior to reconsolidation • Reconsolidation in the oedometer for 24 hr., at following stress levels: in-situ vertical effective stress (σ'_{v0}) - 100 kPa - 150 kPa - 200 kPa • Falling cone tests on specimens reconsolidated in the oedometer at stress levels stated above • Water content measurements after reconsolidation at stress levels stated above • CRS oedometer test up to 800 kPa
Remoulded (manually) by knife	<ul style="list-style-type: none"> • Falling cone test • CRS oedometer test up to 800 kPa • Measurement of water content in the sample built in the oedometer

3.2 Pre-Straining Through Extrusion

3.2.1 Purpose

The purpose of the extrusion through tapered cylinder is to achieve a measurable level of shear mode pre-straining of a clay sample.

3.2.2 Test Equipment

Test equipment used for the extrusion is:

- Steel cylinders with undisturbed clay samples obtained by piston sampling technique. Cylinder diameter is 72.3 mm.
- Extruder cones (tapered cylinders) with opening diameters 54, 60 and 68 mm.
- Hydraulic sample extruder apparatus.
- Ruler for measurement of length of the extruded soil.

3.2.3 Test Procedure

The pre-straining was achieved by extrusion of undisturbed clay samples with length L_1 and diameter D_1 through a tapered cylinder with length L_2 and diameter D_2 . During the extrusion, displacement of the hydraulic sample extruder's piston was measured. The procedure is schematically illustrated in Figure 3.2.1.

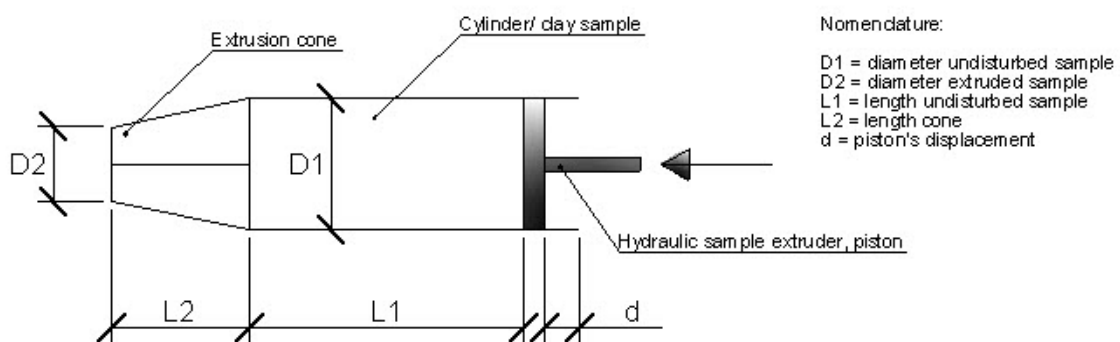


Figure 3.2.1: Pre-straining of clay samples through extrusion.

Initially it was planned to measure the applied force together with the displacement of the piston. The force measurement during pre-straining could be used to find the correlation between the work and the shear strength of pre-strained, non-reconsolidated sample. The objective had to be omitted due to the lack of appropriate equipment.

Cross-sectional areas of undisturbed and pre-strained sample are respectively given as

$$A_1 = \pi \cdot \left(\frac{D_1}{2}\right)^2 \quad (\text{Eq. 3.1})$$

$$A_2 = \pi \cdot \left(\frac{D_2}{2}\right)^2$$

where

D_1 = diameter of the sample before pre-straining (undisturbed sample)

D_2 = diameter of the pre-strained sample

Assuming conservation of volume through the extrusion process, axial strain is given as

$$\varepsilon_a = \left(\frac{A_1}{A_2} - 1\right) \cdot 100\% \quad (\text{Eq. 3.2})$$

Theoretically, mean shear strain is calculated as

$$\gamma_s = \frac{3}{2} \cdot \varepsilon_a \quad (\text{Eq. 3.3})$$

The intact samples obtained at Tiller and Stjørdal test sites were pre-strained by extrusion through $\varnothing 54$ mm, $\varnothing 60$ mm and $\varnothing 68$ mm extruder cones. Table 3.2.1 provides a summary of diameters of extrusion cones (D_2) used in this study, together with calculated strains given by Eq. 3.1-3.3.

The displacement ratio δ_r during the extrusion is given as the relation between the lengths of extruded material and piston displacement:

$$\delta_r = \frac{L_{ext}}{d} \quad (\text{Eq. 3.4})$$

where

L_{ext} = a given length of extruded material

d = piston displacement for the given length of extruded material

Table 3.2.1: Summary of diameters of extruder cones and corresponding degrees of pre-straining.

Diameter of undisturbed sample D_1 , mm	Diameter of extruded sample D_2 , mm	Applied axial strain ϵ_a , %	Applied shear strain γ_s , %	Level of pre-straining	Samples subjected to the pre-straining
72.3	54	78	117	Completely remoulded	T1-H12 S1-H1
72.3	60	44	66	Severely strained	T2-H15 S2-H1
72.3	68	12	18	Moderately strained	T3-H14 S3-H1

The theoretical value of displacement ratio was calculated from the requirement of volume conservation:

$$V_{und} = V_{ext} \quad (\text{Eq. 3.5})$$

$$\pi \cdot \left(\frac{D_1}{2}\right)^2 \cdot d = \pi \cdot \left(\frac{D_2}{2}\right)^2 \cdot L_{ext}$$

$$\delta_r = \frac{L_{ext}}{d} = \frac{\left(\frac{D_1}{2}\right)^2}{\left(\frac{D_2}{2}\right)^2}$$

where

V_{und} = volume of undisturbed material subjected to extrusion

V_{ext} = volume of extruded material

A summary of theoretical values of displacement ratios is given in Table 3.2.2. During the extrusion, the observed value of displacement ratio has been compared to the theoretical one. The comparison was aimed to cross-check whether the assumption of volume conservation, and hence also uniform strain distribution in the cross-section, agreed with the real conditions.

Table 3.2.2: Summary of theoretical displacement ratios during clay extrusion.

Diameter of undisturbed sample D_1, mm	Diameter of extruded sample D_2, mm	Applied axial strain ϵ_a, %	Applied shear strain γ_s, %	Theoretical displacement ratio δ_r, mm/mm
72.3	54	78	117	1.79
72.3	60	44	66	1.45
72.3	68	12	18	1.13

3.3 Density Measurements

3.3.1 Purpose

Density measurements consist of average density calculation, density measurement with small ring and density of the solids determined by pycnometer test. Density of the soil and grain density are both important index parameters which are used in most geotechnical calculations (calculations of unit weight of soil γ , porosity n , void ratio e , etc).

3.3.2 Test Equipment

For average density calculation the test equipment consists of cylinder with sample, ruler and weighing scale.

The density test with small ring is carried out with calibrated small ring with known volume and weight, and the apparatus for pressing the ring in the sample. The test equipment also includes a bowl with known weight for drying of the sample as well as weighing scale.

The pycnometer test equipment consists of calibrated pycnometer with known weight and volume, vacuum-exicator, deaired water, water bath with constant temperature ($20^{\circ}\text{C} \pm 0.1^{\circ}\text{C}$), brush and bowl.

3.3.3 Test Procedure

3.3.3.1 Average Density

Before the extrusion, the sample cylinder with sample was weighed and measured with sealing plug but without end caps. Normally the weighing and length measurement is done without sealing plug as well, however, in this case a sealing plug was kept in sample cylinder due to the specifications of hydraulic extruder apparatus. After the extrusion, the height of plug was measured, the empty cylinder and plug were weighed and the average density and unit weight of soil were calculated.

The average density of whole sample is given as

$$\rho = \frac{m_s + m_w}{V} \left[\frac{g}{cm^3} \right] \quad (\text{Eq. 3.6})$$

The unit weight of soil is determined accordingly from formula

$$\gamma = \frac{(m_s + m_w) \cdot g}{V} \left[\frac{kN}{m^3} \right] \quad (\text{Eq. 3.7})$$

where

- $(m_s + m_w)$ = total mass of sample
- m_s = mass of solid particles
- m_w = mass of water
- V = volume of sample
- g = gravitational acceleration, 9.81 m/s^2

3.3.3.2 Density Determined with Small Ring

The test is standardised in NS 8011:1982 (at the time of writing, the code is about being replaced by NS-EN ISO 17892-2:2014). The density of small sample was determined by pressing a calibrated ring with known volume and weight into cylindrical, undisturbed sample. The material outside of the ring was removed and the weight of the ring and sample was measured. With known volume and weight of the soil in the ring, the density could be calculated in a similar manner as in average density calculation.

After the measurement, the soil inside the ring was collected into a bowl and dried in the oven at 105⁰C for 24 hours. The dry mass was weighed and the dry density could be calculated from the expression

$$\rho_d = \frac{m_s}{V} \quad (\text{Eq. 3.8})$$

where

m_s = mass of solid particles

V = volume of the ring

3.3.3.3 Grain Density (Density of Solids)

The grain density was found by placing an undisturbed specimen with weight > 25 gr. in a bowl and dissolving it with deaired water. The amount of the water was kept as little as possible, not exceeding approximately half of the pycnometer. Brush was used to dissolve the material. When the specimen has been dissolved, the solution was poured into the pycnometer. The pycnometer containing suspended material was placed into the vacuum-exicator for evacuation of air from the material. After evacuation, the pycnometer was refilled with deaired water and placed into the bath for approximately 10 minutes.

After standing in the bath with constant temperature 20⁰C±0.1⁰C, the pycnometer was weighed and the suspension was poured into the bowl with known weight for drying in the oven. The dry weight was reported.

Based on the reported data, the grain density ρ_s was found from the expression

$$\rho_s = \frac{(\text{mass dry sample}) \cdot (\text{density of water})}{(\text{mass waterfilled pycnometer}) + (\text{mass dry sample}) - (\text{mass waterfilled pycnometer} + \text{sample})} \quad (\text{Eq. 3.9})$$

The unit weight of solids is defined as

$$\gamma_{solid} = \frac{m_s \cdot g}{V_s} \left[\frac{kN}{m^3} \right] \quad (\text{Eq. 3.10})$$

where

V_s = volume of solid particles

The test method is suitable for materials with grain size < 4 mm, e.g. for all materials used in this study.

3.4 Natural Water Content

3.4.1 Purpose

Natural water content (w) is one of the key variables in the study. The parameter is used in many geotechnical calculations, among them determination of degree of saturation, porosity and void ratio.

3.4.2 Test Equipment

Test equipment consists of weighing scale and cup with known weight.

3.4.3 Test Procedure

The test is standardised in NS 8013:1982 (at the time of writing, the code is about being replaced by NS-EN ISO 17892-1:2014).

To determine the (natural) water content for a soil sample, the wet sample was placed in a cup and weighed. The sample was dried to constant mass in the oven with temperature 105°C , for 24 hours or longer. Based on the reported wet and dry mass, water content was calculated from the expression

$$w = \frac{m_w}{m_s} \cdot 100 \% \quad [\%] \quad (\text{Eq. 3.11})$$

where

m_w = mass of water

m_s = mass of solid particles

To avoid drying, the first measurements of natural water content were carried out immediately after the sample was extruded out of the sample cylinder. At this stage, following three measurements were reported for each sample cylinder:

- Water content at the bottom of the sample (undisturbed material)
- Water content at the top of the sample (pre-strained material)
- Water content close to the middle of the sample (pre-strained material).

It has been assumed, and confirmed by visual observations, that the extruded (pre-strained) material does not have time to reconsolidate immediately after the extrusion. Hence, immediately after the extrusion, the water content for pre-strained material is assumed to be the same as natural water content for undisturbed material. The measurements were carried out at three different locations to ensure that the sample was homogeneous and without layering. For calculations of other parameters where natural water content was involved, a mean value of these three measurements has been used.

When building up a remoulded clay specimen into the oedometer for testing, a control measurement of water content in the remoulded clay specimen has always been carried out. This has been done due to the quick drying of the remoulded clay.

3.5 Plastic and Liquid Limit

3.5.1 Purpose

Plastic and liquid limits are both involved in calculation of liquidity and plasticity index. The latter index is widely used for classification of clays. In addition to the classification of clays, the plasticity index is closely correlated with ultimate shaft friction of a driven pile. Based on the empirical data, plasticity index enters as one of the main parameters in two most common methods for prediction of ultimate shaft friction (so-called α - and β -method), as proposed by Karlsrud (2012). This makes it reasonable to expect that plasticity index also has large influence on behavior of pre-strained, reconsolidated clay around a drilled shaft and casing.

The factors above make plastic and liquid limit to the key parameters, and determination of these factors to the essential part of index test programme.

3.5.2 Test Equipment

Test equipment for determination of liquid limit consists of Casagrande apparatus, grooving tool, weighing scale, distilled water and cup with known weight for drying of the sample. Figure 3.5.1 shows the Casagrande apparatus with grooving tool used in the study.

For determination of plastic limit, the test equipment consists of glass plate, weighing scale and small glass with known weight.



Figure 3.5.1: Casagrande apparatus with grooving tool.

3.5.3 Test Procedure

3.5.3.1 Liquid Limit

The test procedure for determination of liquid limit is standardised in NS 8001 (1982). The terminology and symbols used in the test are standardised in NS 8000 (1982).

The liquid limit w_L was determined by Casagrande's method. Before the test, the Casagrande apparatus was adjusted in such way that the apparatus' cup was lifted 10 mm at each drop. The determination of liquid limit was carried out by preparing a remoulded clay sample in the Casagrande cup. The paste was divided by a grooving tool to establish 2 mm wide groove. The cup was lifted by means of a crank, and dropped down against the hardwood base of the apparatus with approximate frequency of 2 drops per second, 25 drops in total. When the two halves of the clay mass have touched each other over a length of 12.5 mm after exactly 25 drops, the test was arrested and water content of the clay mass was determined after standard procedure. The water content in this case corresponds to the liquid limit (w_L). Otherwise,

more water has been added and the clay has been remoulded and built into the cup before the test was repeated once again (alternatively, if required, the clay has been remoulded and dried before the test was repeated).

The liquid limit has been determined one time for each of the sample cylinders.

3.5.3.2 *Plastic Limit*

The test procedure for determination of liquid limit is standardised in NS 8003 (1982). The terminology and symbols used in the test are standardised in NS 8000 (1982).

Determination of plastic limit w_p was carried out by forming the remoulded clay mass into a ball, before rolling it by hands on the glass plate. The glass plate caused drying of the clay mass, so that the water content has been reduced through the test. The clay mass was rolled into the threads of diameter 3-4 mm. The test was arrested when the threads started to crumble. At this stage, the threads were collected into the glass with known weight and weighed. The water content in the crumbled threads was determined after standard procedure, and is corresponding to the plastic limit w_p (the lowest water content in the remoulded clay at which the soil is plastic).

The test method described above is suitable for fine-grained soils with plastic behaviour. The plastic limit has been determined one time for each of the sample cylinders.

3.5.3.3 *Plasticity and Liquidity Index. Classification*

Plasticity and liquidity indices were determined for each sample cylinder with known values of natural water content w , liquid limit w_L and plastic limit w_p . The value of natural water content used in the formulas was taken as a mean of three water content measurements carried out for each cylinder directly after sample extrusion.

Liquidity index I_L was found from the formula

$$I_L = \frac{w - w_p}{w_L - w_p} \quad (\text{Eq. 3.12})$$

Plasticity index I_p was found from the expression

$$I_p = w_L - w_p \quad [\%] \quad (\text{Eq. 3.13})$$

Classification of clay after plasticity was carried out in accordance with NGF (1982). The classification chart is given in Table 3.5.1.

Table 3.5.1: Classification of clay after plasticity (after NGF, 1982).

Classification of material	Classification of plasticity	Plasticity index I_p , %
Low plastic	Low plasticity	< 10
Medium plastic	Medium plasticity	10 -20
Highly plastic	High plasticity	> 20

3.6 Degree of Saturation, Void Ratio and Porosity

3.6.1 Purpose

Determination of degree of saturation, void ratio and porosity is a part of any standard index testing programme. The purpose of parameter determination is a systematic assessment of soil's three-phase material.

3.6.2 Determination Procedure

Determination of degree of saturation, void ratio and porosity was carried out with measured and calculated values of natural water content w , unit weight of soil γ and unit weight of solids γ_{solid} .

The degree of saturation S_r describes the share of total pore volume occupied by water. The parameter was calculated from the expression

$$S_r = \frac{V_w}{V_p} = \frac{w \cdot \gamma}{\gamma_w \cdot \left(1 + w - \frac{\gamma}{\gamma_{solid}}\right)} \quad [\%] \text{ or dimensionless} \quad (\text{Eq. 3.14})$$

where

V_w = volume of water

V_p = volume of voids

w = natural water content

γ = unit weight of soil

γ_{solid} = unit weight of solids

γ_w = unit weight of water, 9.81 kN/m³

The void ratio e is a parameter commonly used for clays, and describes the ratio between pore volume and volume of solids. The parameter was calculated from the expression

$$e = \frac{V_p}{V_s} = \frac{\gamma_{solid}(1+w)}{\gamma} - 1 \quad [-] \quad (\text{Eq. 3.15})$$

where

V_s = volume of solids

The porosity n is given by the ratio between volume of voids and the total sample volume. The parameter was calculated from the formula:

$$n = \frac{V_p}{V} = \left(1 - \frac{\gamma}{\gamma_{solid}(1+w)}\right) \cdot 100 \% \quad (\text{Eq. 3.16})$$

V = volume of sample (total volume)

3.7 Grain Size Distribution and Hydrometer Analysis

3.7.1 Purpose

The purpose of hydrometer analysis is to find grain size distribution for fine grained materials with grain diameter < 74 μm . The composition of soil particles is an important part of any index testing programme since the mechanical properties of soils are largely dependent on grain size distribution. Determination of grain size distribution is also an essential procedure for classification of soil with respect to gradation of the material.

3.7.2 Test Equipment

The test equipment for determination of grain size distribution consists of:

- Sieves with different mesh aperture (8, 4, 2, 1, 0.5, 0.25, 0.125, 0.074 mm) and bottom catch pan.
- Brush for wet sieving.
- Distilled water.
- Weighing scale.
- Oven with constant temperature 105⁰C.
- Water bath with constant temperature of 20⁰C \pm 0.1⁰C.

- Calibrated hydrometer.
- Thermometer.
- Stop watch.
- 1000 ml graduated cylinder.
- Dispersive matter.
- Heat resistant bowls for collection of soil material.

3.7.3 Test Procedure

The test is standardised in NS 8005 (1990). Two different methods of sieving are available (dry and wet). Dry sieving method is suitable for materials where fine particles smaller than 74 μm constitute less than 5 % of total mass. For the materials with larger amount of fine grains, the wet sieving with brush and water is used.

Both Tiller and Stjørdal clay were subjected to the wet sieving due to the high content of fines. The amount of clay was chosen so that the weight of material was between 10 and 100 gr. The sieving procedure has shown that all particles have passed 0.125 mm mesh aperture, and only a small amount of particles was held back on the sieve with 0.074 mm mesh aperture. The particles held back on 0.074 mm mesh aperture were dried 24 hours in the oven and weighed after the drying. The particles < 74 μm were subjected to hydrometer analysis.

After the sieving, particles with $d < 74 \mu\text{m}$ dissolved in distilled water were placed in the graduated 1000 ml cylinder. A dispersive matter was added to the suspension to prevent the grains from flocculating. More distilled water was added so that a total volume of 1000 ml could be reached. The cylinder has been shaken in 120 seconds or until no sediment was visible on the bottom, before being placed into the bath with constant temperature ($20^{\circ}\text{C} \pm 0.1^{\circ}\text{C}$). The measurements of water temperature T and stabilization level R on the hydrometer neck were taken inside the cylinder. After the cylinder has been placed in the water-filled bath, the measurements were taken at the given time intervals of 1, 2, 5, 10, 20, 40, 80, 160, 320 minutes and 22 hours. The hydrometer measurements did not have to be corrected since the hydrometer at NTNU laboratory was calibrated.

Based on the measurements, fall velocities and relative weights of several grain fractions could be determined. The calculation procedure is based on Stoke's law for equivalent spheres sedimenting freely in a liquid. Following applies:

$$d_s = K \cdot \sqrt{\frac{Z_r}{t}} \quad (\text{Eq. 3.17})$$

where

d_s = equivalent diameter of solid particle

K = constant, function of water temperature T and grain density ρ_s

Z_r/t = fall velocity of the particles

Z_r = effective depth (distance between top of suspension and the level to which solid particle is sedimenting through a period of time t)

t = time for sedimentation of solid particle to a given level Z_r

The constant K is a function of grain density ρ_s and temperature in the suspension T at the time of a measurement t . The chart for determination of coefficient K is shown in Figure 3.7.1.

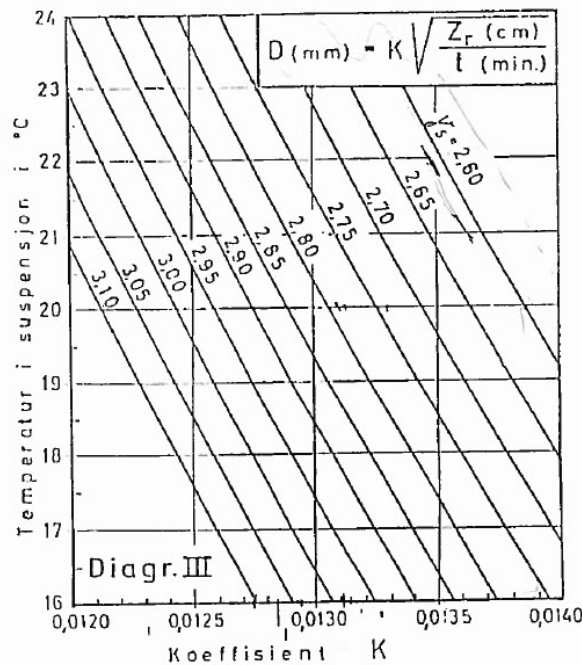


Figure 3.7.1: Chart for determination of constant K in hydrometer analysis.

Effective depth Z_r is a function of measured concentration of the suspension R (stabilization level on the hydrometer neck, in gr/l) at a given time t . The chart for determination of effective depth Z_r is shown in Figure 3.7.2.

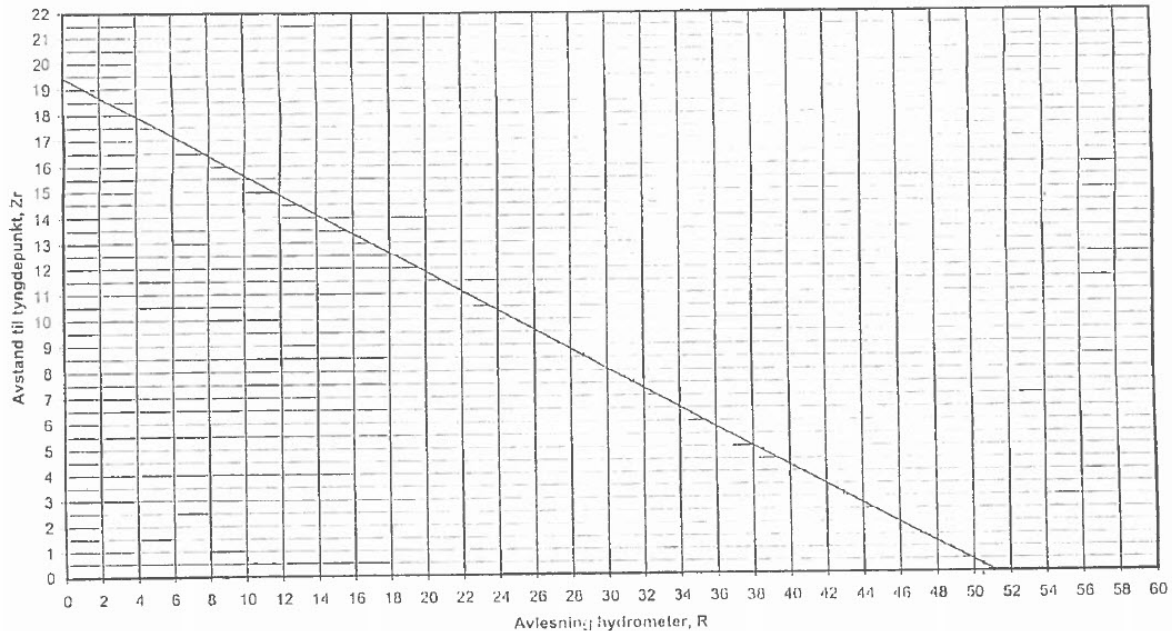


Figure 3.7.2: Chart for determination of effective depth Z_r in hydrometer analysis.

Relative weight N (in %) of the considered particle size or larger is given as

$$N = a \cdot \frac{R}{w_s} \tag{Eq. 3.18}$$

where

a = coefficient

R = concentration of the suspension (stabilization level read on the hydrometer neck)

w_s = dry mass of the material subjected to the hydrometer analysis

Coefficient a is a function of grain density ρ_s . The chart for determination of coefficient a is shown in Figure 3.7.3.

When the measurements were completed, the suspension and the sediment was poured into the heat resistant glass with known weight and dried in the oven. The dry mass of the material subjected to the hydrometer analysis was weighed after drying. Based on the dry mass of the

material in hydrometer analysis, relative weights N and dry mass of the grains held back on sieves, the grain size distribution curve was drawn.

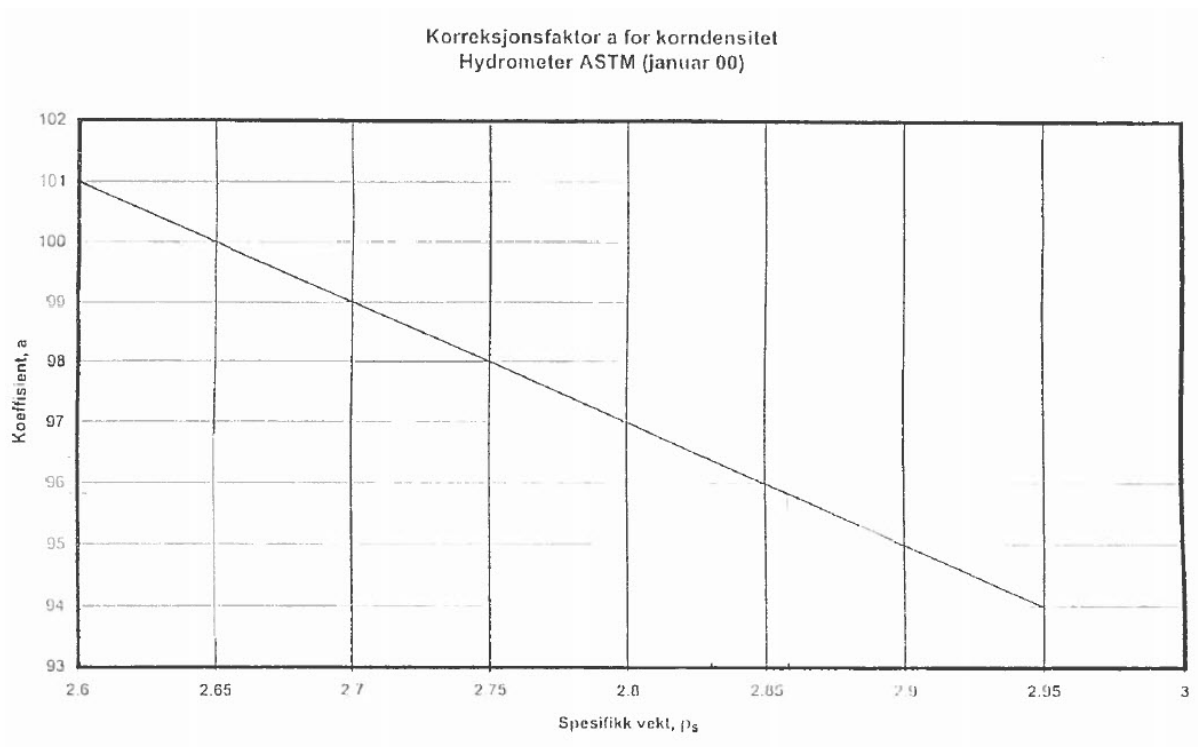


Figure 3.7.3: Chart for determination of coefficient a in hydrometer analysis.

Classification of gradation of the material may be carried out in accordance with NGF (1982) or NS-EN ISO 14688-2 (2004). In this report, classification has been carried out in accordance with NGF (1982) which is the most common practice for Norwegian conditions. The gradation of the material was assessed with uniformity coefficient C_u defined as

$$C_u = \frac{d_{60}}{d_{10}} \quad (\text{Eq. 3.19})$$

where

d_{60} = diameter for 60 % passing

d_{10} = diameter for 10 % passing

Where the ratio d_{60}/d_{10} was not possible to determine for practical reasons, the ratio d_{75}/d_{25} was determined instead.

The chart for classification of material gradation is shown in Table 3.7.1.

Table 3.7.1: Classification of gradation (after NGF, 1982).

Description	Uniformity coefficient $C_u = d_{60}/d_{10}$
Uniformly graded	< 6
Medium graded	6 - 15
Well-graded	> 15

Denotation of soil type is carried out in accordance with NGF (1982). A summary of denotation guidelines is given in Table 3.7.2. The rules for denotation of morainic materials are omitted due to their irrelevance with respect to the materials used in the study.

Table 3.7.2: Denotation of soil type (after NGF, 1982).

Based on clay content (% < 2 μm)	
> 30 %	The soil is described as clay
15 - 30 %	The soil is described as clay, with other fractions in adjective form according to decreasing percentual content
5 - 15 %	The soil is classified as clayey in adjective form
< 5 %	Clay content not given
Based on silt content (% < 60 μm)	
> 45 %	The soil is described as silt, with an additional denotation in adjective form
15 - 45 %	The soil is described as silty
< 15 %	The silt content is not presented
Based on content of sand, gravel or cobbles (% > 0.06 mm)	
> 60 %	The soil is described as sand, gravel or cobbles, but with additional fractions in adjective form
20 - 60 %	The soil is described as sandy, gravelly or cobbly
< 20 %	Fractional content is not presented

3.8 Measurement of Undrained Shear Strength by UCT

3.8.1 Purpose

The purpose of unconfined compression test (UCT) is to evaluate undrained shear strength and the failure strain by loading the sample uniaxially without presence of lateral stresses, at high strain rates.

3.8.2 Test Equipment

Test equipment consists of preparation mould for trimming of the sample to diameter 54 mm, unconfined compression test rig, paper for recording force and displacement, protractor and calibration chart. Figure 3.8.1 shows unconfined compression test rig used in the study.



Figure 3.8.1: Unconfined compression test rig used in the study.

3.8.3 Test Procedure

The test procedure and equipment is standardised in NS 8016 (1988).

The test was carried out on 10 cm high undisturbed test specimen from each sample cylinder. Prior to the test, the specimen was trimmed to diameter 54 mm in a preparation mould so the surfaces were smooth and plane.

After preparation the specimen was installed into the test rig. The recording paper was attached to the barrel and the record of compression load and deformation was done manually on the rig. The test was run by pressing the top cap with high strain rate so the pore water was not allowed to expel from the sample. The strain rate was kept constant throughout the test, usually between 3.5 and 4.5 %/hour. The test was stopped when a considerable decrease in the recorded load was observed. After the test was completed the record paper was attached to the calibration chart from which the axial deformation at failure (in mm) and failure load (in kg) could be read. Because the specimen was exactly 100 mm high, the reading of deformation at failure (δ , in mm) was equal to the value of failure strain (ϵ_a , in percent). The failure strain is given as

$$\epsilon_a = \frac{\delta}{H_0} \cdot 100\% \quad (\text{Eq. 3.20})$$

where

δ = deformation at failure

H_0 = initial height of sample, 100 mm

The angle of failure plane at the test accomplishment was measured by a protractor. Both the shape of sample at failure and the slope of failure plane was documented by photograph and sketch.

Based on the readings the undrained shear strength was calculated. Constant volume requires that loaded area at failure (A) is

$$A = \frac{A_0}{1 - \epsilon_a} \quad (\text{Eq. 3.21})$$

where

A_0 = initial area of sample

In the study, all of the specimens subjected to UCT were trimmed to diameter 54 mm, so the initial area of sample in each test was

$$A_0 = \pi \cdot r^2 = \pi \cdot 27^2 = 2290 \text{ mm}^2 \quad (\text{Eq. 3.22})$$

where

r = initial radius of sample, 27 mm

The major principal stress σ_1 at failure is given as

$$\sigma_1 = \frac{P_f}{A} = \frac{P_f \cdot (1 - \varepsilon_a)}{A_0} \quad (\text{Eq. 3.23})$$

where

P_f = recorded axial load at failure

Since the minor principal stress σ_3 is zero during the test, the undrained shear strength (equal to maximum shear stress) is given as

$$s_u = \tau_{max} = \frac{\sigma_1}{2} = \frac{P_f \cdot (1 - \varepsilon_a)}{2 \cdot A_0} \quad (\text{Eq. 3.24})$$

Figure 3.8.2 shows a graphical representation of the stress state at failure during UCT (Tresca failure criterion).

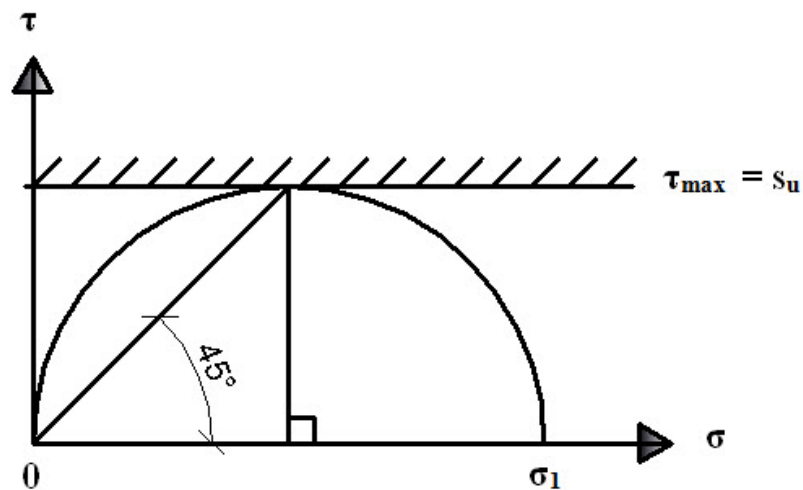


Figure 3.8.2: Graphical representation of Tresca failure criterion during UCT.

Where the distinct failure load and failure strain were lacking, the failure load was read at 10 % axial strain.

The unconfined compression test is regarded as less accurate for evaluation of undrained shear strength. There is however a fairly good agreement between UCT results and falling cone test results in most cases when the tested material is homogeneous. In this study, the UCT results have been cross-checked with falling cone test results for an assessment of homogeneity of the tested material.

3.9 Measurement of Undrained and Remoulded Shear Strength by Fall Cone

3.9.1 Purpose

The purpose of falling cone test is to determine undrained and remoulded shear strength, as well as sensitivity of fine grained soils. Additionally, falling cone test has been carried out for measurement of shear strength of pre-strained clay samples (reconsolidated and non-reconsolidated).

3.9.2 Test Equipment

The test equipment consists of cones in different weights (10, 60, 100 and 400 gr.), test apparatus for falling cone test and calibration charts from Swedish Geotechnical Institute (1946) which have been revised in 1962.

3.9.3 Test Procedure

The test method is standardised in NS 8015 (1988). The test was carried out by mounting the cone in the rig (test apparatus), and adjusting the position in such way that tip of the cone just touched the upper surface of the caly sample. The test was run out on undisturbed, remoulded and pre-strained (reconsolidated and non-reconsolidated) soil samples from each cylinder. Figure 3.9.1 shows test apparatus with mounted cone and undisturbed sample.

When the cone was released the tip penetrated the soil due to the cone's own weight. The intrusion was read in mm from the scale immediately after penetration. The value of shear strength of the soil has been found from calibration chart corresponding to the actual cone's weight.

Normally, the test has been carried out with 100 gr. cone. Where the clay was very soft, 60 gr. cone has been chosen instead.

For the undisturbed soil specimen, the procedure was carried out three times in total, each time at different location on the surface. The mean value of undrained shear strength, s_u , has been reported.



Figure 3.9.1: Falling cone test apparatus with mounted cone and undisturbed sample.

After testing of undisturbed specimen the specimen was remoulded in a cup by a knife, and tested once again for the remoulded shear strength. The testing of remoulded specimen was done in two sets of cone intrusions, each set with two intrusions at different locations. Mean value of remoulded shear strength, s_r , was found for each of the two sets, and the smallest mean value has been reported.

The sensitivity is given as

$$S_t = \frac{s_u}{s_r} \quad (\text{Eq. 3.25})$$

where

s_u = undrained shear strength (intact material)

s_r = remoulded shear strength

Based on undrained shear strength determined by falling cone and UCT, the clay was classified after its strength. The classification after undrained shear strength may be carried out in accordance with NGF (1982) and NS-EN ISO 14688-2 (2004). The classification carried out in this study was done after the guidelines of NGF (1982), which represent the most common practice for Norwegian conditions. The classification chart is shown in Table 3.9.1.

Table 3.9.1: Classification of clay after undrained shear strength determined by falling cone test and UCT (after NGF, 1982).

Classification soil type	Classification shear strength	Undrained shear strength s_u , kPa
Very soft	Very low	< 10
Soft	Low	10 - 25
Medium stiff	Medium	25 - 50
Stiff	High	> 50

Based on the value of S_t , the clay may be classified as low sensitive, medium sensitive or highly sensitive, in accordance with NGF (1982). The classification chart is shown in Table 3.9.2.

Table 3.9.2: Sensitivity classification chart (after NGF, 1982).

Type of clay	Sensitivity description	Value of sensitivity S_t
Low sensitive	Low	< 8
Medium sensitive	Medium	8 - 30
Very sensitive	High	> 30

Testing of pre-strained soil specimens (reconsolidated or non-reconsolidated) was performed in similar manner as for undisturbed specimens. Three cone intrusions have been measured and mean value of shear strength (s_{re} or s) has been reported.

3.10 Reconsolidation in the Oedometer Cell

3.10.1 Purpose

The reconsolidation of pre-strained material to different stress levels in the oedometer cell is carried out in order to simulate the reconsolidation process around a pile. The purpose of simulation is to measure change in properties of pre-strained material after the reconsolidation.

3.10.2 Test Equipment

The test equipment was identical to the equipment in oedometer test. In addition, a bowl was used to collect the sample for drying after reconsolidation (for water content calculation).

3.10.3 Test Procedure

Reconsolidation in the oedometer has been carried out on pre-strained samples from each of the sample cylinders used in the study.

The preparations for the reconsolidation in oedometer were identical to those for CRS oedometer test. When sample was built into oedometer cell, however, the reconsolidation was performed at one step with constant load. The drainage conditions were identical to those during CRS test (on-sided drain, drainage distance 20 mm). The samples were reconsolidated in 24 hr. at following reconsolidation stresses p'_{re} :

- In-situ vertical effective stress, σ'_{v0}
- 100 kPa
- 150 kPa
- 200 kPa

The in-situ vertical effective stress, σ'_{v0} , was calculated from small ring density (ρ). In-situ vertical effective stress σ'_{v0} for the considered test specimen is given as

$$\sigma'_{v0} = \sigma_{v0} - u \quad (\text{Eq. 3.26})$$

$$\sigma_{v0} = \gamma \cdot z$$

$$u = \gamma_w \cdot (z - z_w)$$

where

σ_{v0} = in-situ total vertical stress

u = pore pressure at the considered depth

γ = unit weight of soil (calculated from small ring density)

γ_w = unit weight of water, 9.81 kN/m³

z = depth to the test specimen

z_w = depth to groundwater table

Table 3.10.1 shows summary of reconsolidation stresses equal to in-situ vertical effective stresses σ'_{v0} , for different samples used in the study.

Table 3.10.1: Reconsolidation stresses equal to in-situ vertical effective stresses σ'_{v0} , for reconsolidation in the oedometer.

Sample ID	Density ρ , g/cm ³	Unit weight γ , kN/m ³	Depth to the test specimen z, m	Depth to ground water table z_w , m	In-situ vertical effective stress σ'_{v0} , kPa
T1-H12	1.86 (small ring)	18.25	4.42	0.50	42.2
T2-H15	1.98 (small ring)	19.42	3.19	0.50	35.6
T3-H14	1.96 (small ring)	19.23	3.31	0.50	36.1
S1-H1	1.85 (small ring)	18.15	8.09	2.25	89.5
S2-H1	1.87 (small ring)	18.34	6.22	2.25	75.1
S3-H1	1.80 (small ring)	17.66	7.28	2.25	79.2

Theoretically, primary consolidation time is given as

$$t_p \approx \frac{H^2}{c_v} \quad (\text{Eq. 3.27})$$

where

H = drainage distance (in this case, height of the sample, e.g. 20 mm)

c_v = coefficient of consolidation

However, the samples used for reconsolidation were moderately strained, severely strained and totally remoulded. This makes it reasonable to expect that such clay has lost all traces of

its original microfabric structure, or the original structure was at least heavily damaged. Hence, the soil parameters of this clay samples were expected to be very different from the original parameters, and use of the intact values of c_v in Eq. 3.27 would not provide a realistic estimate of primary consolidation time. Instead, it has been decided to run reconsolidation procedure in 24 hours for all pre-strained samples. During reconsolidation in the oedometer the pore pressure measurements have shown that 24 hours was a sufficient amount of time for reconsolidation for all samples.

After completed reconsolidation at the given load step, the sample was demounted from the oedometer cell and immediately subjected to weight measurement and falling cone test while remaining in the oedometer ring. Because the mass of the ring was known, the weighing made it possible to find the wet mass of the sample after the reconsolidation and thus the amount of expelled pore water. The estimate of expelled water was, however, inaccurate to a small degree since some of the grains were remaining in the oedometer cell's bottom. The falling cone tests on reconsolidated samples have been carried out after the weighing.

To evaluate the effect of reconsolidation, change in shear strength after pre-straining and reconsolidation has been normalised to undrained shear strength, e.g.:

$$\frac{\Delta s}{s_u} = \frac{s_{re} - s_u}{s_u} \quad [\%] \quad (\text{Eq. 3.28})$$

where

Δs = change in shear strength due to the pre-straining and reconsolidation

s_u = undrained shear strength (intact material)

s_{re} = shear strength of pre-strained sample after reconsolidation

In addition, shear strength after pre-straining and reconsolidation has been normalised to reconsolidation stress (e.g., s_{re}/p'_{re} , where p'_{re} is reconsolidation stress).

After the fall cone testing of reconsolidated sample, the oedometer ring was removed and the sample was put into the bowl. The bottom of oedometer cell as well as oedometer ring and filters were cleaned with water. The water from cleaning process was collected in the bowl containing the reconsolidated sample so the dry weight could be measured as accurate as possible. The bowl with sample and collected water has been dried in oven for 24 hours or more before the dry weight was reported. From sample's dry weight, water content prior to and after reconsolidation has been determined. The change in water content due to the reconsolidation was calculated as:

$$\Delta w = w_{re} - w \quad [\%] \quad (\text{Eq. 3.29})$$

where

Δw = change in water content due to the reconsolidation

w = water content prior to reconsolidation

w_{re} = water content after reconsolidation

The volume change due to the reconsolidation at different stress levels was calculated from deformation in the end of each reconsolidation procedure. Since the area of test specimen is constant in the oedometer, volumetric strain at the end of reconsolidation is simply equal to the vertical strain.

3.11 Oedometer Test

3.11.1 Purpose

The purpose of oedometer test is to evaluate the compressibility characteristics of undisturbed, pre-strained and remoulded test samples. For undisturbed specimens, the oedometer test is also used to determine preconsolidation stress p'_c .

3.11.2 Test Equipment

The oedometer cell consists of:

- Oedometer ring of steel with build-in area of 20 cm^2 (diameter $\sim 54 \text{ mm}$) and height 20 mm .
- Top- and bottom porous filters.
- Top cap.
- Pore pressure gauge in the cell's bottom.
- Piston/jack for applying load/deformation on the specimen during the test.
- Gauges for stress/deformation measurements.

Figure 3.11.1 shows typical oedometer cell.

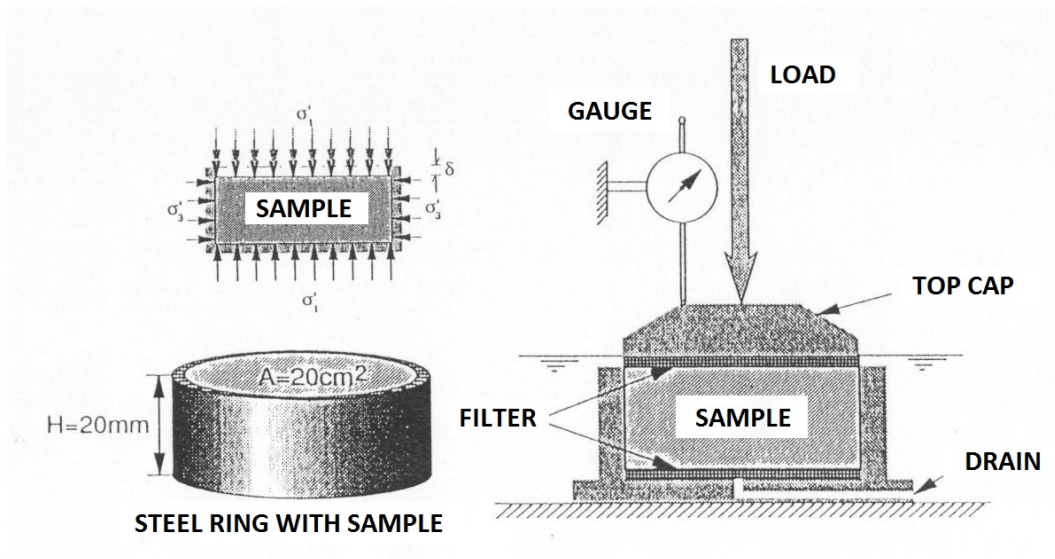


Figure 3.11.1: Cross-section of typical oedometer cell.

The oedometer and the oedometer software used in this study have been developed and built at Geotechnical Division, NTNU. The device is shown in Figure 3.11.2.

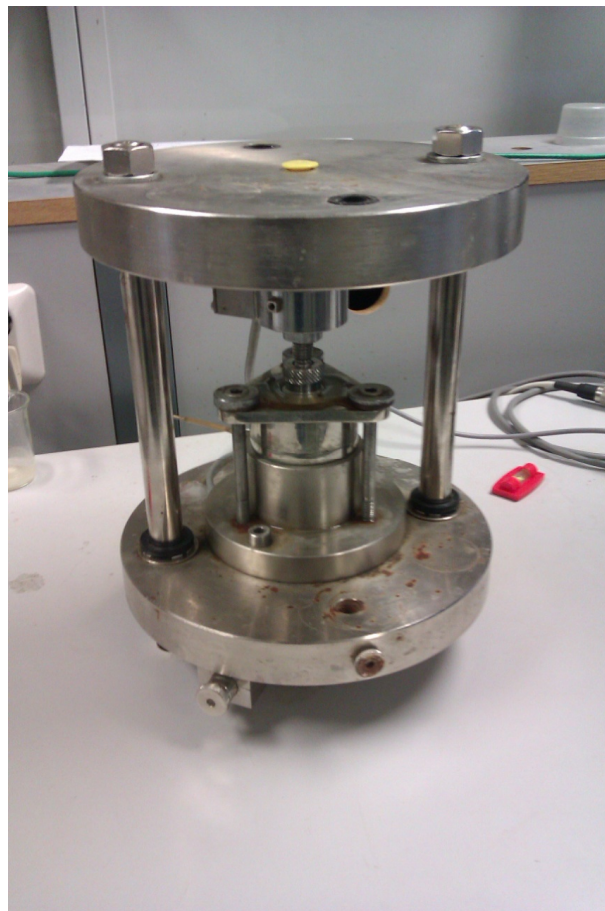


Figure 3.11.2: Oedometer device developed and built at Geotechnical Division, NTNU.

3.11.3 Test Procedure

The oedometer device is capable to execute both IL and CRS oedometer test. In this study it has been decided to use CRS tests. This decision has been made due to the fact that beside of the compressibility parameters of intact and pre-strained clay specimens, the preconsolidation stress p'_c for intact clay specimens should also be verified. The preconsolidation stress may then used to evaluate overconsolidation ratio (OCR) for the intact clay. Although the existing academic literature gives an idea of OCR at Tiller site, the information about OCR is fairly limited for Stjørdal.

Choice of IL oedometer test on intact samples would require several smaller load steps around the expected preconsolidation stress so that the p'_c value could be determined accurately. This, in turn, could be a time-consuming procedure. Instead, CRS procedure was chosen.

Post-processing of the oedometer test results was another reason for selecting continuous loading procedure instead of IL procedure. Post-processing the results from IL procedure is more time-consuming than CRS procedure. On the other hand, an advantage of IL procedure is a possible assessment of creep effects. However, an assessment of creep effects was not a part of this thesis not only due to the longitudinal limitations, but also because more fundamental understanding of the effects of pre-straining is required at the current stage of research programme. This has made CRS procedure to a suitable choice which is able to provide the data relevant for this study, at appropriate time frame.

The preparations for the test were done after standard procedure. The filters were cleaned and deaired. The oedometer steel ring was weighed empty. The steel rings used in the test are standard rings for clay and silt samples, 20 mm high with build-in area of 20 cm². The clay sample was trimmed (when necessary) to easily cut the oedometer ring through the sample. The top and bottom of the clay sample in the ring were trimmed carefully, and the clay rests outside of the ring's walls were removed. Weighing of the ring containing wet specimen has been carried out prior to the installation of the specimen into oedometer cell. The deaired water was then pumped into the oedometer cell base, and the bottom filter has been carefully slid in the water-filled cell base in such way that no air bubbles were present. The sample was locked in the position, the top cap was installed and the whole cell was lifted to the load ram prior to the test start.

The samples were saturated throughout the tests by refilling water on top of the cell. The tests were performed with one-sided drain, e.g., the initial drainage distance, H , is equal to the sample's height, 20 mm.

Since the test was not run for a practical problem, it was not necessary to load the samples to high levels of stresses. For the intact clay for instance, the main objective of the loading beyond preconsolidation stress was to determine the modulus number, m . Determination of the modulus number requires only few data points above p'_c on stress-strain curve. It has been decided to run the test up to 800 kPa, which would give more than enough data points. For the remoulded and pre-strained clay specimens the same maximum load level was used so the test procedure remained the same for all specimens. The strain rate has been chosen as constant standard rate of 0.005 mm/min for all tests.

The CRS oedometer test has been run on the undisturbed, pre-strained and manually remoulded clay specimens from each cylinder. The remoulding of intact clay was carried out on a steel plate with a knife before the remoulded material was built into the oedometer ring. The process was done as quickly as possible to avoid drying of the material. A control measurement of water content for the remoulded clay specimen has always been carried out at the same time as the remoulded material was built into the oedometer ring.

For simplicity's sake, an approximation has been made in the calculations of OCR for each sample cylinder. The value of in-situ vertical effective stress (σ'_{v0}) for CRS oedometer test specimen has been set equal to the relevant value of reconsolidation stress σ'_{v0} provided in Table 3.10.1. The effect of such approximation is insignificant. Although the undisturbed CRS oedometer test specimen and the reconsolidated specimen from each cylinder were located at slightly different depths, the difference is negligible.

Based on the modulus number obtained from oedometer test, intact clay may be classified after its stiffness in normally consolidated range (Janbu, 1970). The classification chart is shown in Table 3.11.1.

The volume changes encountered by undisturbed, pre-strained and remoulded specimens at the end of each test were calculated from the deformation of each specimen. Since the diameter of the test specimen is constant throughout the oedometer test the volumetric strain is simply equal to the vertical strain at the end of the test.

Table 3.11.1: Classification of clay after modulus number (after Janbu, 1970).

Range of modulus number m	Type of clay
$m < 10$	Soft
$10 < m < 20$	Medium stiff
$m > 20$	Stiff

CHAPTER 4 Observations and Results

4.1 Introduction

The chapter describes observations and results of the test programme carried out on each cylinder. More detailed description of the test procedures can be found in Chapter 3. Comparison of the results and discussion are presented the next chapter.

Except for determination of natural water content which was carried out immediately after the sample extrusion, no special attention has been given to the chronological order of the tests in the beginning of the study. The chronological order of the tests was initially neglected since it has been assumed that the storage of pre-strained clay specimens does not affect material properties. After the extrusion of sample T1-H12 it has become clear, however, that storage of pre-strained material causes reconsolidation even in the atmospheric pressure. This observation made it reasonable to assume that the material properties of pre-strained clay may change with time and bring uncertain results in case of long term storage. Therefore, the execution of oedometer and fall cone tests on pre-strained material was given the highest priority after following extrusions.

In the following, measurements of shear strength by falling cone and water content for reconsolidated samples are included in the subchapters dealing with reconsolidation in the appropriate apparatus.

4.2 Test Results for Sample T1-H12

4.2.1 *Extrusion of the Sample*

Sample T1-H12 was extruded in the laboratory at 24.02.2015. The pre-straining was achieved by extrusion of sample from $\varnothing 72.3$ mm to $\varnothing 54$ mm, corresponding to shear strain $\gamma_s = 117$ % (refer to Chapter 3 for more details). Figure 4.2.1 shows the subdivision of the sample during extrusion.

During extrusion of the sample, about 3.5 cm distinct layering has been discovered close to the depth of 4.8 m. The layer has been discarded.

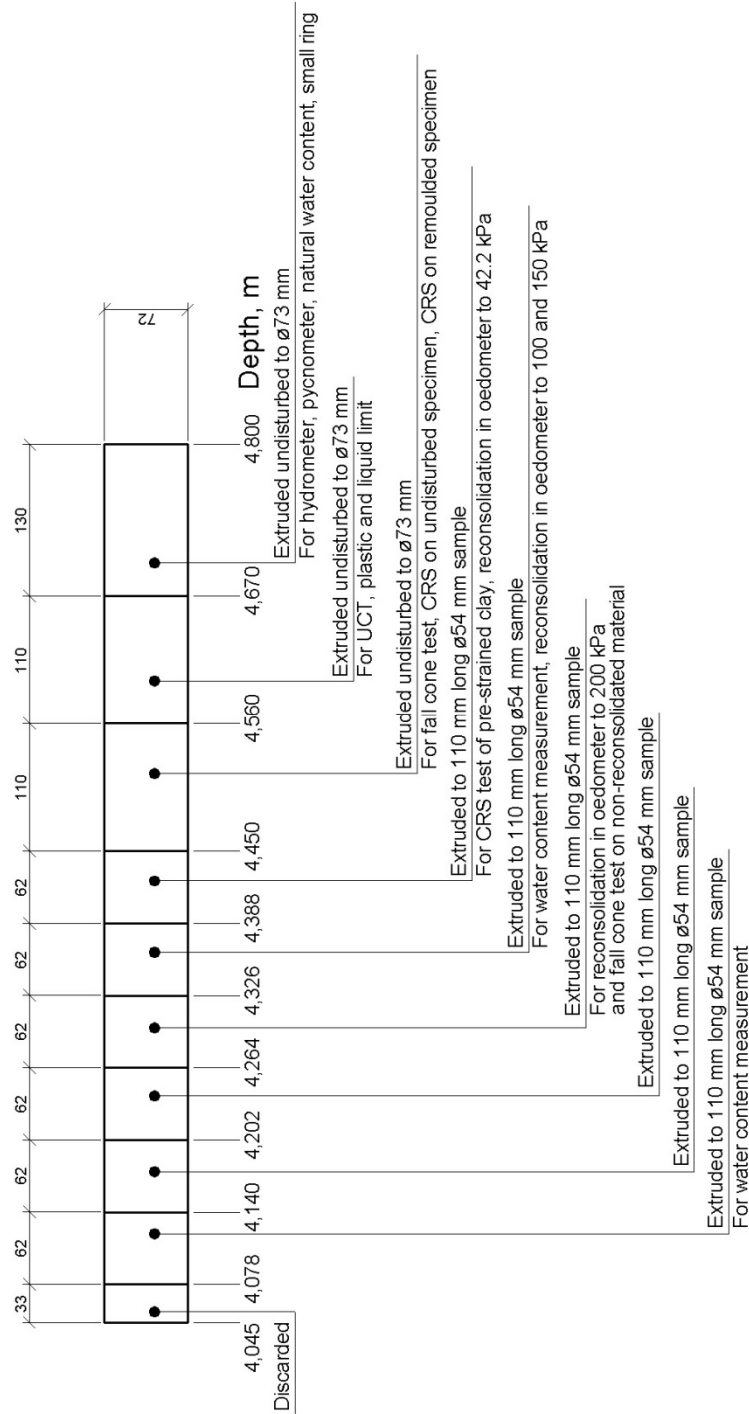


Figure 4.2.1: Sample T1-H12: Extrusion and subdivision.

Displacement ratio is given by Eq. 3.4:

$$\delta_r = \frac{11}{6.2} = 1.77 \text{ mm/mm} \tag{Eq. 4.1}$$

The theoretical displacement ratio is 1.79 mm/mm (refer to Table 3.2.2). The actual displacement ratio is lower than theoretical, indicating some strain variation in the pre-strained clay mass. However, the difference between theoretical and actual value is negligible.

The visual inspection of pre-strained samples indicated that the strains were distributed unevenly over the extruded cross-section. The uneven strain distribution was visible due to the presence of almost perfect circular rings marking the strain boundaries in the cross-section. The material pre-strained in the beginning of the extrusion process experienced more distinct variation of strains in the cross-section than what has been observed for the material pre-strained later on. The strain variation is shown in Figure 4.2.2. The clay mass shown in Figure 4.2.2 (a) has been pre-strained in the beginning of the extrusion process, and has its origin from depth 4.326-4.388 m. The clay mass shown in Figure 4.2.2 (b) has been pre-strained in the end of extrusion process, and belongs to the depth 4.078-4.140 m.



(a)



(b)

Figure 4.2.2: Variation of strains in the cross-section of pre-strained sample T1-H12: (a) Material from depth 4.326-4.388 m pre-strained in the beginning of extrusion process, (b) Material from depth 4.078-4.140 m pre-strained in the end of extrusion process.

In the beginning of the study it has been assumed that storage of the pre-strained samples does not have any impact on the material. After few days, however, it has been observed that pre-strained samples reconsolidated even in the atmospheric pressure. Figure 4.2.3 shows visible traces of dissipated pore water due to the reconsolidation in the atmospheric pressure. When reconsolidation under storage has been observed, it has also been noted that the material became remarkably softer and fell apart more easily.



Figure 4.2.3: Effects of reconsolidation of pre-strained sample T1-H12 in the atmospheric pressure.

4.2.2 Density Measurements

4.2.2.1 Average Density

Table 4.2.1 shows log of measurements made for the calculation of mean density.

Table 4.2.1: Sample T1-H12: Calculation of mean density.

Parameter	Parameter value	Units
Length of sample (L)	75.5	cm
Diameter of sample (D _i)	7.23	cm
Volume of sample (V)	3099.7	cm ³
Mass of cylinder with sample and plug	9455	gr.
Mass of cylinder and plug	3557	gr.
Mass of sample (m)	5898	gr.
Mean density ($\bar{\rho}$)	1.90	gr./cm ³
Unit weight ($\bar{\gamma} = \bar{\rho} \cdot g$)	18.66	kN/m ³

4.2.2.2 Density by Small Ring

Table 4.2.2 contains log of measurements made during calculation of density with small ring.

As seen from Table 4.2.1 and 4.2.2, there is a good agreement between calculated values of densities.

Table 4.2.2: Sample T1-H12: Calculation of density and dry density with small ring.

	Ring	Bowl	
Parameter	Parameter value	Parameter value	Units
Total wet mass	98.28	89.14	gr.
Total dry mass	80.29	71.15	gr.
Mass of ring/bowl	32.10	22.96	gr.
Mass of wet sample ($m_s + m_w$)	66.18	66.18	gr.
Mass of dry sample (m_s)	48.19	48.19	gr.
Volume (V)	35.50	35.50	cm ³
Density (ρ)	1.86	1.86	gr./cm ³
Unit weight of soil (γ)	18.25	18.25	kN/m ³
Dry density (ρ_d)	1.36	1.36	gr./cm ³

4.2.2.3 Grain Density by Pycnometer

Table 4.2.3 shows log of the measurements from pycnometer test. Grain density ρ_s is calculated from Eq. 3.9.

Table 4.2.3: Sample T1-H12: Calculation of grain density and unit weight of solids.

Parameter	Parameter value	Units
Mass of waterfilled pycnometer	148.40	gr.
Mass of pycnometer, water and specimen	154.15	gr.
Total dry mass	301.12	gr.
Mass of bowl	298.28	gr.
Dry mass of specimen (m_s)	8.84	gr.
Density of solids (ρ_s)	2.86	gr./cm ³
Unit weight of solids (γ_{solid})	28.06	kN/m ³

4.2.3 Water Content Measurements

Table 4.2.4 shows log of water content measurements. Test specimen No. 1 was undisturbed, while test specimens No. 2 and 3 were pre-strained.

There is scatter in the values of water content, indicating presence of natural variation and inhomogeneous material.

The mean value of natural water content is

$$w = \frac{33.25+38.42+29.49}{3} = 33.72 \% \quad (\text{Eq. 4.2})$$

Table 4.2.4: Sample T1-H12: Determination of water content.

	Specimen No. 1	Specimen No. 2	Specimen No. 3	
Parameter	Parameter value	Parameter value	Parameter value	Units
Depth	4.670 - 4.800	4.078 - 4.140	4.326 - 4.388	m
Total wet mass	147.74	178.82	236.79	gr.
Total dry mass	132.34	155.01	213.78	gr.
Mass of water (m_w)	15.40	23.81	23.01	gr.
Mass of bowl	86.02	93.03	135.76	gr.
Dry mass (m_s)	46.32	61.98	78.02	gr.
Water content (w)	33.25	38.42	29.49	%

4.2.4 Plastic and Liquid Limit

Table 4.2.5 shows log of plastic and liquid limit calculations.

Table 4.2.5: Sample T1-H12: Calculation of plastic and liquid limit.

	Liquid limit w_L	Plastic limit w_p	
Parameter	Parameter value	Parameter value	Units
Total wet mass	124.29	37.53	gr.
Total dry mass	114.63	36.22	gr.
Mass of water (m_w)	9.66	1.31	gr.
Mass of bowl	89.16	29.61	gr.
Dry mass (m_s)	25.47	6.61	gr.
Water content (w)	37.93	19.82	%

Liquidity and plasticity indices are found from Eq. 3.12 and 3.13, respectively:

$$I_L = \frac{w - w_p}{w_L - w_p} = \frac{33.72 - 19.82}{37.93 - 19.82} = 0.77 \quad (\text{Eq. 4.3})$$

$$I_p = w_L - w_p = 37.93 - 19.82 = 18.11 \%$$

where

w_L = liquid limit

w_p = plastic limit

w = natural water content obtained from Eq. 4.2

4.2.5 Degree of Saturation, Void Ratio and Porosity

Degree of saturation (S_r) is found from Eq. 3.14:

$$S_r = \frac{w \cdot \gamma}{\gamma_w \left(1 + w - \frac{\gamma}{\gamma_{solid}}\right)} = \frac{0.34 \cdot 18.25}{9.81 \cdot \left(1 + 0.34 - \frac{18.25}{28.06}\right)} = 0.92 \quad (\text{Eq. 4.4})$$

Void ratio (e) is found from Eq. 3.15:

$$e = \frac{\gamma_{solid} \cdot (1 + w)}{\gamma} - 1 = \frac{28.06 \cdot (1 + 0.34)}{18.25} - 1 = 1.06 \quad (\text{Eq. 4.5})$$

Porosity (n) is found from Eq. 3.16:

$$n = \left(1 - \frac{\gamma}{\gamma_{solid} \cdot (1 + w)}\right) \cdot 100 \% = \left(1 - \frac{18.25}{28.06 \cdot (1 + 0.34)}\right) \cdot 100 \% = 51.46 \% \quad (\text{Eq. 4.6})$$

Here, the value of natural water content w is obtained from Eq. 4.2, unit weight of soil γ is obtained from Table 4.2.2 and unit weight of solids γ_{solid} is obtained from Table 4.2.3.

4.2.6 Grain Size Distribution

Table 4.2.6 shows observations made during hydrometer test.

Grain size distribution curve for sample T1-H12 is shown in Figure 4.2.4. Ratios d_{60}/d_{10} and d_{75}/d_{25} are not available of practical reasons. Maximum grain size d_{max} is 0.125 mm and average grain size d_{50} is 0.00537 mm. The clay content is approximately 35 % and silt content is approximately 60 %.

Table 4.2.6: Sample T1-H12: Observations from hydrometer test.

Total mass of dried sample (W), gr.		38.78							
Mass of dried sample (w_s) $d < 0.074$ mm, gr.		38.43							
Grain density (ρ_s), gr./cm³		2.86							
Coefficient a		95.8							
Passed time (t), min.	Temp. (T), °C	Concentration (R), gr./l	Eff. depth (Z_r), cm	Constant (K), $\sqrt{\frac{min}{cm}}$	$\sqrt{\frac{Z_r}{t}}$, $\sqrt{\frac{cm}{min}}$	Equiv. grain size (d_s), mm	Rel. weight (N) $d_s < 0.074$ mm, %	Rel. weight total sample, %	
1	21.1	35.1	6.2	0.01271	2.490	0.0316	87.50	86.71	
2	21.1	33.1	6.8	0.01271	1.844	0.0234	82.51	81.77	
5	21.0	30.6	7.8	0.01273	1.249	0.0159	76.28	75.59	
10	20.9	26.6	9.4	0.01275	0.970	0.0124	66.31	65.71	
20	20.8	24.0	10.4	0.01276	0.721	0.0092	59.83	59.29	
40	20.8	22.0	11.1	0.01276	0.527	0.0067	54.84	54.35	
80	20.8	19.5	12	0.01276	0.387	0.0049	48.61	48.17	
160	20.8	17.0	13	0.01276	0.285	0.0036	42.38	42.00	
320	20.8	15.5	13.5	0.01276	0.205	0.0026	38.64	38.29	
1320	20.5	12.5	14.7	0.01280	0.106	0.0014	31.16	30.88	

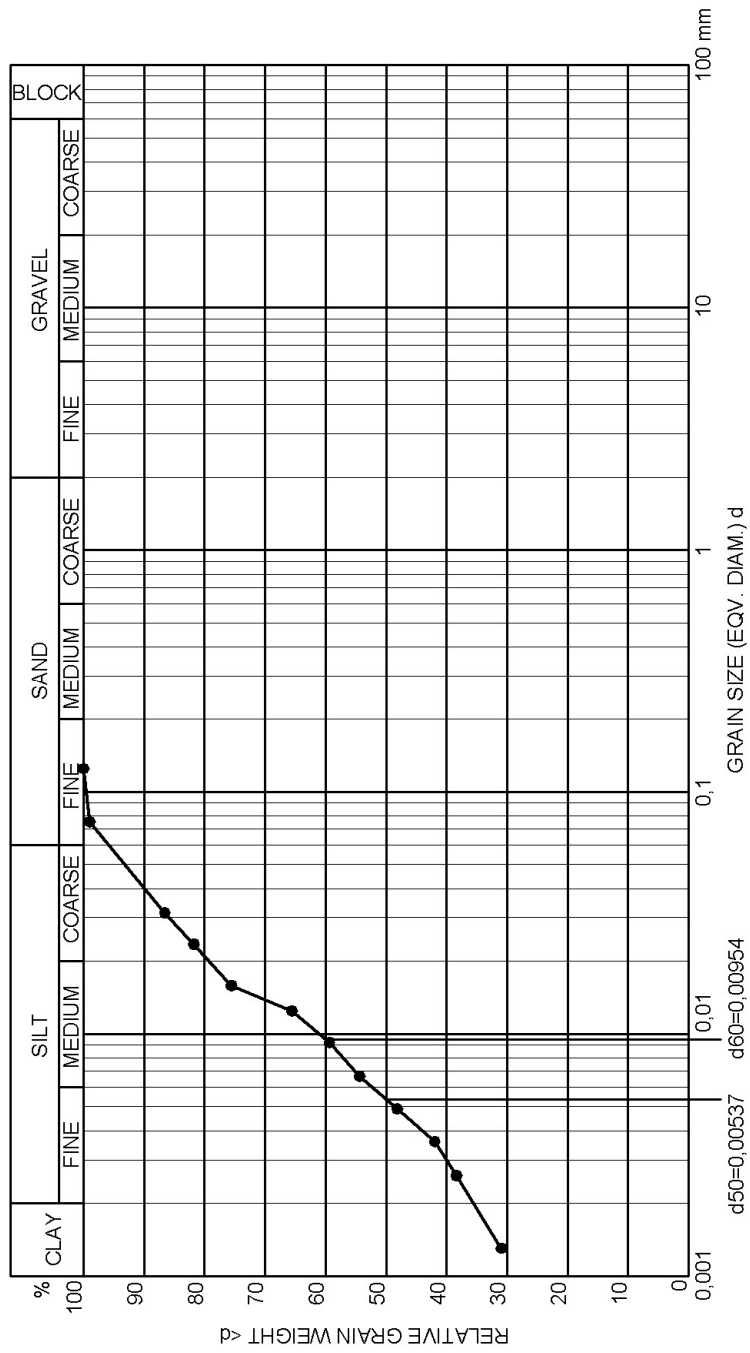


Figure 4.2.4: Sample T1-H12: Grain size distribution curve.

4.2.7 Undrained Shear Strength by UCT

Figure 4.2.5 shows deformation curve from UCT aligned with calibration chart. There is a clear failure load P_f of 12 kg (117.72 N) at failure strain ε_a of 2 %. The failure state can be described as plastic yielding, with almost constant axial stress σ_1 for increasing strain.

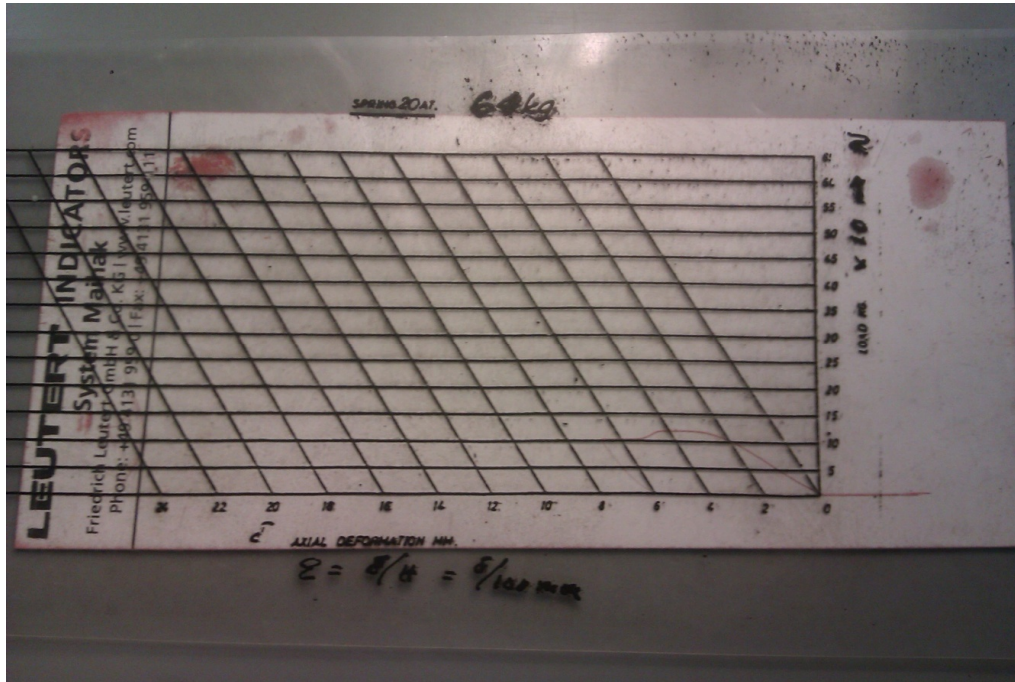


Figure 4.2.5: Sample T1-H12: Recorded deformation curve from UCT.

Undrained shear strength (s_u) is given by Eq. 3.24:

$$s_u = \tau_{max} = \frac{\sigma_1}{2} = \frac{P_f \cdot (1 - \varepsilon_a)}{2 \cdot A_0} = \frac{117.72 \cdot (1 - 0.02)}{2 \cdot 2290} = 0.0252 \text{ N/mm}^2 = 25.2 \text{ kPa} \quad (\text{Eq. 4.7})$$

Figure 4.2.6 shows the sample at failure. The angle between visible failure plane and vertical axis was measured as 35° . A sketch of the shape of sample at failure is shown in Figure 4.2.7.

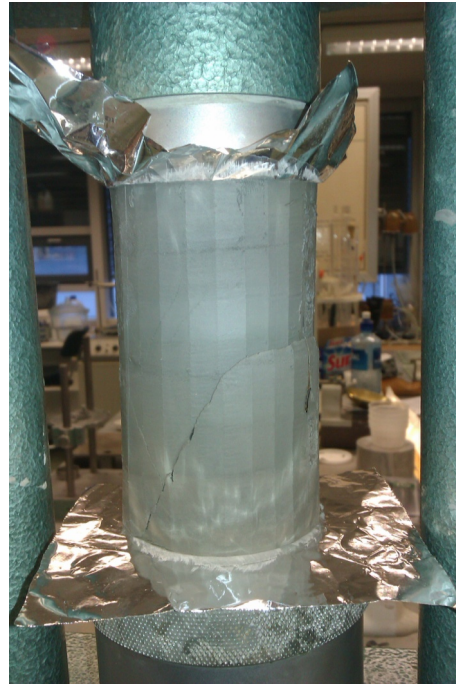


Figure 4.2.6: Sample T1-H12: Specimen at failure during UCT.

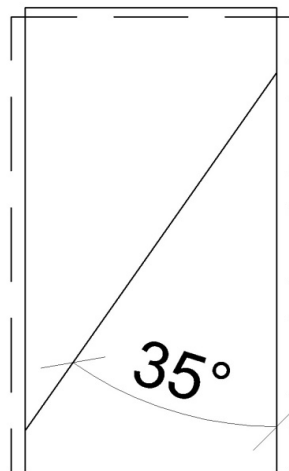


Figure 4.2.7: Sample T1-H12: Shape of specimen at failure during UCT.

4.2.8 Undrained and Remoulded Shear Strength by Fall Cone

Table 4.2.7 shows the results of falling cone test on undisturbed specimen. 100 gr. cone has been used.

Table 4.2.7: Sample T1-H12: Results of falling cone test on undisturbed clay.

Intrusion No.	Intrusion, mm	Undrained shear strength s_u , kPa	Reported (mean) s_u , kPa
1	7.1	23.5	23.7
2	7.2	22.6	
3	6.8	25.0	

As seen from Table 4.2.7, the value of undrained shear strength determined by falling cone agrees reasonably well with the value determined by UCT.

Table 4.2.8 shows the results of falling cone test on remoulded specimen. 60 gr. cone has been used.

Table 4.2.8: Sample T1-H12: Results of falling cone test on remoulded clay.

Set No.	Intrusion, mm	Remoulded shear strength s_r , kPa	Mean remoulded shear strength s_r , kPa	Reported remoulded shear strength s_r , kPa
1	11.0	2.1	2.3	2.3
	10.2	2.4		
2	10.0	2.5	2.5	
	10.0	2.5		

The sensitivity is given by Eq.3.25:

$$S_t = \frac{s_u}{s_r} = \frac{23.7}{2.3} = 10.3 \quad (\text{Eq. 4.8})$$

4.2.9 Shear Strength of Pre-Strained, Non-Reconsolidated Sample by Fall Cone

Table 4.2.9 shows test results from falling cone test on pre-strained, non-reconsolidated sample. 100 gr. cone has been used.

Table 4.2.9: Sample T1-H12: Results of falling cone test on pre-strained non-reconsolidated clay.

Intrusion No.	Intrusion, mm	Shear strength s , kPa	Reported (mean) s , kPa
1	11.4	9.1	8.7
2	11.1	9.6	
3	12.5	7.5	

4.2.10 Reconsolidation of Pre-Strained Specimen in the Oedometer at In-Situ Vertical Effective Stress 42.2 kPa

Table 4.2.10 shows data from calculation of water content for specimen prior to and after reconsolidation. Remaining pore pressure after 24 hrs. reconsolidation time was 3.5 kPa.

Table 4.2.10: Sample T1-H12: Calculation of water content prior to and after reconsolidation at in-situ vertical effective stress 42.2 kPa.

Parameter	Parameter value before reconsolidation	Parameter value after reconsolidation	Units
Mass, oedometer ring with wet specimen	114.02	110.65	gr.
Mass, oedometer ring	39.13	39.13	gr.
Mass of wet specimen	74.89	71.52	gr.
Mass of dry specimen (m_s)	54.48	54.48	gr.
Mass of water (m_w)	20.41	17.04	gr.
Water content (w and w_{re})	37.46	31.28	%

As follows from Table 4.2.10, reconsolidation at 42.2 kPa leads to change in water content:

$$\Delta w = w_{re} - w = 31.28 - 37.46 = -6.18 \% \quad (\text{Eq. 4.9})$$

where

Δw = change in water content due to the reconsolidation

w = water content prior to reconsolidation

w_{re} = water content after reconsolidation

After 24 hrs. reconsolidation at 42.2 kPa, volume of the specimen has been reduced by 8.48 %.

Table 4.2.11 shows the results of falling cone test on reconsolidated specimen. 100 gr. cone has been used in the test.

Table 4.2.11: Sample T1-H12: Results of falling cone test on pre-strained clay reconsolidated at in-situ vertical effective stress 42.2 kPa.

Intrusion No.	Intrusion, mm	Shear strength after reconsolidation s_{re} , kPa	Reported (mean) shear strength after reconsolidation s_{re} , kPa
1	4.2	49.1	47.4
2	4.2	49.1	
3	4.5	44.1	

As follows from Table 4.2.7 and 4.2.11, change in shear strength due to the pre-straining and subsequent reconsolidation at 42.2 kPa is:

$$\Delta s = s_{re} - s_u = 47.4 - 23.7 = 23.7 \text{ kPa} \quad (\text{Eq. 4.10})$$

where

Δs = change in shear strength due to the pre-straining and reconsolidation

s_u = undrained shear strength of intact material

s_{re} = shear strength of pre-strained material after reconsolidation

Normalised change in shear strength due to the pre-straining and reconsolidation is:

$$\frac{\Delta s}{s_u} = \frac{s_{re} - s_u}{s_u} \cdot 100 \% = \frac{47.4 - 23.7}{23.7} \cdot 100 \% = 100.00 \% \quad (\text{Eq. 4.11})$$

4.2.11 Reconsolidation of Pre-Strained Specimen in the Oedometer at 100 kPa

Table 4.2.12 shows data for calculation of water content in specimen prior to and after reconsolidation. Remaining pore pressure after 24 hrs. reconsolidation time was 1.2 kPa.

Table 4.2.12: Sample T1-H12: Calculation of water content prior to and after reconsolidation at 100 kPa.

Parameter	Parameter value before reconsolidation	Parameter value after reconsolidation	Units
Mass, oedometer ring with wet specimen	115.66	111.33	gr.
Mass, oedometer ring	39.18	39.18	gr.
Mass of wet specimen	76.48	72.15	gr.
Mass of dry specimen (m_s)	57.08	57.08	gr.
Mass of water (m_w)	19.40	15.07	gr.
Water content (w and w_{re})	33.99	26.40	%

As follows from Table 4.2.12, reconsolidation at 100 kPa leads to change in water content:

$$\Delta w = w_{re} - w = 26.40 - 33.99 = -7.59 \% \quad (\text{Eq. 4.12})$$

After 24 hrs. reconsolidation at 100 kPa, volume of the specimen has been reduced by 11.79 %.

Table 4.2.13 shows the results of falling cone test on reconsolidated specimen. 100 gr. cone has been used in the test.

As follows from Table 4.2.7 and 4.2.13, change in shear strength due to the pre-straining and subsequent reconsolidation at 100 kPa is:

$$\Delta s = s_{re} - s_u = 73.6 - 23.7 = 49.9 \text{ kPa} \quad (\text{Eq. 4.13})$$

Normalised change in shear strength due to the pre-straining and reconsolidation is:

$$\frac{\Delta s}{s_u} = \frac{s_{re} - s_u}{s_u} \cdot 100 \% = \frac{73.6 - 23.7}{23.7} \cdot 100 \% = 210.55 \% \quad (\text{Eq. 4.14})$$

Table 4.2.13: Sample T1-H12: Results of falling cone test on pre-strained clay reconsolidated at 100 kPa.

Intrusion No.	Intrusion, mm	Shear strength after reconsolidation s_{re} , kPa	Reported (mean) shear strength after reconsolidation s_{re} , kPa
1	3.3	66.7	73.6
2	2.9	77.0	
3	2.9	77.0	

4.2.12 Reconsolidation of Pre-Strained Specimen in the Oedometer at 150 kPa

Table 4.2.14 shows data for calculation of water content for the specimen prior to and after reconsolidation. Remaining pore pressure after 24 hrs. reconsolidation time was 0.4 kPa.

Table 4.2.14: Sample T1-H12: Calculation of water content prior to and after reconsolidation at 150 kPa.

Parameter	Parameter value before reconsolidation	Parameter value after reconsolidation	Units
Mass, oedometer ring with wet specimen	114.91	110.38	gr.
Mass, oedometer ring	38.72	38.72	gr.
Mass of wet specimen	76.19	71.66	gr.
Mass of dry specimen (m_s)	56.77	56.77	gr.
Mass of water (m_w)	19.42	14.89	gr.
Water content (w and w_{re})	34.21	26.23	%

As follows from Table 4.2.14, reconsolidation at 150 kPa leads to change in water content:

$$\Delta w = w_{re} - w = 26.23 - 34.21 = -7.98 \% \quad (\text{Eq. 4.15})$$

After 24 hrs. reconsolidation at 150 kPa, volume of the specimen has been reduced by 13.91 %.

Table 4.2.15 shows the results of falling cone test on reconsolidated specimen. 100 gr. cone has been used in the test.

Table 4.2.15: Sample T1-H12: Results of falling cone test on pre-strained clay reconsolidated at 150 kPa.

Intrusion No.	Intrusion, mm	Shear strength after reconsolidation s_{re} , kPa	Reported (mean) shear strength after reconsolidation s_{re} , kPa
1	2.3	94.7	85.5
2	3.0	74.1	
3	2.5	87.8	

As follows from Table 4.2.7 and 4.2.15, change in shear strength due to the pre-straining and subsequent reconsolidation at 150 kPa is

$$\Delta s = s_{re} - s_u = 85.5 - 23.7 = 61.8 \text{ kPa} \quad (\text{Eq. 4.16})$$

Normalised change in shear strength due to the pre-straining and reconsolidation is:

$$\frac{\Delta s}{s_u} = \frac{s_{re} - s_u}{s_u} \cdot 100 \% = \frac{85.5 - 23.7}{23.7} \cdot 100 \% = 260.76 \% \quad (\text{Eq. 4.17})$$

4.2.13 Reconsolidation of Pre-Strained Specimen in the Oedometer at 200 kPa

Table 4.2.16 shows data for calculation of water content for the specimen prior to and after reconsolidation. Remaining pore pressure after 24 hrs. reconsolidation time was 5.2 kPa.

As follows from Table 4.2.16, reconsolidation at 200 kPa leads to change in water content:

$$\Delta w = w_{re} - w = 26.54 - 35.96 = -9.42 \% \quad (\text{Eq. 4.18})$$

After 24 hrs. reconsolidation at 200 kPa, volume of the specimen has been reduced by 16.61 %.

Table 4.2.16: Sample T1-H12: Calculation of water content prior to and after reconsolidation at 200 kPa.

Parameter	Parameter value before reconsolidation	Parameter value after reconsolidation	Units
Mass, oedometer ring with wet specimen	113.64	108.35	gr.
Mass, oedometer ring	37.31	37.31	gr.
Mass of wet specimen	76.33	71.04	gr.
Mass of dry specimen (m_s)	56.14	56.14	gr.
Mass of water (m_w)	20.19	14.90	gr.
Water content (w and w_{re})	35.96	26.54	%

Table 4.2.17 shows the results of falling cone test on reconsolidated specimen. 100 gr. cone has been used in the test.

Table 4.2.17: Sample T1-H12: Results of falling cone test on pre-strained clay reconsolidated at 200 kPa.

Intrusion No.	Intrusion, mm	Shear strength after reconsolidation s_{re} , kPa	Reported (mean) shear strength after reconsolidation s_{re} , kPa
1	3.1	71.6	80.9
2	3.0	74.1	
3	2.2	97.0	

As follows from Table 4.2.7 and 4.2.17, change in shear strength due to the pre-straining and subsequent reconsolidation at 200 kPa is:

$$\Delta s = s_{re} - s_u = 80.9 - 23.7 = 57.2 \text{ kPa} \quad (\text{Eq. 4.19})$$

Normalised change in shear strength due to the pre-straining and reconsolidation is:

$$\frac{\Delta s}{s_u} = \frac{s_{re} - s_u}{s_u} \cdot 100 \% = \frac{80.9 - 23.7}{23.7} \cdot 100 \% = 241.35 \% \quad (\text{Eq. 4.20})$$

4.2.14 CRS Oedometer Test on Undisturbed Clay

Calculation of index parameters for the test specimen is given in Table 4.2.18. The value of grain density ρ_s used in the calculation is obtained from the results of pycnometer test (refer to Chapter 4.2.2).

As follows from Table 4.2.18, the calculated water content and degree of saturation for oedometer test specimen are similar to the the values calculated for the whole sample T1-H12 (refer to Chapters 4.2.3 and 4.2.5). The value of void ratio shows some deviation.

Figures 4.2.8-4.2.12 show the results of CRS oedometer test on undisturbed sample T1-H12. The presented results consist of:

- Stress vs. strain plot ($\sigma'_m - \varepsilon$), Figure 4.2.8.
- Stress vs. pore pressure at sample base ($\sigma'_m - u_b$), Figure 4.2.9.
- Stress vs. modulus plot ($\sigma'_m - M$), Figure 4.2.10 and 4.2.11.
- Stress vs. coefficient of consolidation ($\sigma'_m - c_v$), Figure 4.2.12.

As follows from the test results presented in Figure 4.2.8-4.2.12, preconsolidation stress p'_c for sample T1-H12 is approximately 180-200 kPa. Constrained moduli in the overconsolidated range (M_o) and at the preconsolidation stress (M_n) are 5 MPa and 3.7 MPa, respectively. For normally consolidated range, the modulus number (m) is 22.7.

Overconsolidation ratio for sample T1-H12 is given as

$$OCR = \frac{p'_c}{\sigma'_{v0}} = \frac{180}{42.2} = 4.3 \quad (\text{Eq. 4.21})$$

where

p'_c = preconsolidation stress

σ'_{v0} = in-situ vertical effective stress (see Table 3.10.1)

Coefficients of consolidation in the overconsolidated zone (c_{v0}) and at about p'_c (c_{vn}) are approximately 200 and 50 m^2/yr , respectively. The values of coefficient of consolidation in Figure 4.2.12 appear to be unreasonably high. A discussion on the values of c_v is given in Chapter 5.

Table 4.2.18: Sample T1-H12: Calculation of index parameters for undisturbed specimen subjected to CRS oedometer test.

Parameter	Parameter value	Units
Height of specimen (h_0)	20	mm
Area of specimen (A)	20	cm ²
Volume of specimen (V_0)	40	cm ³
Mass, oedometer ring with specimen	116.61	gr.
Mass of oedometer ring	39.25	gr.
Mass of wet specimen (m_s+m_w)	77.36	gr.
Mass of dry specimen (m_s)	58.46	gr.
Mass of water (m_w)	18.90	gr.
Water content (w)	32.33	%
Grain density (ρ_s)	2.86	gr./cm ³
Solids ($h_s = \frac{m_s}{A \cdot \rho_s}$)	1.02	cm
Void ratio ($e_0 = \frac{h_0 - h_s}{h_s}$)	0.96	-
Degree of saturation ($S_t = \frac{\rho_s \cdot w}{\rho_w \cdot e_0}$)	0.96	-

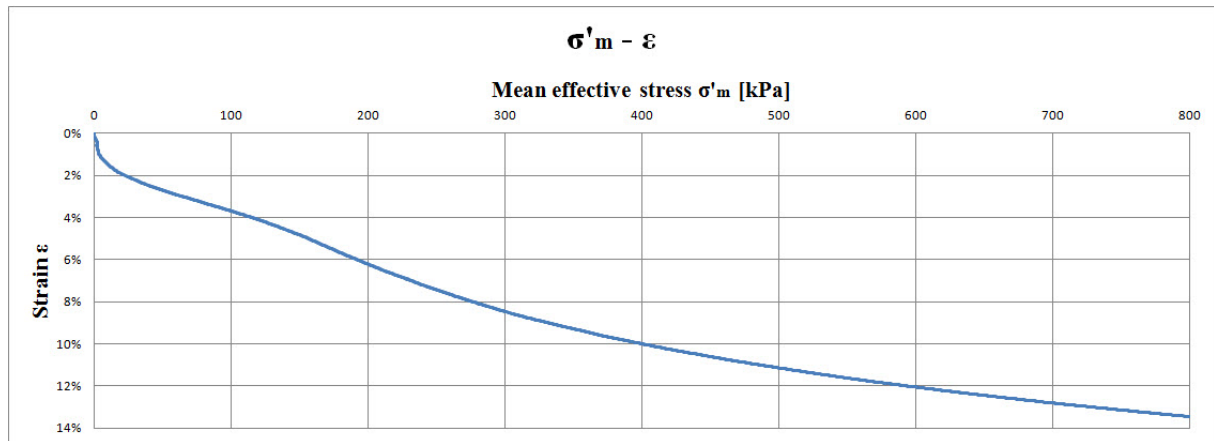


Figure 4.2.8: Sample T1-H12: Stress vs. strain from CRS oedometer test on undisturbed specimen.

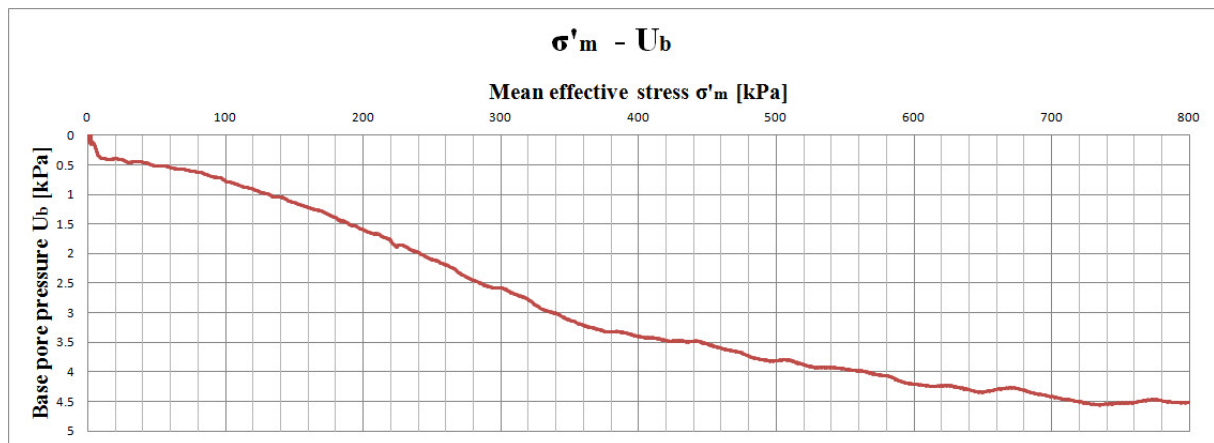


Figure 4.2.9: Sample T1-H12: Stress vs. pore pressure from CRS oedometer test on undisturbed specimen.

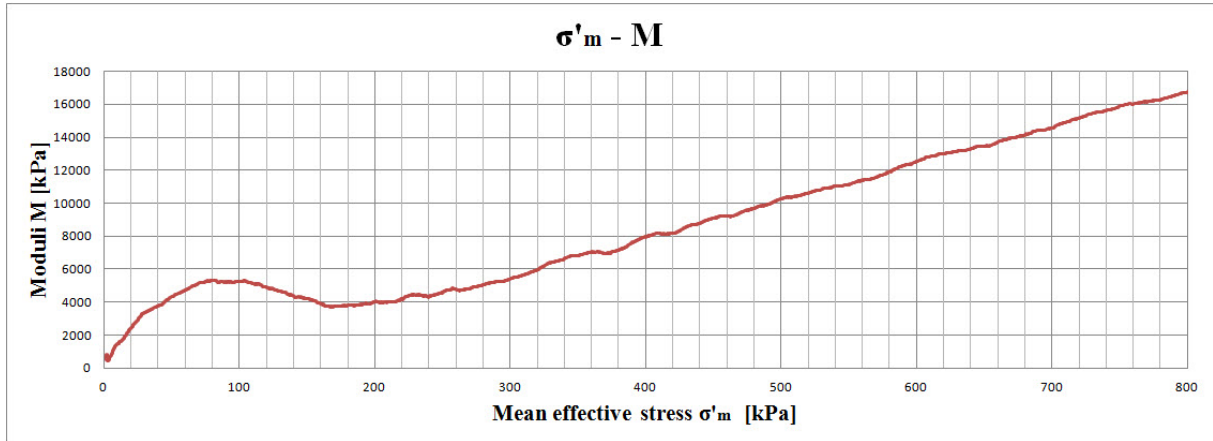


Figure 4.2.10: Sample T1-H12: Stress vs. oedometer modulus from CRS oedometer test on undisturbed specimen.

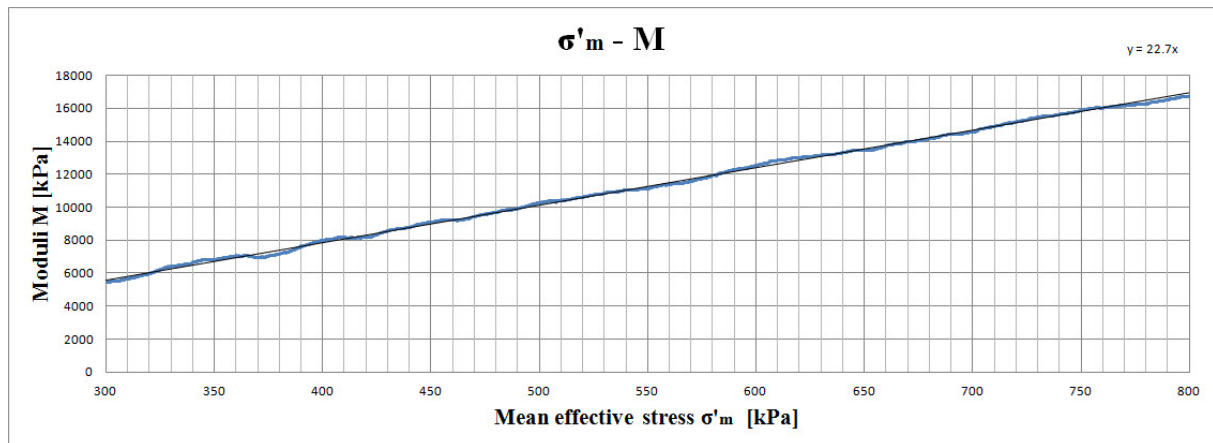


Figure 4.2.11: Sample T1-H12: Modulus number from CRS oedometer test on undisturbed specimen.

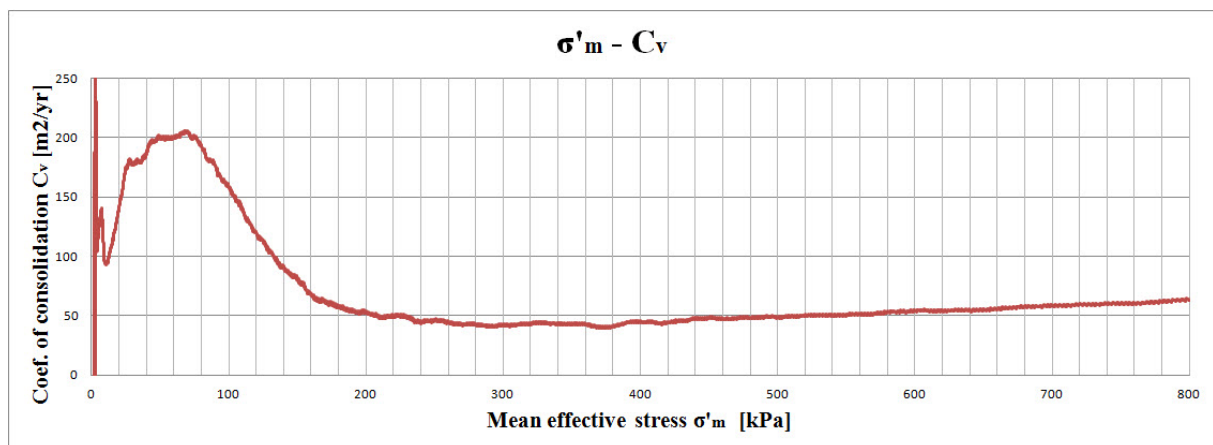


Figure 4.2.12: Sample T1-H12: Stress vs. coefficient of consolidation from CRS oedometer test on undisturbed specimen.

4.2.15 CRS Oedometer Test on Pre-Strained Clay

Calculation of water content for the test specimen is given in Table 4.2.19.

As seen from Table 4.2.19, calculated value of water content for the test specimen agrees well with water content values for the whole sample T1-H12 (refer to Chapter 4.2.3).

Figures 4.2.13-4.2.17 show the results of CRS oedometer test on sample T1-H12 pre-strained to shear strain $\gamma_s = 117\%$. The presented results consist of:

- Stress vs. strain plot ($\sigma'_m - \varepsilon$), Figure 4.2.13.
- Stress vs. pore pressure at sample base ($\sigma'_m - u_b$), Figure 4.2.14.
- Stress vs. modulus plot ($\sigma'_m - M$), Figure 4.2.15 and 4.2.16.
- Stress vs. coefficient of consolidation ($\sigma'_m - c_v$), Figure 4.2.17.

As follows from the results presented in Figure 4.2.13-4.2.17, the modulus number (m) for the specimen pre-strained to shear strain $\gamma_s = 117\%$ is constant and equal to 32.9 in the stress range of 0-580 kPa.

Table 4.2.19: Sample T1-H12: Calculation of water content for pre-strained specimen subjected to CRS oedometer test.

Parameter	Parameter value	Units
Mass, oedometer ring with specimen	115.49	gr.
Mass of oedometer ring	39.15	gr.
Mass of wet specimen ($m_s + m_w$)	76.34	gr.
Mass of dry specimen (m_s)	56.79	gr.
Mass of water (m_w)	19.55	gr.
Water content (w)	34.43	%

The results for constrained modulus and coefficient of consolidation show an inconsistency in the stress range 580-800 kPa. Also for the stresses between 34 and 37 kPa, a negligible inconsistency may be seen from all plots. The inconsistencies might have been caused by uneven strain distribution in the cross-section of the pre-strained specimen. This problem has

been encountered several times during other tests in the test programme. The effects of such uneven straining was usually easy to identify both from visual observations of the specimens after the tests as well as from stress-strain plots. Normally the tests have been repeated every time such problem has occurred. However, the oedometer test on pre-strained specimen T1-H12 has not been repeated since a sufficient amount of data points has been secured for the stresses up to 580 kPa.

Coefficient of consolidation (c_v) shows the same trend as the constrained modulus. The coefficient is evenly increasing from 0 to approximately $30 \text{ m}^2/\text{yr}$. in the stress range 0-580 kPa. The results are inconsistent for the stresses above 580 kPa.

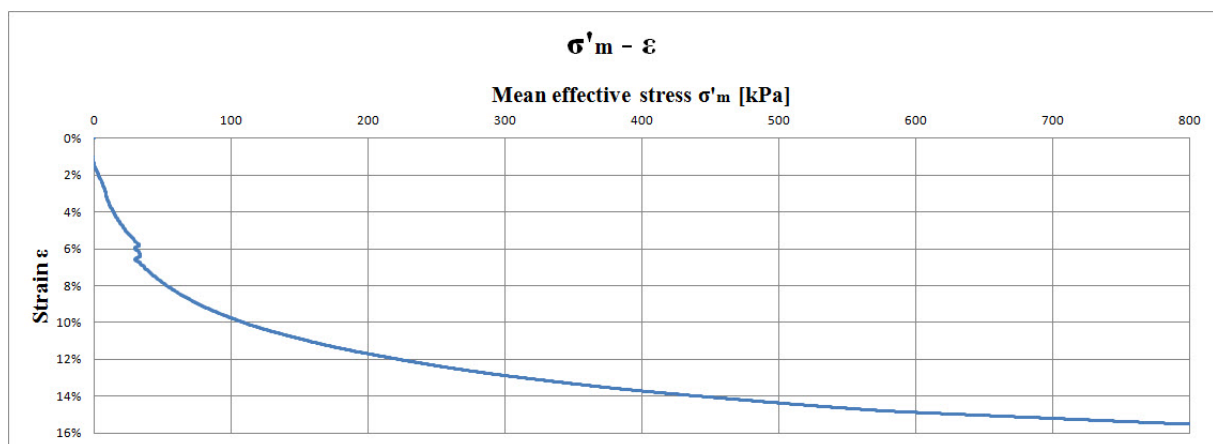


Figure 4.2.13: Sample T1-H12: Stress vs. strain from CRS oedometer test on specimen pre-strained to $\gamma_s = 117 \%$.

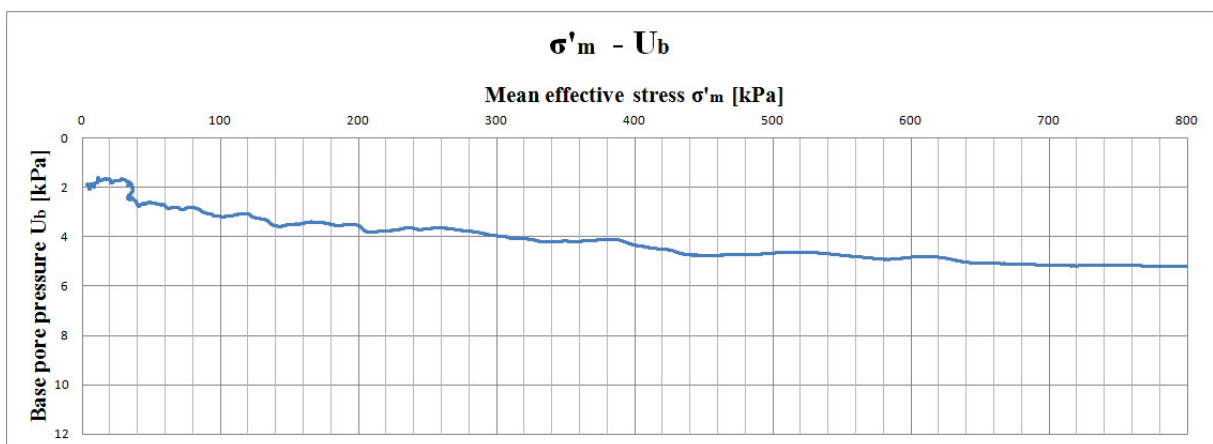


Figure 4.2.14: Sample T1-H12: Stress vs. pore pressure from CRS oedometer test on specimen pre-strained to $\gamma_s = 117 \%$.

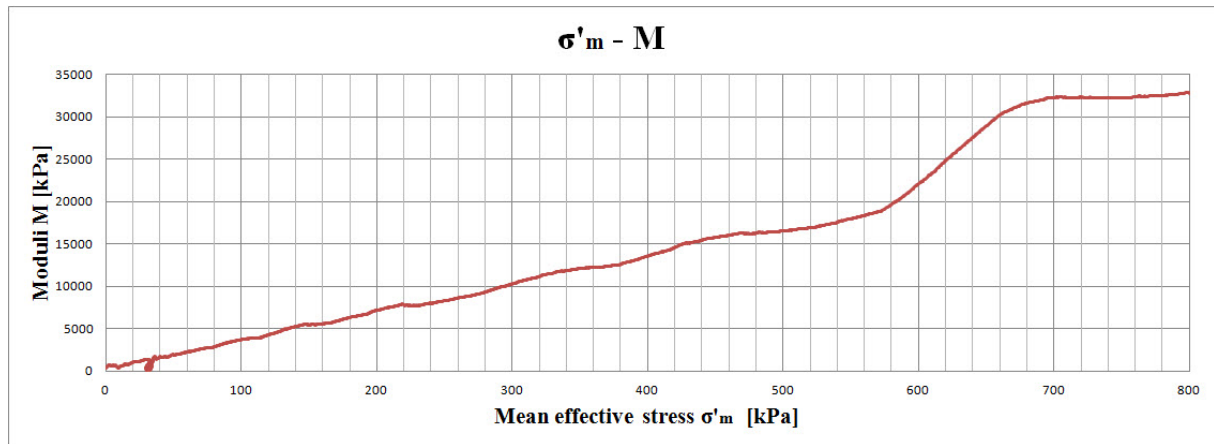


Figure 4.2.15: Sample T1-H12: Stress vs. oedometer modulus from CRS oedometer test on specimen pre-strained to $\gamma_s = 117\%$.

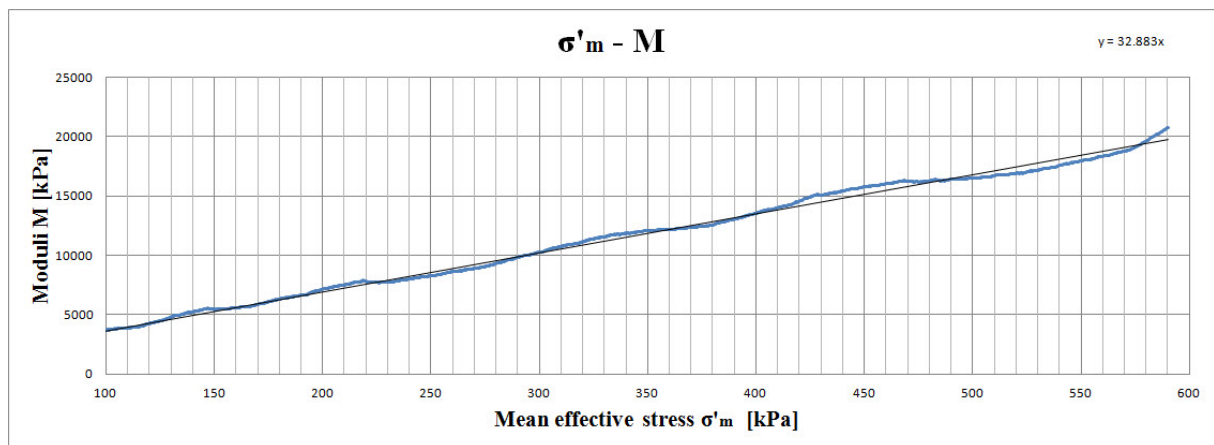


Figure 4.2.16: Sample T1-H12: Modulus number from CRS oedometer test on specimen pre-strained to $\gamma_s = 117\%$.

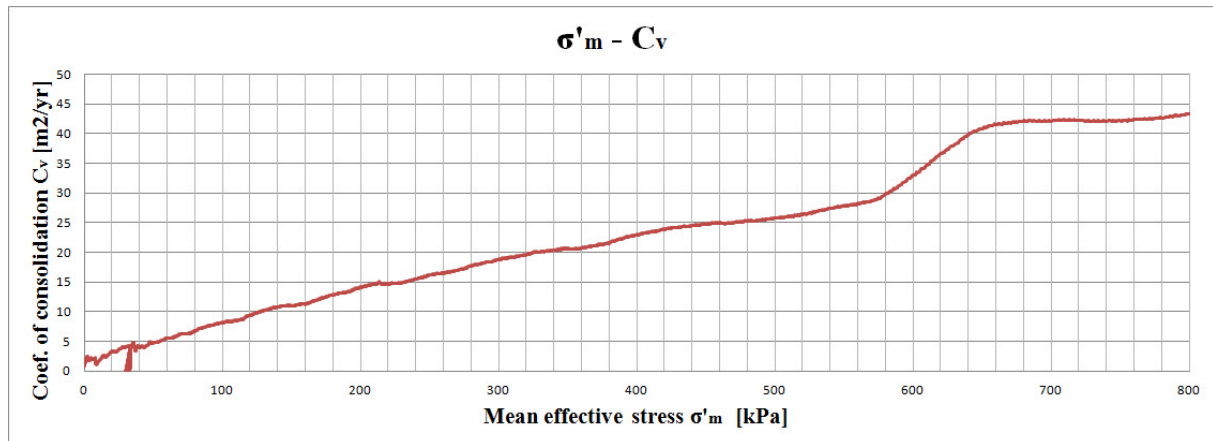


Figure 4.2.17: Sample T1-H12: Stress vs. coefficient of consolidation from CRS oedometer test on specimen pre-strained to $\gamma_s = 117\%$.

4.2.16 CRS Oedometer Test on Remoulded Clay

Calculation of water content for the test specimen is given in Table 4.2.20.

As follows from Table 4.2.20, the value of water content for remoulded clay specimen agrees reasonably well with the values calculated for the whole sample T1-H12 (refer to Chapter 4.2.3). An additional control measurement of water content has been done for the remoulded clay mass at the same time as the remoulded specimen was built into the oedometer. The control measurement showed water content $w = 29.49\%$.

Table 4.2.20: Sample T1-H12: Calculation of water content for remoulded specimen subjected to CRS oedometer test.

Parameter	Parameter value	Units
Mass, oedometer ring with specimen	116.19	gr.
Mass of oedometer ring	39.25	gr.
Mass of wet specimen (m_s+m_w)	76.94	gr.
Mass of dry specimen (m_s)	58.69	gr.
Mass of water (m_w)	18.25	gr.
Water content (w)	31.10	%

Figures 4.2.18-4.2.21 show the results of CRS oedometer test on totally remoulded clay sample T1-H12. The presented results consist of:

- Stress vs. strain plot ($\sigma'_m - \epsilon$), Figure 4.2.18.
- Stress vs. pore pressure at sample base ($\sigma'_m - u_b$), Figure 4.2.19.
- Stress vs. modulus plot ($\sigma'_m - M$), Figure 4.2.20.
- Stress vs. coefficient of consolidation ($\sigma'_m - c_v$), Figure 4.2.21.

As follows from the results presented in Figure 4.2.18-4.2.21, the modulus number (m) for the remoulded specimen is constant and equal to 34.3. Coefficient of consolidation (c_v) is increasing non-linearly with the stress level and is reaching its maximum of 26 $m^2/yr.$ at 800 kPa.

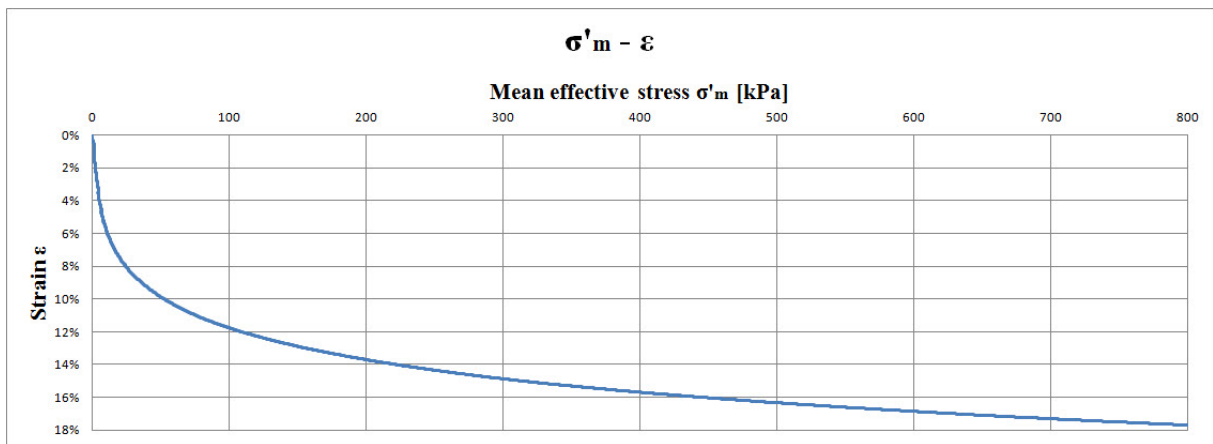


Figure 4.2.18: Sample T1-H12: Stress vs. strain from CRS oedometer test on remoulded specimen.

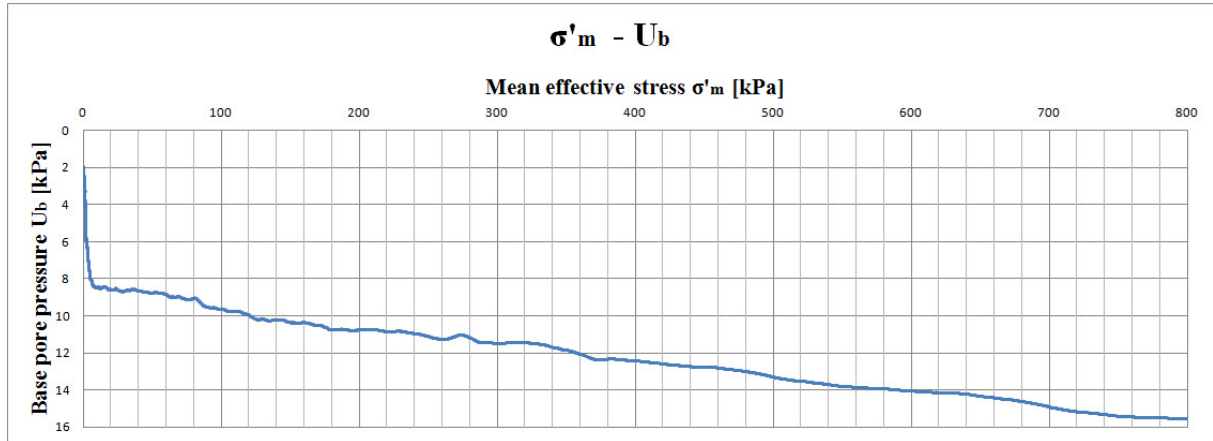


Figure 4.2.19: Sample T1-H12: Stress vs. pore pressure from CRS oedometer test on remoulded specimen.

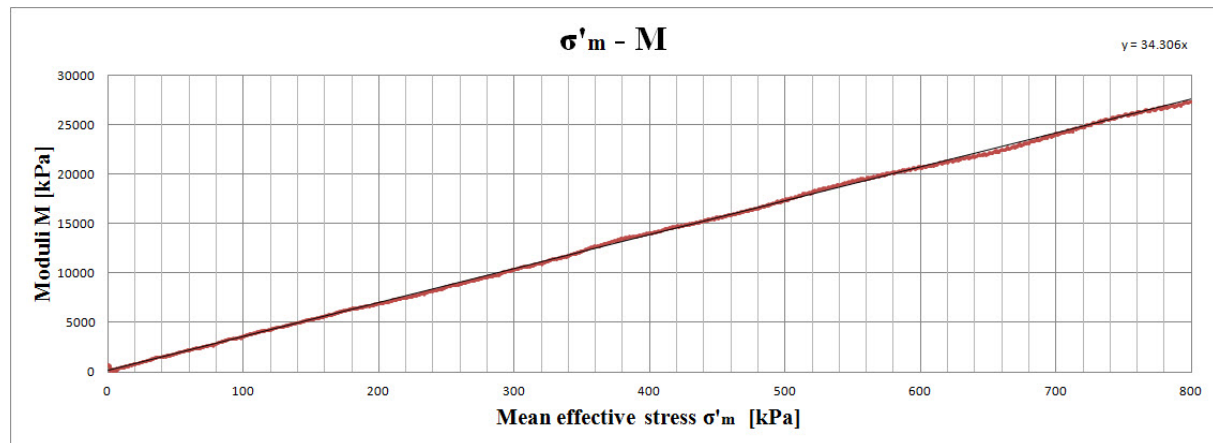


Figure 4.2.20: Sample T1-H12: Stress vs. oedometer modulus from CRS oedometer test on remoulded specimen.

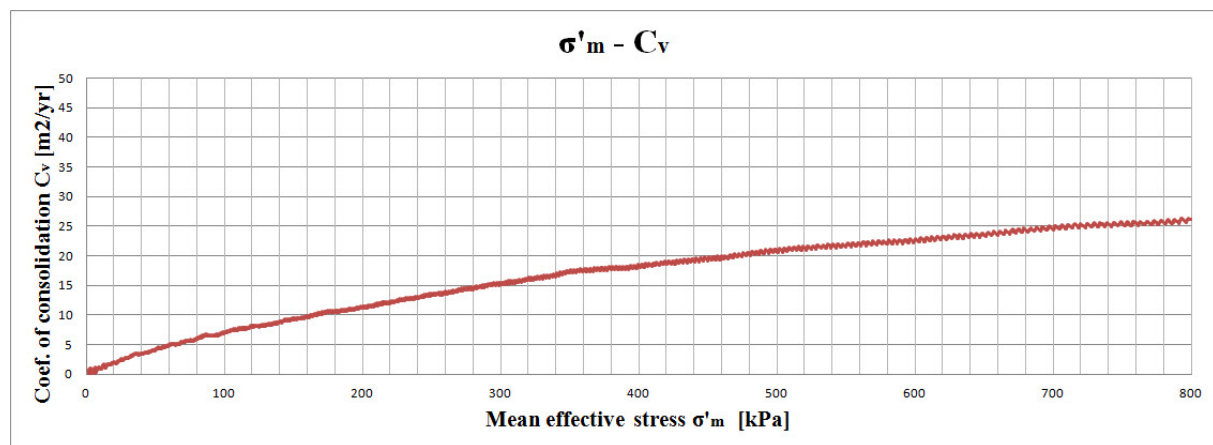


Figure 4.2.21: Sample T1-H12: Stress vs. coefficient of consolidation from CRS oedometer test on remoulded specimen.

4.3 Test Results for Sample T2-H15

4.3.1 Extrusion of the Sample

Sample T2-H15 was extruded in the laboratory at 23.03.2015. The pre-straining was achieved by extrusion of sample from $\varnothing 72.3$ mm to $\varnothing 60$ mm, corresponding to shear strain $\gamma_s = 66$ % (refer to Chapter 3 for more details). Figure 4.3.1 shows subdivision of the sample during extrusion.

During the pre-straining, it has been observed that the first parts of pre-strained material had similarly distinct strain variations in its cross-section as in the sample T1-H12.

Displacement ratio is given by Eq. 3.4:

$$\delta_r = \frac{11}{7.6} = 1.45 \text{ mm/mm} \quad (\text{Eq. 4.22})$$

The observed displacement ratio is equal to the theoretical displacement ratio (1.45 mm/mm) shown in Table 3.2.2.

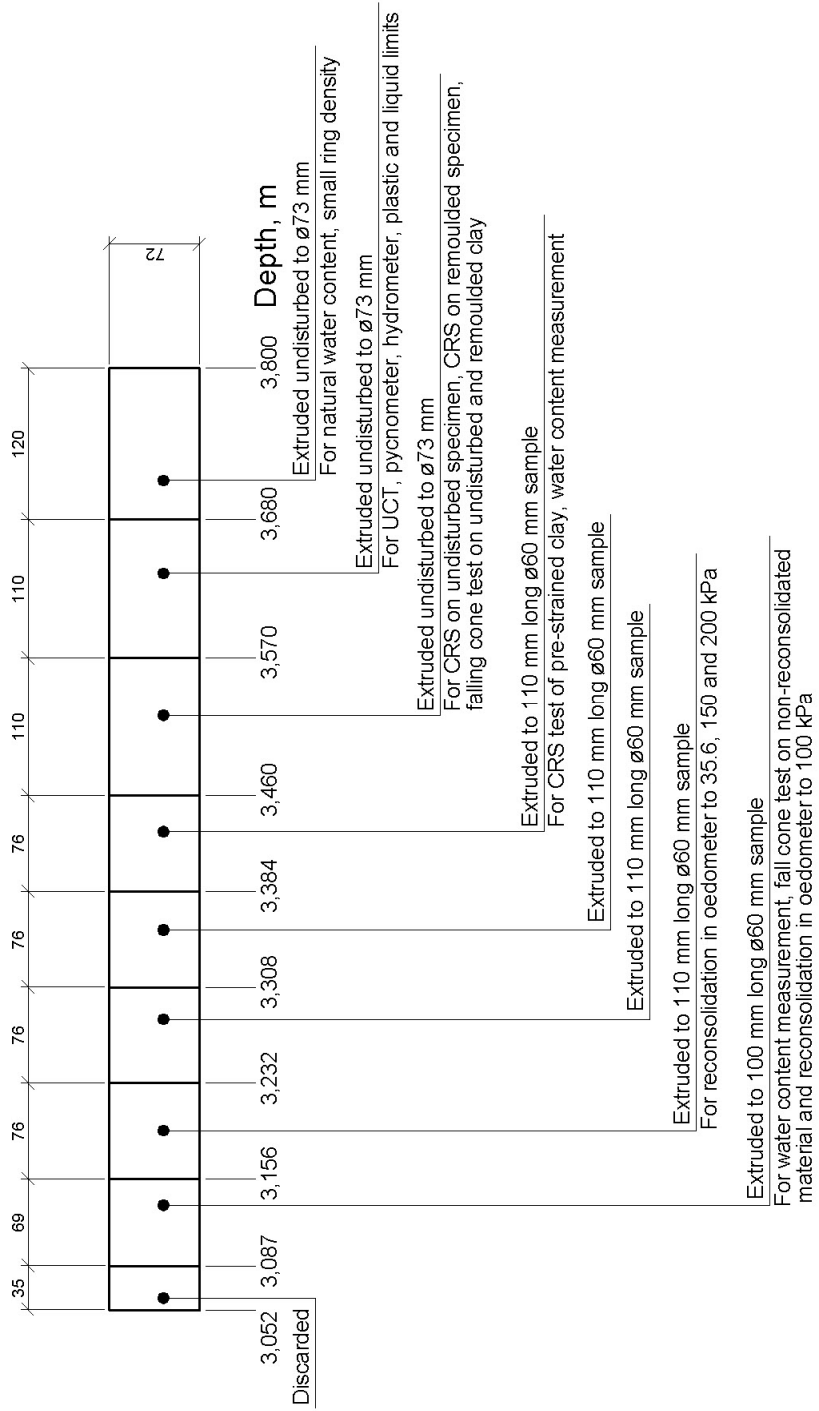


Figure 4.3.1: Sample T2-H15: Extrusion and subdivision.

4.3.2 Density Measurements

4.3.2.1 Average Density

Table 4.3.1 shows log of measurements made during calculation of mean density.

Table 4.3.1: Sample T2-H15: Calculation of mean density.

Parameter	Parameter value	Units
Length of sample (L)	74.8	cm
Diameter of sample (D _i)	7.23	cm
Volume of sample (V)	3070.9	cm ³
Mass of cylinder with sample and plug	9659	gr.
Mass of cylinder and plug	3564	gr.
Mass of sample (m)	6095	gr.
Mean density ($\bar{\rho}$)	1.98	gr./cm ³
Unit weight ($\bar{\gamma} = \bar{\rho} \cdot g$)	19.42	kN/m ³

4.3.2.2 Density by Small Ring

Table 4.3.2 contains log of measurements made for the calculation of density with small ring.

Table 4.3.2: Sample T2-H15: Calculation of density and dry density with small ring.

	Ring	Bowl	
Parameter	Parameter value	Parameter value	Units
Total wet mass	102.23	222.49	gr.
Total dry mass	85.81	206.07	gr.
Mass of ring/bowl	32.10	152.36	gr.
Mass of wet sample ($m_s + m_w$)	70.13	70.13	gr.
Mass of dry sample (m_s)	53.71	53.71	gr.
Volume (V)	35.50	35.50	cm ³
Density (ρ)	1.98	1.98	gr./cm ³
Unit weight of soil (γ)	19.42	19.42	kN/m ³
Dry density (ρ_d)	1.51	1.51	gr./cm ³

As seen from Table 4.3.1 and 4.3.2, there is a very good agreement between the calculated values of densities.

4.3.2.3 Grain Density by Pycnometer

Table 4.3.3 shows log of the measurements from pycnometer test. Grain density ρ_s is calculated from Eq. 3.9.

Table 4.3.3: Sample T2-H15: Calculation of grain density and unit weight of solids.

Parameter	Parameter value	Units
Mass of waterfilled pycnometer	148.47	gr.
Mass of pycnometer, water and specimen	157.39	gr.
Total dry mass	314.93	gr.
Mass of bowl	301.01	gr.
Dry mass of specimen (m_s)	13.92	gr.
Density of solids (ρ_s)	2.78	gr./cm ³
Unit weight of solids (γ_{solid})	27.27	kN/m ³

4.3.3 Water Content Measurements

Table 4.3.4 shows log of water content measurements. Test specimen No. 1 was undisturbed, while test specimens No. 2 and 3 were pre-strained.

As Table 4.3.4 shows, measurements of water content are consistent. The mean value of natural water content is

$$w = \frac{27.80+28.34+27.03}{3} = 27.72 \% \quad (\text{Eq. 4.23})$$

Table 4.3.4: Sample T2-H15: Determination of water content.

	Specimen No. 1	Specimen No. 2	Specimen No. 3	
Parameter	Parameter value	Parameter value	Parameter value	Units
Depth	3.680 - 3.800	3.087 - 3.156	3.384 - 3.460	m
Total wet mass	130.86	81.01	102.45	gr.
Total dry mass	112.22	73.96	90.94	gr.
Mass of water (m_w)	18.64	7.05	11.51	gr.
Mass of bowl	45.18	49.08	48.36	gr.
Dry mass (m_s)	67.04	24.88	42.58	gr.
Water content (w)	27.80	28.34	27.03	%

4.3.4 Plastic and Liquid Limit

Table 4.3.5 shows log of plastic and liquid limit measurements.

Liquidity and plasticity indices are found from Eq. 3.12 and 3.13, respectively:

$$I_L = \frac{w - w_p}{w_L - w_p} = \frac{27.72 - 18.83}{28.74 - 18.83} = 0.90 \quad (\text{Eq. 4.24})$$

$$I_p = w_L - w_p = 28.74 - 18.83 = 9.91 \%$$

The value of natural water content in Eq. 4.24 is obtained from Eq. 4.23.

Table 4.3.5: Sample T2-H15: Calculation of plastic and liquid limit.

	Liquid limit w_L	Plastic limit w_p	
Parameter	Parameter value	Parameter value	Units
Total wet mass	57.60	36.32	gr.
Total dry mass	50.62	35.26	gr.
Mass of water (m_w)	6.98	1.06	gr.
Mass of bowl	26.33	29.63	gr.
Dry mass (m_s)	24.29	5.63	gr.
Water content (w_L and w_p)	28.74	18.83	%

4.3.5 Degree of Saturation, Void Ratio and Porosity

Degree of saturation (S_r) is found from Eq. 3.14:

$$S_r = \frac{w \cdot \gamma}{\gamma_w \cdot \left(1 + w - \frac{\gamma}{\gamma_{solid}}\right)} = \frac{0.28 \cdot 19.42}{9.81 \cdot \left(1 + 0.28 - \frac{19.42}{27.27}\right)} = 0.98 \quad (\text{Eq. 4.25})$$

Void ratio (e) is found from Eq. 3.15:

$$e = \frac{\gamma_{solid} \cdot (1+w)}{\gamma} - 1 = \frac{27.27 \cdot (1+0.28)}{19.42} - 1 = 0.80 \quad (\text{Eq. 4.26})$$

Porosity (n) is found from Eq. 3.16:

$$n = \left(1 - \frac{\gamma}{\gamma_{solid} \cdot (1+w)}\right) \cdot 100 \% = \left(1 - \frac{19.42}{27.27 \cdot (1+0.28)}\right) \cdot 100 \% = 44.36 \% \quad (\text{Eq. 4.27})$$

Here, the value of natural water content w is obtained from Eq. 4.23, unit weight of soil γ is obtained from Table 4.3.2 and unit weight of solids γ_{solid} is obtained from Table 4.3.3.

4.3.6 Grain Size Distribution

Table 4.3.6 shows observations made during hydrometer test.

Table 4.3.6: Sample T2-H15: Observations from hydrometer test.

Total mass of dried sample (W), gr.		40.23							
Mass of dried sample (w_s) $d < 0.074$ mm, gr.		40.13							
Grain density (ρ_s), gr./cm³		2.78							
Coefficient a		97.3							
Passed time (t), min.	Temp. (T), °C	Concentration (R), gr./l	Eff. depth (Z_r), cm	Constant (K), $\sqrt{\frac{min}{cm}}$	$\sqrt{\frac{Z_r}{t}}$, $\sqrt{\frac{cm}{min}}$	Equiv. grain size (d_s), mm	Rel. weight (N) $d_s < 0.074$ mm, %	Rel. weight total sample, %	
1	21.9	35.2	6.0	0.01282	2.449	0.0314	85.35	85.14	
2	21.6	32.5	7.2	0.01285	1.897	0.0244	78.80	78.60	
5	21.6	27.5	9.0	0.01285	1.342	0.0172	66.68	66.51	
10	21.6	24.5	10.2	0.01285	1.010	0.0130	59.40	59.25	
20	21.3	21.2	11.5	0.01294	0.758	0.0098	51.40	51.27	
40	21.2	18.0	12.6	0.01295	0.561	0.0073	43.64	43.53	
80	21.3	15.5	13.7	0.01294	0.414	0.0054	37.58	37.49	
160	21.3	13.5	14.3	0.01294	0.299	0.0039	32.73	32.65	
320	21.6	12.2	14.7	0.01285	0.214	0.0027	29.58	29.51	
1320	21.1	9.5	15.8	0.01298	0.109	0.0014	23.03	22.97	

Grain size distribution curve for sample T2-H15 is shown in Figure 4.3.2. Ratio d_{60}/d_{10} is not available due to practical reasons. Ratio d_{75}/d_{25} is calculated from data in Figure 4.3.2:

$$\frac{d_{75}}{d_{25}} = \frac{0.02188}{0.00173} = 12.6$$

(Eq. 4.28)

Maximum grain size d_{max} is 0.125 mm and average grain size d_{50} is 0.00934 mm. The clay content is 26 % and silt content is approximately 70 %.

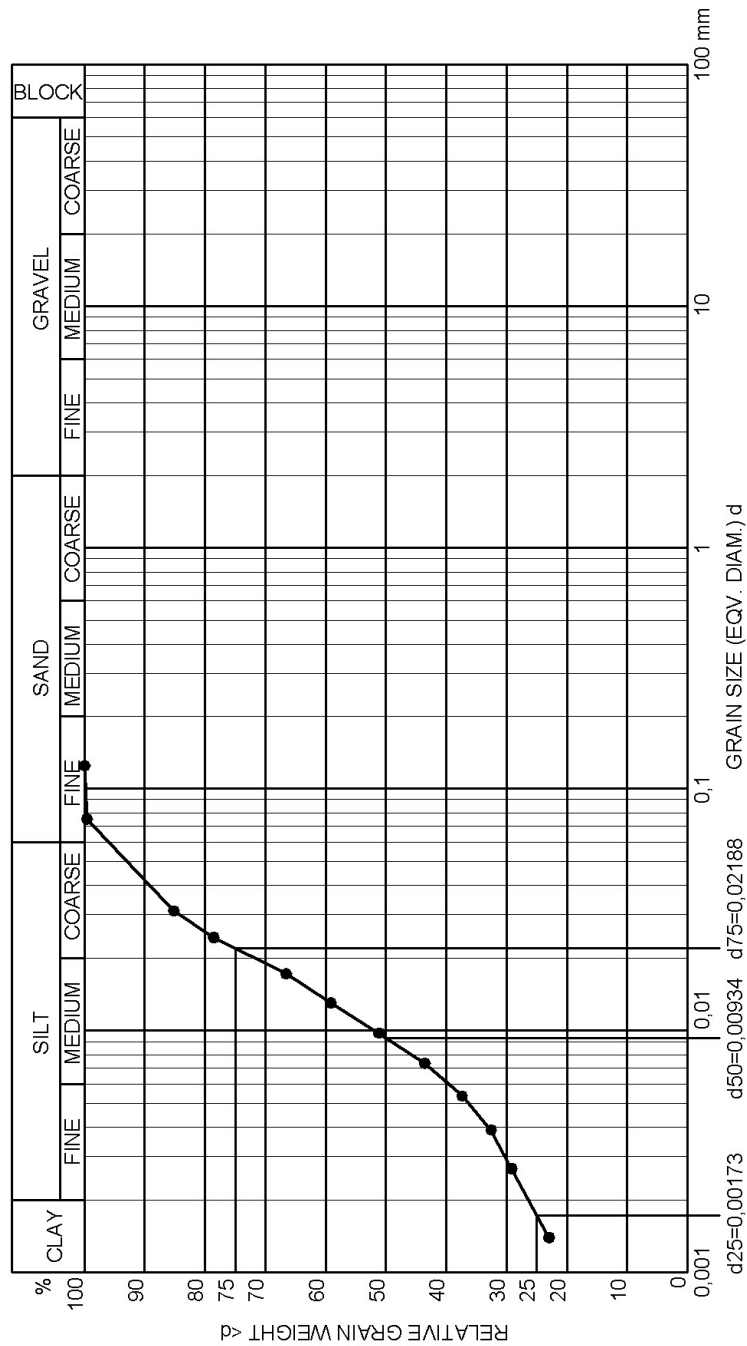


Figure 4.3.2: Sample T2-H15: Grain size distribution curve.

4.3.7 Undrained Shear Strength by UCT

Figure 4.3.3 shows deformation curve from UCT aligned with calibration chart. The sample demonstrates clearly dilatant behaviour, without any distinct failure load, yield strain or visible failure plane. The strain is increasing continuously and non-linearly with increasing load. The recorded deformation vs. load curve indicates a possible sample disturbance. However, such result may also be due to the high silt content.

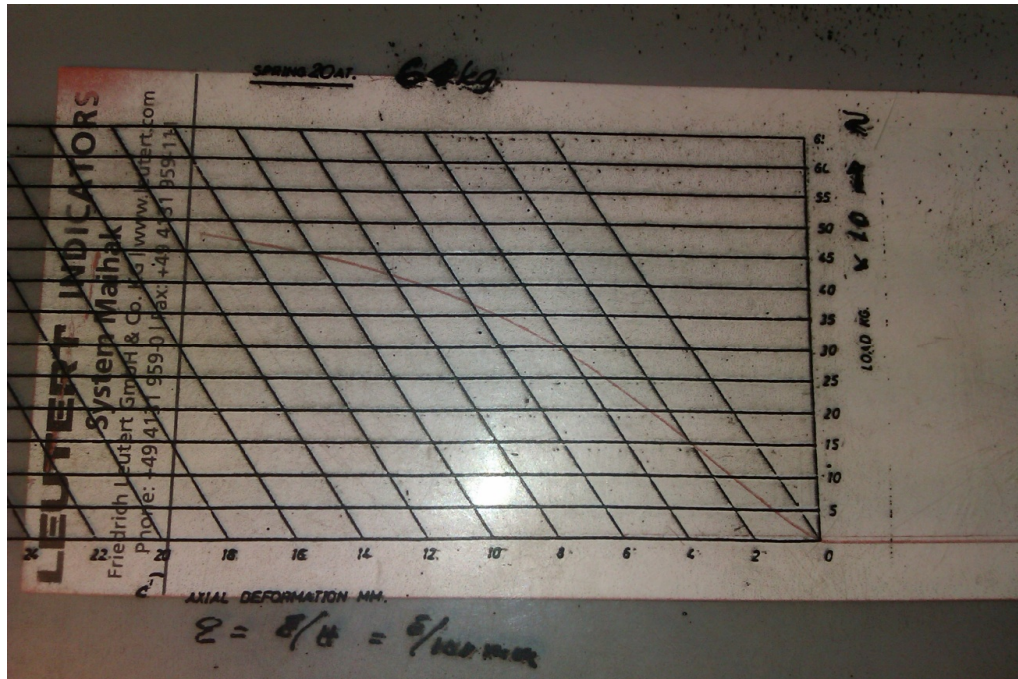


Figure 4.3.3: Sample T2-H15: Recorded deformation curve from UCT.

Since any well-defined failure load is lacking, the failure strain ϵ_a is set to 10 %. The corresponding axial load is 45 kg (441.45 N). Undrained shear strength (s_u) at $\epsilon_a = 10\%$ is given by Eq. 3.24:

$$s_u = \tau_{max} = \frac{\sigma_1}{2} = \frac{P_f \cdot (1 - \epsilon_a)}{2 \cdot A_0} = \frac{441.45 \cdot (1 - 0.10)}{2 \cdot 2290} = 0.0867 \text{ N/mm}^2 = 86.7 \text{ kPa} \quad (\text{Eq. 4.29})$$

The test result should not be considered as reliable. This is, however, not significant since the undrained shear strength is also measured by falling cone.

Figure 4.3.4 shows the sample at the end of the test. A sketch of the shape of sample at failure is shown in Figure 4.3.5.



Figure 4.3.4: Sample T2-H15: Specimen at the end of UCT.

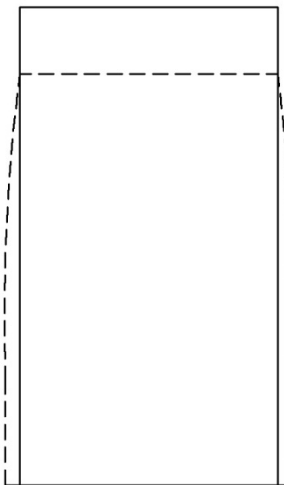


Figure 4.3.5: Sample T2-H15: Shape of specimen at the end of UCT.

4.3.8 Undrained and Remoulded Shear Strength by Fall Cone

Table 4.3.7 shows the results of falling cone test on undisturbed specimen. 100 gr. cone has been used.

Table 4.3.7: Sample T2-H15: Results of falling cone test on undisturbed clay.

Intrusion No.	Intrusion, mm	Undrained shear strength s_u , kPa	Reported (mean) s_u , kPa
1	3.2	69.2	71.0
2	2.9	77.0	
3	3.3	66.7	

Table 4.3.8 shows the results of falling cone test on remoulded specimen. 60 gr. cone has been used.

Table 4.3.8: Sample T2-H15: Results of falling cone test on remoulded clay.

Set No.	Intrusion, mm	Remoulded shear strength s_r , kPa	Mean remoulded shear strength s_r , kPa	Reported remoulded shear strength s_r , kPa
1	5.8	7.0	6.6	6.6
	6.2	6.2		
2	5.2	8.4	7.4	
	6.1	6.4		

The sensitivity is given by Eq.3.25:

$$S_t = \frac{s_u}{s_r} = \frac{71.0}{6.6} = 10.8 \quad (\text{Eq. 4.30})$$

4.3.9 Shear Strength of Pre-Strained, Non-Reconsolidated Sample by Fall Cone

Table 4.3.9 shows test results from falling cone test on pre-strained, non-reconsolidated sample. 100 gr. cone has been used.

Table 4.3.9: Sample T2-H15: Results of falling cone test on pre-strained non-reconsolidated clay.

Intrusion No.	Intrusion, mm	Shear strength s , kPa	Reported (mean) s , kPa
1	7.1	23.5	20.4
2	7.9	19.1	
3	8.0	18.6	

4.3.10 Reconsolidation of Pre-Strained Specimen in the Oedometer at In-Situ Vertical Effective Stress 35.6 kPa

Table 4.3.10 shows data for calculation of water content in specimen prior to and after reconsolidation. Remaining pore pressure after 24 hrs. reconsolidation time was 0.6 kPa.

Table 4.3.10: Sample T2-H15: Calculation of water content prior to and after reconsolidation at in-situ vertical effective stress 35.6 kPa.

Parameter	Parameter value before reconsolidation	Parameter value after reconsolidation	Units
Mass, oedometer ring with wet specimen	114.49	112.62	gr.
Mass, oedometer ring	38.64	38.64	gr.
Mass of wet specimen	75.85	73.98	gr.
Mass of dry specimen (m_s)	56.35	56.35	gr.
Mass of water (m_w)	19.50	17.63	gr.
Water content (w and w_{re})	34.61	31.29	%

As follows from Table 4.3.10, reconsolidation at 35.6 kPa leads to change in water content:

$$\Delta w = w_{re} - w = 31.29 - 34.61 = -3.32 \% \quad (\text{Eq. 4.31})$$

After 24 hrs. reconsolidation at 35.6 kPa, volume of the specimen has been reduced by 6.67 %.

Table 4.3.11 shows the results of falling cone test on reconsolidated specimen. 100 gr. cone has been used in the test.

Table 4.3.11: Sample T2-H15: Results of falling cone test on pre-strained clay reconsolidated at in-situ vertical effective stress 35.6 kPa.

Intrusion No.	Intrusion, mm	Shear strength after reconsolidation s_{re} , kPa	Reported (mean) shear strength after reconsolidation s_{re} , kPa
1	5.8	31.9	35.8
2	5.2	36.8	
3	5.0	38.7	

As follows from Table 4.3.7 and 4.3.11, change in shear strength due to the pre-straining and subsequent reconsolidation at 35.6 kPa is:

$$\Delta s = s_{re} - s_u = 35.8 - 71.0 = -35.2 \text{ kPa} \quad (\text{Eq. 4.32})$$

Normalised change in shear strength due to the pre-straining and reconsolidation is:

$$\frac{\Delta s}{s_u} = \frac{s_{re} - s_u}{s_u} \cdot 100 \% = \frac{35.8 - 71.0}{71.0} \cdot 100 \% = -49.58 \% \quad (\text{Eq. 4.33})$$

4.3.11 Reconsolidation of Pre-Strained Specimen in the Oedometer at 100 kPa

Table 4.3.12 shows data for calculation of water content in specimen prior to and after reconsolidation. Remaining pore pressure after 24 hrs. reconsolidation time was 1.7 kPa.

As follows from Table 4.3.12, reconsolidation at 100 kPa leads to change in water content:

$$\Delta w = w_{re} - w = 22.20 - 26.61 = -4.41 \% \quad (\text{Eq. 4.34})$$

After 24 hrs. reconsolidation at 100 kPa, volume of the specimen has been reduced by 7.17 %.

Table 4.3.12: Sample T2-H15: Calculation of water content prior to and after reconsolidation at 100 kPa.

Parameter	Parameter value before reconsolidation	Parameter value after reconsolidation	Units
Mass, oedometer ring with wet specimen	120.01	117.20	gr.
Mass, oedometer ring	39.26	39.26	gr.
Mass of wet specimen	80.75	77.94	gr.
Mass of dry specimen (m_s)	63.78	63.78	gr.
Mass of water (m_w)	16.97	14.16	gr.
Water content (w and w_{re})	26.61	22.20	%

Table 4.3.13 shows the results of falling cone test on reconsolidated specimen. 100 gr. cone has been used in the test.

Table 4.3.13: Sample T2-H15: Results of falling cone test on pre-strained clay reconsolidated at 100 kPa.

Intrusion No.	Intrusion, mm	Shear strength after reconsolidation s_{re} , kPa	Reported (mean) shear strength after reconsolidation s_{re} , kPa
1	2.2	97.0	103.3
2	1.8	108.0	
3	1.9	105.0	

As follows from Table 4.3.7 and 4.3.13, change in shear strength due to the pre-straining and subsequent reconsolidation at 100 kPa is:

$$\Delta s = s_{re} - s_u = 103.3 - 71.0 = 32.3 \text{ kPa} \quad (\text{Eq. 4.35})$$

Normalised change in shear strength due to the pre-straining and reconsolidation is:

$$\frac{\Delta s}{s_u} = \frac{s_{re} - s_u}{s_u} \cdot 100 \% = \frac{103.3 - 71.0}{71.0} \cdot 100 \% = 45.49 \% \quad (\text{Eq. 4.36})$$

4.3.12 Reconsolidation of Pre-Strained Specimen in the Oedometer at 150 kPa

Table 4.3.14 shows data for calculation of water content in specimen prior to and after reconsolidation. Remaining pore pressure after 24 hrs. reconsolidation time was 4.3 kPa.

Table 4.3.14: Sample T2-H15: Calculation of water content prior to and after reconsolidation at 150 kPa.

Parameter	Parameter value before reconsolidation	Parameter value after reconsolidation	Units
Mass, oedometer ring with wet specimen	116.58	113.59	gr.
Mass, oedometer ring	38.70	38.70	gr.
Mass of wet specimen	77.88	74.89	gr.
Mass of dry specimen (m_s)	59.15	59.15	gr.
Mass of water (m_w)	18.73	15.74	gr.
Water content (w and w_{re})	31.67	26.61	%

As follows from Table 4.3.14, reconsolidation at 150 kPa leads to change in water content:

$$\Delta w = w_{re} - w = 26.61 - 31.67 = -5.06 \% \quad (\text{Eq. 4.37})$$

After 24 hrs. reconsolidation at 150 kPa, volume of the specimen has been reduced by 8.14 %.

Table 4.3.15 shows the results of falling cone test on reconsolidated specimen. 100 gr. cone has been used in the test.

As follows from Table 4.3.7 and 4.3.15, change in shear strength due to the pre-straining and subsequent reconsolidation at 150 kPa is

$$\Delta s = s_{re} - s_u = 120.7 - 71.0 = 49.7 \text{ kPa} \quad (\text{Eq. 4.38})$$

Normalised change in shear strength due to the pre-straining and reconsolidation is:

$$\frac{\Delta s}{s_u} = \frac{s_{re} - s_u}{s_u} \cdot 100 \% = \frac{120.7 - 71.0}{71.0} \cdot 100 \% = 70.00 \% \quad (\text{Eq. 4.39})$$

Table 4.3.15: Sample T2-H15: Results of falling cone test on pre-strained clay reconsolidated at 150 kPa.

Intrusion No.	Intrusion, mm	Shear strength after reconsolidation s_{re} , kPa	Reported (mean) shear strength after reconsolidation s_{re} , kPa
1	1.3	123.0	120.7
2	1.5	116.0	
3	1.3	123.0	

4.3.13 Reconsolidation of Pre-Strained Specimen in the Oedometer at 200 kPa

Table 4.3.16 shows data for calculation of water content in specimen prior to and after reconsolidation. Remaining pore pressure after 24 hrs. reconsolidation time was 3.2 kPa.

Table 4.3.16: Sample T2-H15: Calculation of water content prior to and after reconsolidation at 200 kPa.

Parameter	Parameter value before reconsolidation	Parameter value after reconsolidation	Units
Mass, oedometer ring with wet specimen	116.39	113.04	gr.
Mass, oedometer ring	39.26	39.26	gr.
Mass of wet specimen	77.13	73.78	gr.
Mass of dry specimen (m_s)	57.93	57.93	gr.
Mass of water (m_w)	19.20	15.85	gr.
Water content (w and w_{re})	33.14	27.36	%

As follows from Table 4.3.16, reconsolidation at 200 kPa leads to change in water content:

$$\Delta w = w_{re} - w = 27.36 - 33.14 = -5.78 \% \quad (\text{Eq. 4.40})$$

After 24 hrs. reconsolidation at 200 kPa, volume of the specimen has been reduced by 11.37 %.

Table 4.3.17 shows the results of falling cone test on reconsolidated specimen. 100 gr. cone has been used in the test.

Table 4.3.17: Sample T2-H15: Results of falling cone test on pre-strained clay reconsolidated at 200 kPa.

Intrusion No.	Intrusion, mm	Shear strength after reconsolidation s_{re} , kPa	Reported (mean) shear strength after reconsolidation s_{re} , kPa
1	2.9	77.0	81.6
2	2.6	85.3	
3	2.7	82.4	

As follows from Table 4.3.7 and 4.3.17, change in shear strength due to the pre-straining and subsequent reconsolidation at 200 kPa is:

$$\Delta s = s_{re} - s_u = 81.6 - 71.0 = 10.6 \text{ kPa} \quad (\text{Eq. 4.41})$$

Normalised change in shear strength due to the pre-straining and reconsolidation is:

$$\frac{\Delta s}{s_u} = \frac{s_{re} - s_u}{s_u} \cdot 100 \% = \frac{81.6 - 71.0}{71.0} \cdot 100 \% = 14.93 \% \quad (\text{Eq. 4.42})$$

4.3.14 CRS Oedometer Test on Undisturbed Clay

Calculation of index parameters for the test specimen is given in Table 4.3.18. The value of grain density ρ_s used in the calculation is obtained from the results of pycnometer test (refer to Chapter 4.3.2).

As follows from Table 4.3.18, the value of degree of saturation for oedometer test specimen is similar to the the value calculated for the whole sample T2-H15 (refer to Chapters 4.3.5). There is a small deviation (3.7 %) between water content values for the oedometer specimen and for the whole sample (refer to Chapter 4.3.3). Furthermore, there is a minor deviation (Δe

= 0.07) between the values of void ratio for oedometer test specimen and for the whole sample (refer to Chapter 4.3.5 for the latter).

Table 4.3.18: Sample T2-H15: Calculation of index parameters for undisturbed specimen subjected to CRS oedometer test.

Parameter	Parameter value	Units
Height of specimen (h_0)	20	mm
Area of specimen (A)	20	cm ²
Volume of specimen (V_0)	40	cm ³
Mass, oedometer ring with specimen	117.39	gr.
Mass of oedometer ring	39.25	gr.
Mass of wet specimen (m_s+m_w)	78.14	gr.
Mass of dry specimen (m_s)	59.48	gr.
Mass of water (m_w)	18.66	gr.
Water content (w)	31.37	%
Grain density (ρ_s)	2.78	gr./cm ³
Solids ($h_s = \frac{m_s}{A \cdot \rho_s}$)	1.07	cm
Void ratio ($e_0 = \frac{(h_0-h_s)}{h_s}$)	0.87	-
Degree of saturation ($S_t = \frac{\rho_s \cdot w}{\rho_w \cdot e_0}$)	1.00	-

Figures 4.3.6-4.3.10 show the results of CRS oedometer test on undisturbed sample T2-H15.

The presented results consist of:

- Stress vs. strain plot ($\sigma'_m - \epsilon$), Figure 4.3.6.
- Stress vs. pore pressure at sample base ($\sigma'_m - u_b$), Figure 4.3.7.

- Stress vs. modulus plot ($\sigma'_m - M$), Figure 4.3.8 and 4.3.9.
- Stress vs. coefficient of consolidation ($\sigma'_m - c_v$), Figure 4.3.10.

As follows from the test results presented in Figure 4.3.6-4.3.10, preconsolidation stress p'_c for sample T2-H15 is approximately 120 kPa. Constrained moduli in the overconsolidated range (M_o) and at the preconsolidation stress (M_n) are 3 MPa and 2 MPa, respectively. For normally consolidated range, the modulus number (m) is 22.2.

Coefficients of consolidation in the overconsolidated zone (c_{vo}) and at about p'_c (c_{vn}) are 23 and 8 m^2/yr , respectively.

Overconsolidation ratio for sample T2-H15 is given as

$$OCR = \frac{p'_c}{\sigma'_{v0}} = \frac{120}{35.6} = 3.4 \tag{Eq. 4.43}$$

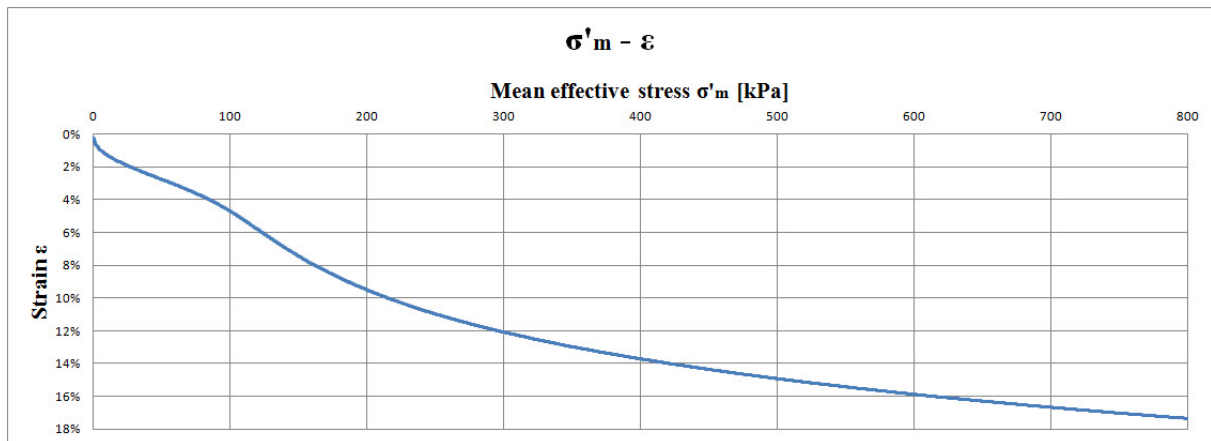


Figure 4.3.6: Sample T2-H15: Stress vs. strain from CRS oedometer test on undisturbed specimen.

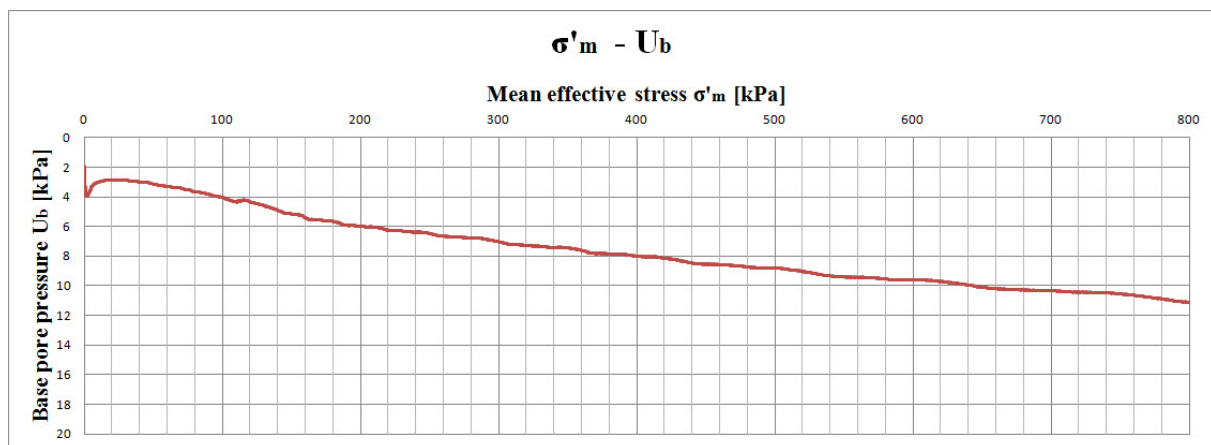


Figure 4.3.7: Sample T2-H15: Stress vs. pore pressure from CRS oedometer test on undisturbed specimen.

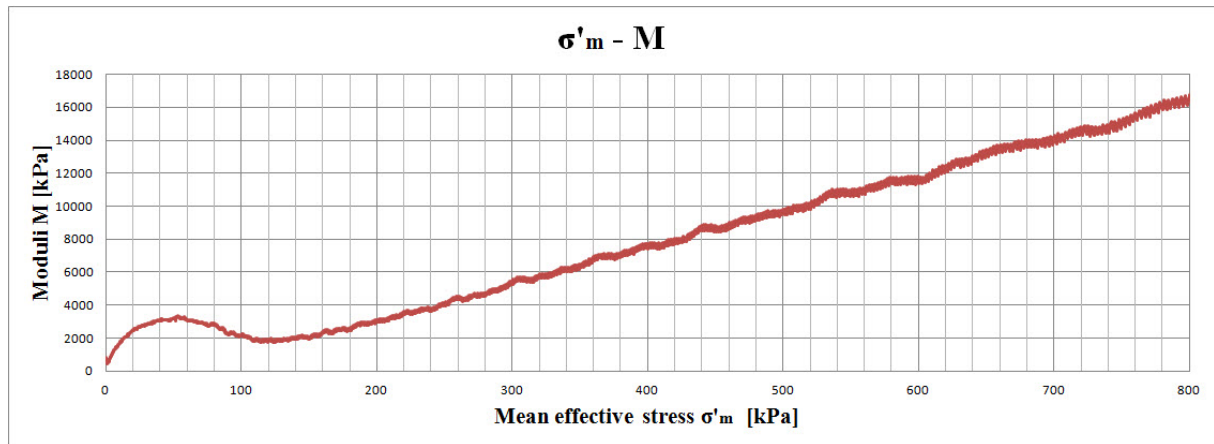


Figure 4.3.8: Sample T2-H15: Stress vs. oedometer modulus from CRS oedometer test on undisturbed specimen.

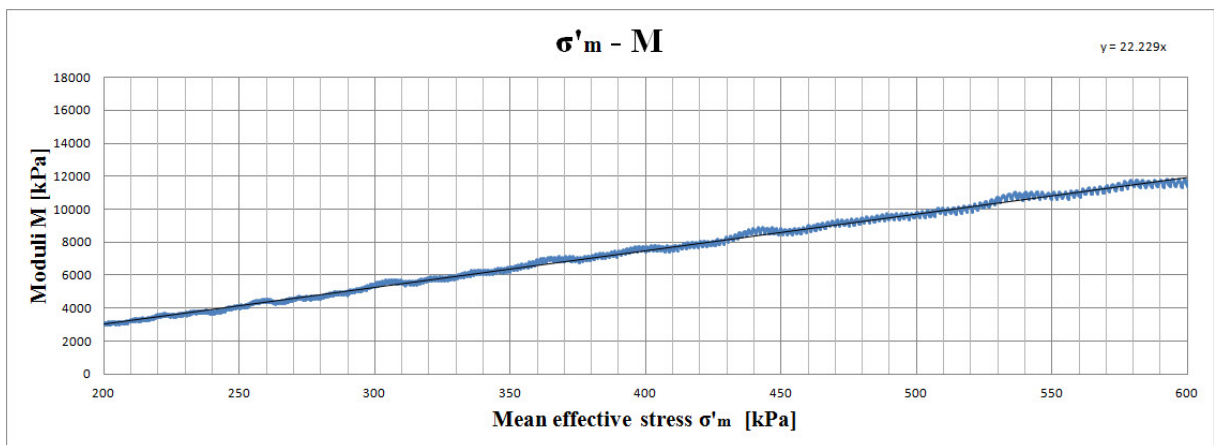


Figure 4.3.9: Sample T2-H15: Modulus number from CRS oedometer test on undisturbed specimen.

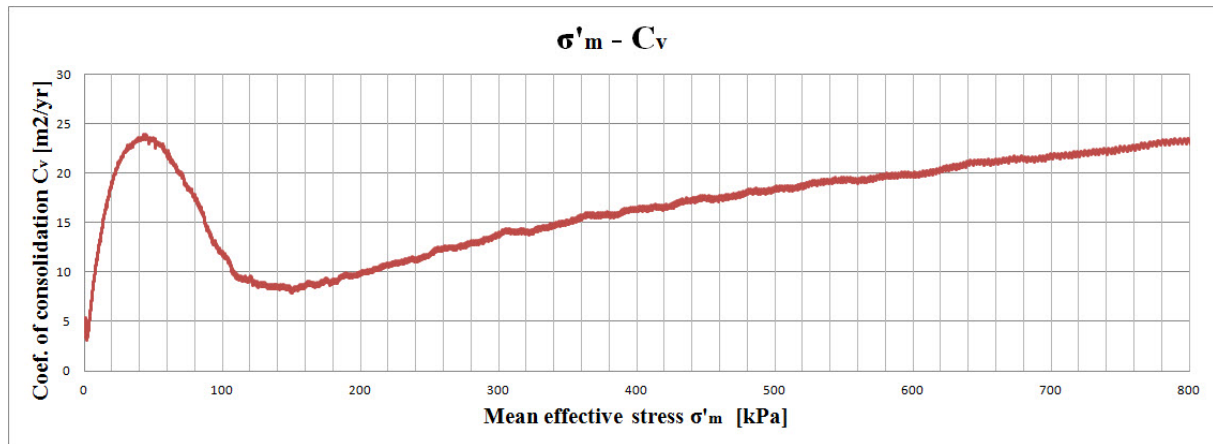


Figure 4.3.10: Sample T2-H15: Stress vs. coefficient of consolidation from CRS oedometer test on undisturbed specimen.

4.3.15 CRS Oedometer Test on Pre-Strained Clay

Calculation of water content for the test specimen is given in Table 4.3.19.

Table 4.3.19: Sample T2-H15: Calculation of water content for pre-strained specimen subjected to CRS oedometer test.

Parameter	Parameter value	Units
Mass, oedometer ring with specimen	115.47	gr.
Mass of oedometer ring	37.30	gr.
Mass of wet specimen (m_s+m_w)	78.17	gr.
Mass of dry specimen (m_s)	58.91	gr.
Mass of water (m_w)	19.26	gr.
Water content (w)	32.69	%

As seen from Table 4.3.19, there is a deviation of almost 5 % between calculated values of water content for the test specimen and for the whole sample T2-H15 (refer to Chapter 4.3.3). The deviation is likely to be caused by natural variation, and indicates that the material is less homogeneous than what has been assumed.

Figures 4.3.11-4.3.14 show the results of CRS oedometer test on sample T2-H15 pre-strained to shear strain $\gamma_s = 66 \%$. The presented results consist of:

- Stress vs. strain plot ($\sigma'_m - \epsilon$), Figure 4.3.11.
- Stress vs. pore pressure at sample base ($\sigma'_m - u_b$), Figure 4.3.12.
- Stress vs. modulus plot ($\sigma'_m - M$), Figure 4.3.13.
- Stress vs. coefficient of consolidation ($\sigma'_m - c_v$), Figure 4.3.14.

As follows from the results presented in Figure 4.3.11-4.3.14, the modulus number (m) for the specimen pre-strained to shear strain $\gamma_s = 66 \%$ is constant and equal to 25.4. Coefficient of consolidation (c_v) increases almost linearly with stress level, reaching the peak value of 23 m^2/yr at 800 kPa.

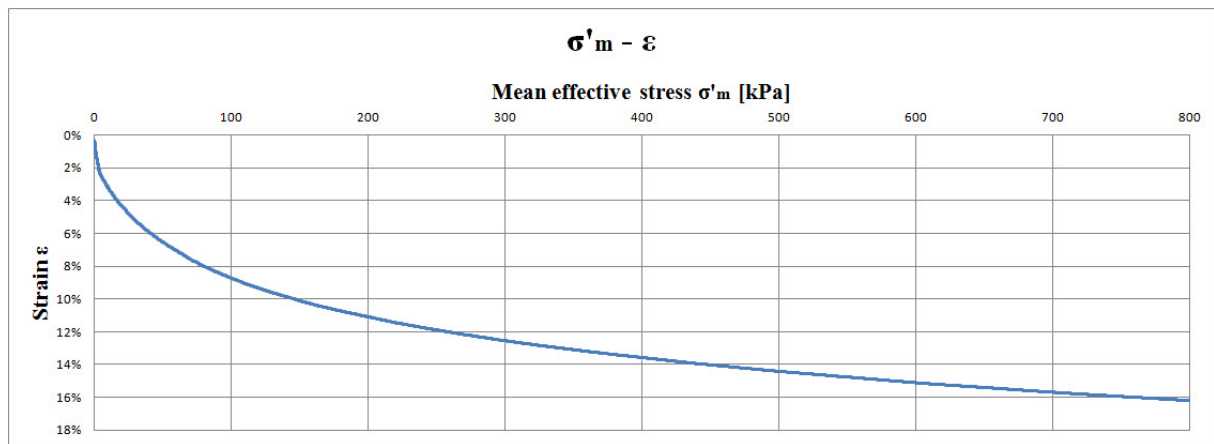


Figure 4.3.11: Sample T2-H15: Stress vs. strain from CRS oedometer test on specimen pre-strained to $\gamma_s = 66 \%$.

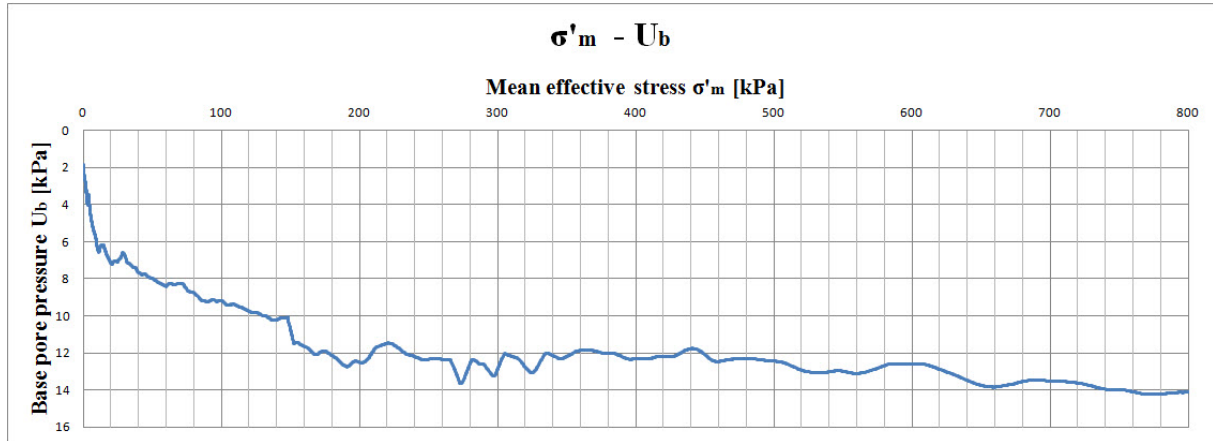


Figure 4.3.12: Sample T2-H15: Stress vs. pore pressure from CRS oedometer test on specimen pre-strained to $\gamma_s = 66\%$.

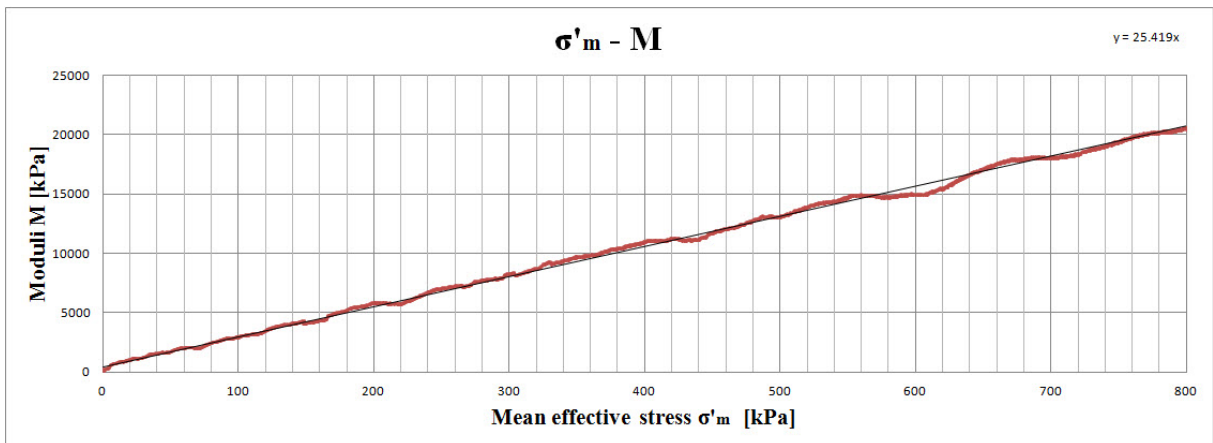


Figure 4.3.13: Sample T2-H15: Stress vs. oedometer modulus from CRS oedometer test on specimen pre-strained to $\gamma_s = 66\%$.

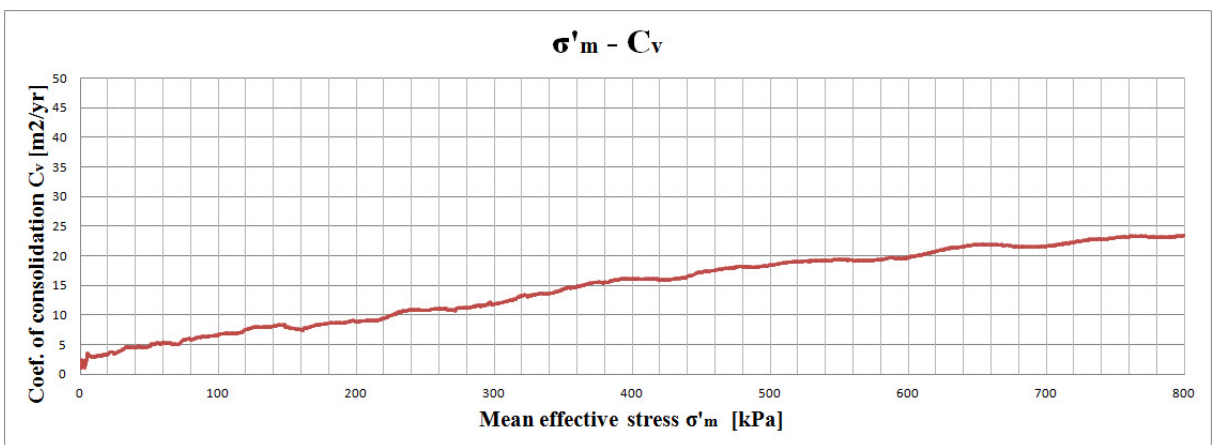


Figure 4.3.14: Sample T2-H15: Stress vs. coefficient of consolidation from CRS oedometer test on specimen pre-strained to $\gamma_s = 66\%$.

4.3.16 CRS Oedometer Test on Remoulded Clay

Calculation of water content for the test specimen is given in Table 4.3.20.

Table 4.3.20: Sample T2-H15: Calculation of water content for remoulded specimen subjected to CRS oedometer test.

Parameter	Parameter value	Units
Mass, oedometer ring with specimen	114.23	gr.
Mass of oedometer ring	39.56	gr.
Mass of wet specimen (m_s+m_w)	74.67	gr.
Mass of dry specimen (m_s)	56.03	gr.
Mass of water (m_w)	18.64	gr.
Water content (w)	33.27	%

As follows from Table 4.3.20, the value of water content for remoulded clay specimen agrees reasonably well with those values calculated for undisturbed and pre-strained specimens (Chapters 4.3.14 and 4.3.15, respectively). However, the water content value for remoulded clay specimen deviates by 5.6 % from the value calculated for the whole sample T2-H15 (27.72 %, refer to Chapter 4.3.3). An additional control measurement of water content has been done for the remoulded clay mass at the same time as the remoulded specimen was built into the oedometer. The control measurement showed water content $w = 31.72$ %.

Figures 4.3.15-4.3.18 show the results of CRS oedometer test on totally remoulded clay sample T2-H15. The presented results consist of:

- Stress vs. strain plot ($\sigma'_m - \epsilon$), Figure 4.3.15.
- Stress vs. pore pressure at sample base ($\sigma'_m - u_b$), Figure 4.3.16.
- Stress vs. modulus plot ($\sigma'_m - M$), Figure 4.3.17.
- Stress vs. coefficient of consolidation ($\sigma'_m - c_v$), Figure 4.3.18.

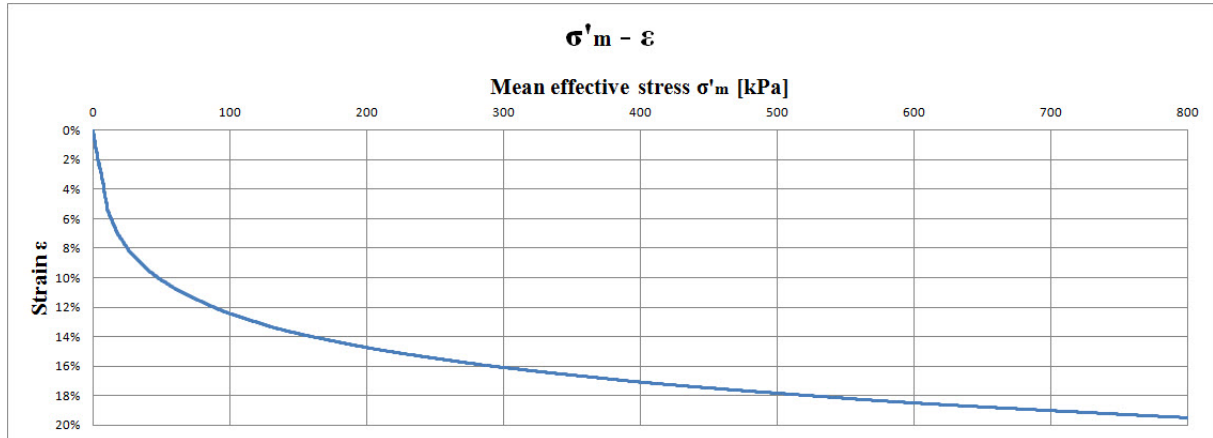


Figure 4.3.15: Sample T2-H15: Stress vs. strain from CRS oedometer test on remoulded specimen.

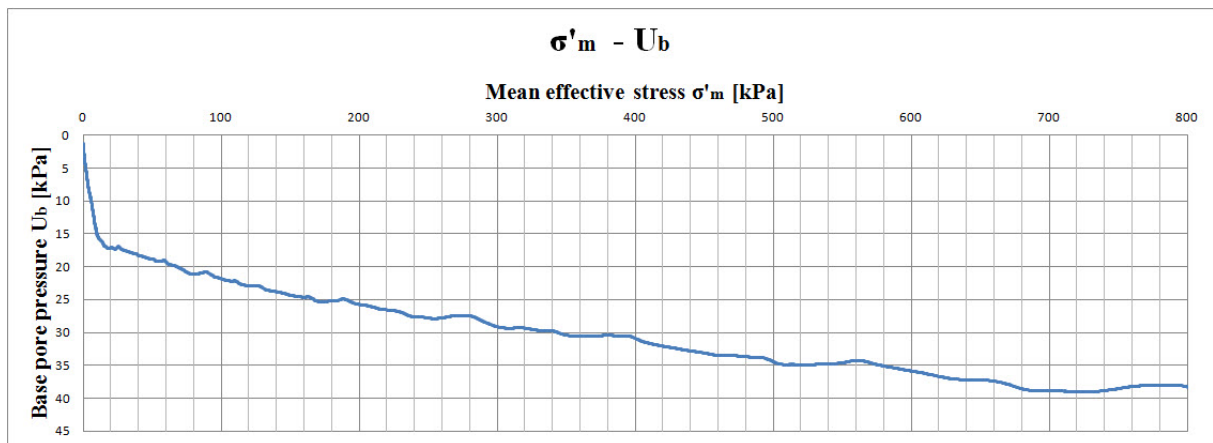


Figure 4.3.16: Sample T2-H15: Stress vs. pore pressure from CRS oedometer test on remoulded specimen.

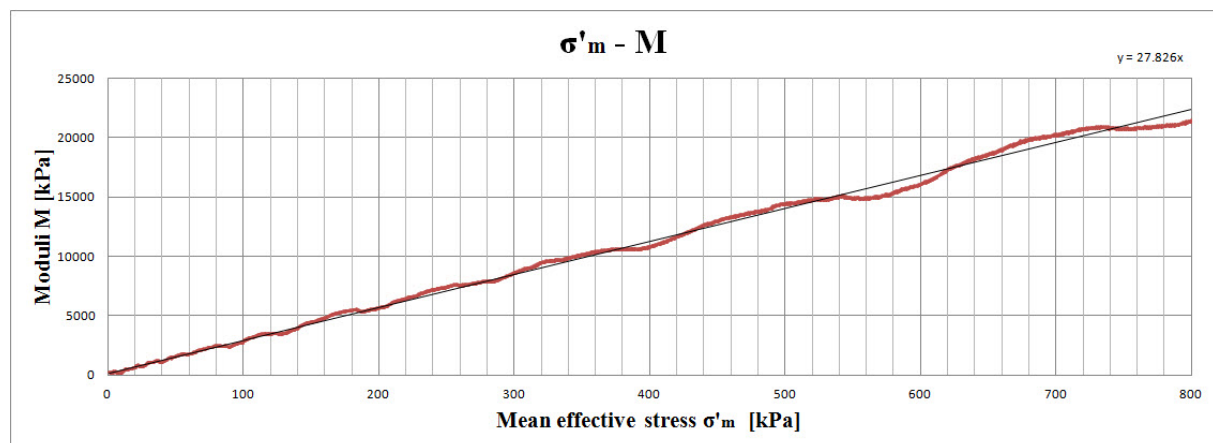


Figure 4.3.17: Sample T2-H15: Stress vs. oedometer modulus from CRS oedometer test on remoulded specimen.

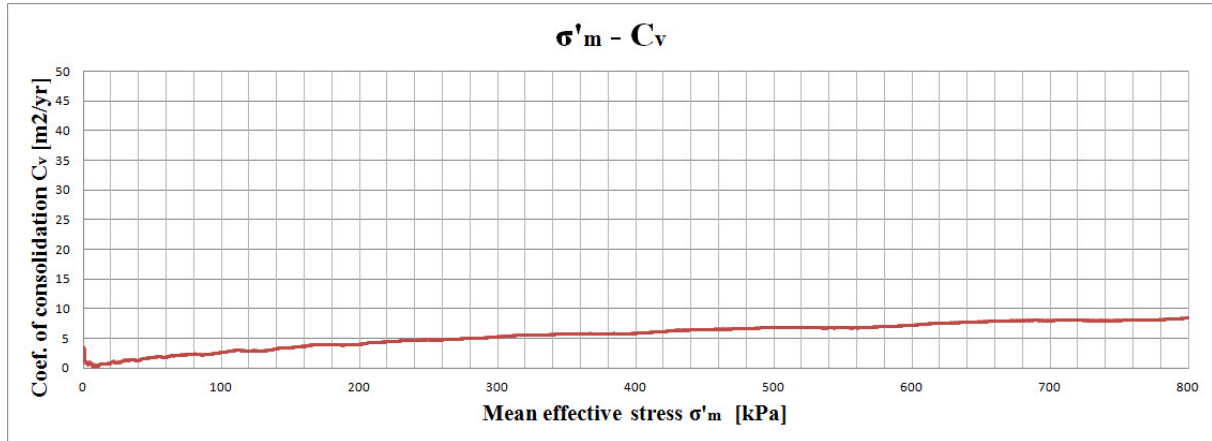


Figure 4.3.18: Sample T2-H15: Stress vs. coefficient of consolidation from CRS oedometer test on remoulded specimen.

As follows from the results presented in Figure 4.3.15-4.3.18, the modulus number (m) for the remoulded specimen is constant and equal to 27.8. Coefficient of consolidation (c_v) is slightly increasing with the stress level and is reaching its maximum of 8.3 m²/yr. at 800 kPa.

4.4 Test Results for Sample T3-H14

4.4.1 Extrusion of the Sample

Sample T3-H14 was extruded in the laboratory at 08.04.2015. The pre-straining was achieved by extrusion of the sample from $\phi 72.3$ mm to $\phi 68$ mm, corresponding to shear strain $\gamma_s = 18$ % (refer to Chapter 3 for more details). Figure 4.4.1 shows subdivision of the sample during extrusion.

Contrary to the samples extruded to shear strains of 117 % and 66 %, no strain variation has been observed in the cross-section of pre-strained sample T3-H14.

Displacement ratio is given by Eq. 3.4:

$$\delta_r = \frac{11}{10.1} = 1.09 \text{ mm/mm} \tag{Eq. 4.44}$$

There is a minor deviation between observed and theoretical displacement ratio (1.13 mm/mm, shown in Table 3.2.2).

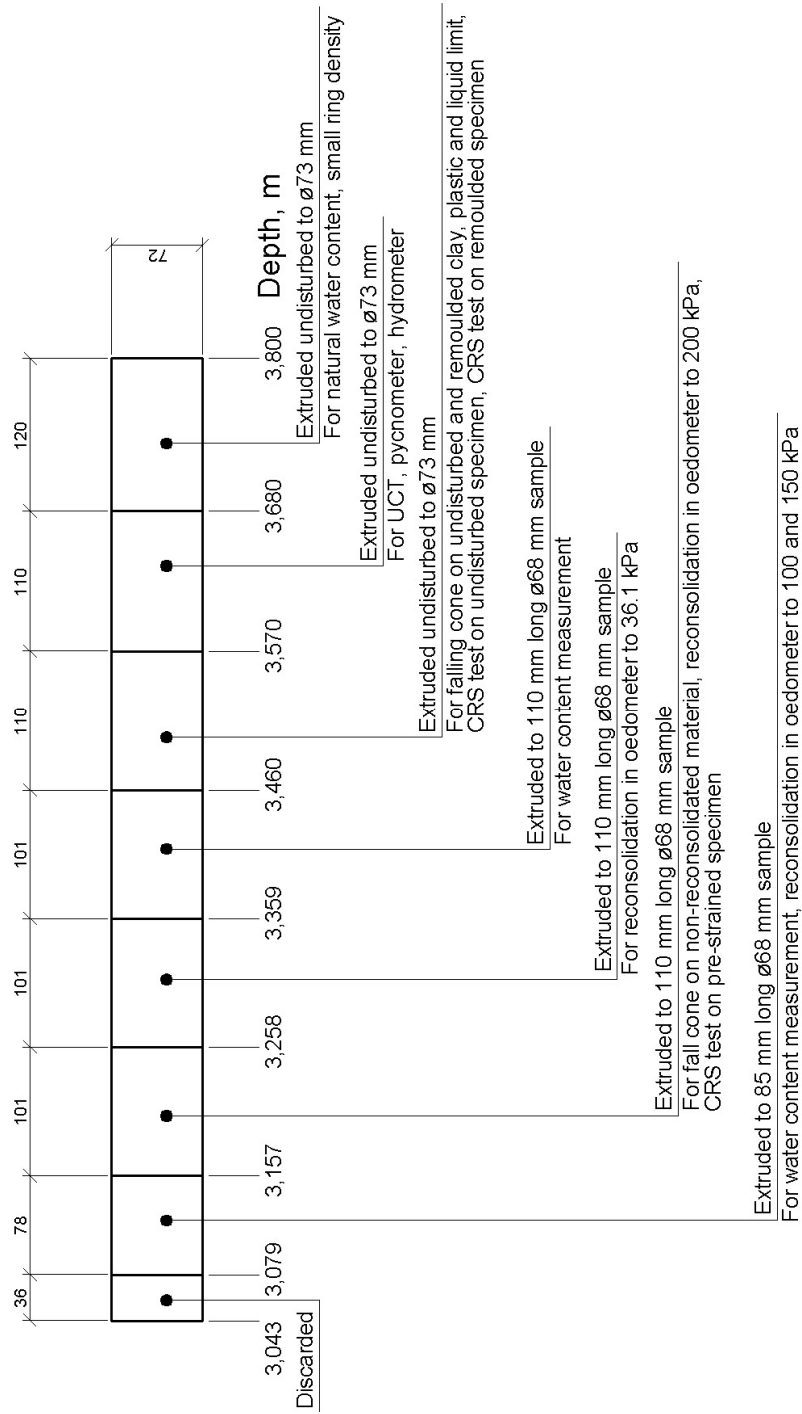


Figure 4.4.1: Sample T3-H14: Extrusion and subdivision.

4.4.2 Density Measurements

4.4.2.1 Average Density

Table 4.4.1 shows log of measurements made during calculation of mean density.

Table 4.4.1: Sample T3-H14: Calculation of mean density.

Parameter	Parameter value	Units
Length of sample (L)	75.7	cm
Diameter of sample (D _i)	7.23	cm
Volume of sample (V)	3107.9	cm ³
Mass of cylinder with sample and plug	9671	gr.
Mass of cylinder and plug	3556	gr.
Mass of sample (m)	6115	gr.
Mean density ($\bar{\rho}$)	1.97	gr./cm ³
Unit weight ($\bar{\gamma} = \bar{\rho} \cdot g$)	19.33	kN/m ³

4.4.2.2 Density by Small Ring

Table 4.4.2 contains log of measurements made during calculation of density with small ring.

Table 4.4.2: Sample T3-H14: Calculation of density and dry density with small ring.

	Ring	Bowl	
Parameter	Parameter value	Parameter value	Units
Total wet mass	101.63	119.37	gr.
Total dry mass	85.44	103.18	gr.
Mass of ring/bowl	32.10	49.84	gr.
Mass of wet sample ($m_s + m_w$)	69.53	69.53	gr.
Mass of dry sample (m_s)	53.34	53.34	gr.
Volume (V)	35.50	35.50	cm ³
Density (ρ)	1.96	1.96	gr./cm ³
Unit weight of soil (γ)	19.23	19.23	kN/m ³
Dry density (ρ_d)	1.50	1.50	gr./cm ³

As seen from Table 4.4.1 and 4.4.2, there is a close agreement between calculated values of densities.

4.4.2.3 Grain Density by Pycnometer

Table 4.4.3 shows log of measurements from pycnometer test. Grain density ρ_s is calculated from Eq. 3.9.

Table 4.4.3: Sample T3-H14: Calculation of grain density and unit weight of solids.

Parameter	Parameter value	Units
Mass of waterfilled pycnometer	146.92	gr.
Mass of pycnometer, water and specimen	157.85	gr.
Total dry mass	308.25	gr.
Mass of bowl	291.26	gr.
Dry mass of specimen (m_s)	16.99	gr.
Density of solids (ρ_s)	2.80	gr./cm ³
Unit weight of solids (γ_{solid})	27.47	kN/m ³

4.4.3 Water Content Measurements

Table 4.4.4 shows log of water content measurements. Test specimen No. 1 was undisturbed, while test specimens No. 2 and 3 were pre-strained.

As Table 4.4.4 shows, measurements of water content are somewhat inconsistent, indicating a possible inhomogeneity of the material. The mean value of natural water content is

$$w = \frac{28.25+25.73+30.77}{3} = 28.25 \% \quad (\text{Eq. 4.45})$$

Table 4.4.4: Sample T3-H14: Determination of water content.

	Specimen No. 1	Specimen No. 2	Specimen No. 3	
Parameter	Parameter value	Parameter value	Parameter value	Units
Depth	3.680 - 3.800	3.079 - 3.157	3.359 - 3.460	m
Total wet mass	97.36	128.64	89.08	gr.
Total dry mass	86.95	111.56	79.50	gr.
Mass of water (m_w)	10.41	17.08	9.58	gr.
Mass of bowl	50.10	45.19	48.37	gr.
Dry mass (m_s)	36.85	66.37	31.13	gr.
Water content (w)	28.25	25.73	30.77	%

4.4.4 Plastic and Liquid Limit

Table 4.4.5 shows log of plastic and liquid limit measurements.

Table 4.4.5: Sample T3-H14: Calculation of plastic and liquid limit.

	Liquid limit w_L	Plastic limit w_p	
Parameter	Parameter value	Parameter value	Units
Total wet mass	83.22	42.53	gr.
Total dry mass	74.48	40.72	gr.
Mass of water (m_w)	8.74	1.81	gr.
Mass of bowl	45.70	31.22	gr.
Dry mass (m_s)	28.78	9.50	gr.
Water content (w_L and w_p)	30.37	19.05	%

Liquidity and plasticity indices are found from Eq. 3.12 and 3.13, respectively:

$$I_L = \frac{w - w_p}{w_L - w_p} = \frac{28.25 - 19.05}{30.37 - 19.05} = 0.81 \quad (\text{Eq. 4.46})$$

$$I_p = w_L - w_p = 30.37 - 19.05 = 11.32 \%$$

The value of natural water content in Eq. 4.46 is obtained from Eq. 4.45.

4.4.5 Degree of Saturation, Void Ratio and Porosity

Degree of saturation (S_r) is found from Eq. 3.14:

$$S_r = \frac{w \cdot \gamma}{\gamma_w \cdot \left(1 + w - \frac{\gamma}{\gamma_{\text{solid}}}\right)} = \frac{0.28 \cdot 19.23}{9.81 \cdot \left(1 + 0.28 - \frac{19.23}{27.47}\right)} = 0.95 \quad (\text{Eq. 4.47})$$

Void ratio (e) is found from Eq. 3.15:

$$e = \frac{\gamma_{\text{solid}} \cdot (1 + w)}{\gamma} - 1 = \frac{27.47 \cdot (1 + 0.28)}{19.23} - 1 = 0.83 \quad (\text{Eq. 4.48})$$

Porosity (n) is found from Eq. 3.16:

$$n = \left(1 - \frac{\gamma}{\gamma_{\text{solid}} \cdot (1 + w)}\right) \cdot 100 \% = \left(1 - \frac{19.23}{27.47 \cdot (1 + 0.28)}\right) \cdot 100 \% = 45.31 \% \quad (\text{Eq. 4.49})$$

Here, the value of natural water content w is obtained from Eq. 4.45, unit weight of soil γ is obtained from Table 4.4.2 and unit weight of solids γ_{solid} is obtained from Table 4.4.3.

4.4.6 Grain Size Distribution

Table 4.4.6 shows observations made during hydrometer test.

Grain size distribution curve for sample T3-H14 is shown in Figure 4.4.2. Ratio d_{60}/d_{10} is not available due to practical reasons. Ratio d_{75}/d_{25} is calculated from data in Figure 4.4.2:

$$\frac{d_{75}}{d_{25}} = \frac{0.02409}{0.00176} = 13.7 \quad (\text{Eq. 4.50})$$

Maximum grain size d_{max} is 0.125 mm and average grain size d_{50} is 0.01051 mm. The clay content is 27 % and silt content is approximately 69 %.

Table 4.4.6: Sample T3-H14: Observations from hydrometer test.

Total mass of dried sample (W), gr.		37.59							
Mass of dried sample (w_s) $d < 0.074$ mm, gr.		37.52							
Grain density (ρ_s), gr./cm³		2.80							
Coefficient a		97.0							
Passed time (t), min.	Temp. (T), °C	Concentration (R), gr./l	Eff. depth (Z_r), cm	Constant (K), $\sqrt{\frac{min}{cm}}$	$\sqrt{\frac{Z_r}{t}}$, $\sqrt{\frac{cm}{min}}$	Equiv. grain size (d_s), mm	Rel. weight (N) $d_s < 0.074$ mm, %	Rel. weight total sample, %	
1	21.3	32.5	7.2	0.01287	2.683	0.0345	84.02	83.86	
2	21.2	30.0	8.0	0.01288	2.000	0.0258	77.56	77.42	
5	21.2	25.0	10.0	0.01288	1.414	0.0182	64.63	64.51	
10	21.0	22.0	11.2	0.01290	1.058	0.0136	56.88	56.77	
20	20.7	19.0	12.2	0.01297	0.781	0.0101	49.12	49.03	
40	20.6	16.5	13.2	0.01298	0.574	0.0075	42.66	42.58	
80	20.4	15.0	13.7	0.01300	0.414	0.0054	38.78	38.71	
160	20.4	13.0	14.5	0.01300	0.301	0.0039	33.61	33.55	
320	20.7	12.0	14.8	0.01297	0.215	0.0028	31.02	30.96	
1320	21.0	8.5	16.3	0.01290	0.111	0.0014	21.97	21.93	

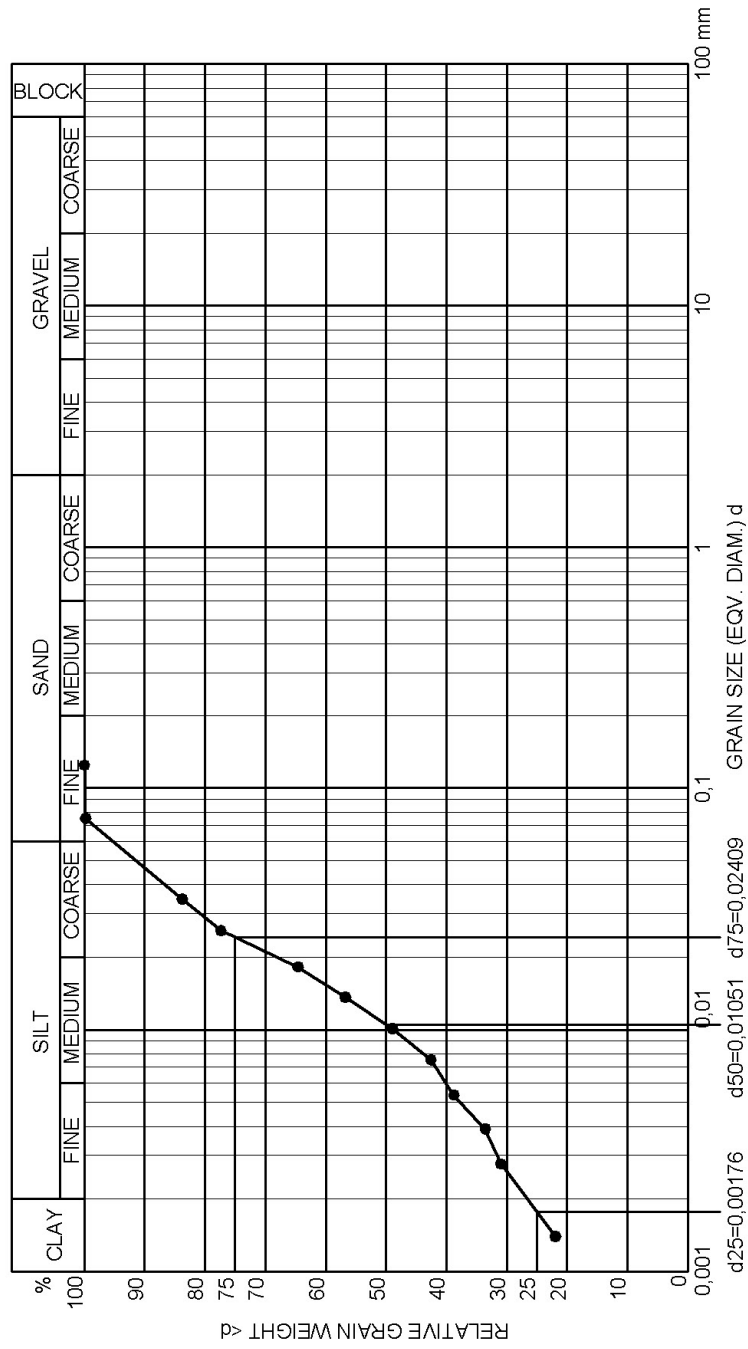


Figure 4.4.2: Sample T3-H14: Grain size distribution curve.

4.4.7 Undrained Shear Strength by UCT

Figure 4.4.3 shows deformation curve from UCT aligned with calibration chart. The sample demonstrates plastic yielding at strain $\epsilon_a = 12\%$ for maximum load $P = 47\text{ kg}$ (461.07 N). After the peak load is reached, the load is nearly constant for an increasing strain.

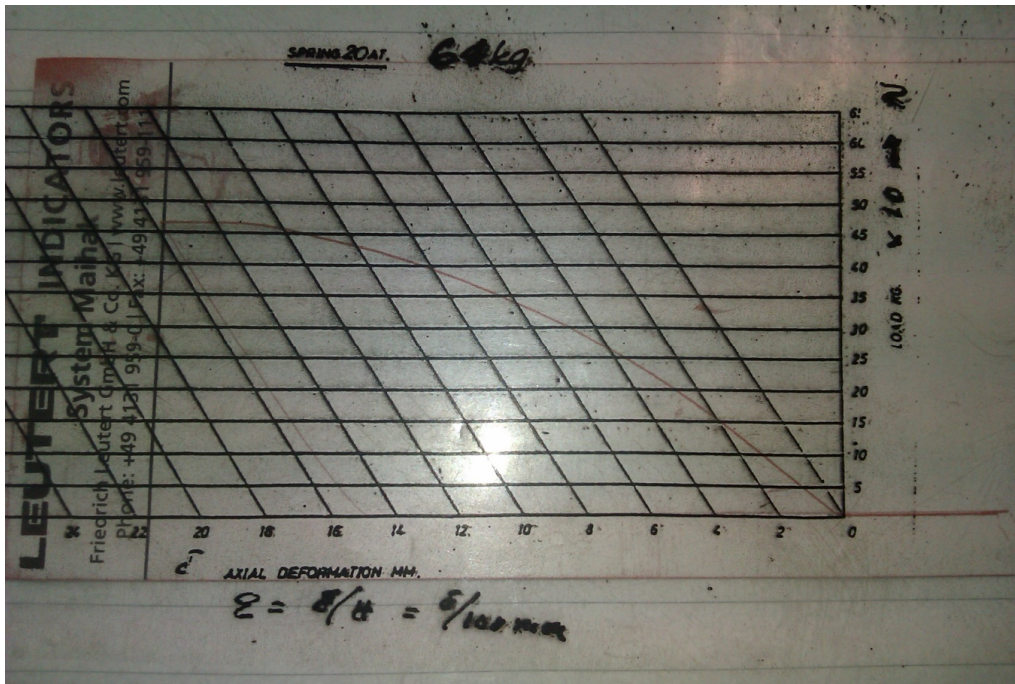


Figure 4.4.3: Sample T3-H14: Recorded deformation curve from UCT.

Undrained shear strength (s_u) is given by Eq. 3.24:

$$s_u = \tau_{max} = \frac{\sigma_1}{2} = \frac{P_f \cdot (1 - \epsilon_a)}{2 \cdot A_0} = \frac{461.07 \cdot (1 - 0.12)}{2 \cdot 2290} = 0.0886 \text{ N/mm}^2 = 88.6 \text{ kPa} \quad (\text{Eq. 4.51})$$

Figure 4.4.4 shows the sample at the end of the test. A sketch of the shape of sample at failure is shown in Figure 4.4.5. In the end of the test, a clearly visible failure plane was located at an angle of 15° from vertical axis.

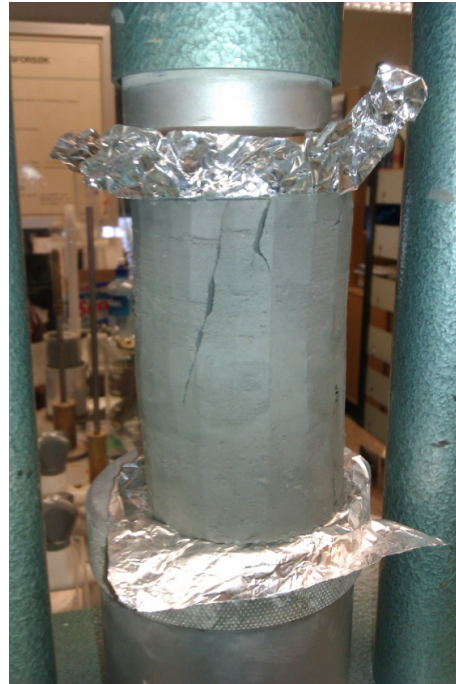


Figure 4.4.4: Sample T3-H14: Specimen at failure during UCT.

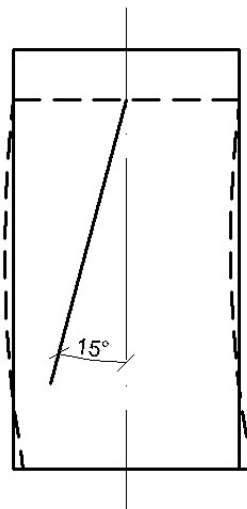


Figure 4.4.5: Sample T3-H14: Shape of specimen at failure during UCT.

4.4.8 Undrained and Remoulded Shear Strength by Fall Cone

Table 4.4.7 shows results of falling cone test on undisturbed specimen. 100 gr. cone has been used.

As seen from Table 4.4.7, there is a deviation between values of undrained shear strength determined by falling cone and UCT. One possible explanation of the deviation is a disturbance in the sample close to the cylinder's end, from where the specimen has been obtained for UCT.

Table 4.4.7: Sample T3-H14: Results of falling cone test on undisturbed clay.

Intrusion No.	Intrusion, mm	Undrained shear strength s_u , kPa	Reported (mean) s_u , kPa
1	4.2	49.1	46.1
2	4.3	47.6	
3	4.7	41.7	

Table 4.4.8 shows results of falling cone test on remoulded specimen. 60 gr. cone has been used.

Table 4.4.8: Sample T3-H14: Results of falling cone test on remoulded clay.

Set No.	Intrusion, mm	Remoulded shear strength s_r , kPa	Mean remoulded shear strength s_r , kPa	Reported remoulded shear strength s_r , kPa
1	7.8	3.9	4.2	4.2
	7.2	4.5		
2	7.0	4.8	4.7	
	7.2	4.5		

The sensitivity is given by Eq.3.25:

$$S_t = \frac{s_u}{s_r} = \frac{46.1}{4.2} = 11.0 \quad (\text{Eq. 4.52})$$

4.4.9 Shear Strength of Pre-Strained, Non-Reconsolidated Sample by Fall Cone

Table 4.4.9 shows test results from falling cone test on pre-strained non-reconsolidated sample. 100 gr. cone has been used.

Table 4.4.9: Sample T3-H14: Results of falling cone test on pre-strained non-reconsolidated clay.

Intrusion No.	Intrusion, mm	Shear strength s , kPa	Reported (mean) s , kPa
1	6.1	29.9	30.6
2	6.0	30.4	
3	5.9	31.4	

4.4.10 Reconsolidation of Pre-Strained Specimen in the Oedometer at In-Situ Vertical Effective Stress 36.1 kPa

Table 4.4.10 shows data for calculation of water content in specimen prior to and after reconsolidation. Remaining pore pressure after 24 hrs. reconsolidation time was 0.1 kPa.

Table 4.4.10: Sample T3-H14: Calculation of water content prior to and after reconsolidation at in-situ vertical effective stress 36.1 kPa.

Parameter	Parameter value before reconsolidation	Parameter value after reconsolidation	Units
Mass, oedometer ring with wet specimen	115.15	114.25	gr.
Mass, oedometer ring	39.12	39.12	gr.
Mass of wet specimen	76.03	75.13	gr.
Mass of dry specimen (m_s)	55.98	55.98	gr.
Mass of water (m_w)	20.05	19.15	gr.
Water content (w and w_{re})	35.82	34.21	%

As follows from Table 4.4.10, reconsolidation at 36.1 kPa leads to change in water content:

$$\Delta w = w_{re} - w = 34.21 - 35.82 = -1.61 \% \quad (\text{Eq. 4.53})$$

After 24 hrs. reconsolidation at 36.1 kPa, volume of the specimen has been reduced by 5.04 %.

Table 4.4.11 shows results of falling cone test on reconsolidated specimen. 100 gr. cone has been used in the test.

Table 4.4.11: Sample T3-H14: Results of falling cone test on pre-strained clay reconsolidated at in-situ vertical effective stress 36.1 kPa.

Intrusion No.	Intrusion, mm	Shear strength after reconsolidation s_{re} , kPa	Reported (mean) shear strength after reconsolidation s_{re} , kPa
1	5.0	38.7	42.0
2	4.3	47.6	
3	4.9	39.7	

As follows from Table 4.4.7 and 4.4.11, change in shear strength due to the pre-straining and subsequent reconsolidation at 36.1 is:

$$\Delta s = s_{re} - s_u = 42.0 - 46.1 = -4.1 \text{ kPa} \quad (\text{Eq. 4.54})$$

Normalised change in shear strength due to the pre-straining and reconsolidation is:

$$\frac{\Delta s}{s_u} = \frac{s_{re} - s_u}{s_u} \cdot 100 \% = \frac{42.0 - 46.1}{46.1} \cdot 100 \% = -8.89 \% \quad (\text{Eq. 4.55})$$

4.4.11 Reconsolidation of Pre-Strained Specimen in the Oedometer at 100 kPa

Table 4.4.12 shows data for calculation of water content in specimen prior to and after reconsolidation. Remaining pore pressure after 24 hrs. reconsolidation time was 0.8 kPa.

As follows from Table 4.4.12, reconsolidation at 100 kPa leads to change in water content:

$$\Delta w = w_{re} - w = 25.62 - 28.91 = -3.29 \% \quad (\text{Eq. 4.56})$$

After 24 hrs. reconsolidation at 100 kPa, volume of the specimen has been reduced by 8.85 %.

Table 4.4.12: Sample T3-H14: Calculation of water content prior to and after reconsolidation at 100 kPa.

Parameter	Parameter value before reconsolidation	Parameter value after reconsolidation	Units
Mass, oedometer ring with wet specimen	117.56	115.51	gr.
Mass, oedometer ring	37.30	37.30	gr.
Mass of wet specimen	80.26	78.21	gr.
Mass of dry specimen (m_s)	62.26	62.26	gr.
Mass of water (m_w)	18.00	15.95	gr.
Water content (w and w_{re})	28.91	25.62	%

Table 4.4.13 shows the results of falling cone test on reconsolidated specimen. 100 gr. cone has been used in the test.

Table 4.4.13: Sample T3-H14: Results of falling cone test on pre-strained clay reconsolidated at 100 kPa.

Intrusion No.	Intrusion, mm	Shear strength after reconsolidation s_{re} , kPa	Reported (mean) shear strength after reconsolidation s_{re} , kPa
1	3.1	71.6	75.2
2	2.9	77.0	
3	2.9	77.0	

As follows from Table 4.4.7 and 4.4.13, change in shear strength due to the pre-straining and subsequent reconsolidation at 100 kPa is:

$$\Delta s = s_{re} - s_u = 75.2 - 46.1 = 29.1 \text{ kPa} \quad (\text{Eq. 4.57})$$

Normalised change in shear strength due to the pre-straining and reconsolidation is:

$$\frac{\Delta s}{s_u} = \frac{s_{re} - s_u}{s_u} \cdot 100 \% = \frac{75.2 - 46.1}{46.1} \cdot 100 \% = 63.12 \% \quad (\text{Eq. 4.58})$$

4.4.12 Reconsolidation of Pre-Strained Specimen in the Oedometer at 150 kPa

Table 4.4.14 shows data for calculation of water content in specimen prior to and after reconsolidation. Remaining pore pressure after 24 hrs. reconsolidation time was 1.9 kPa.

Table 4.4.14: Sample T3-H14: Calculation of water content prior to and after reconsolidation at 150 kPa.

Parameter	Parameter value before reconsolidation	Parameter value after reconsolidation	Units
Mass, oedometer ring with wet specimen	118.05	115.64	gr.
Mass, oedometer ring	37.30	37.30	gr.
Mass of wet specimen	80.75	78.34	gr.
Mass of dry specimen (m_s)	62.79	62.79	gr.
Mass of water (m_w)	17.96	15.55	gr.
Water content (w and w_{re})	28.60	24.77	%

As follows from Table 4.4.14, reconsolidation at 150 kPa leads to change in water content:

$$\Delta w = w_{re} - w = 24.77 - 28.60 = -3.83 \% \quad (\text{Eq. 4.59})$$

After 24 hrs. reconsolidation at 150 kPa, volume of the specimen has been reduced by 9.45 %.

Table 4.4.15 shows the results of falling cone test on reconsolidated specimen. 100 gr. cone has been used in the test.

As follows from Table 4.4.7 and 4.4.15, change in shear strength due to the pre-straining and subsequent reconsolidation at 150 kPa is:

$$\Delta s = s_{re} - s_u = 102.6 - 46.1 = 56.5 \text{ kPa} \quad (\text{Eq. 4.60})$$

Normalised change in shear strength due to the pre-straining and reconsolidation is:

$$\frac{\Delta s}{s_u} = \frac{s_{re} - s_u}{s_u} \cdot 100 \% = \frac{102.6 - 46.1}{46.1} \cdot 100 \% = 122.56 \% \quad (\text{Eq. 4.61})$$

Table 4.4.15: Sample T3-H14: Results of falling cone test on pre-strained clay reconsolidated at 150 kPa.

Intrusion No.	Intrusion, mm	Shear strength after reconsolidation s_{re} , kPa	Reported (mean) shear strength after reconsolidation s_{re} , kPa
1	1.8	108.0	102.6
2	2.3	94.7	
3	1.9	105.0	

4.4.13 Reconsolidation of Pre-Strained Specimen in the Oedometer at 200 kPa

Table 4.4.16 shows data for calculation of water content in specimen prior to and after reconsolidation. Remaining pore pressure after 24 hrs. reconsolidation time was 0.3 kPa.

Table 4.4.16: Sample T3-H14: Calculation of water content prior to and after reconsolidation at 200 kPa.

Parameter	Parameter value before reconsolidation	Parameter value after reconsolidation	Units
Mass, oedometer ring with wet specimen	114.21	110.21	gr.
Mass, oedometer ring	37.30	37.30	gr.
Mass of wet specimen	76.91	72.91	gr.
Mass of dry specimen (m_s)	56.91	56.91	gr.
Mass of water (m_w)	20.00	16.00	gr.
Water content (w and w_{re})	35.14	28.11	%

As follows from Table 4.4.16, reconsolidation at 200 kPa leads to change in water content:

$$\Delta w = w_{re} - w = 28.11 - 35.14 = -7.03 \% \quad (\text{Eq. 4.62})$$

After 24 hrs. reconsolidation at 200 kPa, volume of the specimen has been reduced by 13.24 %.

Table 4.4.17 shows the results of falling cone test on reconsolidated specimen. 100 gr. cone has been used in the test.

Table 4.4.17: Sample T3-H14: Results of falling cone test on pre-strained clay reconsolidated at 200 kPa.

Intrusion No.	Intrusion, mm	Shear strength after reconsolidation s_{re} , kPa	Reported (mean) shear strength after reconsolidation s_{re} , kPa
1	1.9	105.0	102.3
2	2.1	100.0	
3	2.0	102.0	

As follows from Table 4.4.7 and 4.4.17, change in shear strength due to the pre-straining and subsequent reconsolidation at 200 kPa is:

$$\Delta s = s_{re} - s_u = 102.3 - 46.1 = 56.2 \text{ kPa} \quad (\text{Eq. 4.63})$$

Normalised change in shear strength due to the pre-straining and reconsolidation is:

$$\frac{\Delta s}{s_u} = \frac{s_{re} - s_u}{s_u} \cdot 100 \% = \frac{102.3 - 46.1}{46.1} \cdot 100 \% = 121.91 \% \quad (\text{Eq. 4.64})$$

4.4.14 CRS Oedometer Test on Undisturbed Clay

Calculation of index parameters for the test specimen is given in Table 4.4.18. The value of grain density ρ_s used in the calculation is obtained from the results of pycnometer test (refer to Chapter 4.4.2).

As follows from Table 4.4.18, there are small deviations between calculated values of water content, degree of saturation and void ratio for oedometer test specimen and whole sample T3-H14 (refer to Chapters 4.4.3 and 4.4.5). The deviation between values of water content, degree of saturation and void ratio are 3.28 %, 0.04 and 0.06, respectively. The deviations are negligible.

Table 4.4.18: Sample T3-H14: Calculation of index parameters for undisturbed specimen subjected to CRS oedometer test.

Parameter	Parameter value	Units
Height of specimen (h_0)	20	mm
Area of specimen (A)	20	cm ²
Volume of specimen (V_0)	40	cm ³
Mass, oedometer ring with specimen	118.07	gr.
Mass of oedometer ring	39.64	gr.
Mass of wet specimen (m_s+m_w)	78.43	gr.
Mass of dry specimen (m_s)	59.63	gr.
Mass of water (m_w)	18.80	gr.
Water content (w)	31.53	%
Grain density (ρ_s)	2.80	gr./cm ³
Solids ($h_s = \frac{m_s}{A \cdot \rho_s}$)	1.06	cm
Void ratio ($e_0 = \frac{h_0 - h_s}{h_s}$)	0.89	-
Degree of saturation ($S_t = \frac{\rho_s \cdot w}{\rho_w \cdot e_0}$)	0.99	-

Figures 4.4.6-4.4.10 show the results of CRS oedometer test on undisturbed sample T3-H14.

The presented results consist of:

- Stress vs. strain plot ($\sigma'_m - \varepsilon$), Figure 4.4.6.
- Stress vs. pore pressure at sample base ($\sigma'_m - u_b$), Figure 4.4.7.
- Stress vs. modulus plot ($\sigma'_m - M$), Figure 4.4.8 and 4.4.9.
- Stress vs. coefficient of consolidation ($\sigma'_m - c_v$), Figure 4.4.10.

As follows from the test results presented in Figure 4.4.6-4.4.10, preconsolidation stress p'_c for sample T3-H14 is approximately 120 kPa. Constrained moduli in the overconsolidated range (M_o) and at the preconsolidation stress (M_n) are 5 MPa and 4 MPa, respectively. For normally consolidated range, the modulus number (m) is 23.5.

With $p'_c = 120$ kPa, the overconsolidation ratio for sample T3-H14 can be estimated as

$$OCR = \frac{p'_c}{\sigma'_{v0}} = \frac{120}{36.1} = 3.3 \tag{Eq. 4.65}$$

Coefficients of consolidation in the overconsolidated zone (c_{vo}) and at about p'_c (c_{vn}) are 9 and 6 m^2/yr , respectively.

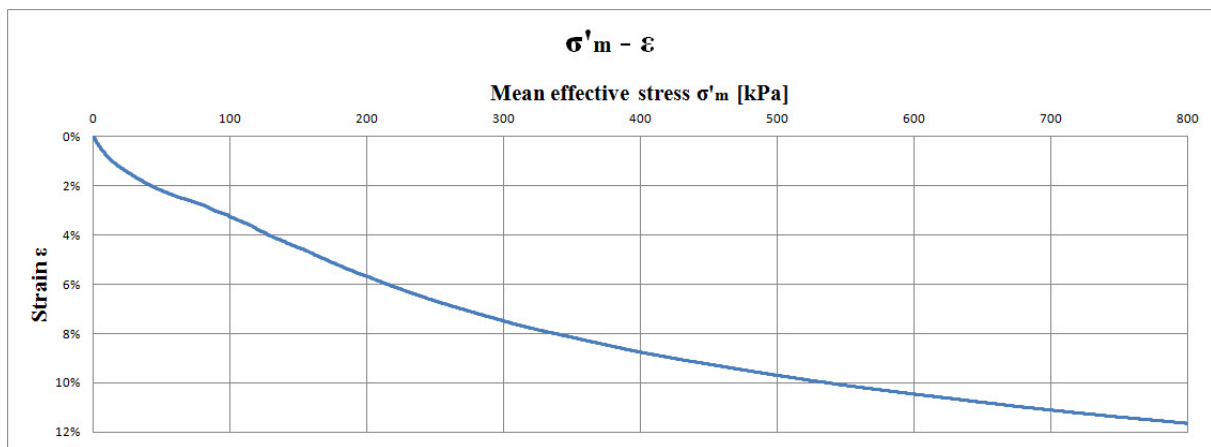


Figure 4.4.6: Sample T3-H14: Stress vs. strain from CRS oedometer test on undisturbed specimen.

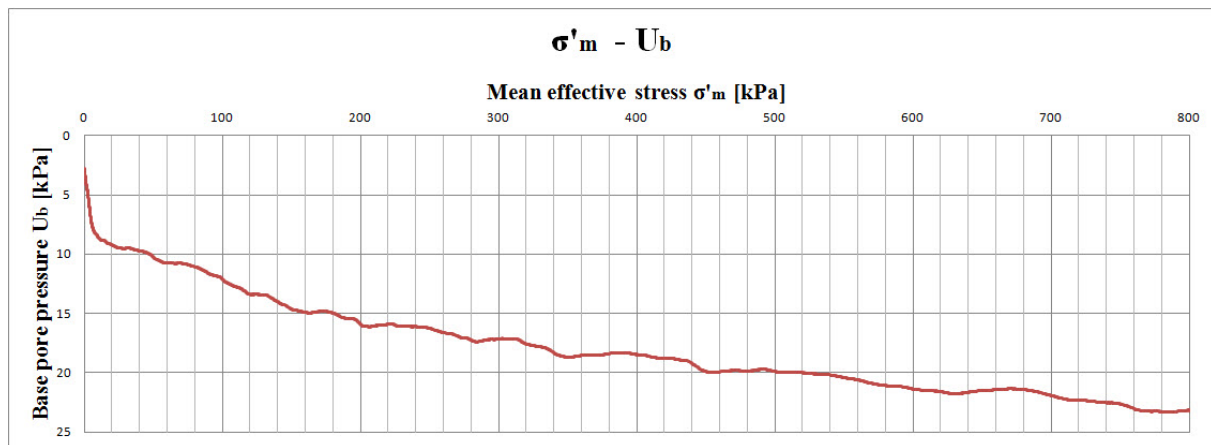


Figure 4.4.7: Sample T3-H14: Stress vs. pore pressure from CRS oedometer test on undisturbed specimen.

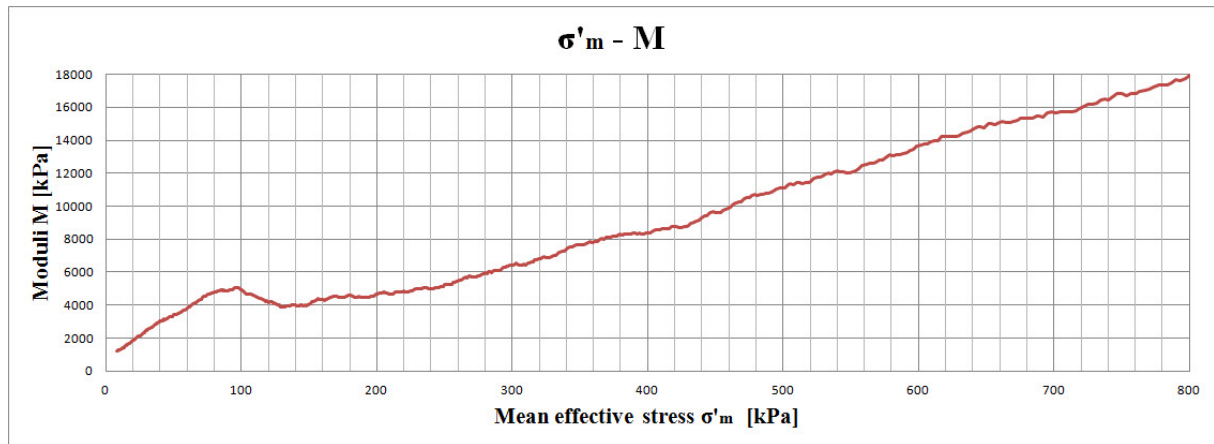


Figure 4.4.8: Sample T3-H14: Stress vs. oedometer modulus from CRS oedometer test on undisturbed specimen.

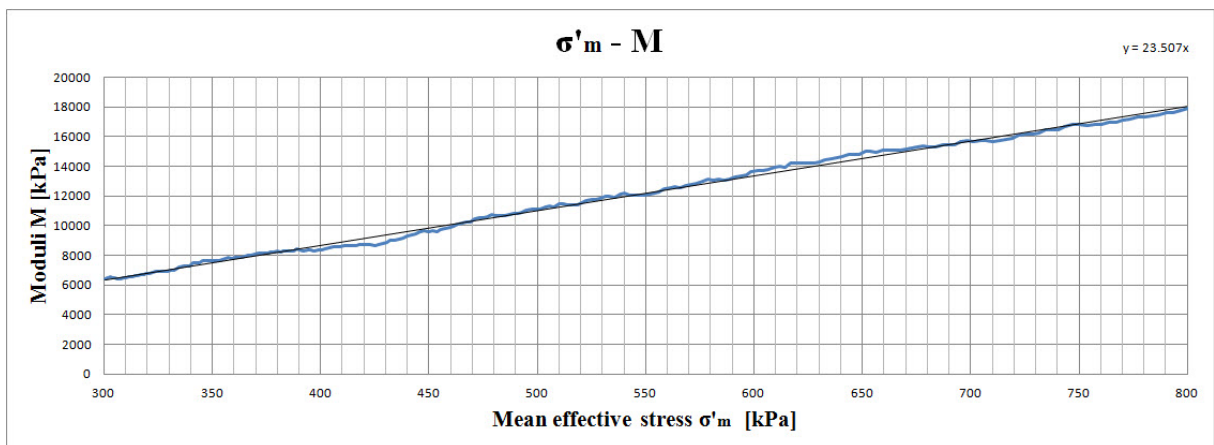


Figure 4.4.9: Sample T3-H14: Modulus number from CRS oedometer test on undisturbed specimen.

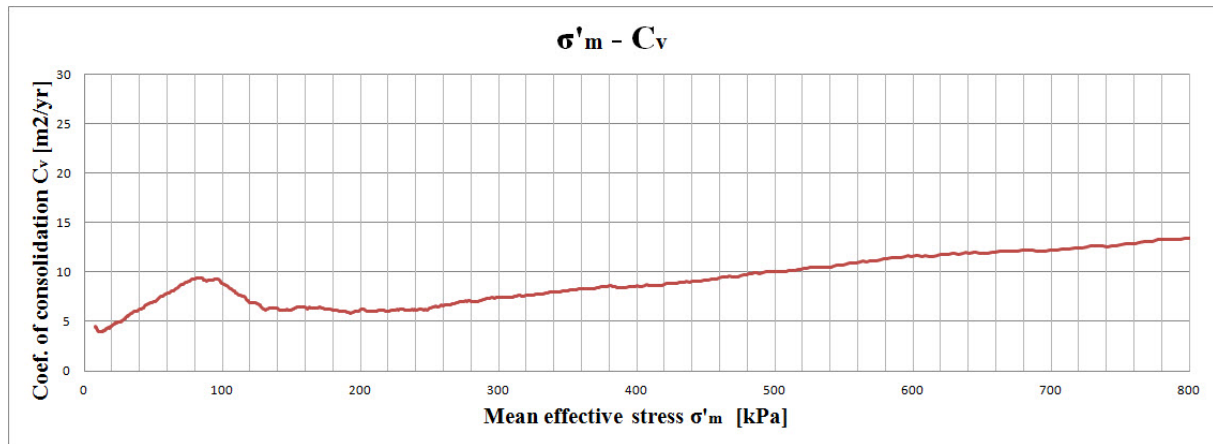


Figure 4.4.10: Sample T3-H14: Stress vs. coefficient of consolidation from CRS oedometer test on undisturbed specimen.

4.4.15 CRS Oedometer Test on Pre-Strained Clay

Calculation of water content for the test specimen is given in Table 4.4.19.

Table 4.4.19: Sample T3-H14: Calculation of water content for pre-strained specimen subjected to CRS oedometer test.

Parameter	Parameter value	Units
Mass, oedometer ring with specimen	116.09	gr.
Mass of oedometer ring	39.64	gr.
Mass of wet specimen (m_s+m_w)	76.45	gr.
Mass of dry specimen (m_s)	56.54	gr.
Mass of water (m_w)	19.91	gr.
Water content (w)	35.21	%

As seen from Table 4.4.19, there is a deviation of almost 7 % between calculated values of water content for the test specimen and for the whole sample T3-H14 (refer to Chapter 4.4.3). The deviation may indicate that sample T3-H14 consists of inhomogeneous material.

Figures 4.4.11-4.4.14 show the results of CRS oedometer test on sample T3-H14 pre-strained to shear strain $\gamma_s = 18$ %. The presented results consist of:

- Stress vs. strain plot ($\sigma'_m - \epsilon$), Figure 4.4.11.
- Stress vs. pore pressure at sample base ($\sigma'_m - u_b$), Figure 4.4.12.
- Stress vs. modulus plot ($\sigma'_m - M$), Figure 4.4.13.
- Stress vs. coefficient of consolidation ($\sigma'_m - c_v$), Figure 4.4.14.

As follows from the results presented in Figure 4.4.11-4.4.14, the modulus number (m) for the specimen pre-strained to shear strain $\gamma_s = 18\%$ is constant and equal to 22.1. Coefficient of consolidation (c_v) is increasing with stress level, reaching the peak value of $10 \text{ m}^2/\text{yr}$ at 800 kPa.

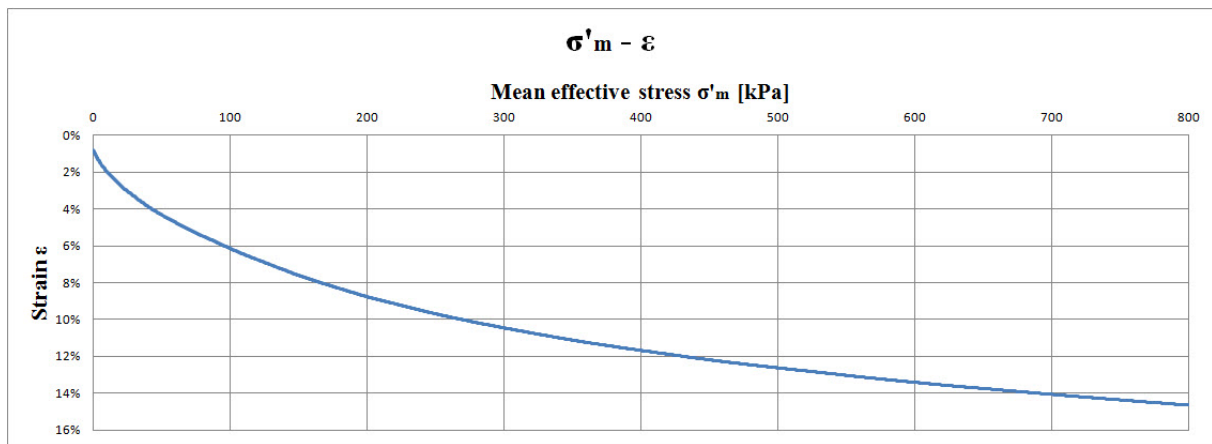


Figure 4.4.11: Sample T3-H14: Stress vs. strain from CRS oedometer test on specimen pre-strained to $\gamma_s = 18\%$.

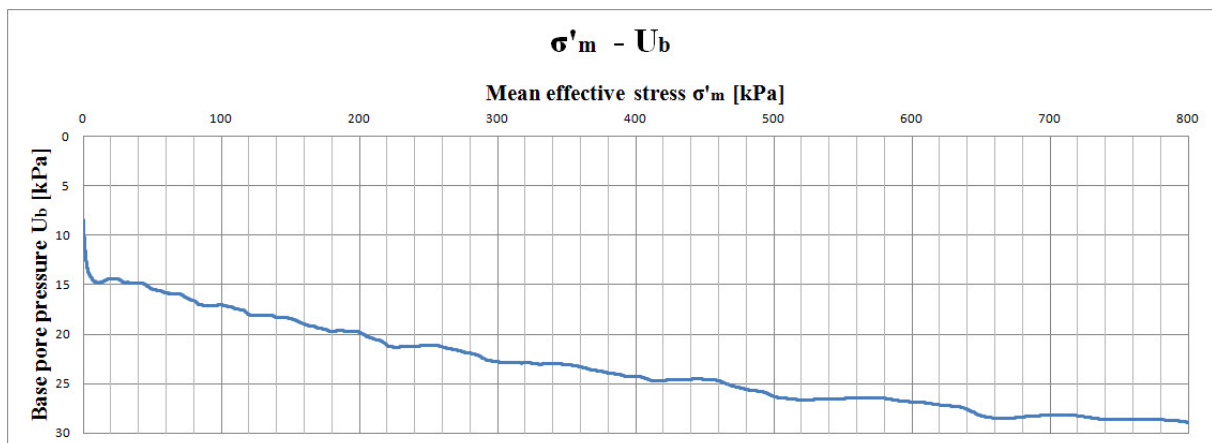


Figure 4.4.12: Sample T3-H14: Stress vs. pore pressure from CRS oedometer test on specimen pre-strained to $\gamma_s = 18\%$.

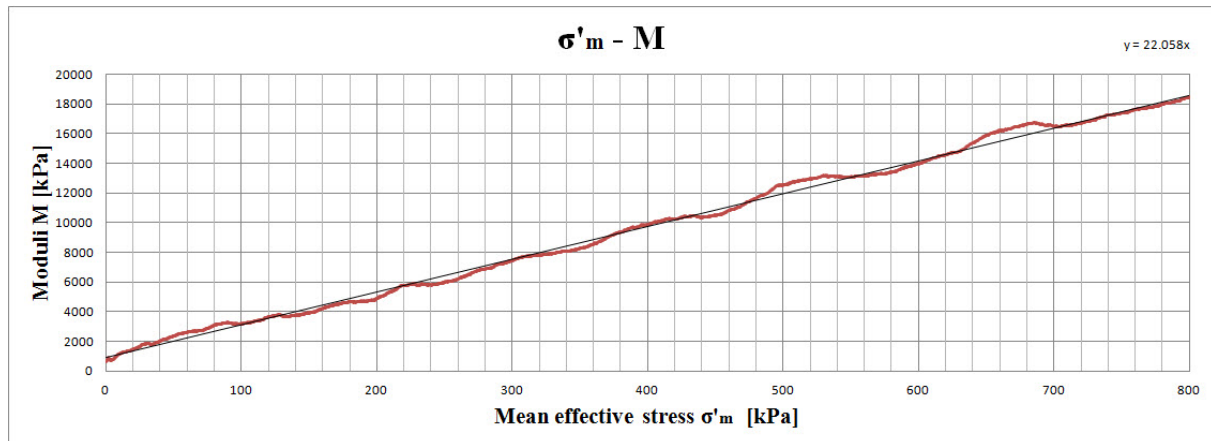


Figure 4.4.13: Sample T3-H14: Stress vs. oedometer modulus from CRS oedometer test on specimen pre-strained to $\gamma_s = 18\%$.

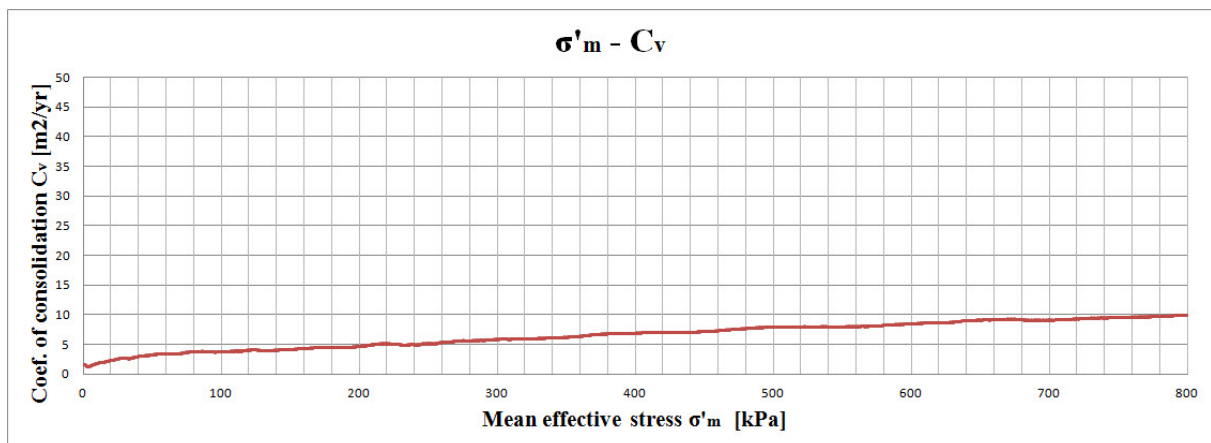


Figure 4.4.14: Sample T3-H14: Stress vs. coefficient of consolidation from CRS oedometer test on specimen pre-strained to $\gamma_s = 18\%$.

4.4.16 CRS Oedometer Test on Remoulded Clay

Calculation of water content for the test specimen is given in Table 4.4.20.

As follows from Table 4.4.20, there is a deviation between the value of water content for remoulded clay specimen and the values calculated for the whole sample T3-H14, undisturbed and pre-strained specimens (refer to Chapter 4.4.3, Chapters 4.4.14 and 4.4.15, respectively). The deviations in water content values are within 5%. An additional control measurement of water content has been done for the remoulded clay mass at the same time as the remoulded specimen was built into the oedometer. The control measurement showed water content $w = 32.14\%$.

Table 4.4.20: Sample T3-H14: Calculation of water content for remoulded specimen subjected to CRS oedometer test.

Parameter	Parameter value	Units
Mass, oedometer ring with specimen	114.15	gr.
Mass of oedometer ring	37.33	gr.
Mass of wet specimen (m_s+m_w)	76.82	gr.
Mass of dry specimen (m_s)	58.95	gr.
Mass of water (m_w)	17.87	gr.
Water content (w)	30.31	%

Figures 4.4.15-4.4.18 show the results of CRS oedometer test on totally remoulded clay sample T3-H14. The presented results consist of:

- Stress vs. strain plot ($\sigma'_m - \varepsilon$), Figure 4.4.15.
- Stress vs. pore pressure at sample base ($\sigma'_m - u_b$), Figure 4.4.16.
- Stress vs. modulus plot ($\sigma'_m - M$), Figure 4.4.17.
- Stress vs. coefficient of consolidation ($\sigma'_m - c_v$), Figure 4.4.18.

As follows from the results presented in Figures 4.4.15-4.4.18, the modulus number (m) for the remoulded specimen is constant and equal to 28.9. Coefficient of consolidation (c_v) is increasing with the stress level and is reaching its maximum of 11.9 m²/yr. at 800 kPa.

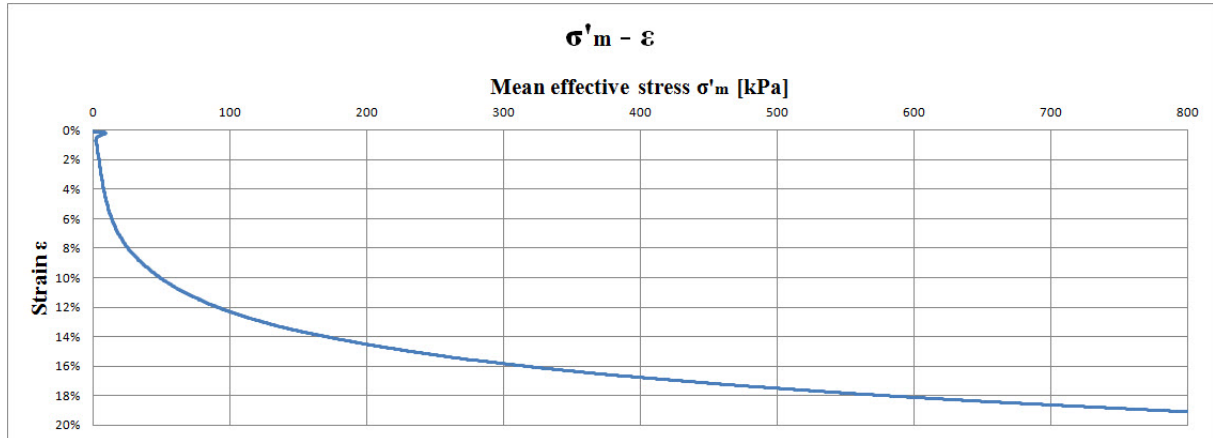


Figure 4.4.15: Sample T3-H14: Stress vs. strain from CRS oedometer test on remoulded specimen.

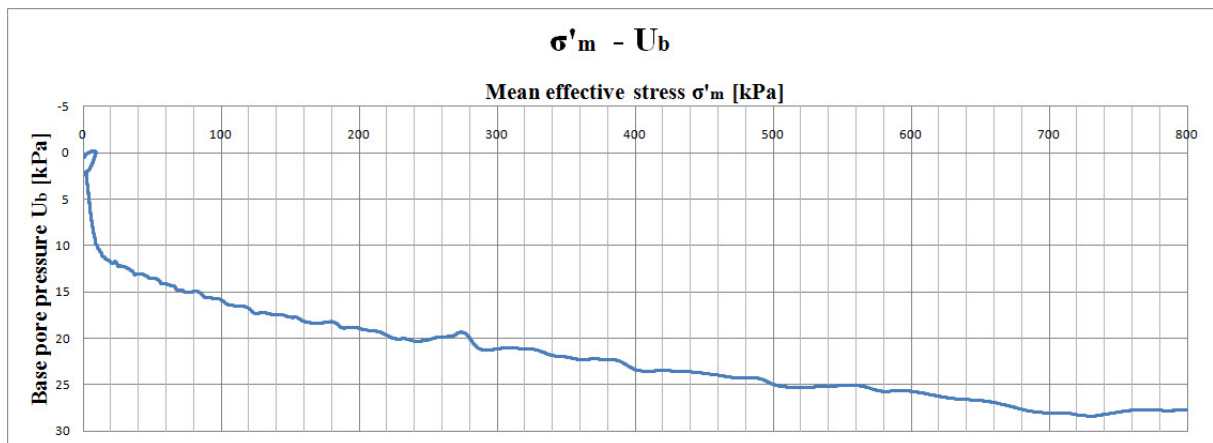


Figure 4.4.16: Sample T3-H14: Stress vs. pore pressure from CRS oedometer test on remoulded specimen.

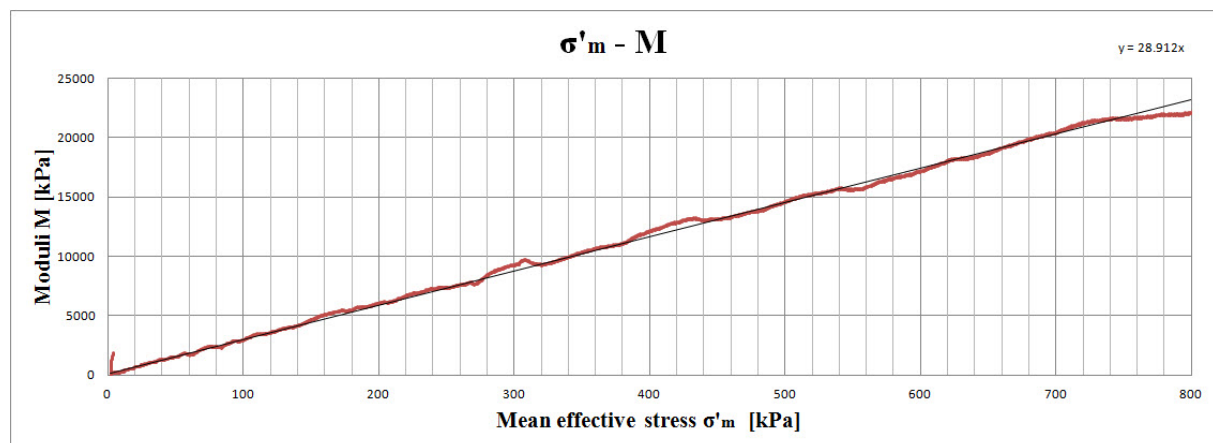


Figure 4.4.17: Sample T3-H14: Stress vs. oedometer modulus from CRS oedometer test on remoulded specimen.

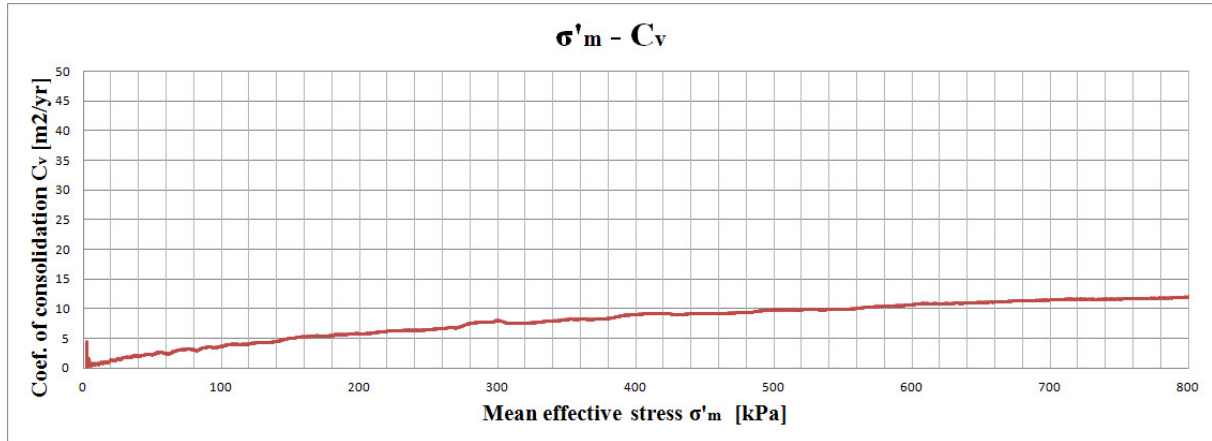


Figure 4.4.18: Sample T3-H14: Stress vs. coefficient of consolidation from CRS oedometer test on remoulded specimen.

4.5 Test Results for Sample S1-H1

4.5.1 Extrusion of the Sample

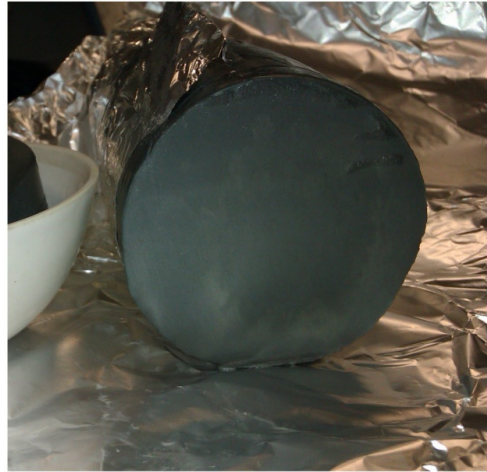
Sample S1-H1 was extruded in the laboratory at 13.04.2015. The pre-straining was achieved by extrusion of sample from $\phi 72.3$ mm to $\phi 54$ mm, corresponding to shear strain $\gamma_s = 117\%$ (refer to Chapter 3 for more details). Figure 4.5.1 shows subdivision of the sample during extrusion.

Displacement ratio is given by Eq. 3.4:

$$\delta_r = \frac{11}{6.4} = 1.72 \text{ mm/mm} \tag{Eq. 4.66}$$

The theoretical displacement ratio is 1.79 mm/mm as it has been shown in Table 3.2.2. The actual displacement ratio is lower than theoretical.

From visual observation of the sample, the clay was highly plastic and had a high water content. Contrary to the sample T1-H12 from Tiller, a visual inspection of pre-strained sample S1-H1 suggested that the strains were almost uniformly distributed since no distinct rings were observed in the pre-strained cross-section. The nearly uniform strain distribution was probably caused by the high plasticity of the material.



(a)



(b)

Figure 4.5.2: Variation of strains in the cross-section of pre-strained sample S1-H1: (a) Material from depth 8.376-8.440 m pre-strained in the beginning of extrusion process, (b) Material from depth 8.069-8.120 m pre-strained in the end of extrusion process.

4.5.2 Density Measurements

4.5.2.1 Average Density

Table 4.5.1 shows log of measurements made during calculation of mean density.

Table 4.5.1: Sample S1-H1: Calculation of mean density.

Parameter	Parameter value	Units
Length of sample (L)	75.7	cm
Diameter of sample (D _i)	7.23	cm
Volume of sample (V)	3107.9	cm ³
Mass of cylinder with sample and plug	9318	gr.
Mass of cylinder and plug	3578	gr.
Mass of sample (m)	5740	gr.
Mean density ($\bar{\rho}$)	1.85	gr./cm ³
Unit weight ($\bar{\gamma} = \bar{\rho} \cdot g$)	18.15	kN/m ³

4.5.2.2 Density by Small Ring

Table 4.5.2 contains log of measurements made during calculation of density with small ring.

Table 4.5.2: Sample S1-H1: Calculation of density and dry density with small ring.

	Ring	Bowl	
Parameter	Parameter value	Parameter value	Units
Total wet mass	97.75	92.34	gr.
Total dry mass	79.21	73.80	gr.
Mass of ring/bowl	32.10	26.69	gr.
Mass of wet sample ($m_s + m_w$)	65.65	65.65	gr.
Mass of dry sample (m_s)	47.11	47.11	gr.
Volume (V)	35.50	35.50	cm ³
Density (ρ)	1.85	1.85	gr./cm ³
Unit weight of soil (γ)	18.15	18.15	kN/m ³
Dry density (ρ_d)	1.33	1.33	gr./cm ³

As seen from Table 4.5.1 and 4.5.2, the calculated values of densities agree well.

4.5.2.3 Grain Density by Pycnometer

Table 4.5.3 shows log of measurements from pycnometer test. Grain density ρ_s is calculated from Eq. 3.9.

Table 4.5.3: Sample S1-H1: Calculation of grain density and unit weight of solids.

Parameter	Parameter value	Units
Mass of waterfilled pycnometer	148.47	gr.
Mass of pycnometer, water and specimen	160.04	gr.
Total dry mass	297.79	gr.
Mass of bowl	279.83	gr.
Dry mass of specimen (m_s)	17.96	gr.
Density of solids (ρ_s)	2.81	gr./cm ³
Unit weight of solids (γ_{solid})	27.57	kN/m ³

4.5.3 Water Content Measurements

Table 4.5.4 shows log of water content measurements. Test specimen No. 1 was undisturbed, while test specimens No. 2 and 3 were pre-strained.

As follows from Table 4.5.4, there is a fair agreement between the values of water content.

The mean value of natural water content is

$$w = \frac{39.86+40.45+43.62}{3} = 41.31 \% \quad (\text{Eq. 4.67})$$

Table 4.5.4: Sample S1-H1: Determination of water content.

	Specimen No. 1	Specimen No. 2	Specimen No. 3	
Parameter	Parameter value	Parameter value	Parameter value	Units
Depth	8.680 - 8.800	8.069 - 8.120	8.376 - 8.440	m
Total wet mass	167.25	140.23	152.93	gr.
Total dry mass	133.51	112.84	121.39	gr.
Mass of water (m_w)	33.74	27.39	31.54	gr.
Mass of bowl	48.87	45.12	49.09	gr.
Dry mass (m_s)	84.64	67.72	72.30	gr.
Water content (w)	39.86	40.45	43.62	%

4.5.4 Plastic and Liquid Limit

Table 4.5.5 shows log of plastic and liquid limit measurements.

Table 4.5.5: Sample S1-H1: Calculation of plastic and liquid limit.

	Liquid limit w_L	Plastic limit w_p	
Parameter	Parameter value	Parameter value	Units
Total wet mass	75.48	37.21	gr.
Total dry mass	66.05	35.81	gr.
Mass of water (m_w)	9.43	1.40	gr.
Mass of bowl	45.17	29.09	gr.
Dry mass (m_s)	20.88	6.72	gr.
Water content (w)	45.16	20.83	%

Liquidity and plasticity indices are found from Eq. 3.12 and 3.13, respectively:

$$I_L = \frac{w-w_p}{w_L-w_p} = \frac{41.31-20.83}{45.16-20.83} = 0.84 \quad (\text{Eq. 4.68})$$

$$I_p = w_L - w_p = 45.16 - 20.83 = 24.33 \%$$

In the calculation above, the value of natural water content is obtained from Eq. 4.67.

4.5.5 Degree of Saturation, Void Ratio and Porosity

Degree of saturation (S_r) is found from Eq. 3.14:

$$S_r = \frac{w \cdot \gamma}{\gamma_w \left(1 + w - \frac{\gamma}{\gamma_{solid}}\right)} = \frac{0.41 \cdot 18.15}{9.81 \cdot \left(1 + 0.41 - \frac{18.15}{27.57}\right)} = 1.00 \quad (\text{Eq. 4.69})$$

Void ratio (e) is found from Eq. 3.15:

$$e = \frac{\gamma_{solid} \cdot (1+w)}{\gamma} - 1 = \frac{27.57 \cdot (1+0.41)}{18.15} - 1 = 1.14 \quad (\text{Eq. 4.70})$$

Porosity (n) is found from Eq. 3.16:

$$n = \left(1 - \frac{\gamma}{\gamma_{solid} \cdot (1+w)}\right) \cdot 100 \% = \left(1 - \frac{18.15}{27.57 \cdot (1+0.41)}\right) \cdot 100 \% = 53.31 \% \quad (\text{Eq. 4.71})$$

Here, the value of natural water content w is obtained from Eq. 4.67, unit weight of soil γ is obtained from Table 4.5.2 and unit weight of solids γ_{solid} is obtained from Table 4.5.3.

4.5.6 Grain Size Distribution

Table 4.5.6 shows observations from hydrometer test.

Grain size distribution curve for sample S1-H1 is shown in Figure 4.5.3. The material consists of high percentage of clay particles. More than 60 % of grains are smaller than 0.002 mm (clay fraction), while about 35 % of grains belongs to silt fraction. Average grain size d_{50} and ratios d_{60}/d_{10} , d_{75}/d_{25} are not available of practical reasons. Maximum grain size d_{max} is 0.074 mm.

Table 4.5.6: Sample S1-H1: Observations from hydrometer test.

Total mass of dried sample (W), gr.		33.58							
Mass of dried sample (w_s) $d < 0.074$ mm, gr.		33.58							
Grain density (ρ_s), gr./cm³		2.81							
Coefficient a		96.75							
Passed time (t), min.	Temp. (T), °C	Concentration (R), gr./l	Eff. depth (Z_r), cm	Constant (K), $\sqrt{\frac{min}{cm}}$	$\sqrt{\frac{Z_r}{t}}$, $\sqrt{\frac{cm}{min}}$	Equiv. grain size (d_s), mm	Rel. weight (N) $d_s < 0.074$ mm, %	Rel. weight total sample, %	
1	22.1	33.5	6.7	0.01268	2.588	0.0328	96.52	96.52	
2	22.0	33.2	6.8	0.01272	1.844	0.0235	95.66	95.66	
5	21.7	33.0	6.9	0.01278	1.175	0.0150	95.08	95.08	
10	21.7	32.8	7.0	0.01278	0.837	0.0107	94.50	94.50	
20	21.7	32.5	7.2	0.01278	0.600	0.0077	93.64	93.64	
40	21.8	31.5	7.6	0.01274	0.436	0.0056	90.76	90.76	
80	21.7	29.0	8.5	0.01278	0.326	0.0042	83.55	83.55	
160	21.3	26.0	9.6	0.01282	0.245	0.0031	74.91	74.91	
320	21.2	23.0	10.8	0.01286	0.184	0.0024	66.27	66.27	
1320	21.1	18.5	12.4	0.01287	0.097	0.0012	53.30	53.30	

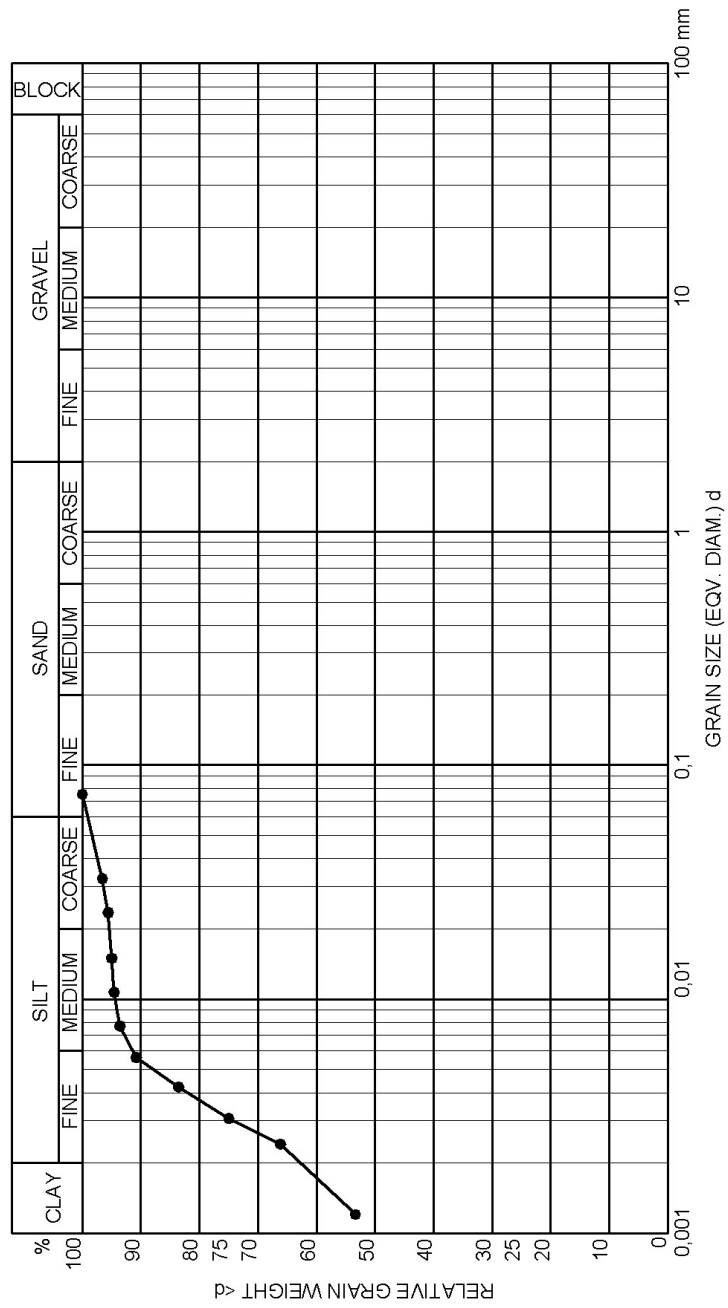


Figure 4.5.3: Sample S1-H1: Grain size distribution curve.

4.5.7 Undrained Shear Strength by UCT

Figure 4.5.4 shows deformation curve from UCT aligned with calibration chart. There is a clear brittle failure, with rapid decrease in load for small decrease in deformation. The failure occurs at load P_f of 44 kg (431.64 N) and failure strain ϵ_a of 5 %.

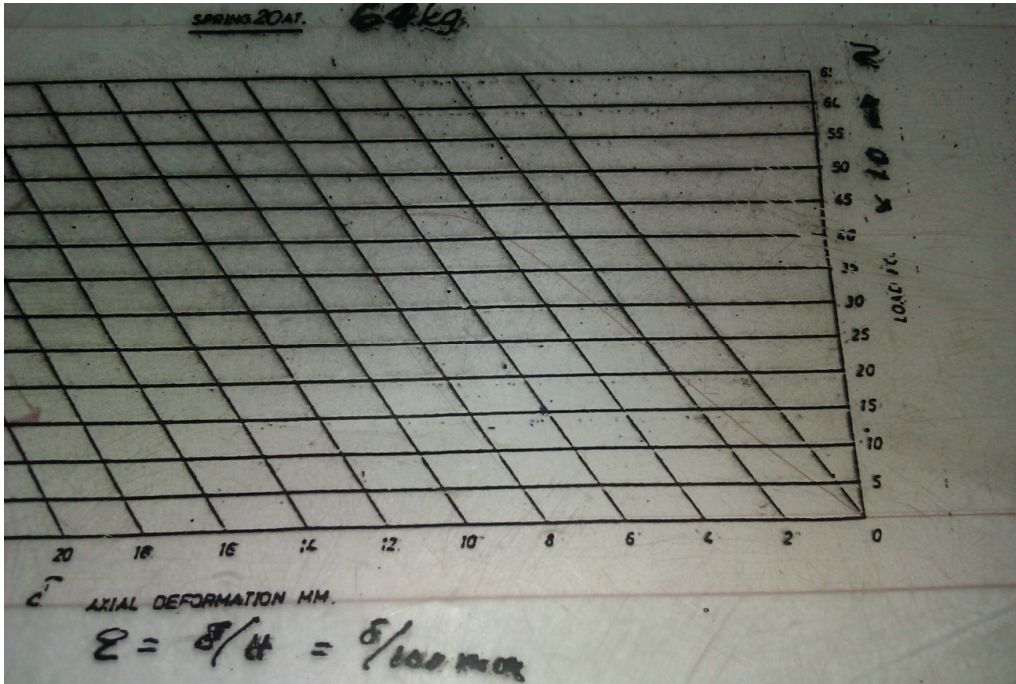


Figure 4.5.4: Sample S1-H1: Recorded deformation curve from UCT.

Undrained shear strength (s_u) is given by Eq. 3.24:

$$s_u = \tau_{max} = \frac{\sigma_1}{2} = \frac{P_f \cdot (1 - \epsilon_a)}{2 \cdot A_0} = \frac{431.64 \cdot (1 - 0.05)}{2 \cdot 2290} = 0.0895 \text{ N/mm}^2 = 89.5 \text{ kPa} \quad (\text{Eq. 4.72})$$

Figure 4.5.5 shows specimen at failure. The angle between visible failure plane and vertical axis was measured to 30° . A sketch of the shape of specimen at failure is shown in Figure 4.5.6.

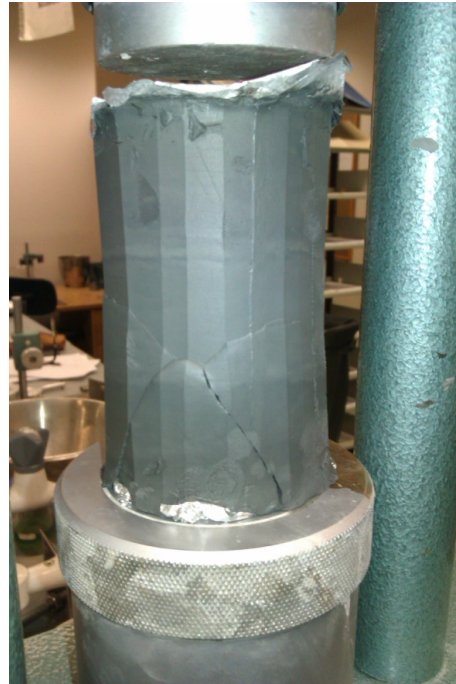


Figure 4.5.5: Sample S1-H1: Specimen at failure during UCT.

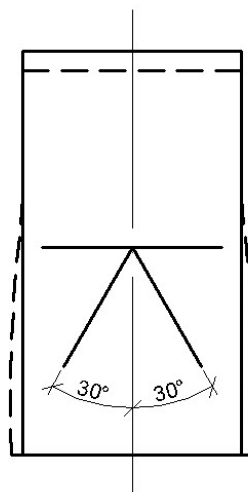


Figure 4.5.6: Sample S1-H1: Shape of specimen at failure during UCT.

4.5.8 Undrained and Remoulded Shear Strength by Fall Cone

Table 4.5.7 shows the results of falling cone test on undisturbed specimen. 100 gr. cone has been used.

There is a lacking agreement between the values of undrained shear strength determined by falling cone and by UCT. One of the possible explanations of the discrepancy is inhomogeneity of the material.

Table 4.5.7: Sample S1-H1: Results of falling cone test on undisturbed clay.

Intrusion No.	Intrusion, mm	Undrained shear strength s_u , kPa	Reported (mean) s_u , kPa
1	4.8	40.7	40.7
2	4.8	40.7	
3	4.8	40.7	

Table 4.5.8 shows the results of falling cone test on remoulded specimen. 60 gr. cone has been used.

Table 4.5.8: Sample S1-H1: Results of falling cone test on remoulded clay.

Set No.	Intrusion, mm	Remoulded shear strength s_r , kPa	Mean remoulded shear strength s_r , kPa	Reported remoulded shear strength s_r , kPa
1	6.8	5.1	5.2	5.1
	6.7	5.2		
2	6.9	4.9	5.1	
	6.7	5.2		

Sensitivity is given by Eq.3.25:

$$S_t = \frac{s_u}{s_r} = \frac{40.7}{5.1} = 8.0 \quad (\text{Eq. 4.73})$$

4.5.9 Shear Strength of Pre-Strained, Non-Reconsolidated Sample by Fall Cone

Table 4.5.9 shows test results from falling cone test on pre-strained, non-reconsolidated sample. 100 gr. cone has been used.

Table 4.5.9: Sample S1-H1: Results of falling cone test on pre-strained non-reconsolidated clay.

Intrusion No.	Intrusion, mm	Shear strength s , kPa	Reported (mean) s , kPa
1	10.9	10.0	9.3
2	11.4	9.1	
3	11.5	8.9	

4.5.10 Reconsolidation of Pre-Strained Specimen in the Oedometer at In-Situ Vertical Effective Stress 89.5 kPa

Table 4.5.10 shows data for calculation of water content in specimen prior to and after reconsolidation. Remaining pore pressure after 24 hrs. reconsolidation time was 1.1 kPa.

Table 4.5.10: Sample S1-H1: Calculation of water content prior to and after reconsolidation at in-situ vertical effective stress 89.5 kPa.

Parameter	Parameter value before reconsolidation	Parameter value after reconsolidation	Units
Mass, oedometer ring with wet specimen	112.71	109.84	gr.
Mass, oedometer ring	37.30	37.30	gr.
Mass of wet specimen	75.41	72.54	gr.
Mass of dry specimen (m_s)	54.58	54.58	gr.
Mass of water (m_w)	20.83	17.96	gr.
Water content (w and w_{re})	38.16	32.91	%

As follows from Table 4.5.10, reconsolidation at 89.5 kPa leads to change in water content:

$$\Delta w = w_{re} - w = 32.91 - 38.16 = -5.25 \% \quad (\text{Eq. 4.74})$$

After 24 hrs. reconsolidation at 89.5 kPa, volume of the specimen has been reduced by 9.59 %.

Table 4.5.11 shows the results of falling cone test on reconsolidated specimen. 100 gr. cone has been used in the test.

Table 4.5.11: Sample S1-H1: Results of falling cone test on pre-strained clay reconsolidated at in-situ vertical effective stress 89.5 kPa.

Intrusion No.	Intrusion, mm	Shear strength after reconsolidation s_{re} , kPa	Reported (mean) shear strength after reconsolidation s_{re} , kPa
1	3.0	74.1	69.2
2	3.3	66.7	
3	3.3	66.7	

As follows from Table 4.5.7 and 4.5.11, change in shear strength due to the pre-straining and subsequent reconsolidation at 89.5 kPa is:

$$\Delta s = s_{re} - s_u = 69.2 - 40.7 = 28.5 \text{ kPa} \quad (\text{Eq. 4.75})$$

Normalised change in shear strength due to the pre-straining and reconsolidation is:

$$\frac{\Delta s}{s_u} = \frac{s_{re} - s_u}{s_u} \cdot 100 \% = \frac{69.2 - 40.7}{40.7} \cdot 100 \% = 70.02 \% \quad (\text{Eq. 4.76})$$

4.5.11 Reconsolidation of Pre-Strained Specimen in the Oedometer at 100 kPa

Table 4.5.12 shows data for calculation of water content in specimen prior to and after reconsolidation. Remaining pore pressure after 24 hrs. reconsolidation time was 0.5 kPa.

As follows from Table 4.5.12, reconsolidation at 100 kPa leads to change in water content:

$$\Delta w = w_{re} - w = 35.70 - 42.47 = -6.77 \% \quad (\text{Eq. 4.77})$$

After 24 hrs. reconsolidation at 100 kPa, volume of the specimen has been reduced by 11.46 %.

Table 4.5.12: Sample S1-H1: Calculation of water content prior to and after reconsolidation at 100 kPa.

Parameter	Parameter value before reconsolidation	Parameter value after reconsolidation	Units
Mass, oedometer ring with wet specimen	112.93	109.45	gr.
Mass, oedometer ring	39.66	39.66	gr.
Mass of wet specimen	73.27	69.79	gr.
Mass of dry specimen (m_s)	51.43	51.43	gr.
Mass of water (m_w)	21.84	18.36	gr.
Water content (w and w_{re})	42.47	35.70	%

Table 4.5.13 shows the results of falling cone test on reconsolidated specimen. 100 gr. cone has been used in the test.

Table 4.5.13: Sample S1-H1: Results of falling cone test on pre-strained clay reconsolidated at 100 kPa.

Intrusion No.	Intrusion, mm	Shear strength after reconsolidation s_{re} , kPa	Reported (mean) shear strength after reconsolidation s_{re} , kPa
1	3.0	74.1	75.9
2	3.0	74.1	
3	2.8	79.5	

As follows from Table 4.5.7 and 4.5.13, change in shear strength due to the pre-straining and subsequent reconsolidation at 100 kPa is:

$$\Delta s = s_{re} - s_u = 75.9 - 40.7 = 35.2 \text{ kPa} \quad (\text{Eq. 4.78})$$

Normalised change in shear strength due to the pre-straining and reconsolidation is:

$$\frac{\Delta s}{s_u} = \frac{s_{re} - s_u}{s_u} \cdot 100 \% = \frac{75.9 - 40.7}{40.7} \cdot 100 \% = 86.49 \% \quad (\text{Eq. 4.79})$$

4.5.12 Reconsolidation of Pre-Strained Specimen in the Oedometer at 150 kPa

Table 4.5.14 shows data for calculation of water content in specimen prior to and after reconsolidation. Remaining pore pressure after 24 hrs. reconsolidation time was 0.9 kPa.

Table 4.5.14: Sample S1-H1: Calculation of water content prior to and after reconsolidation at 150 kPa.

Parameter	Parameter value before reconsolidation	Parameter value after reconsolidation	Units
Mass, oedometer ring with wet specimen	111.25	107.20	gr.
Mass, oedometer ring	37.29	37.29	gr.
Mass of wet specimen	73.96	69.91	gr.
Mass of dry specimen (m_s)	52.34	52.34	gr.
Mass of water (m_w)	21.62	17.57	gr.
Water content (w and w_{re})	41.31	33.57	%

As follows from Table 4.5.14, reconsolidation at 150 kPa leads to change in water content:

$$\Delta w = w_{re} - w = 33.57 - 41.31 = -7.74 \% \quad (\text{Eq. 4.80})$$

After 24 hrs. reconsolidation at 150 kPa, volume of the specimen has been reduced by 13.16 %.

Table 4.5.15 shows the results of falling cone test on reconsolidated specimen. 100 gr. cone has been used in the test.

As follows from Table 4.5.7 and 4.5.15, change in shear strength due to the pre-straining and subsequent reconsolidation at 150 kPa is:

$$\Delta s = s_{re} - s_u = 74.2 - 40.7 = 33.5 \text{ kPa} \quad (\text{Eq. 4.81})$$

Normalised change in shear strength due to the pre-straining and reconsolidation is:

$$\frac{\Delta s}{s_u} = \frac{s_{re} - s_u}{s_u} \cdot 100 \% = \frac{74.2 - 40.7}{40.7} \cdot 100 \% = 82.31 \% \quad (\text{Eq. 4.82})$$

Table 4.5.15: Sample S1-H1: Results of falling cone test on pre-strained clay reconsolidated at 150 kPa.

Intrusion No.	Intrusion, mm	Shear strength after reconsolidation s_{re} , kPa	Reported (mean) shear strength after reconsolidation s_{re} , kPa
1	2.9	77.0	74.2
2	3.1	71.6	
3	3.0	74.1	

4.5.13 Reconsolidation of Pre-Strained Specimen in the Oedometer at 200 kPa

Table 4.5.16 shows data for calculation of water content in specimen prior to and after reconsolidation. Remaining pore pressure after 24 hrs. reconsolidation time was 1.2 kPa.

Table 4.5.16: Sample S1-H1: Calculation of water content prior to and after reconsolidation at 200 kPa.

Parameter	Parameter value before reconsolidation	Parameter value after reconsolidation	Units
Mass, oedometer ring with wet specimen	112.67	108.42	gr.
Mass, oedometer ring	39.15	39.15	gr.
Mass of wet specimen	73.52	69.27	gr.
Mass of dry specimen (m_s)	52.21	52.21	gr.
Mass of water (m_w)	21.31	17.06	gr.
Water content (w and w_{re})	40.82	32.68	%

As follows from Table 4.5.16, reconsolidation at 200 kPa leads to change in water content:

$$\Delta w = w_{re} - w = 32.68 - 40.82 = -8.14 \% \quad (\text{Eq. 4.83})$$

After 24 hrs. reconsolidation at 200 kPa, volume of the specimen has been reduced by 14.39 %.

Table 4.5.17 shows the results of falling cone test on reconsolidated specimen. 100 gr. cone has been used in the test.

Table 4.5.17: Sample S1-H1: Results of falling cone test on pre-strained clay reconsolidated at 200 kPa.

Intrusion No.	Intrusion, mm	Shear strength after reconsolidation s_{re} , kPa	Reported (mean) shear strength after reconsolidation s_{re} , kPa
1	2.1	100.0	86.5
2	2.9	77.0	
3	2.7	82.4	

As follows from Table 4.5.7 and 4.5.17, change in shear strength due to the pre-straining and subsequent reconsolidation at 200 kPa is:

$$\Delta s = s_{re} - s_u = 86.5 - 40.7 = 45.8 \text{ kPa} \quad (\text{Eq. 4.84})$$

Normalised change in shear strength due to the pre-straining and reconsolidation is:

$$\frac{\Delta s}{s_u} = \frac{s_{re} - s_u}{s_u} \cdot 100 \% = \frac{86.5 - 40.7}{40.7} \cdot 100 \% = 112.53 \% \quad (\text{Eq. 4.85})$$

4.5.14 CRS Oedometer Test on Undisturbed Clay

Calculation of index parameters for the test specimen is given in Table 4.5.18. The value of grain density ρ_s used in the calculation is obtained from the results of pycnometer test (refer to Chapter 4.5.2).

As follows from Table 4.5.18, the calculated degree of saturation for oedometer test specimen agrees closely with the value calculated for the whole sample S1-H1 (refer to Chapter 4.5.5).

The deviation between values of water content and void ratio are 2.71 % and 0.08, respectively (refer to Chapters 4.5.3 and 4.5.5). The deviations are negligible.

Table 4.5.18: Sample S1-H1: Calculation of index parameters for undisturbed specimen subjected to CRS oedometer test.

Parameter	Parameter value	Units
Height of specimen (h_0)	20	mm
Area of specimen (A)	20	cm ²
Volume of specimen (V_0)	40	cm ³
Mass, oedometer ring with specimen	112.09	gr.
Mass of oedometer ring	39.65	gr.
Mass of wet specimen (m_s+m_w)	72.44	gr.
Mass of dry specimen (m_s)	50.30	gr.
Mass of water (m_w)	22.14	gr.
Water content (w)	44.02	%
Grain density (ρ_s)	2.81	gr./cm ³
Solids ($h_s = \frac{m_s}{A \cdot \rho_s}$)	0.90	cm
Void ratio ($e_0 = \frac{(h_0-h_s)}{h_s}$)	1.22	-
Degree of saturation ($S_t = \frac{\rho_s \cdot w}{\rho_w \cdot e_0}$)	1.00	-

Figures 4.5.7-4.5.11 show the results of CRS oedometer test on undisturbed sample S1-H1.

The presented results consist of:

- Stress vs. strain plot ($\sigma'_m - \epsilon$), Figure 4.5.7.
- Stress vs. pore pressure at sample base ($\sigma'_m - u_b$), Figure 4.5.8.
- Stress vs. modulus plot ($\sigma'_m - M$), Figure 4.5.9 and 4.5.10.

- Stress vs. coefficient of consolidation ($\sigma'_m - c_v$), Figure 4.5.11.

As follows from the test results presented in Figures 4.5.7-4.5.11, preconsolidation stress p'_c for sample S1-H1 is approximately 270 kPa. Constrained moduli in the overconsolidated range (M_o) and at the preconsolidation stress (M_n) are 5.5 MPa and 2.5 MPa, respectively. For normally consolidated range, the modulus number (m) is 19.3.

Overconsolidation ratio for sample S1-H1 is given as

$$OCR = \frac{p'_c}{\sigma'_{v0}} = \frac{270}{89.5} = 3.0 \tag{Eq. 4.86}$$

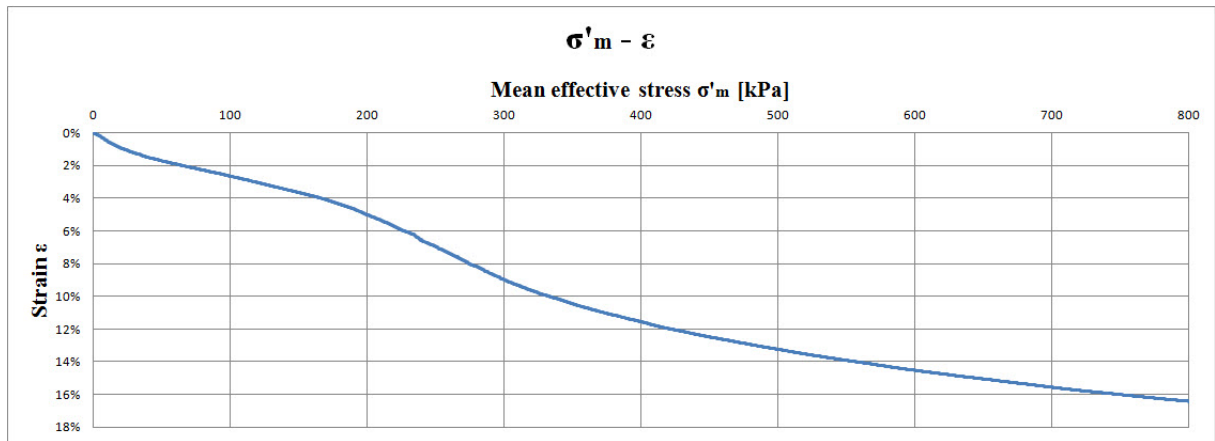


Figure 4.5.7: Sample S1-H1: Stress vs. strain from CRS oedometer test on undisturbed specimen.

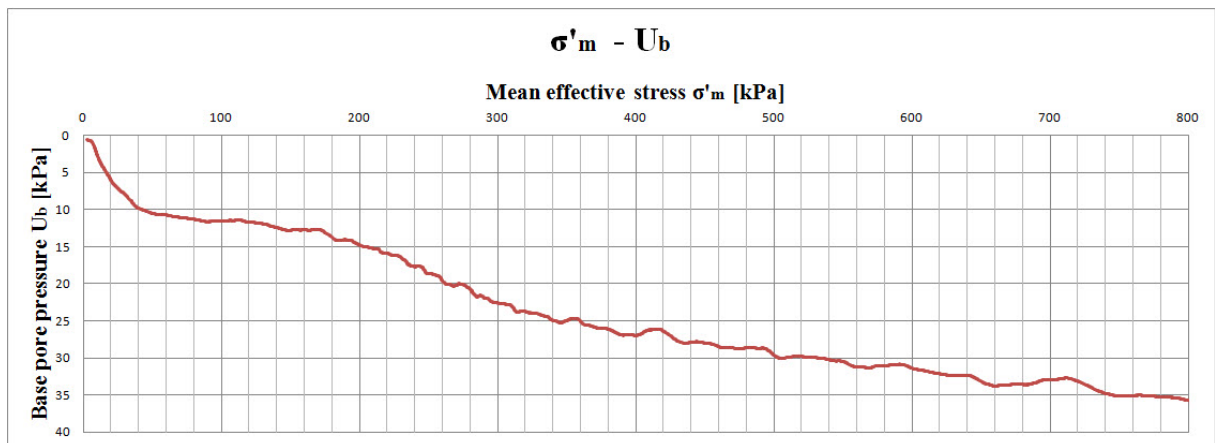


Figure 4.5.8: Sample S1-H1: Stress vs. pore pressure from CRS oedometer test on undisturbed specimen.

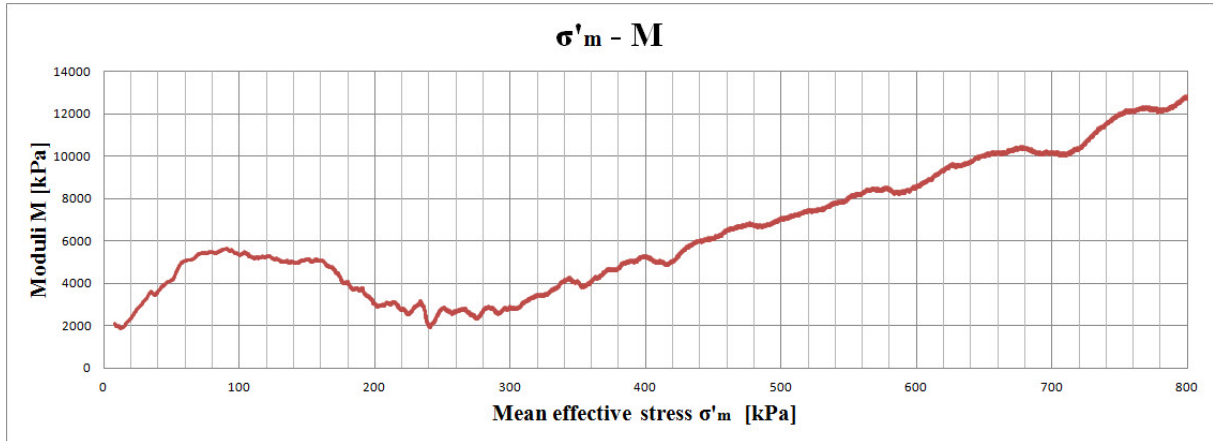


Figure 4.5.9: Sample S1-H1: Stress vs. oedometer modulus from CRS oedometer test on undisturbed specimen.

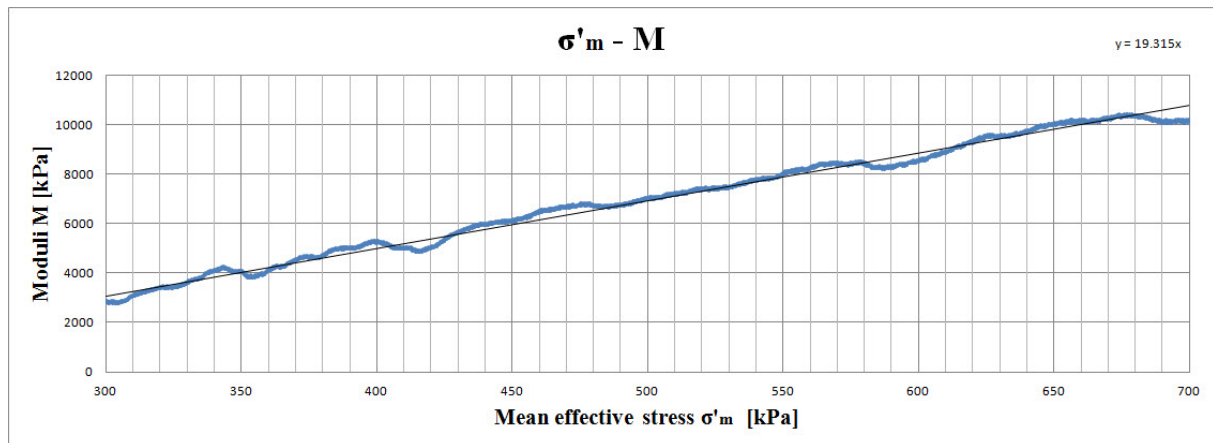


Figure 4.5.10: Sample S1-H1: Modulus number from CRS oedometer test on undisturbed specimen.

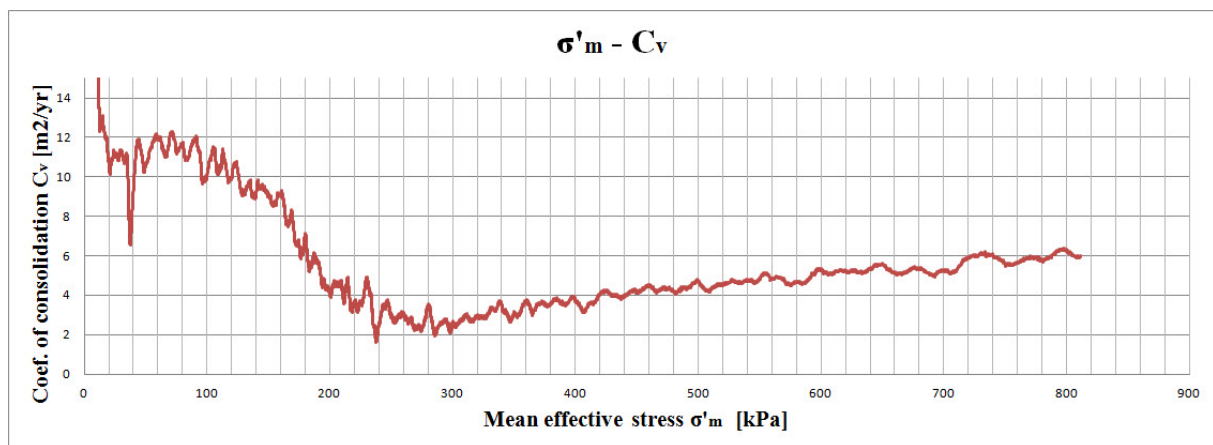


Figure 4.5.11: Sample S1-H1: Stress vs. coefficient of consolidation from CRS oedometer test on undisturbed specimen.

The plot of coefficient of consolidation suggests some disturbance of the sample. The results are however readable. Coefficients of consolidation in the overconsolidated zone (c_{v0}) and at about p'_c (c_{v1}) are $11 \text{ m}^2/\text{yr.}$ and $3 \text{ m}^2/\text{yr.}$, respectively.

4.5.15 CRS Oedometer Test on Pre-Strained Clay

Calculation of water content for the test specimen is given in Table 4.5.19.

Table 4.5.19: Sample S1-H1: Calculation of water content for pre-strained specimen subjected to CRS oedometer test.

Parameter	Parameter value	Units
Mass, oedometer ring with specimen	112.66	gr.
Mass of oedometer ring	39.65	gr.
Mass of wet specimen (m_s+m_w)	73.01	gr.
Mass of dry specimen (m_s)	51.43	gr.
Mass of water (m_w)	21.58	gr.
Water content (w)	41.96	%

As seen from Table 4.5.19, calculated value of water content for the test specimen agrees well with water content values for the whole sample S1-H1 (refer to Chapter 4.5.3).

Figures 4.5.12-4.5.15 show the results of CRS oedometer test on sample S1-H1 pre-strained to shear strain $\gamma_s = 117 \%$. The presented results consist of:

- Stress vs. strain plot ($\sigma'_m - \epsilon$), Figure 4.5.12.
- Stress vs. pore pressure at sample base ($\sigma'_m - u_b$), Figure 4.5.13.
- Stress vs. modulus plot ($\sigma'_m - M$), Figure 4.5.14.
- Stress vs. coefficient of consolidation ($\sigma'_m - c_v$), Figure 4.5.15.

As follows from the results presented in Figures 4.5.12-4.5.15, the modulus number (m) for the specimen S1-H1 pre-strained to shear strain $\gamma_s = 117 \%$ is equal to 22.2.

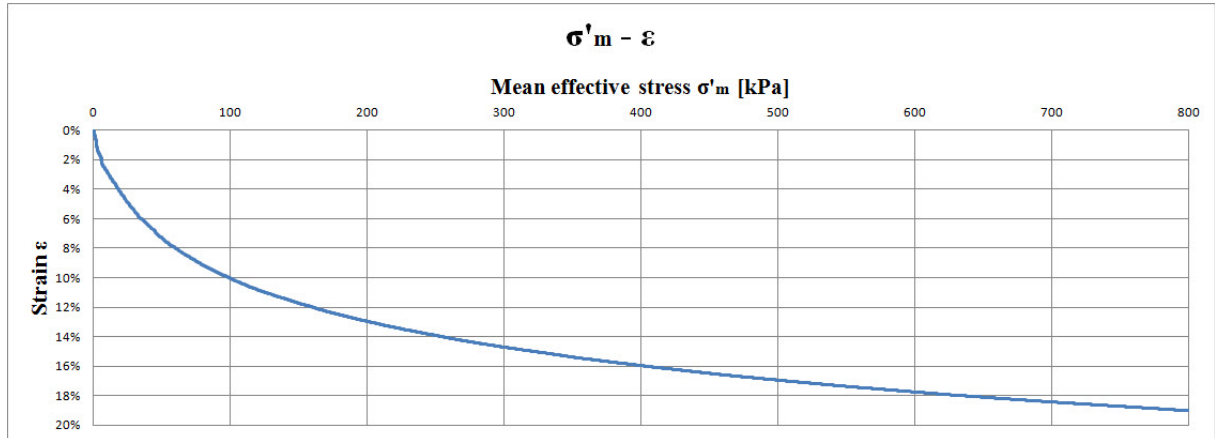


Figure 4.5.12: Sample S1-H1: Stress vs. strain from CRS oedometer test on specimen pre-strained to $\gamma_s = 117\%$.

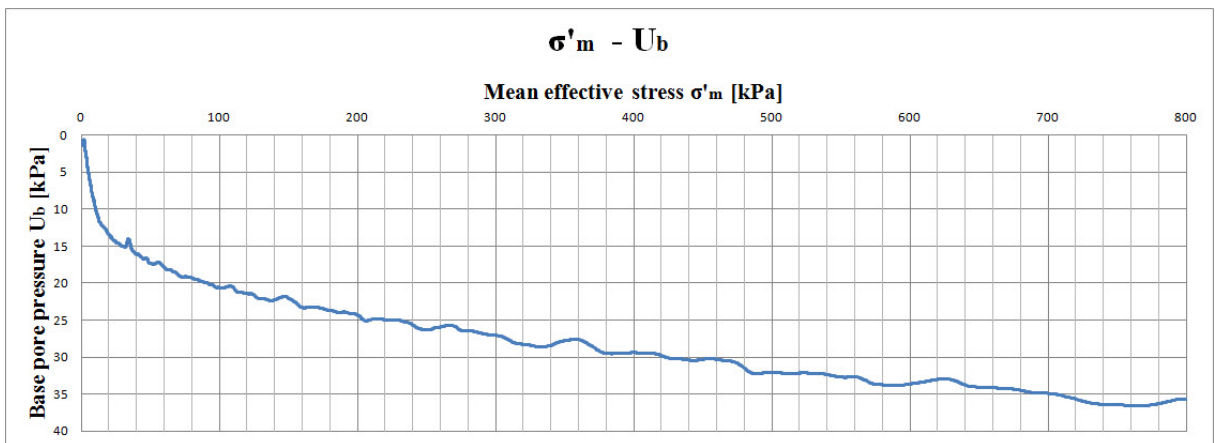


Figure 4.5.13: Sample S1-H1: Stress vs. pore pressure from CRS oedometer test on specimen pre-strained to $\gamma_s = 117\%$.

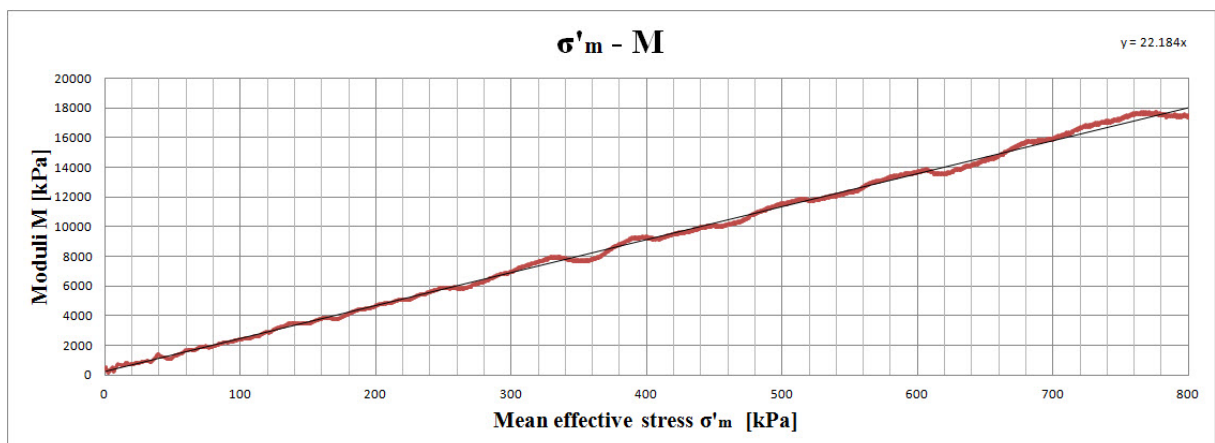


Figure 4.5.14: Sample S1-H1: Stress vs. oedometer modulus from CRS oedometer test on specimen pre-strained to $\gamma_s = 117\%$.

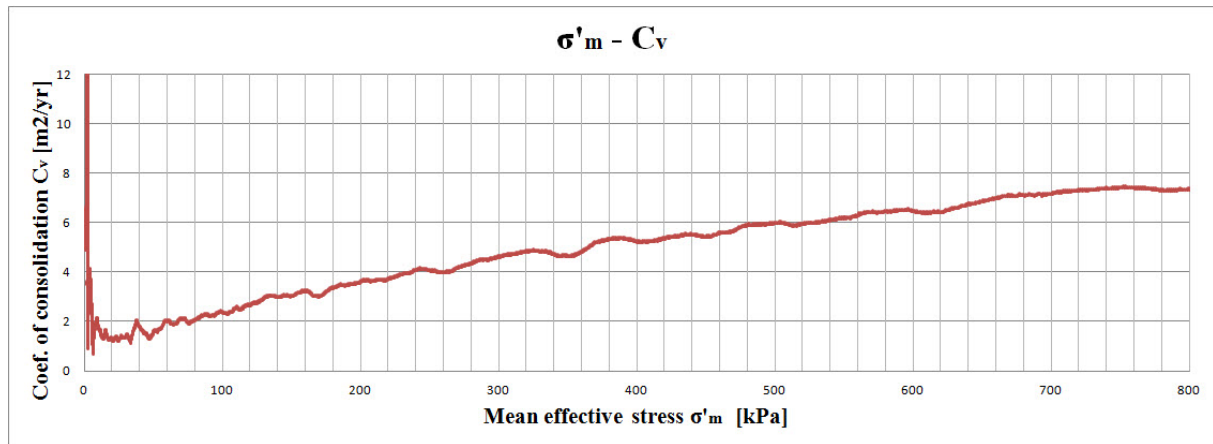


Figure 4.5.15: Sample S1-H1: Stress vs. coefficient of consolidation from CRS oedometer test on specimen pre-strained to $\gamma_s = 117\%$.

Coefficient of consolidation (c_v) is increasing almost linearly with the stress level, reaching a maximum of $7.3 \text{ m}^2/\text{yr}$. at stress level of 800 kPa.

4.5.16 CRS Oedometer Test on Remoulded Clay

Calculation of water content for the test specimen is given in Table 4.5.20.

An additional control measurement of water content has been done for the remoulded clay mass at the same time as the remoulded specimen was built into the oedometer. The control measurement showed water content $w = 41.29\%$.

Figures 4.5.16-4.5.19 show the results of CRS oedometer test on remoulded clay sample S1-H1. The presented results consist of:

- Stress vs. strain plot ($\sigma'_m - \varepsilon$), Figure 4.5.16.
- Stress vs. pore pressure at sample base ($\sigma'_m - u_b$), Figure 4.5.17.
- Stress vs. modulus plot ($\sigma'_m - M$), Figure 4.5.18.
- Stress vs. coefficient of consolidation ($\sigma'_m - c_v$), Figure 4.5.19.

As follows from the results presented in Figures 4.5.16-4.5.19, the modulus number (m) for the remoulded specimen is constant and equal to 28.0. Coefficient of consolidation (c_v) is increasing with the stress level and is reaching its maximum of $4.6 \text{ m}^2/\text{yr}$. at 800 kPa.

Table 4.5.20: Sample S1-H1: Calculation of water content for remoulded specimen subjected to CRS oedometer test.

Parameter	Parameter value	Units
Mass, oedometer ring with specimen	110.88	gr.
Mass of oedometer ring	39.15	gr.
Mass of wet specimen (m_s+m_w)	71.73	gr.
Mass of dry specimen (m_s)	50.12	gr.
Mass of water (m_w)	21.61	gr.
Water content (w)	43.12	%

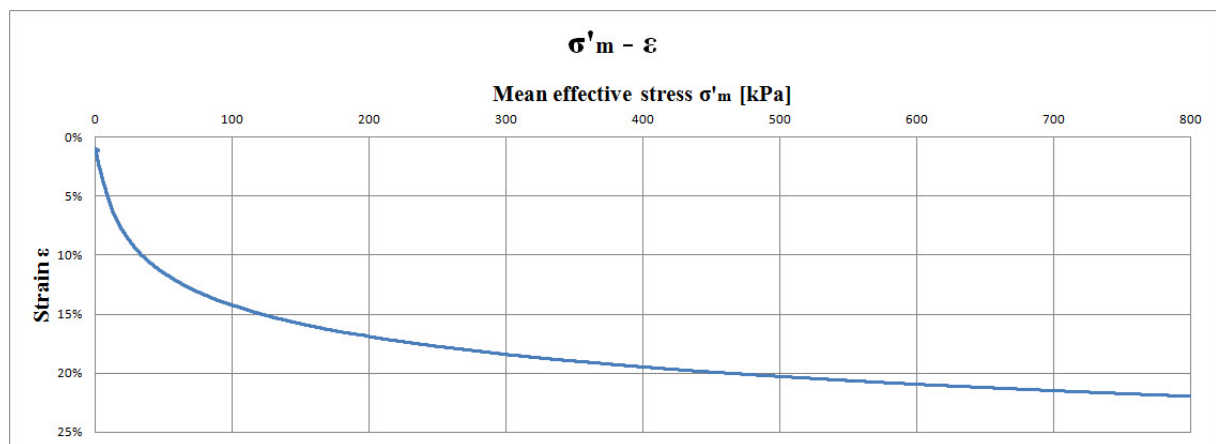


Figure 4.5.16: Sample S1-H1: Stress vs. strain from CRS oedometer test on remoulded specimen.

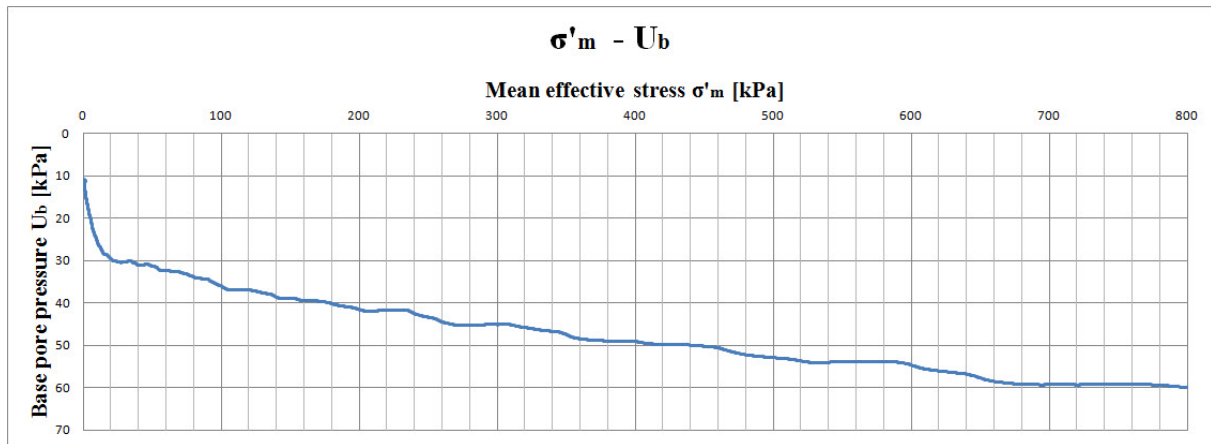


Figure 4.5.17: Sample S1-H1: Stress vs. pore pressure from CRS oedometer test on remoulded specimen.

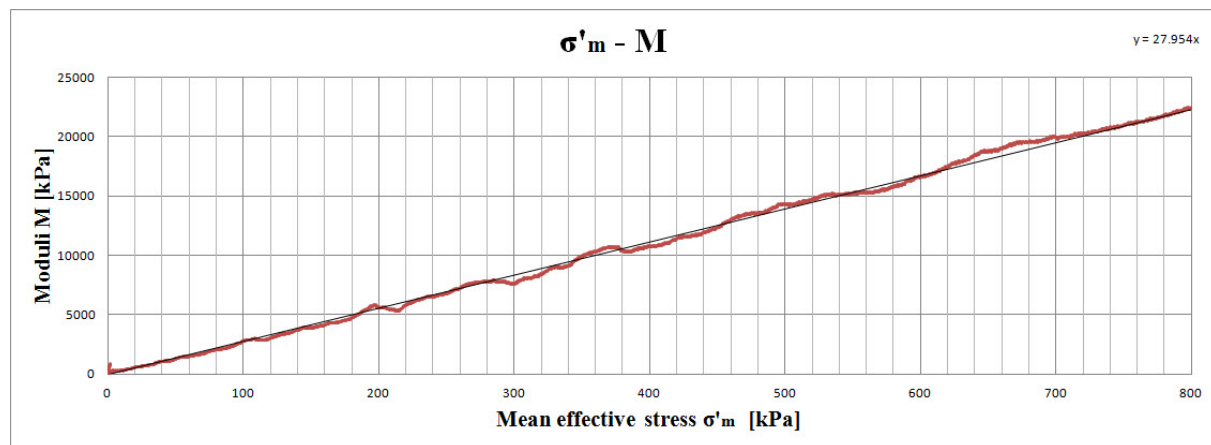


Figure 4.5.18: Sample S1-H1: Stress vs. oedometer modulus from CRS oedometer test on remoulded specimen.

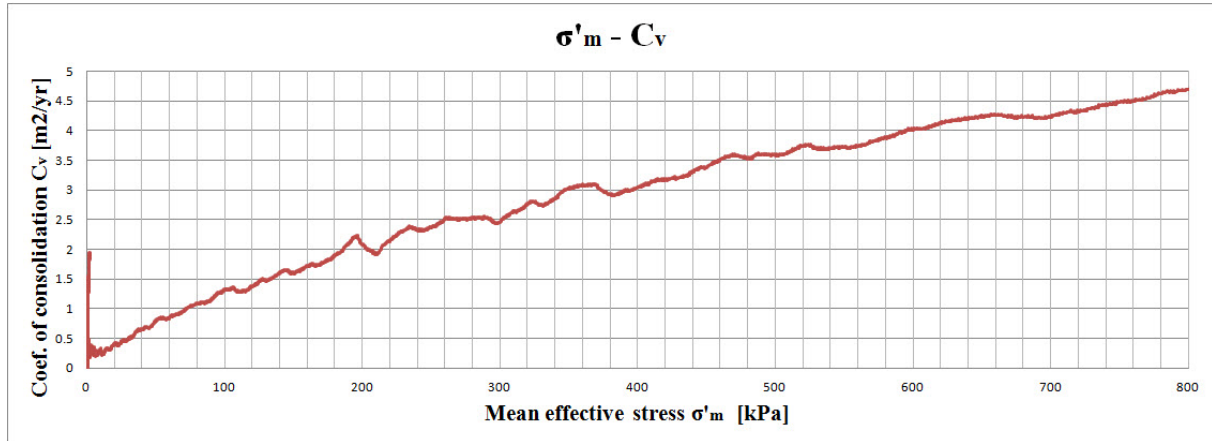


Figure 4.5.19: Sample S1-H1: Stress vs. coefficient of consolidation from CRS oedometer test on remoulded specimen.

4.6 Test Results for Sample S2-H1

4.6.1 Extrusion of the Sample

Sample S2-H1 was extruded in the laboratory at 17.04.2015. The pre-straining was achieved by extrusion of the sample from $\phi 72.3$ mm to $\phi 60$ mm, corresponding to shear strain $\gamma_s = 66$ % (refer to Chapter 3 for more details). Figure 4.6.1 shows subdivision of the sample during extrusion.

Displacement ratio is given by Eq. 3.4:

$$\delta_r = \frac{11}{8.1} = 1.36 \text{ mm/mm} \quad (\text{Eq. 4.87})$$

The observed displacement ratio is lower than theoretical displacement ratio (1.45 mm/mm) shown in Table 3.2.2.

Nearly no strain variation has been noticed in the pre-strained cross-section. Figure 4.6.2 shows cross-section of the material pre-strained in the beginning and in the end of pre-straining process. The strain variation in these two cross-sections is almost identical and hardly visible.

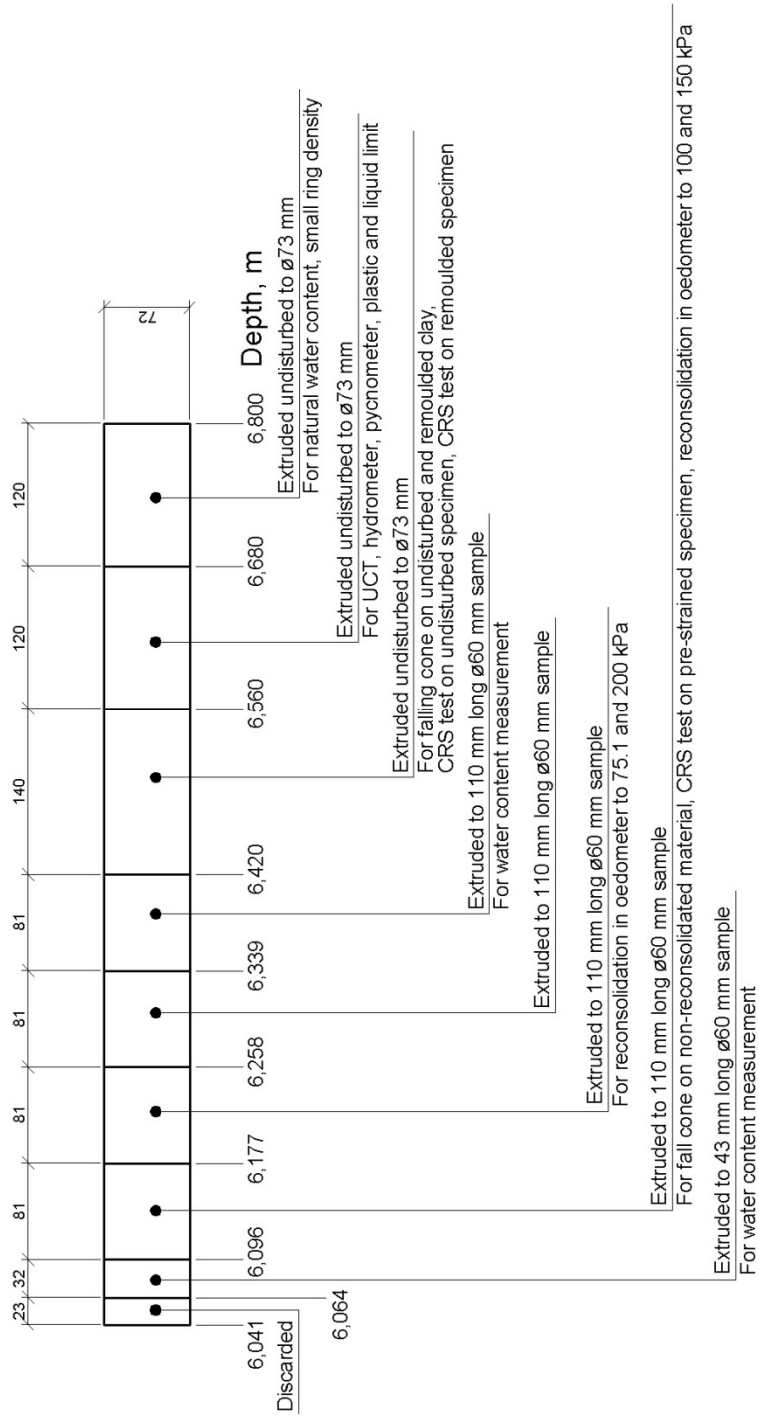


Figure 4.6.1: Sample S2-H1: Extrusion and subdivision.

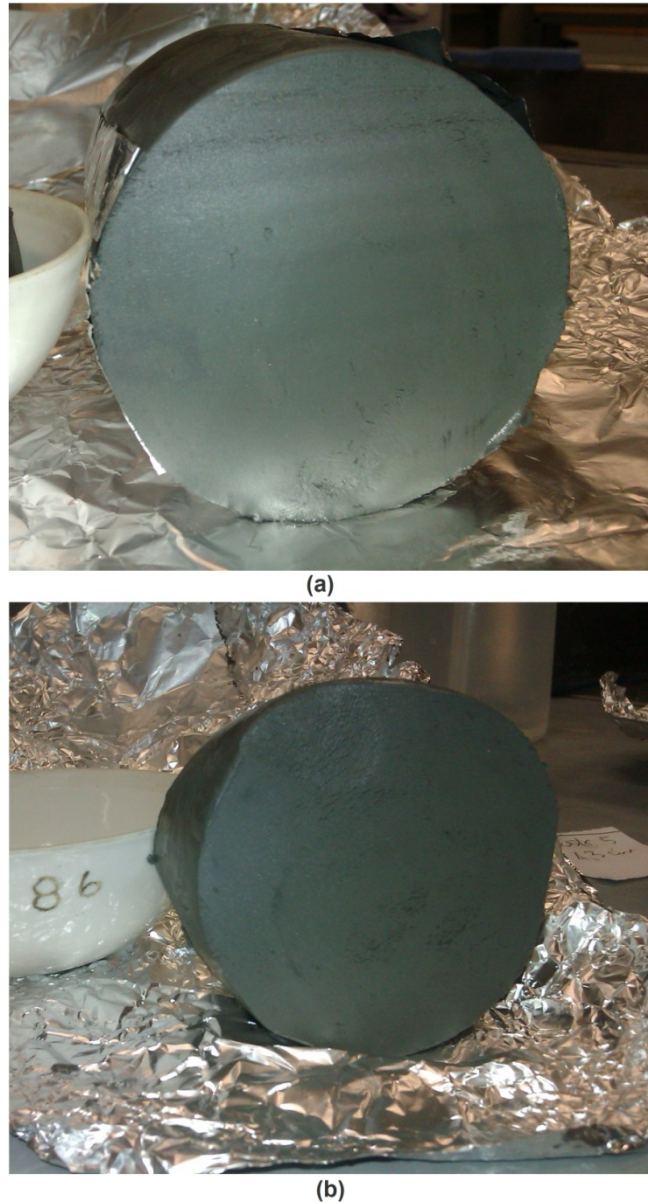


Figure 4.6.2: Variation of strains in the cross-section of pre-strained sample S2-H1: (a) Material from depth 6.339-6.420 m pre-strained in the beginning of pre-straining process, (b) Material from depth 6.064-6.096 m pre-strained in the end of pre-straining process.

4.6.2 Density Measurements

4.6.2.1 Average Density

Table 4.6.1 shows log of measurements carried out for the calculation of mean density.

Table 4.6.1: Sample S2-H1: Calculation of mean density.

Parameter	Parameter value	Units
Length of sample (L)	75.9	cm
Diameter of sample (D _i)	7.23	cm
Volume of sample (V)	3116.1	cm ³
Mass of cylinder with sample and plug	9623	gr.
Mass of cylinder and plug	3547	gr.
Mass of sample (m)	6076	gr.
Mean density ($\bar{\rho}$)	1.95	gr./cm ³
Unit weight ($\bar{\gamma} = \bar{\rho} \cdot g$)	19.13	kN/m ³

4.6.2.2 Density by Small Ring

Table 4.6.2 contains log of measurements carried out for the calculation of density with small ring.

Table 4.6.2: Sample S2-H1: Calculation of density and dry density with small ring.

	Ring	Bowl	
Parameter	Parameter value	Parameter value	Units
Total wet mass	98.64	115.41	gr.
Total dry mass	80.65	97.42	gr.
Mass of ring/bowl	32.10	48.87	gr.
Mass of wet sample ($m_s + m_w$)	66.54	66.54	gr.
Mass of dry sample (m_s)	48.55	48.55	gr.
Volume (V)	35.50	35.50	cm ³
Density (ρ)	1.87	1.87	gr./cm ³
Unit weight of soil (γ)	18.34	18.34	kN/m ³
Dry density (ρ_d)	1.37	1.37	gr./cm ³

As seen from Table 4.6.1 and 4.6.2, there is a fair agreement between the calculated values of densities.

4.6.2.3 Grain Density by Pycnometer

Table 4.6.3 shows log of measurements from pycnometer test. Grain density ρ_s is calculated from Eq. 3.9.

Table 4.6.3: Sample S2-H1: Calculation of grain density and unit weight of solids.

Parameter	Parameter value	Units
Mass of waterfilled pycnometer	148.47	gr.
Mass of pycnometer, water and specimen	153.22	gr.
Total dry mass	217.91	gr.
Mass of bowl	210.51	gr.
Dry mass of specimen (m_s)	7.40	gr.
Density of solids (ρ_s)	2.79	gr./cm ³
Unit weight of solids (γ_{solid})	27.37	kN/m ³

4.6.3 Water Content Measurements

Table 4.6.4 shows log of water content measurements. Test specimen No. 1 was undisturbed, while test specimens No. 2 and 3 were pre-strained.

As Table 4.6.4 shows, there is some scatter in the measurements of water content. The mean value of water content is

$$w = \frac{36.09+29.49+32.65}{3} = 32.74 \% \quad (\text{Eq. 4.88})$$

Table 4.6.4: Sample S2-H1: Determination of water content.

	Specimen No. 1	Specimen No. 2	Specimen No. 3	
Parameter	Parameter value	Parameter value	Parameter value	Units
Depth	6.680 - 6.800	6.064 - 6.096	6.339 - 6.420	m
Total wet mass	148.02	140.25	185.71	gr.
Total dry mass	122.05	118.72	151.90	gr.
Mass of water (m_w)	25.97	21.53	33.81	gr.
Mass of bowl	50.10	45.70	48.36	gr.
Dry mass (m_s)	71.95	73.02	103.54	gr.
Water content (w)	36.09	29.49	32.65	%

4.6.4 Plastic and Liquid Limit

Table 4.6.5 shows log of plastic and liquid limit measurements.

Liquidity and plasticity indices are found from Eq. 3.12 and 3.13, respectively:

$$I_L = \frac{w - w_p}{w_L - w_p} = \frac{32.74 - 19.33}{38.46 - 19.33} = 0.70 \quad (\text{Eq. 4.89})$$

$$I_p = w_L - w_p = 38.46 - 19.33 = 19.13 \%$$

The value of natural water content in Eq. 4.89 is obtained from Eq. 4.88.

Table 4.6.5: Sample S2-H1: Calculation of plastic and liquid limit.

	Liquid limit w_L	Plastic limit w_p	
Parameter	Parameter value	Parameter value	Units
Total wet mass	86.88	36.72	gr.
Total dry mass	76.38	35.57	gr.
Mass of water (m_w)	10.50	1.15	gr.
Mass of bowl	49.08	29.62	gr.
Dry mass (m_s)	27.30	5.95	gr.
Water content (w_L and w_p)	38.46	19.33	%

4.6.5 Degree of Saturation, Void Ratio and Porosity

Degree of saturation (S_r) is found from Eq. 3.14:

$$S_r = \frac{w \cdot \gamma}{\gamma_w \cdot \left(1 + w - \frac{\gamma}{\gamma_{solid}}\right)} = \frac{0.33 \cdot 18.34}{9.81 \cdot \left(1 + 0.33 - \frac{18.34}{27.37}\right)} = 0.93 \quad (\text{Eq. 4.90})$$

Void ratio (e) is found from Eq. 3.15:

$$e = \frac{\gamma_{solid} \cdot (1+w)}{\gamma} - 1 = \frac{27.37 \cdot (1+0.33)}{18.34} - 1 = 0.98 \quad (\text{Eq. 4.91})$$

Porosity (n) is found from Eq. 3.16:

$$n = \left(1 - \frac{\gamma}{\gamma_{solid} \cdot (1+w)}\right) \cdot 100 \% = \left(1 - \frac{18.34}{27.37 \cdot (1+0.33)}\right) \cdot 100 \% = 49.62 \% \quad (\text{Eq. 4.92})$$

Here, the value of natural water content w is obtained from Eq. 4.88, unit weight of soil γ is obtained from Table 4.6.2 and unit weight of solids γ_{solid} is obtained from Table 4.6.3.

4.6.6 Grain Size Distribution

Table 4.6.6 shows observations from hydrometer test.

Table 4.6.6: Sample S2-H1: Observations from hydrometer test.

Total mass of dried sample (W), gr.		37.43						
Mass of dried sample (w_s) $d < 0.074$ mm, gr.		37.40						
Grain density (ρ_s), gr./cm³		2.79						
Coefficient a		97.2						
Passed time (t), min.	Temp. (T), °C	Concentration (R), gr./l	Eff. depth (Z_r), cm	Constant (K), $\sqrt{\frac{min}{cm}}$	$\sqrt{\frac{Z_r}{t}}$, $\sqrt{\frac{cm}{min}}$	Equiv. grain size (d_s), mm	Rel. weight (N) $d_s < 0.074$ mm, %	Rel. weight total sample, %
1	21.7	36	5.7	0.01285	2.387	0.0307	93.56	93.49
2	21.7	35.5	6.0	0.01285	1.732	0.0223	92.26	92.19
5	21.2	34.0	6.5	0.01291	1.140	0.0147	88.36	88.29
10	21.2	32.0	7.3	0.01291	0.854	0.0110	83.17	83.10
20	20.9	28.3	8.6	0.01296	0.656	0.0085	73.55	73.49
40	20.8	26.2	9.4	0.01298	0.485	0.0063	68.09	68.04
80	20.8	23.5	10.5	0.01298	0.362	0.0047	61.07	61.02
160	20.8	20.5	11.7	0.01298	0.270	0.0035	53.28	53.24
320	20.8	18.5	12.4	0.01298	0.197	0.0026	48.08	48.04
1320	20.8	15.5	13.5	0.01298	0.101	0.0013	40.28	40.25

Grain size distribution curve for sample S2-H1 is shown in Figure 4.6.3. Ratios d_{60}/d_{10} and d_{75}/d_{25} are not available of practical reasons. Maximum grain size d_{max} is 0.125 mm and

average grain size d_{50} is 0.00292 mm. The clay content is 45 % and silt content is approximately 53 %.

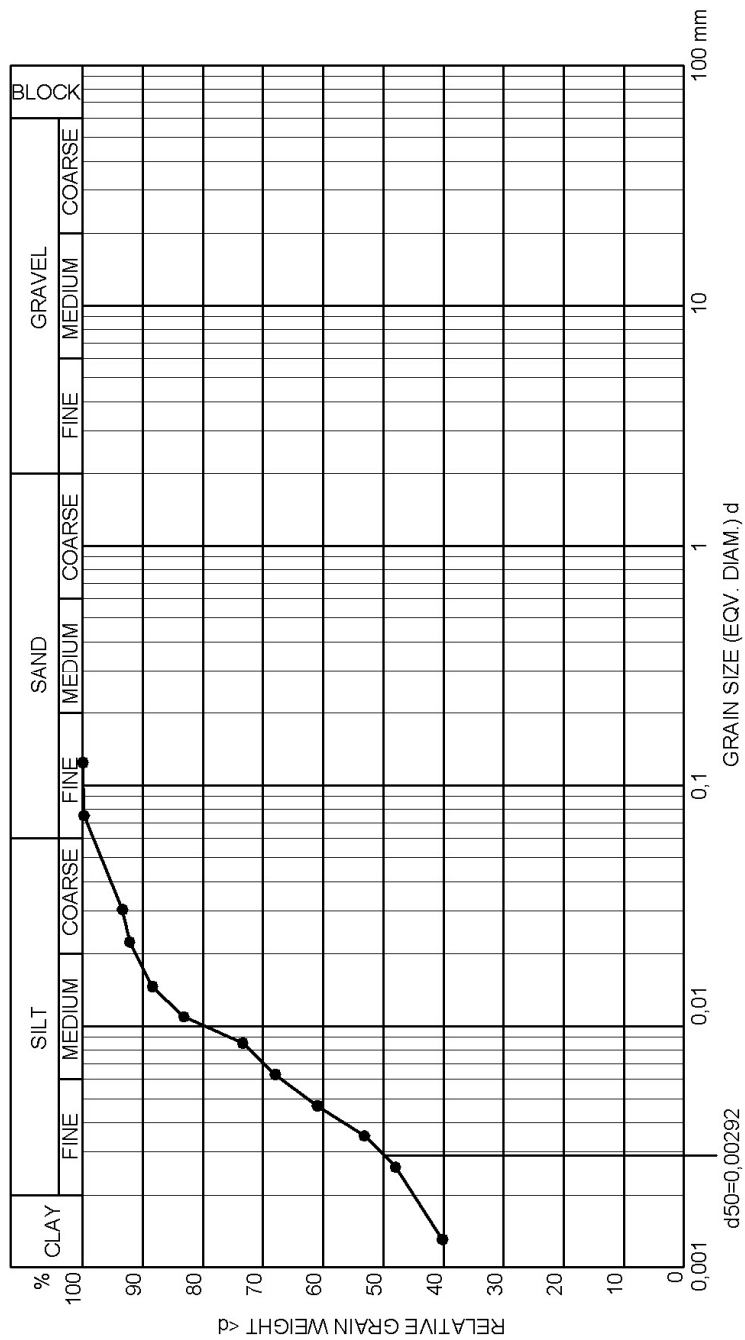


Figure 4.6.3: Sample S2-H1: Grain size distribution curve.

4.6.7 Undrained Shear Strength by UCT

Figure 4.6.4 shows deformation curve from UCT aligned with calibration chart. There is a clear failure load P_f of 43 kg (421.83 N) at failure strain ε_a of 7 %. The failure state can be described as plastic yielding, with almost constant axial stress σ_1 for increasing strain.

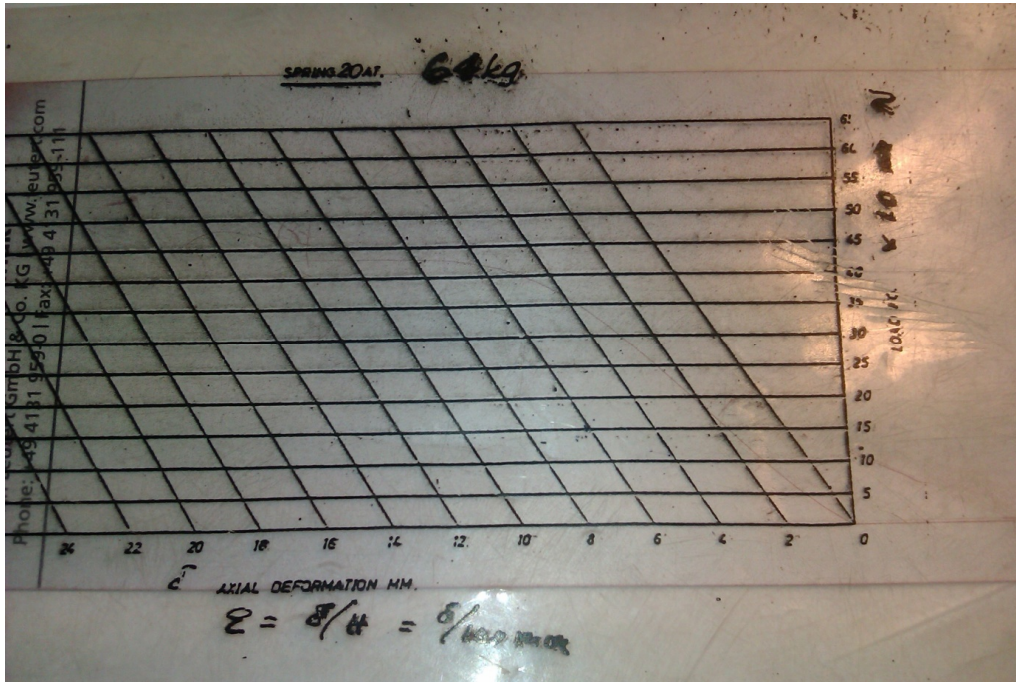


Figure 4.6.4: Sample S2-H1: Recorded deformation curve from UCT.

Undrained shear strength (s_u) is given by Eq. 3.24:

$$s_u = \tau_{max} = \frac{\sigma_1}{2} = \frac{P_f \cdot (1 - \varepsilon_a)}{2 \cdot A_0} = \frac{421.83 \cdot (1 - 0.07)}{2 \cdot 2290} = 0.0857 \text{ N/mm}^2 = 85.7 \text{ kPa} \quad (\text{Eq. 4.93})$$

Figure 4.6.5 shows specimen at failure. The angle between visible failure plane and vertical axis was measured as 35° . A sketch of the shape of specimen at failure is shown in Figure 4.6.6.

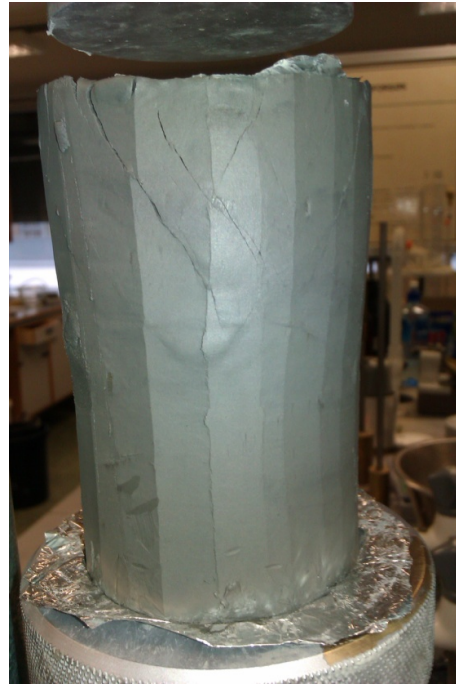


Figure 4.6.5: Sample S2-H1: Specimen at failure during UCT.

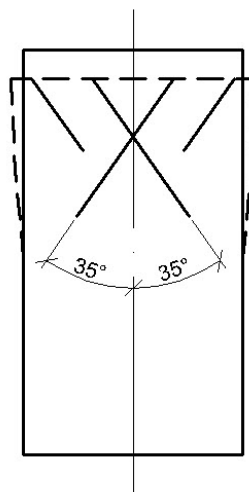


Figure 4.6.6: Sample S2-H1: Shape of specimen at failure during UCT.

4.6.8 Undrained and Remoulded Shear Strength by Fall Cone

Table 4.6.7 shows the results of falling cone test on undisturbed specimen. 100 gr. cone has been used.

Table 4.6.7: Sample S2-H1: Results of falling cone test on undisturbed clay.

Intrusion No.	Intrusion, mm	Undrained shear strength s_u , kPa	Reported (mean) s_u , kPa
1	2.9	77.0	72.6
2	3.3	66.7	
3	3.0	74.1	

Table 4.6.8 shows the results of falling cone test on remoulded specimen. 60 gr. cone has been used.

Table 4.6.8: Sample S2-H1: Results of falling cone test on remoulded clay.

Set No.	Intrusion, mm	Remoulded shear strength s_r , kPa	Mean remoulded shear strength s_r , kPa	Reported remoulded shear strength s_r , kPa
1	5.2	8.4	8.2	7.5
	5.4	7.9		
2	5.6	7.5	7.5	
	5.6	7.5		

The sensitivity is given by Eq.3.25:

$$S_t = \frac{s_u}{s_r} = \frac{72.6}{7.5} = 9.7 \quad (\text{Eq. 4.94})$$

4.6.9 Shear Strength of Pre-Strained, Non-Reconsolidated Sample by Fall Cone

Table 4.6.9 shows test results from falling cone test on pre-strained, non-reconsolidated sample. 100 gr. cone has been used.

Table 4.6.9: Sample S2-H1: Results of falling cone test on pre-strained non-reconsolidated clay.

Intrusion No.	Intrusion, mm	Shear strength s , kPa	Reported (mean) s , kPa
1	5.2	36.8	37.1
2	5.0	38.7	
3	5.3	35.8	

4.6.10 Reconsolidation of Pre-Strained Specimen in the Oedometer at In-Situ Vertical Effective Stress 75.1 kPa

Table 4.6.10 shows data for calculation of water content in specimen prior to and after reconsolidation. Remaining pore pressure after 24 hrs. reconsolidation time was 0.5 kPa.

Table 4.6.10: Sample S2-H1: Calculation of water content prior to and after reconsolidation at in-situ vertical effective stress 75.1 kPa.

Parameter	Parameter value before reconsolidation	Parameter value after reconsolidation	Units
Mass, oedometer ring with wet specimen	116.81	114.86	gr.
Mass, oedometer ring	37.36	37.36	gr.
Mass of wet specimen	79.45	77.50	gr.
Mass of dry specimen (m_s)	60.77	60.77	gr.
Mass of water (m_w)	18.68	16.73	gr.
Water content (w and w_{re})	30.74	27.53	%

As follows from Table 4.6.10, reconsolidation at 75.1 kPa leads to change in water content:

$$\Delta w = w_{re} - w = 27.53 - 30.74 = -3.21 \% \quad (\text{Eq. 4.95})$$

After 24 hrs. reconsolidation at 75.1 kPa, volume of the specimen has been reduced by 7.94 %.

Table 4.6.11 shows the results of falling cone test on reconsolidated specimen. 100 gr. cone has been used in the test.

Table 4.6.11: Sample S2-H1: Results of falling cone test on pre-strained clay reconsolidated at in-situ vertical effective stress 75.1 kPa.

Intrusion No.	Intrusion, mm	Shear strength after reconsolidation s_{re} , kPa	Reported (mean) shear strength after reconsolidation s_{re} , kPa
1	3.1	71.6	71.1
2	3.4	64.7	
3	2.9	77.0	

As follows from Tables 4.6.7 and 4.6.11, change in shear strength due to the pre-straining and subsequent reconsolidation at 75.1 kPa is:

$$\Delta s = s_{re} - s_u = 71.1 - 72.6 = -1.5 \text{ kPa} \quad (\text{Eq. 4.96})$$

Normalised change in shear strength due to the pre-straining and reconsolidation is:

$$\frac{\Delta s}{s_u} = \frac{s_{re} - s_u}{s_u} \cdot 100 \% = \frac{71.1 - 72.6}{72.6} \cdot 100 \% = -2.07 \% \quad (\text{Eq. 4.97})$$

4.6.11 Reconsolidation of Pre-Strained Specimen in the Oedometer at 100 kPa

Table 4.6.12 shows data for calculation of water content in specimen prior to and after reconsolidation. Remaining pore pressure after 24 hrs. reconsolidation time was 0.2 kPa.

As follows from Table 4.6.12, reconsolidation at 100 kPa leads to change in water content:

$$\Delta w = w_{re} - w = 26.39 - 30.01 = -3.62 \% \quad (\text{Eq. 4.98})$$

After 24 hrs. reconsolidation at 100 kPa, volume of the specimen has been reduced by 8.31 %.

Table 4.6.12: Sample S2-H1: Calculation of water content prior to and after reconsolidation at 100 kPa.

Parameter	Parameter value before reconsolidation	Parameter value after reconsolidation	Units
Mass, oedometer ring with wet specimen	118.12	115.92	gr.
Mass, oedometer ring	39.15	39.15	gr.
Mass of wet specimen	78.97	76.77	gr.
Mass of dry specimen (m_s)	60.74	60.74	gr.
Mass of water (m_w)	18.23	16.03	gr.
Water content (w and w_{re})	30.01	26.39	%

Table 4.6.13 shows the results of falling cone test on reconsolidated specimen. 100 gr. cone has been used in the test.

Table 4.6.13: Sample S2-H1: Results of falling cone test on pre-strained clay reconsolidated at 100 kPa.

Intrusion No.	Intrusion, mm	Shear strength after reconsolidation s_{re} , kPa	Reported (mean) shear strength after reconsolidation s_{re} , kPa
1	2.6	85.3	86.5
2	2.4	91.7	
3	2.7	82.4	

As follows from Table 4.6.7 and 4.6.13, change in shear strength due to the pre-straining and subsequent reconsolidation at 100 kPa is:

$$\Delta s = s_{re} - s_u = 86.5 - 72.6 = 13.9 \text{ kPa} \quad (\text{Eq. 4.99})$$

Normalised change in shear strength due to the pre-straining and reconsolidation is:

$$\frac{\Delta s}{s_u} = \frac{s_{re} - s_u}{s_u} \cdot 100 \% = \frac{86.5 - 72.6}{72.6} \cdot 100 \% = 19.15 \% \quad (\text{Eq. 4.100})$$

4.6.12 Reconsolidation of Pre-Strained Specimen in the Oedometer at 150 kPa

Table 4.6.14 shows data for calculation of water content in specimen prior to and after reconsolidation. Remaining pore pressure after 24 hrs. reconsolidation time was 1.3 kPa.

Table 4.6.14: Sample S2-H1: Calculation of water content prior to and after reconsolidation at 150 kPa.

Parameter	Parameter value before reconsolidation	Parameter value after reconsolidation	Units
Mass, oedometer ring with wet specimen	116.78	114.04	gr.
Mass, oedometer ring	37.31	37.31	gr.
Mass of wet specimen	79.47	76.73	gr.
Mass of dry specimen (m_s)	60.91	60.91	gr.
Mass of water (m_w)	18.56	15.82	gr.
Water content (w and w_{re})	30.47	25.97	%

As follows from Table 4.6.14, reconsolidation at 150 kPa leads to change in water content:

$$\Delta w = w_{re} - w = 25.97 - 30.47 = -4.50 \% \quad (\text{Eq. 4.101})$$

After 24 hrs. reconsolidation at 150 kPa, volume of the specimen has been reduced by 9.85 %.

Table 4.6.15 shows the results of falling cone test on reconsolidated specimen. 100 gr. cone has been used in the test.

As follows from Table 4.6.7 and 4.6.15, change in shear strength due to the pre-straining and subsequent reconsolidation at 150 kPa is:

$$\Delta s = s_{re} - s_u = 102.3 - 72.6 = 29.7 \text{ kPa} \quad (\text{Eq. 4.102})$$

Normalised change in shear strength due to the pre-straining and reconsolidation is:

$$\frac{\Delta s}{s_u} = \frac{s_{re} - s_u}{s_u} \cdot 100 \% = \frac{102.3 - 72.6}{72.6} \cdot 100 \% = 40.91 \% \quad (\text{Eq. 4.103})$$

Table 4.6.15: Sample S2-H1: Results of falling cone test on pre-strained clay reconsolidated at 150 kPa.

Intrusion No.	Intrusion, mm	Shear strength after reconsolidation s_{re} , kPa	Reported (mean) shear strength after reconsolidation s_{re} , kPa
1	1.9	105.0	102.3
2	2.2	97.0	
3	1.9	105.0	

4.6.13 Reconsolidation of Pre-Strained Specimen in the Oedometer at 200 kPa

Table 4.6.16 shows data for calculation of water content in specimen prior to and after reconsolidation. Remaining pore pressure after 24 hrs. reconsolidation time was 0.1 kPa.

Table 4.6.16: Sample S2-H1: Calculation of water content prior to and after reconsolidation at 200 kPa.

Parameter	Parameter value before reconsolidation	Parameter value after reconsolidation	Units
Mass, oedometer ring with wet specimen	116.75	113.04	gr.
Mass, oedometer ring	39.15	39.15	gr.
Mass of wet specimen	77.60	73.89	gr.
Mass of dry specimen (m_s)	58.54	58.54	gr.
Mass of water (m_w)	19.06	15.35	gr.
Water content (w and w_{re})	32.56	26.22	%

As follows from Table 4.6.16, reconsolidation at 200 kPa leads to change in water content:

$$\Delta w = w_{re} - w = 26.22 - 32.56 = -6.34 \% \quad (\text{Eq. 4.104})$$

After 24 hrs. reconsolidation at 200 kPa, volume of the specimen has been reduced by 11.17 %.

Table 4.6.17 shows the results of falling cone test on reconsolidated specimen. 100 gr. cone has been used in the test.

Table 4.6.17: Sample S2-H1: Results of falling cone test on pre-strained clay reconsolidated at 200 kPa.

Intrusion No.	Intrusion, mm	Shear strength after reconsolidation s_{re} , kPa	Reported (mean) shear strength after reconsolidation s_{re} , kPa
1	1.9	105.0	105.0
2	1.8	108.0	
3	2.0	102.0	

As follows from Table 4.6.7 and 4.6.17, change in shear strength due to the pre-straining and subsequent reconsolidation at 200 kPa is:

$$\Delta s = s_{re} - s_u = 105.0 - 72.6 = 32.4 \text{ kPa} \quad (\text{Eq. 4.105})$$

Normalised change in shear strength due to the pre-straining and reconsolidation is:

$$\frac{\Delta s}{s_u} = \frac{s_{re} - s_u}{s_u} \cdot 100 \% = \frac{105.0 - 72.6}{72.6} \cdot 100 \% = 44.63 \% \quad (\text{Eq. 4.106})$$

4.6.14 CRS Oedometer Test on Undisturbed Clay

Calculation of index parameters for the test specimen is given in Table 4.6.18. The value of grain density ρ_s used in the calculation is obtained from the results of pycnometer test (refer to Chapter 4.6.2).

As follows from Table 4.6.18, the value of natural water content for oedometer test specimen is similar to the value calculated for the whole sample S2-H1 (refer to Chapters 4.6.3). There is some scatter in the values of degree of saturation (the deviation is 0.07) and void ratio (the deviation is 0.07) calculated for oedometer test specimen and for the whole sample (refer to Chapter 4.6.5 for details).

Table 4.6.18: Sample S2-H1: Calculation of index parameters for undisturbed specimen subjected to CRS oedometer test.

Parameter	Parameter value	Units
Height of specimen (h_0)	20	mm
Area of specimen (A)	20	cm ²
Volume of specimen (V_0)	40	cm ³
Mass, oedometer ring with specimen	116.86	gr.
Mass of oedometer ring	39.15	gr.
Mass of wet specimen (m_s+m_w)	77.71	gr.
Mass of dry specimen (m_s)	58.39	gr.
Mass of water (m_w)	19.32	gr.
Water content (w)	33.09	%
Grain density (ρ_s)	2.79	gr./cm ³
Solids ($h_s = \frac{m_s}{A \cdot \rho_s}$)	1.05	cm
Void ratio ($e_0 = \frac{h_0 - h_s}{h_s}$)	0.91	-
Degree of saturation ($S_t = \frac{\rho_s \cdot w}{\rho_w \cdot e_0}$)	1.00	-

Figures 4.6.7-4.6.11 show the results of CRS oedometer test on undisturbed sample S2-H1.

The presented results consist of:

- Stress vs. strain plot ($\sigma'_m - \epsilon$), Figure 4.6.7.
- Stress vs. pore pressure at sample base ($\sigma'_m - u_b$), Figure 4.6.8.
- Stress vs. modulus plot ($\sigma'_m - M$), Figure 4.6.9 and 4.6.10.
- Stress vs. coefficient of consolidation ($\sigma'_m - c_v$), Figure 4.6.11.

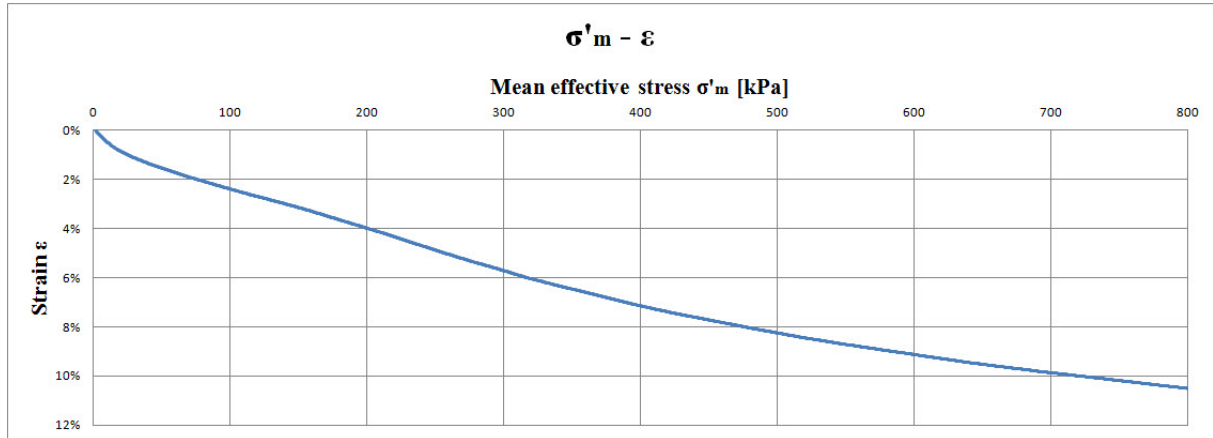


Figure 4.6.7: Sample S2-H1: Stress vs. strain from CRS oedometer test on undisturbed specimen.

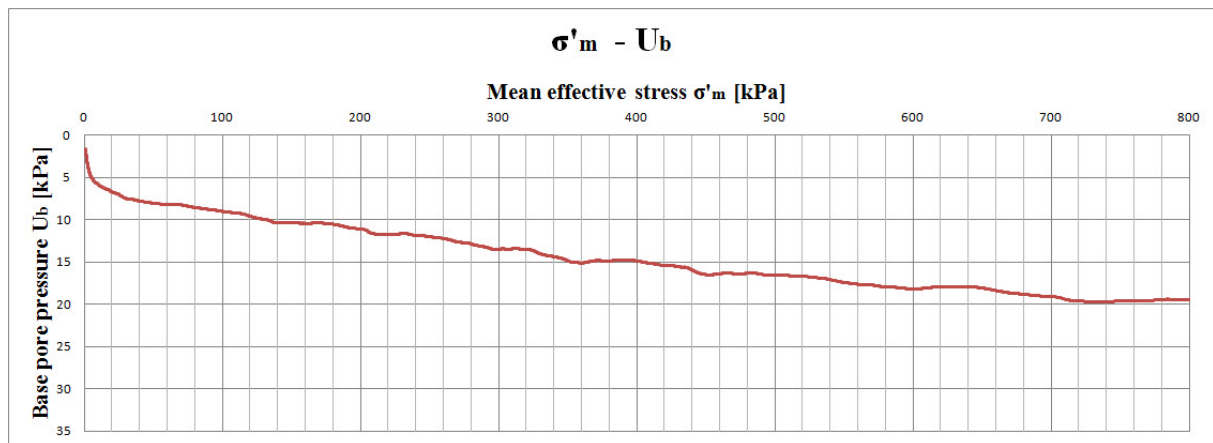


Figure 4.6.8: Sample S2-H1: Stress vs. pore pressure from CRS oedometer test on undisturbed specimen.

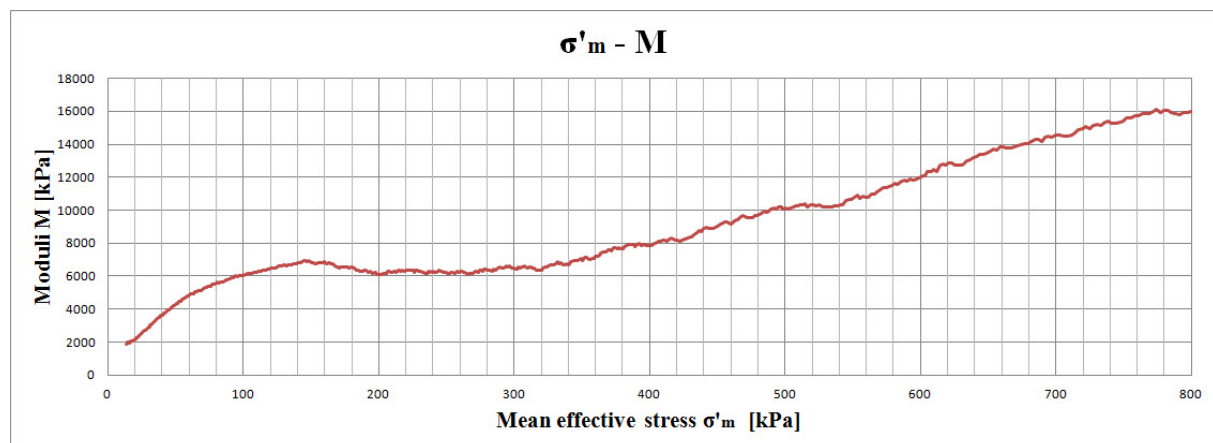


Figure 4.6.9: Sample S2-H1: Stress vs. oedometer modulus from CRS oedometer test on undisturbed specimen.

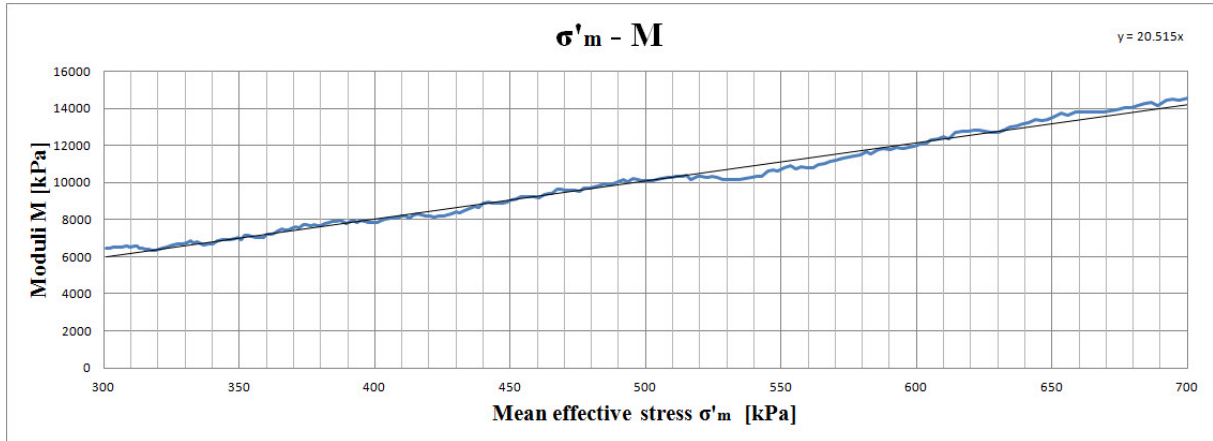


Figure 4.6.10: Sample S2-H1: Modulus number from CRS oedometer test on undisturbed specimen.

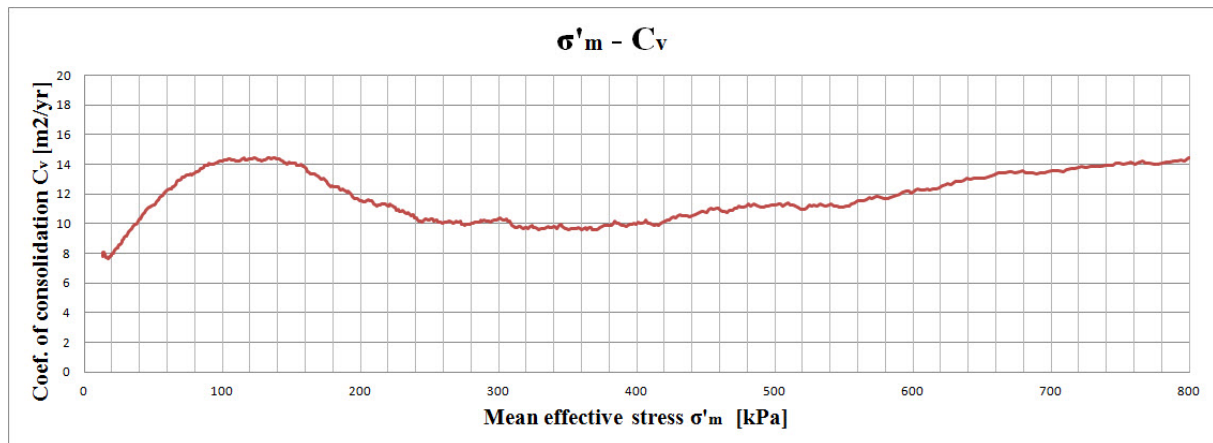


Figure 4.6.11: Sample S2-H1: Stress vs. coefficient of consolidation from CRS oedometer test on undisturbed specimen.

As follows from the test results presented in Figures 4.6.7-4.6.11, preconsolidation stress p'_c for sample S2-H1 is approximately 250 kPa. Constrained moduli in the overconsolidated range (M_o) and at the preconsolidation stress (M_n) are 6.9 MPa and 6.1 MPa, respectively. For normally consolidated range, the modulus number (m) is 20.5. Coefficients of consolidation in overconsolidated zone (c_{v_o}) and at about p'_c (c_{v_n}) are 14 m²/yr. and 10 m²/yr., respectively.

Overconsolidation ratio for sample S2-H1 is given as

$$OCR = \frac{p'_c}{\sigma'_{v0}} = \frac{250}{75.1} = 3.3 \tag{Eq. 4.107}$$

4.6.15 CRS Oedometer Test on Pre-Strained Clay

Calculation of water content for the test specimen is given in Table 4.6.19.

Table 4.6.19: Sample S2-H1: Calculation of water content for pre-strained specimen subjected to CRS oedometer test.

Parameter	Parameter value	Units
Mass, oedometer ring with specimen	118.65	gr.
Mass of oedometer ring	39.64	gr.
Mass of wet specimen (m_s+m_w)	79.01	gr.
Mass of dry specimen (m_s)	60.55	gr.
Mass of water (m_w)	18.46	gr.
Water content (w)	30.49	%

As seen from Table 4.6.19, there is a small deviation (2.25 %) between calculated values of water content for the test specimen and for the whole sample S2-H1 (refer to Chapter 4.6.3).

Figures 4.6.12-4.6.15 show the results of CRS oedometer test on sample S2-H1 pre-strained to shear strain $\gamma_s = 66\%$. The presented results consist of:

- Stress vs. strain plot ($\sigma'_m - \varepsilon$), Figure 4.6.12.
- Stress vs. pore pressure at sample base ($\sigma'_m - u_b$), Figure 4.6.13.
- Stress vs. modulus plot ($\sigma'_m - M$), Figure 4.6.14.
- Stress vs. coefficient of consolidation ($\sigma'_m - c_v$), Figure 4.6.15.

As follows from the results presented in Figure 4.6.12-4.6.15, the modulus number (m) for the specimen pre-strained to shear strain $\gamma_s = 66\%$ is constant and equal to 28.7. Coefficient of consolidation (c_v) increases non-linearly with the stress level, reaching the peak value of 16.5 $m^2/yr.$ at 800 kPa.

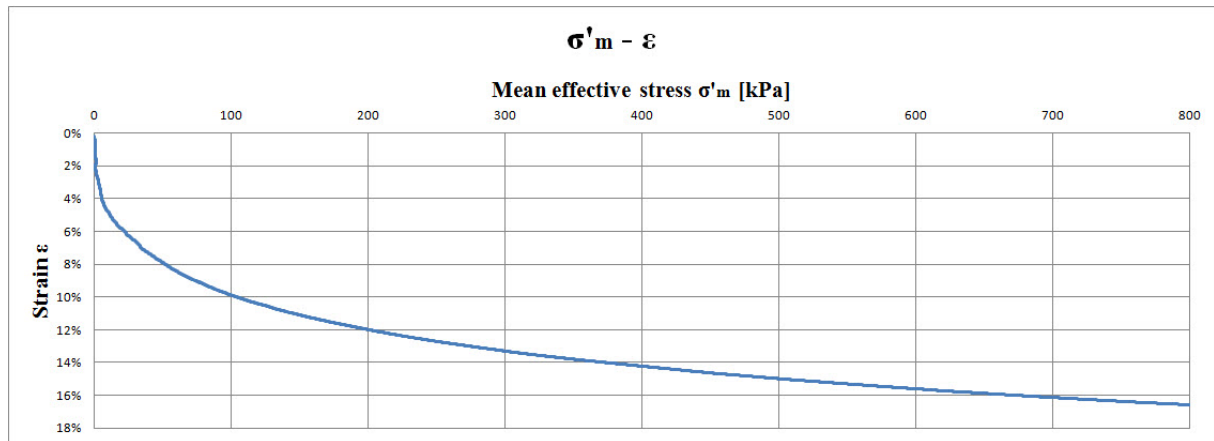


Figure 4.6.12: Sample S2-H1: Stress vs. strain from CRS oedometer test on specimen pre-strained to $\gamma_s = 66\%$.

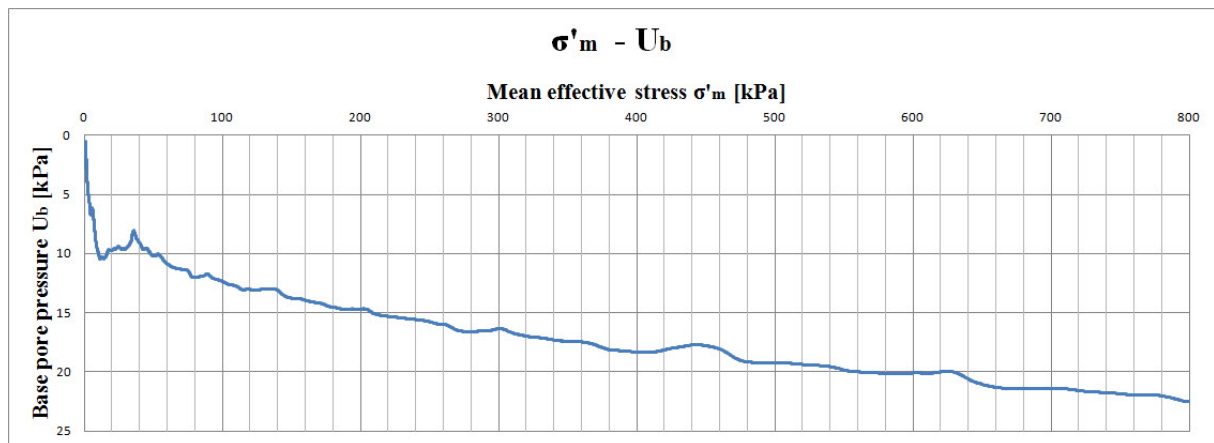


Figure 4.6.13: Sample S2-H1: Stress vs. pore pressure from CRS oedometer test on specimen pre-strained to $\gamma_s = 66\%$.

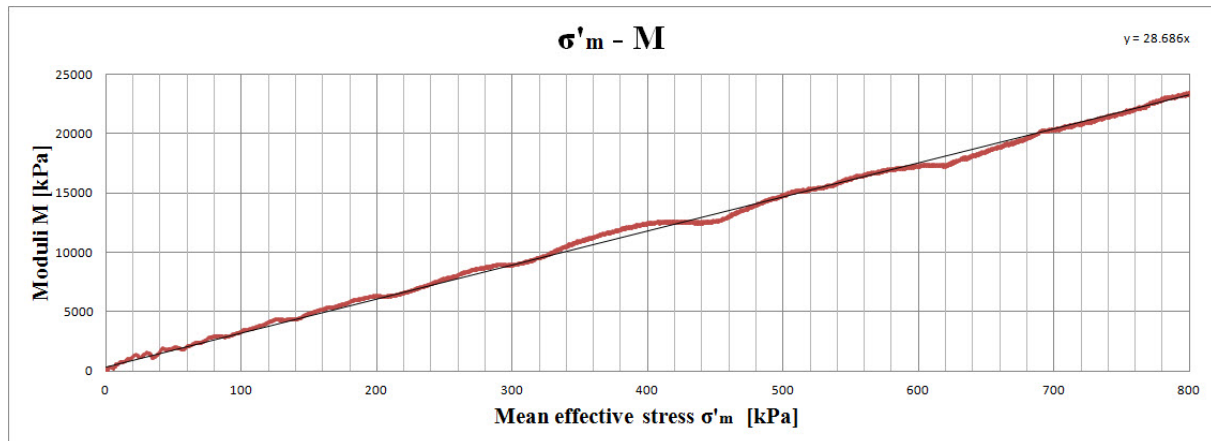


Figure 4.6.14: Sample S2-H1: Stress vs. oedometer modulus from CRS oedometer test on specimen pre-strained to $\gamma_s = 66\%$.

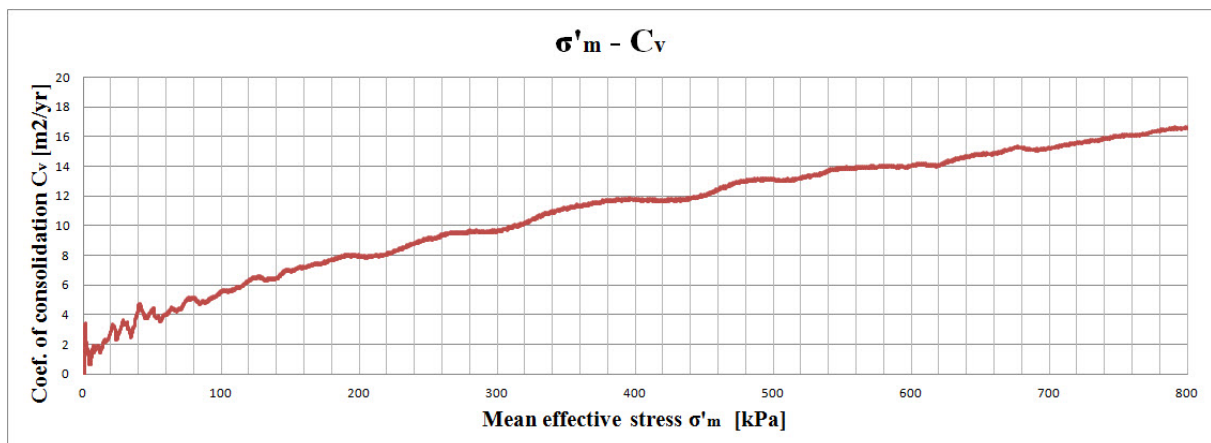


Figure 4.6.15: Sample S2-H1: Stress vs. coefficient of consolidation from CRS oedometer test on specimen pre-strained to $\gamma_s = 66\%$.

4.6.16 CRS Oedometer Test on Remoulded Clay

Calculation of water content for the test specimen is given in Table 4.6.20.

As follows from Table 4.6.20, there is a fair agreement between values of water content for the remoulded clay specimen and the whole sample S2-H1 (refer to Chapter 4.6.3). An additional control measurement of water content has been carried out for the remoulded clay mass at the same time as the remoulded specimen was built into the oedometer. The control measurement showed water content $w = 31.45\%$.

Table 4.6.20: Sample S2-H1: Calculation of water content for remoulded specimen subjected to CRS oedometer test.

Parameter	Parameter value	Units
Mass, oedometer ring with specimen	114.55	gr.
Mass of oedometer ring	37.36	gr.
Mass of wet specimen (m_s+m_w)	77.19	gr.
Mass of dry specimen (m_s)	58.67	gr.
Mass of water (m_w)	18.52	gr.
Water content (w)	31.57	%

Figures 4.6.16-4.6.19 show the results of CRS oedometer test on remoulded clay sample S2-H1. The presented results consist of:

- Stress vs. strain plot ($\sigma'_m - \epsilon$), Figure 4.6.16.
- Stress vs. pore pressure at sample base ($\sigma'_m - u_b$), Figure 4.6.17.
- Stress vs. modulus plot ($\sigma'_m - M$), Figure 4.6.18.
- Stress vs. coefficient of consolidation ($\sigma'_m - c_v$), Figure 4.6.19.

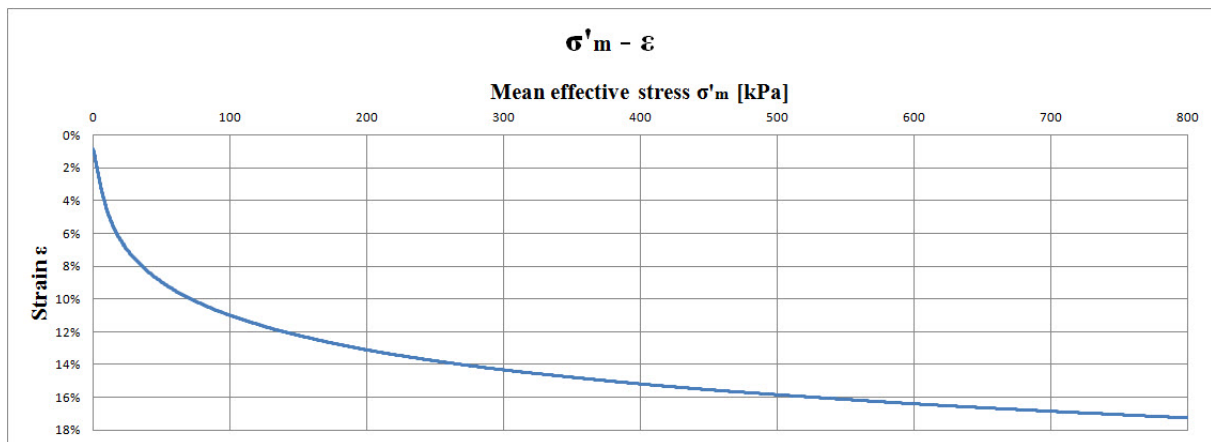


Figure 4.6.16: Sample S2-H1: Stress vs. strain from CRS oedometer test on remoulded specimen.

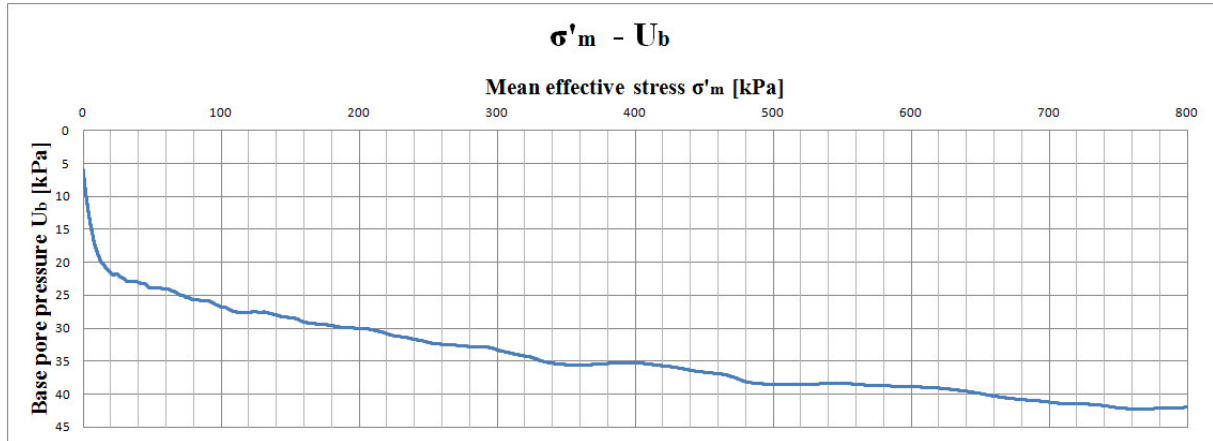


Figure 4.6.17: Sample S2-H1: Stress vs. pore pressure from CRS oedometer test on remoulded specimen.

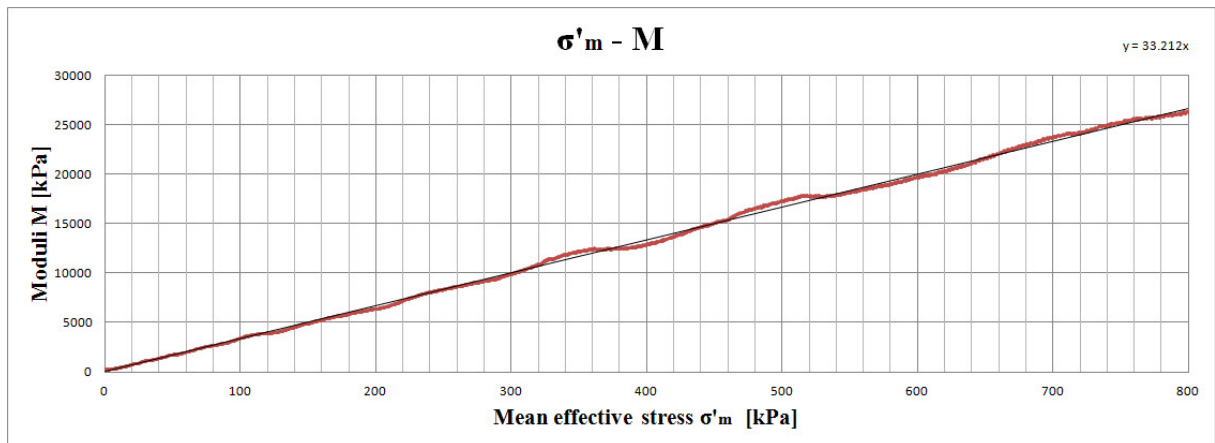


Figure 4.6.18: Sample S2-H1: Stress vs. oedometer modulus from CRS oedometer test on remoulded specimen.

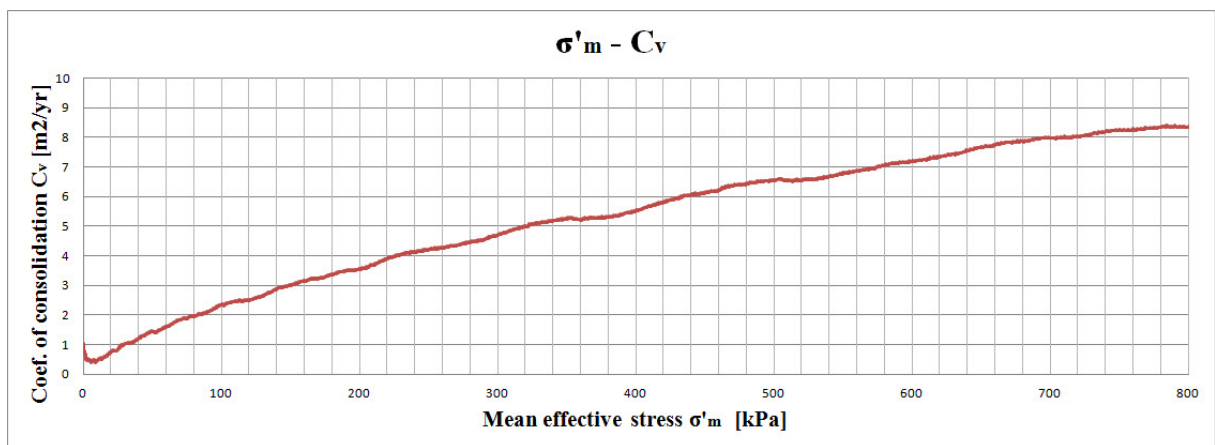


Figure 4.6.19: Sample S2-H1: Stress vs. coefficient of consolidation from CRS oedometer test on remoulded specimen.

As follows from the results presented in Figures 4.6.16-4.6.19, the modulus number (m) for the remoulded specimen is constant and equal to 33.2. Coefficient of consolidation (c_v) is increasing non-linearly with the stress level and is reaching its maximum of 8.4 m²/yr. at 800 kPa.

4.7 Test Results for Sample S3-H1

4.7.1 Extrusion of the Sample

Sample S3-H1 was extruded in the laboratory at 27.04.2015. The pre-straining was achieved by extrusion of sample from $\varnothing 72.3$ mm to $\varnothing 68$ mm, corresponding to shear strain $\gamma_s = 18$ % (refer to Chapter 3 for more details). Figure 4.7.1 shows subdivision of the sample during extrusion.

No strain variation has been observed in the cross-section of pre-strained sample S3-H1.

Displacement ratio is given by Eq. 3.4:

$$\delta_r = \frac{11}{10} = 1.10 \text{ mm/mm} \quad (\text{Eq. 4.108})$$

There is a minor deviation between observed and theoretical displacement ratio (1.13 mm/mm, refer to Table 3.2.2).

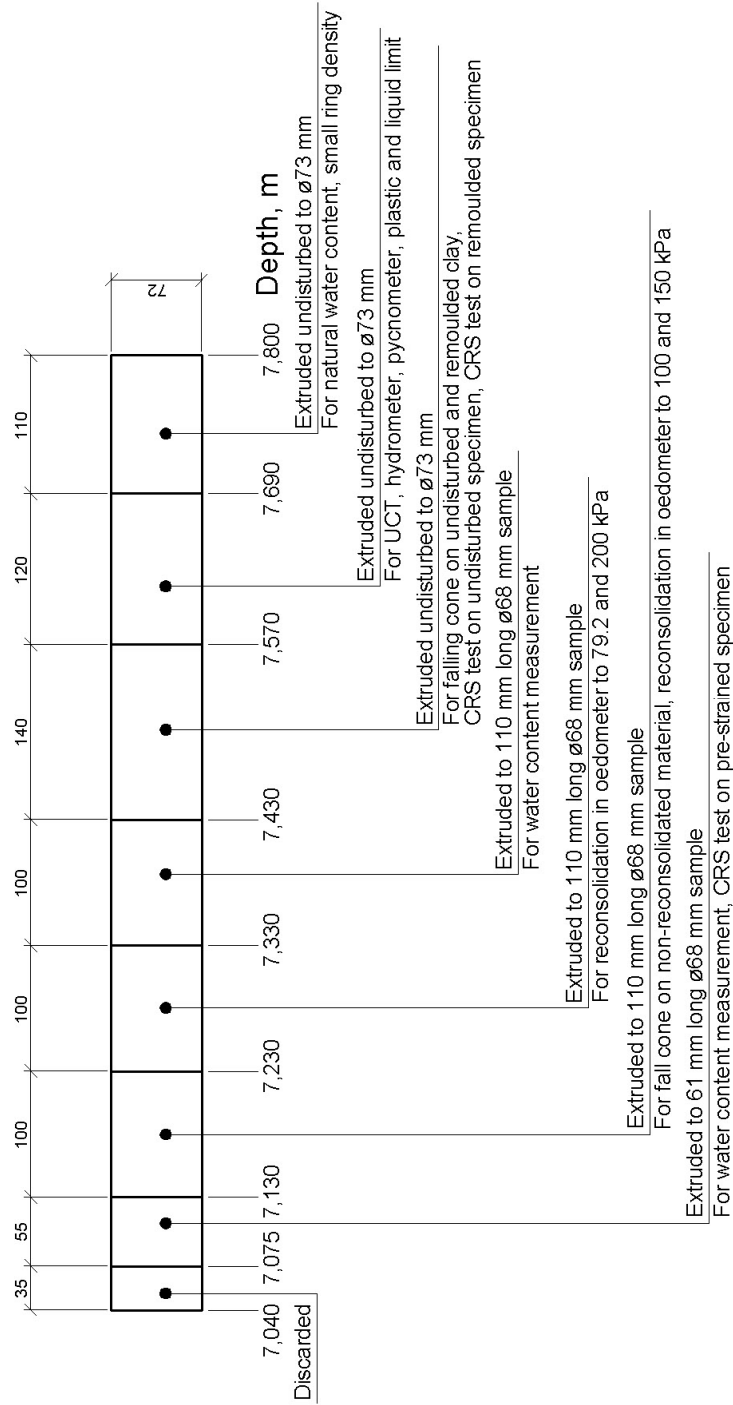


Figure 4.7.1: Sample S3-H1: Extrusion and subdivision.

4.7.2 Density Measurements

4.7.2.1 Average Density

Table 4.7.1 shows log of measurements carried out for calculation of mean density.

Table 4.7.1: Sample S3-H1: Calculation of mean density.

Parameter	Parameter value	Units
Length of sample (L)	76.0	cm
Diameter of sample (D _i)	7.23	cm
Volume of sample (V)	3120.2	cm ³
Mass of cylinder with sample and plug	9232	gr.
Mass of cylinder and plug	3564	gr.
Mass of sample (m)	5668	gr.
Mean density ($\bar{\rho}$)	1.82	gr./cm ³
Unit weight ($\bar{\gamma} = \bar{\rho} \cdot g$)	17.85	kN/m ³

4.7.2.2 Density by Small Ring

Table 4.7.2 contains log of measurements carried out for calculation of density with small ring.

Table 4.7.2: Sample S3-H1: Calculation of density and dry density with small ring.

	Ring	Bowl	
Parameter	Parameter value	Parameter value	Units
Total wet mass	95.86	169.85	gr.
Total dry mass	76.15	150.14	gr.
Mass of ring/bowl	32.11	106.10	gr.
Mass of wet sample ($m_s + m_w$)	63.75	63.75	gr.
Mass of dry sample (m_s)	44.04	44.04	gr.
Volume (V)	35.50	35.50	cm ³
Density (ρ)	1.80	1.80	gr./cm ³
Unit weight of soil (γ)	17.66	17.66	kN/m ³
Dry density (ρ_d)	1.24	1.24	gr./cm ³

As seen from Tables 4.7.1 and 4.7.2, there is close agreement between the calculated values of densities.

4.7.2.3 Grain Density by Pycnometer

Table 4.7.3 shows log of measurements from pycnometer test. Grain density ρ_s is given by Eq. 3.9.

Table 4.7.3: Sample S3-H1: Calculation of grain density and unit weight of solids.

Parameter	Parameter value	Units
Mass of waterfilled pycnometer	148.47	gr.
Mass of pycnometer, water and specimen	152.53	gr.
Total dry mass	298.73	gr.
Mass of bowl	292.39	gr.
Dry mass of specimen (m_s)	6.34	gr.
Density of solids (ρ_s)	2.78	gr./cm ³
Unit weight of solids (γ_{solid})	27.27	kN/m ³

4.7.3 Water Content Measurements

Table 4.7.4 shows log of water content measurements. Test specimen No. 1 was undisturbed, while test specimens No. 2 and 3 were pre-strained.

As follows from Table 4.7.4, the values of water content are consistent. The mean value of water content is

$$w = \frac{43.28+43.84+43.67}{3} = 43.60 \% \quad (\text{Eq. 4.109})$$

Table 4.7.4: Sample S3-H1: Determination of water content.

	Specimen No. 1	Specimen No. 2	Specimen No. 3	
Parameter	Parameter value	Parameter value	Parameter value	Units
Depth	7.690 - 7.800	7.075 - 7.130	7.330 - 7.430	m
Total wet mass	136.11	119.17	126.41	gr.
Total dry mass	110.13	97.59	102.90	gr.
Mass of water (m_w)	25.98	21.58	23.51	gr.
Mass of bowl	50.10	48.36	49.07	gr.
Dry mass (m_s)	60.03	49.23	53.83	gr.
Water content (w)	43.28	43.84	43.67	%

4.7.4 Plastic and Liquid Limit

Table 4.7.5 shows log of plastic and liquid limit measurements.

Liquidity and plasticity indices are found from Eq. 3.12 and 3.13, respectively:

$$I_L = \frac{w - w_p}{w_L - w_p} = \frac{43.60 - 21.56}{48.40 - 21.56} = 0.82 \quad (\text{Eq. 4.110})$$

$$I_p = w_L - w_p = 48.40 - 21.56 = 26.84 \%$$

The value of natural water content in Eq. 4.110 is obtained from Eq. 4.109.

Table 4.7.5: Sample S3-H1: Calculation of plastic and liquid limit.

	Liquid limit w_L	Plastic limit w_p	
Parameter	Parameter value	Parameter value	Units
Total wet mass	81.71	34.30	gr.
Total dry mass	69.78	33.47	gr.
Mass of water (m_w)	11.93	0.83	gr.
Mass of bowl	45.13	29.62	gr.
Dry mass (m_s)	24.65	3.85	gr.
Water content (w_L and w_p)	48.40	21.56	%

4.7.5 Degree of Saturation, Void Ratio and Porosity

Degree of saturation (S_r) is found from Eq. 3.14:

$$S_r = \frac{w \cdot \gamma}{\gamma_w \cdot \left(1 + w - \frac{\gamma}{\gamma_{solid}}\right)} = \frac{0.44 \cdot 17.66}{9.81 \cdot \left(1 + 0.44 - \frac{17.66}{27.27}\right)} = 1.00 \quad (\text{Eq. 4.111})$$

Void ratio (e) is found from Eq. 3.15:

$$e = \frac{\gamma_{solid} \cdot (1+w)}{\gamma} - 1 = \frac{27.27 \cdot (1+0.44)}{17.66} - 1 = 1.22 \quad (\text{Eq. 4.112})$$

Porosity (n) is found from Eq. 3.16:

$$n = \left(1 - \frac{\gamma}{\gamma_{solid} \cdot (1+w)}\right) \cdot 100 \% = \left(1 - \frac{17.66}{27.27 \cdot (1+0.44)}\right) \cdot 100 \% = 55.03 \% \quad (\text{Eq. 4.113})$$

In the equations above, the value of natural water content w is obtained from Eq. 4.109, unit weight of soil γ is obtained from Table 4.7.2 and unit weight of solids γ_{solid} is obtained from Table 4.7.3.

4.7.6 Grain Size Distribution

Table 4.7.6 shows observations from hydrometer test.

Table 4.7.6: Sample S3-H1: Observations from hydrometer test.

Total mass of dried sample (W), gr.		43.52							
Mass of dried sample (w_s) $d < 0.074$ mm, gr.		43.52							
Grain density (ρ_s), gr./cm³		2.78							
Coefficient a		97.3							
Passed time (t), min.	Temp. (T), °C	Concentration (R), gr./l	Eff. depth (Z_r), cm	Constant (K), $\sqrt{\frac{min}{cm}}$	$\sqrt{\frac{Z_r}{t}}$, $\sqrt{\frac{cm}{min}}$	Equiv. grain size (d_s), mm	Rel. weight (N) $d_s < 0.074$ mm, %	Rel. weight total sample, %	
1	22.2	43.5	3.0	0.01275	1.732	0.0221	97.26	97.26	
2	22.1	43.0	3.2	0.01276	1.265	0.0161	96.14	96.14	
5	21.7	41.5	3.7	0.01283	0.860	0.0110	92.78	92.78	
10	21.6	40.0	4.2	0.01285	0.648	0.0083	89.43	89.43	
20	21.3	38.0	5.0	0.01294	0.500	0.0065	84.96	84.96	
40	21.2	36.5	5.6	0.01295	0.374	0.0048	81.61	81.61	
80	21.2	34.0	6.5	0.01295	0.285	0.0037	76.02	76.02	
160	21.1	32.0	7.3	0.01298	0.214	0.0028	71.54	71.54	
320	21.1	29.5	8.3	0.01298	0.161	0.0021	65.95	65.95	
1320	21.2	24.0	10.3	0.01295	0.088	0.0011	53.66	53.66	

Grain size distribution curve for sample S3-H1 is shown in Figure 4.7.2. The material contains a large amount of fines. 65 % of particles fall in clay fraction and 34 % of particles

fall in silt fraction. Maximum grain size d_{max} is 0.074 mm. Average grain size d_{50} , ratio d_{60}/d_{10} and ratio d_{75}/d_{25} are not available due to the practical reasons.

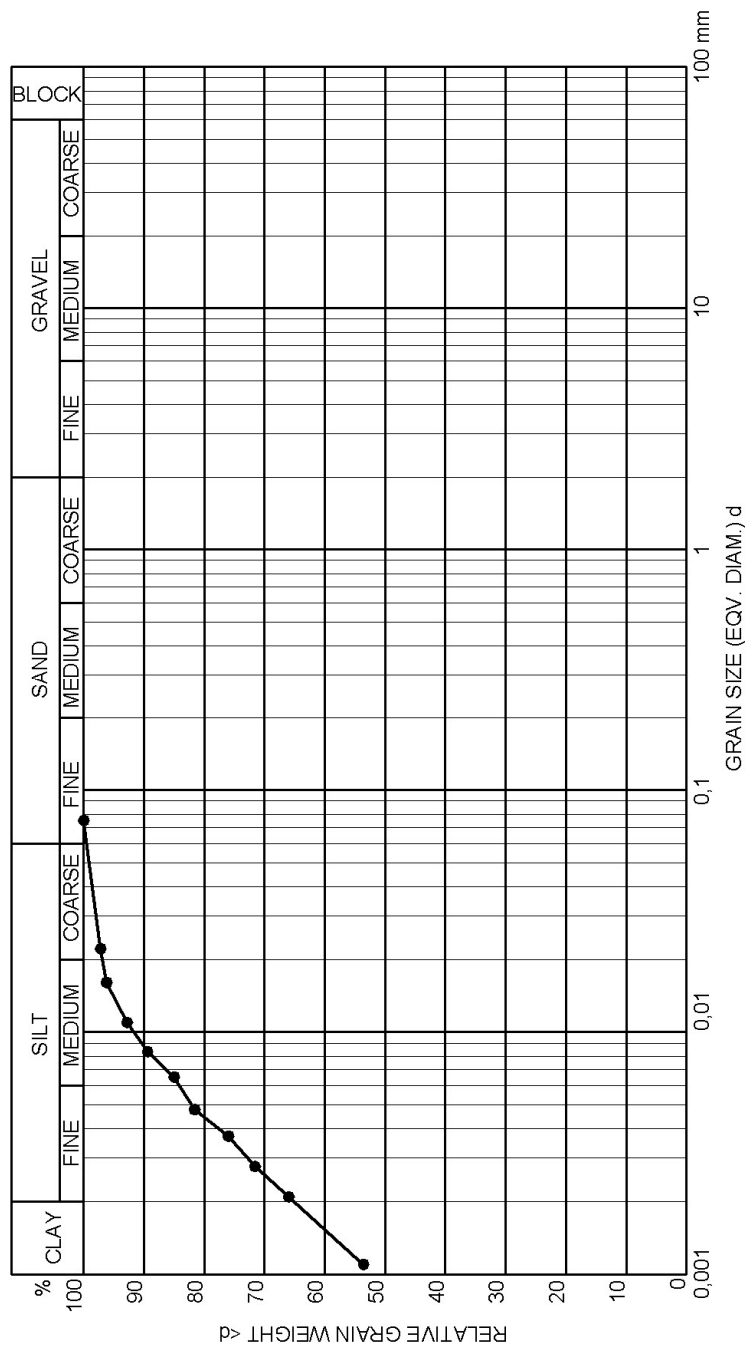


Figure 4.7.2: Sample S3-H1: Grain size distribution curve.

4.7.7 Undrained Shear Strength by UCT

Figure 4.7.3 shows deformation curve from UCT aligned with calibration chart. The sample demonstrates plastic yielding at strain $\varepsilon_a = 14\%$ for maximum load $P_f = 33\text{ kg}$ (323.73 N). Softening occurs at strain $\varepsilon_a = 17\%$, after which the load record drops down to $P = 27\text{ kg}$ (264.87 N).

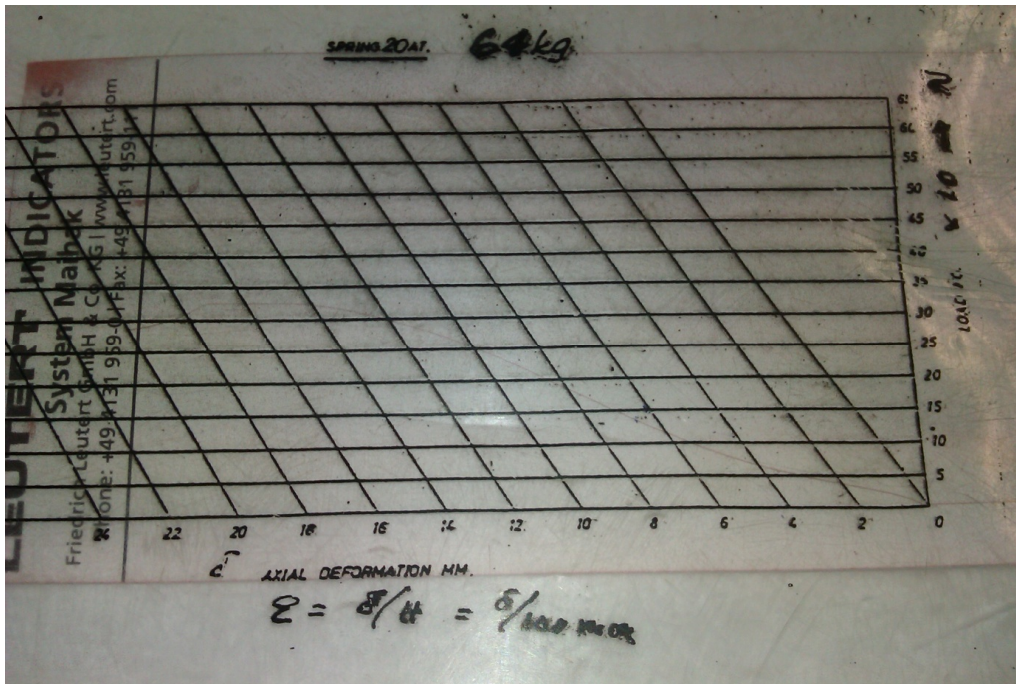


Figure 4.7.3: Sample S3-H1: Recorded deformation curve from UCT.

Undrained shear strength (s_u) is given by Eq. 3.24:

$$s_u = \tau_{max} = \frac{\sigma_1}{2} = \frac{P_f \cdot (1 - \varepsilon_a)}{2 \cdot A_0} = \frac{323.73 \cdot (1 - 0.14)}{2 \cdot 2290} = 0.0608 \text{ N/mm}^2 = 60.8 \text{ kPa} \quad (\text{Eq. 4.114})$$

Figure 4.7.4 shows specimen at failure. Sketch of the shape of specimen at failure is shown in Figure 4.7.5. In the end of the test, a clearly visible failure plane was located at angle of 40° from vertical axis.

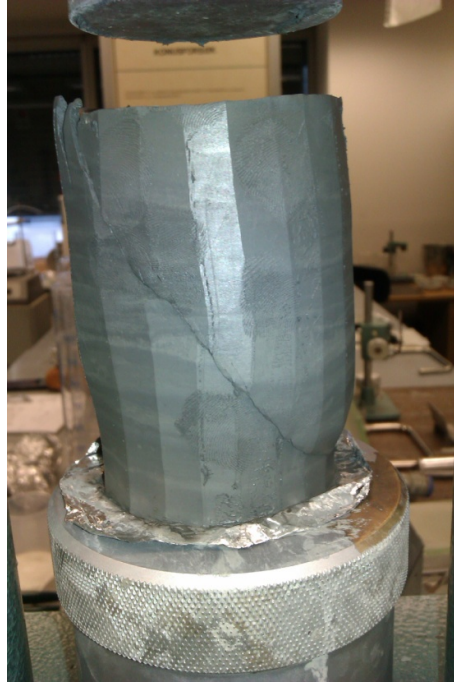


Figure 4.7.4: Sample S3-H1: Specimen at failure during UCT.

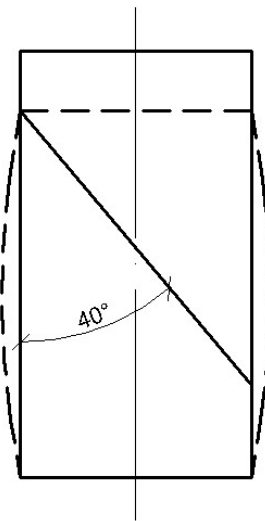


Figure 4.7.5: Sample S3-H1: Shape of specimen at failure during UCT.

4.7.8 Undrained and Remoulded Shear Strength by Fall Cone

Table 4.7.7 shows the results of falling cone test on undisturbed specimen. 100 gr. cone has been used.

As seen from Table 4.7.7, there is a deviation between values of undrained shear strength determined by falling cone and UCT.

Table 4.7.7: Sample S3-H1: Results of falling cone test on undisturbed clay.

Intrusion No.	Intrusion, mm	Undrained shear strength s_u , kPa	Reported (mean) s_u , kPa
1	5.0	38.7	39.0
2	4.9	39.7	
3	5.0	38.7	

Table 4.7.8 shows the results of falling cone test on remoulded specimen. 60 gr. cone has been used.

Table 4.7.8: Sample S3-H1: Results of falling cone test on remoulded clay.

Set No.	Intrusion, mm	Remoulded shear strength s_r , kPa	Mean remoulded shear strength s_r , kPa	Reported remoulded shear strength s_r , kPa
1	6.9	4.9	5.3	5.3
	6.5	5.6		
2	6.2	6.2	5.9	
	6.5	5.6		

The sensitivity is given by Eq.3.25:

$$S_t = \frac{s_u}{s_r} = \frac{39.0}{5.3} = 7.4 \quad (\text{Eq. 4.115})$$

4.7.9 Shear Strength of Pre-Strained, Non-Reconsolidated Sample by Fall Cone

Table 4.7.9 shows test results from falling cone test on pre-strained non-reconsolidated sample. 100 gr. cone has been used.

Table 4.7.9: Sample S3-H1: Results of falling cone test on pre-strained non-reconsolidated clay.

Intrusion No.	Intrusion, mm	Shear strength s , kPa	Reported (mean) s , kPa
1	7.7	20.1	19.9
2	7.5	21.1	
3	8.0	18.6	

4.7.10 Reconsolidation of Pre-Strained Specimen in the Oedometer at In-Situ Vertical Effective Stress 79.2 kPa

Table 4.7.10 shows data for calculation of water content in specimen prior to and after reconsolidation. Remaining pore pressure after 24 hrs. reconsolidation time was 0.9 kPa.

Table 4.7.10: Sample S3-H1: Calculation of water content prior to and after reconsolidation at in-situ vertical effective stress 79.2 kPa.

Parameter	Parameter value before reconsolidation	Parameter value after reconsolidation	Units
Mass, oedometer ring with wet specimen	109.61	108.43	gr.
Mass, oedometer ring	37.37	37.37	gr.
Mass of wet specimen	72.24	71.06	gr.
Mass of dry specimen (m_s)	49.80	49.80	gr.
Mass of water (m_w)	22.44	21.26	gr.
Water content (w and w_{re})	45.06	42.69	%

As follows from Table 4.7.10, reconsolidation at 79.2 kPa leads to change in water content:

$$\Delta w = w_{re} - w = 42.69 - 45.06 = -2.37 \% \quad (\text{Eq. 4.116})$$

After 24 hrs. reconsolidation at 79.2 kPa, volume of the specimen has been reduced by 6.61 %.

Table 4.7.11 shows the results of falling cone test on reconsolidated specimen. 100 gr. cone has been used in the test.

Table 4.7.11: Sample S3-H1: Results of falling cone test on pre-strained clay reconsolidated at in-situ vertical effective stress 79.2 kPa.

Intrusion No.	Intrusion, mm	Shear strength after reconsolidation s_{re} , kPa	Reported (mean) shear strength after reconsolidation s_{re} , kPa
1	6.5	27.0	30.3
2	5.8	31.9	
3	5.8	31.9	

As follows from Tables 4.7.7 and 4.7.11, change in shear strength due to the pre-straining and subsequent reconsolidation at 79.2 kPa is:

$$\Delta s = s_{re} - s_u = 30.3 - 39.0 = -8.7 \text{ kPa} \quad (\text{Eq. 4.117})$$

Normalised change in shear strength due to the pre-straining and reconsolidation is:

$$\frac{\Delta s}{s_u} = \frac{s_{re} - s_u}{s_u} \cdot 100 \% = \frac{30.3 - 39.0}{39.0} \cdot 100 \% = -22.31 \% \quad (\text{Eq. 4.118})$$

4.7.11 Reconsolidation of Pre-Strained Specimen in the Oedometer at 100 kPa

Table 4.7.12 shows data for calculation of water content in specimen prior to and after reconsolidation. Remaining pore pressure after 24 hrs. reconsolidation time was 1.9 kPa.

As follows from Table 4.7.12, reconsolidation at 100 kPa leads to change in water content:

$$\Delta w = w_{re} - w = 38.48 - 43.69 = -5.21 \% \quad (\text{Eq. 4.119})$$

After 24 hrs. reconsolidation at 100 kPa, volume of the specimen has been reduced by 8.92 %.

Table 4.7.12: Sample S3-H1: Calculation of water content prior to and after reconsolidation at 100 kPa.

Parameter	Parameter value before reconsolidation	Parameter value after reconsolidation	Units
Mass, oedometer ring with wet specimen	111.40	108.78	gr.
Mass, oedometer ring	39.14	39.14	gr.
Mass of wet specimen	72.26	69.64	gr.
Mass of dry specimen (m_s)	50.29	50.29	gr.
Mass of water (m_w)	21.97	19.35	gr.
Water content (w and w_{re})	43.69	38.48	%

Table 4.7.13 shows the results of falling cone test on reconsolidated specimen. 100 gr. cone has been used in the test.

Table 4.7.13: Sample S3-H1: Results of falling cone test on pre-strained clay reconsolidated at 100 kPa.

Intrusion No.	Intrusion, mm	Shear strength after reconsolidation s_{re} , kPa	Reported (mean) shear strength after reconsolidation s_{re} , kPa
1	4.2	49.1	50.4
2	4.1	51.0	
3	4.1	51.0	

As follows from Tables 4.7.7 and 4.7.13, change in shear strength due to the pre-straining and subsequent reconsolidation at 100 kPa is:

$$\Delta s = s_{re} - s_u = 50.4 - 39.0 = 11.4 \text{ kPa} \tag{Eq. 4.120}$$

Normalised change in shear strength due to the pre-straining and reconsolidation is:

$$\frac{\Delta s}{s_u} = \frac{s_{re} - s_u}{s_u} \cdot 100 \% = \frac{50.4 - 39.0}{39.0} \cdot 100 \% = 29.23 \% \quad (\text{Eq. 4.121})$$

4.7.12 Reconsolidation of Pre-Strained Specimen in the Oedometer at 150 kPa

Table 4.7.14 shows data for calculation of water content in specimen prior to and after reconsolidation. Remaining pore pressure after 24 hrs. reconsolidation time was 0.1 kPa.

Table 4.7.14: Sample S3-H1: Calculation of water content prior to and after reconsolidation at 150 kPa.

Parameter	Parameter value before reconsolidation	Parameter value after reconsolidation	Units
Mass, oedometer ring with wet specimen	111.02	108.23	gr.
Mass, oedometer ring	37.31	37.31	gr.
Mass of wet specimen	73.71	70.92	gr.
Mass of dry specimen (m_s)	51.85	51.85	gr.
Mass of water (m_w)	21.86	19.07	gr.
Water content (w and w_{re})	42.16	36.78	%

As follows from Table 4.7.14, reconsolidation at 150 kPa leads to change in water content:

$$\Delta w = w_{re} - w = 36.78 - 42.16 = -5.38 \% \quad (\text{Eq. 4.122})$$

After 24 hrs. reconsolidation at 150 kPa, volume of the specimen has been reduced by 8.66 %.

Table 4.7.15 shows the results of falling cone test on reconsolidated specimen. 100 gr. cone has been used in the test.

As follows from Tables 4.7.7 and 4.7.15, change in shear strength due to the pre-straining and subsequent reconsolidation at 150 kPa is:

$$\Delta s = s_{re} - s_u = 67.7 - 39.0 = 28.7 \text{ kPa} \quad (\text{Eq. 4.123})$$

Normalised change in shear strength due to the pre-straining and reconsolidation is:

$$\frac{\Delta s}{s_u} = \frac{s_{re} - s_u}{s_u} \cdot 100 \% = \frac{67.7 - 39.0}{39.0} \cdot 100 \% = 73.59 \% \quad (\text{Eq. 4.124})$$

Table 4.7.15: Sample S3-H1: Results of falling cone test on pre-strained clay reconsolidated at 150 kPa.

Intrusion No.	Intrusion, mm	Shear strength after reconsolidation s_{re} , kPa	Reported (mean) shear strength after reconsolidation s_{re} , kPa
1	3.1	71.6	67.7
2	3.4	64.7	
3	3.3	66.7	

4.7.13 Reconsolidation of Pre-Strained Specimen in the Oedometer at 200 kPa

Table 4.7.16 shows data for calculation of water content in specimen prior to and after reconsolidation. Remaining pore pressure after 24 hrs. reconsolidation time was 0.4 kPa.

Table 4.7.16: Sample S3-H1: Calculation of water content prior to and after reconsolidation at 200 kPa.

Parameter	Parameter value before reconsolidation	Parameter value after reconsolidation	Units
Mass, oedometer ring with wet specimen	109.98	106.19	gr.
Mass, oedometer ring	38.75	38.75	gr.
Mass of wet specimen	71.23	67.44	gr.
Mass of dry specimen (m_s)	48.70	48.70	gr.
Mass of water (m_w)	22.53	18.74	gr.
Water content (w and w_{re})	46.26	38.48	%

As follows from Table 4.7.16, reconsolidation at 200 kPa leads to change in water content:

$$\Delta w = w_{re} - w = 38.48 - 46.26 = -7.78 \% \quad (\text{Eq. 4.125})$$

After 24 hrs. reconsolidation at 200 kPa, volume of the specimen has been reduced by 11.32 %.

Table 4.7.17 shows the results of falling cone test on reconsolidated specimen. 100 gr. cone has been used in the test.

Table 4.7.17: Sample S3-H1: Results of falling cone test on pre-strained clay reconsolidated at 200 kPa.

Intrusion No.	Intrusion, mm	Shear strength after reconsolidation s_{re} , kPa	Reported (mean) shear strength after reconsolidation s_{re} , kPa
1	3.2	69.2	71.6
2	3.0	74.1	
3	3.1	71.6	

As follows from Tables 4.7.7 and 4.7.17, change in shear strength due to the pre-straining and reconsolidation at 200 kPa is:

$$\Delta s = s_{re} - s_u = 71.6 - 39.0 = 32.6 \text{ kPa} \quad (\text{Eq. 4.126})$$

Normalised change in shear strength due to the pre-straining and reconsolidation is:

$$\frac{\Delta s}{s_u} = \frac{s_{re} - s_u}{s_u} \cdot 100 \% = \frac{71.6 - 39.0}{39.0} \cdot 100 \% = 83.59 \% \quad (\text{Eq. 4.127})$$

4.7.14 CRS Oedometer Test on Undisturbed Clay

Calculation of index parameters for the test specimen is given in Table 4.7.18. The value of grain density ρ_s used in the calculation is obtained from the results of pycnometer test (refer to Chapter 4.7.2).

As follows from Table 4.7.18, there are small deviations between calculated values of water content and void ratio for the oedometer test specimen and the whole sample S3-H1 (refer to Chapters 4.7.3 and 4.7.5). The deviation between values of water content and void ratio are 2.62 % and 0.05, respectively. The deviations are negligible.

Table 4.7.18: Sample S3-H1: Calculation of index parameters for undisturbed specimen subjected to CRS oedometer test.

Parameter	Parameter value	Units
Height of specimen (h_0)	20	mm
Area of specimen (A)	20	cm ²
Volume of specimen (V_0)	40	cm ³
Mass, oedometer ring with specimen	111.45	gr.
Mass of oedometer ring	39.70	gr.
Mass of wet specimen (m_s+m_w)	71.75	gr.
Mass of dry specimen (m_s)	49.07	gr.
Mass of water (m_w)	22.68	gr.
Water content (w)	46.22	%
Grain density (ρ_s)	2.78	gr./cm ³
Solids ($h_s = \frac{m_s}{A \cdot \rho_s}$)	0.88	cm
Void ratio ($e_0 = \frac{h_0 - h_s}{h_s}$)	1.27	-
Degree of saturation ($S_t = \frac{\rho_s \cdot w}{\rho_w \cdot e_0}$)	1.00	-

Figures 4.7.6-4.7.10 show the results of CRS oedometer test on undisturbed sample S3-H1.

The presented results consist of:

- Stress vs. strain plot ($\sigma'_m - \varepsilon$), Figure 4.7.6.
- Stress vs. pore pressure at sample base ($\sigma'_m - u_b$), Figure 4.7.7.
- Stress vs. modulus plot ($\sigma'_m - M$), Figure 4.7.8 and 4.7.9.
- Stress vs. coefficient of consolidation ($\sigma'_m - c_v$), Figure 4.7.10.

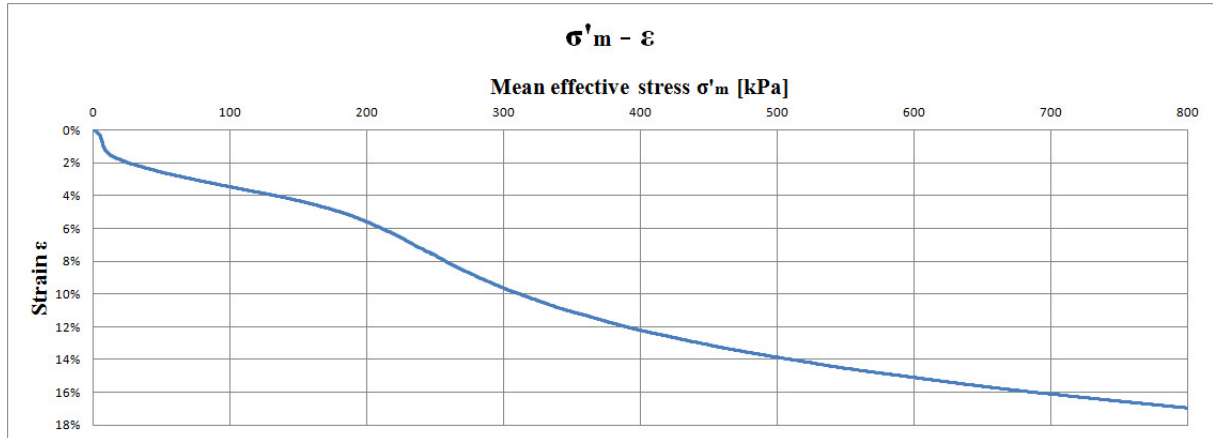


Figure 4.7.6: Sample S3-H1: Stress vs. strain from CRS oedometer test on undisturbed specimen.

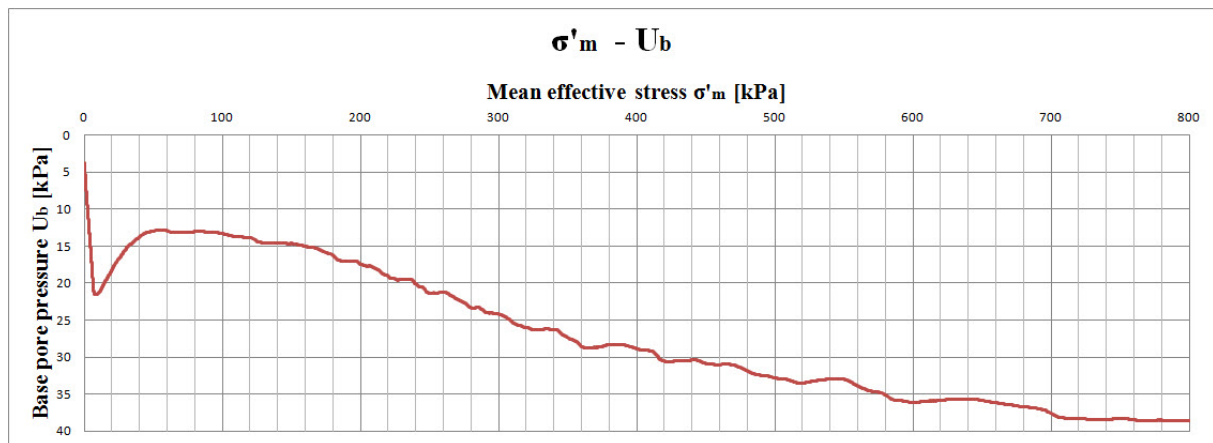


Figure 4.7.7: Sample S3-H1: Stress vs. pore pressure from CRS oedometer test on undisturbed specimen.

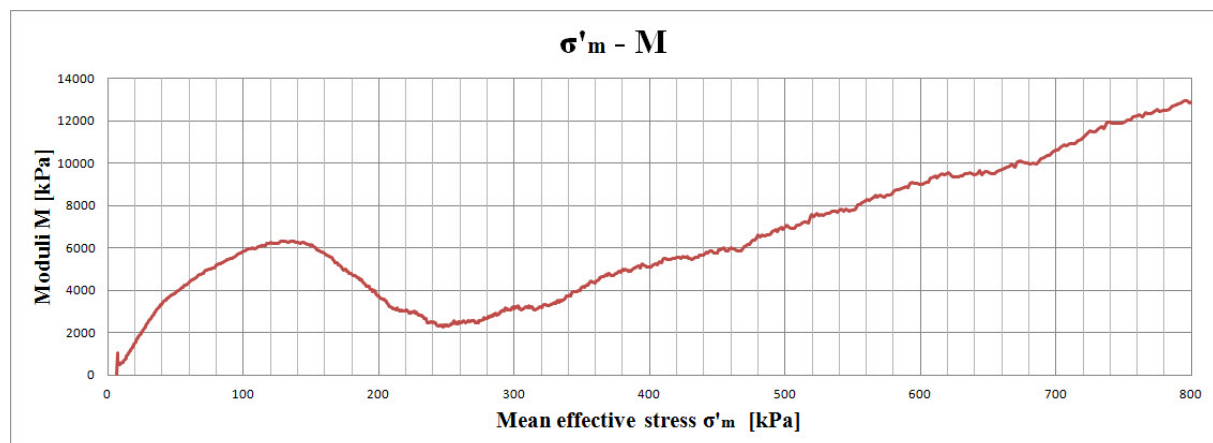


Figure 4.7.8: Sample S3-H1: Stress vs. oedometer modulus from CRS oedometer test on undisturbed specimen.

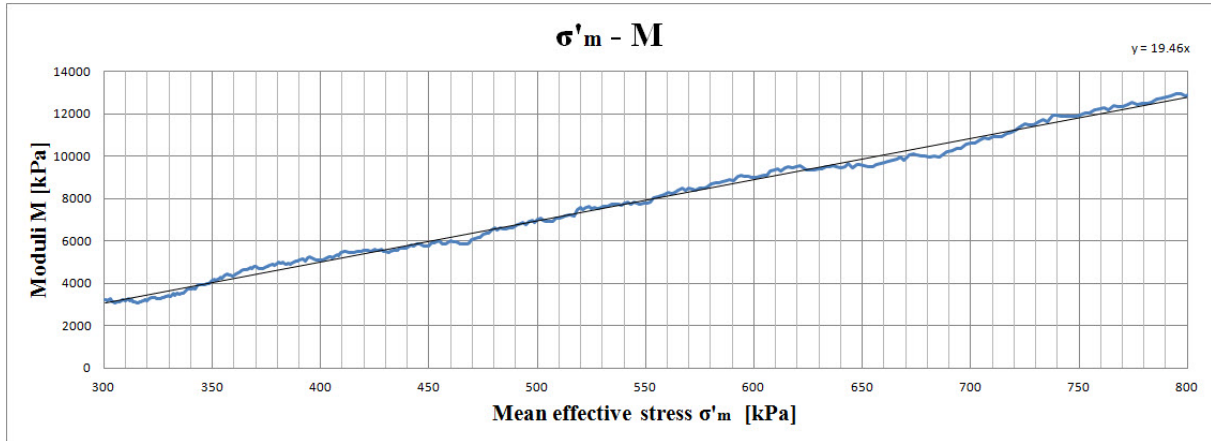


Figure 4.7.9: Sample S3-H1: Modulus number from CRS oedometer test on undisturbed specimen.

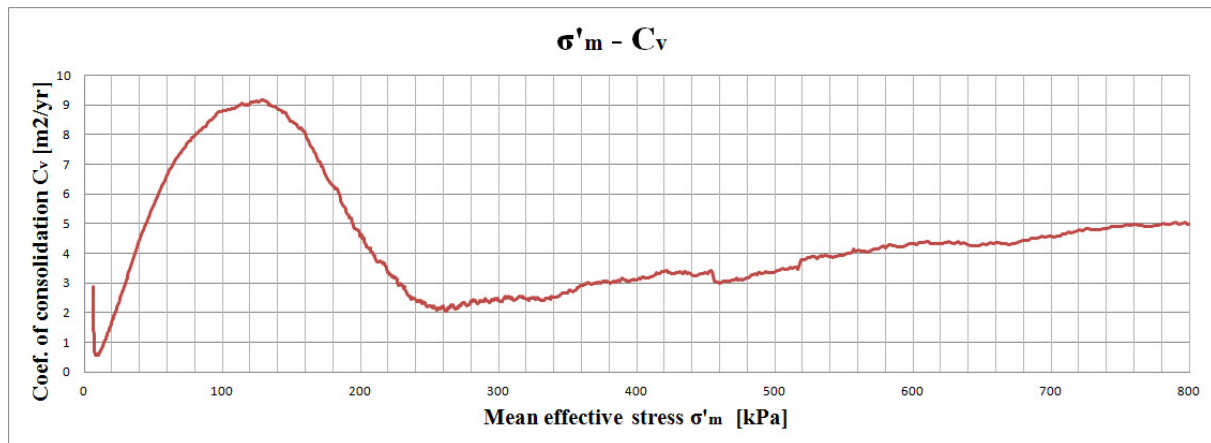


Figure 4.7.10: Sample S3-H1: Stress vs. coefficient of consolidation from CRS oedometer test on undisturbed specimen.

As follows from the test results presented in Figures 4.7.6-4.7.10, preconsolidation stress p'_c for sample S3-H1 is approximately 240 kPa. Constrained moduli in the overconsolidated range (M_o) and at the preconsolidation stress (M_n) are 6.3 MPa and 2.4 MPa, respectively. In normally consolidated range, the modulus number (m) is 19.5. Coefficients of consolidation in the overconsolidated zone (c_{v0}) and at about p'_c (c_{vn}) are $9.1 \text{ m}^2/\text{yr.}$ and $2.0 \text{ m}^2/\text{yr.}$, respectively.

With $p'_c = 240 \text{ kPa}$, the overconsolidation ratio for sample S3-H1 can be estimated as

$$OCR = \frac{p'_c}{\sigma'_{v0}} = \frac{240}{79.2} = 3.0 \tag{Eq. 4.128}$$

4.7.15 CRS Oedometer Test on Pre-Strained Clay

Calculation of water content for the test specimen is given in Table 4.7.19.

Table 4.7.19: Sample S3-H1: Calculation of water content for pre-strained specimen subjected to CRS oedometer test.

Parameter	Parameter value	Units
Mass, oedometer ring with specimen	111.42	gr.
Mass of oedometer ring	39.70	gr.
Mass of wet specimen (m_s+m_w)	71.72	gr.
Mass of dry specimen (m_s)	49.45	gr.
Mass of water (m_w)	22.27	gr.
Water content (w)	45.04	%

As seen from Table 4.7.19, there is a deviation of 1.44 % between calculated values of water content for the test specimen and for the whole sample S3-H1 (refer to Chapter 4.7.3).

Figures 4.7.11-4.7.14 show the results of CRS oedometer test on sample S3-H1 pre-strained to shear strain $\gamma_s = 18\%$. The presented results consist of:

- Stress vs. strain plot ($\sigma'_m - \varepsilon$), Figure 4.7.11.
- Stress vs. pore pressure at sample base ($\sigma'_m - u_b$), Figure 4.7.12.
- Stress vs. modulus plot ($\sigma'_m - M$), Figure 4.7.13.
- Stress vs. coefficient of consolidation ($\sigma'_m - c_v$), Figure 4.7.14.

As follows from the results presented in Figures 4.7.11-4.7.14, the modulus number (m) for the specimen pre-strained to shear strain $\gamma_s = 18\%$ is constant and equal to 18.7. Coefficient of consolidation (c_v) increases almost linearly with stress level after 100 kPa, reaching the peak value of 7.9 $m^2/yr.$ at 800 kPa.

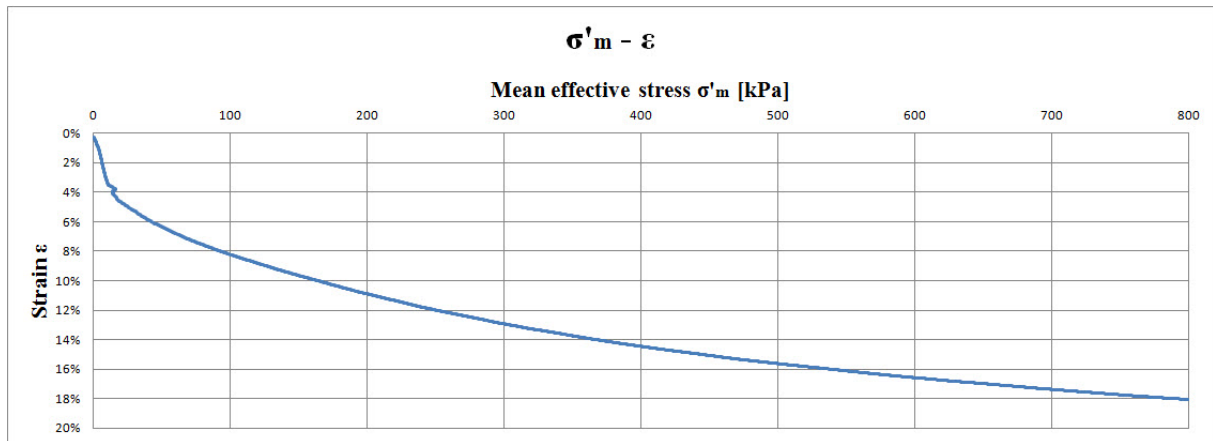


Figure 4.7.11: Sample S3-H1: Stress vs. strain from CRS oedometer test on specimen pre-strained to $\gamma_s = 18\%$.

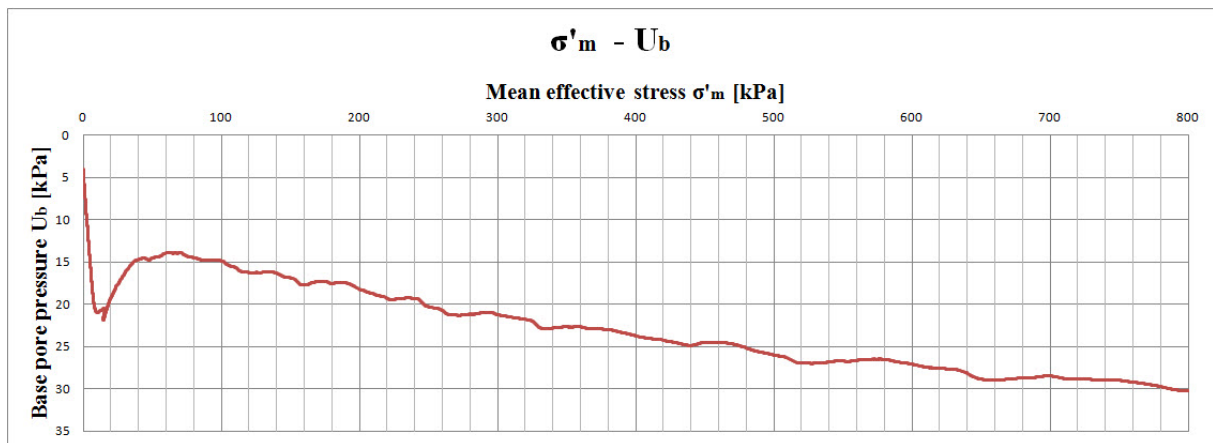


Figure 4.7.12: Sample S3-H1: Stress vs. pore pressure from CRS oedometer test on specimen pre-strained to $\gamma_s = 18\%$.

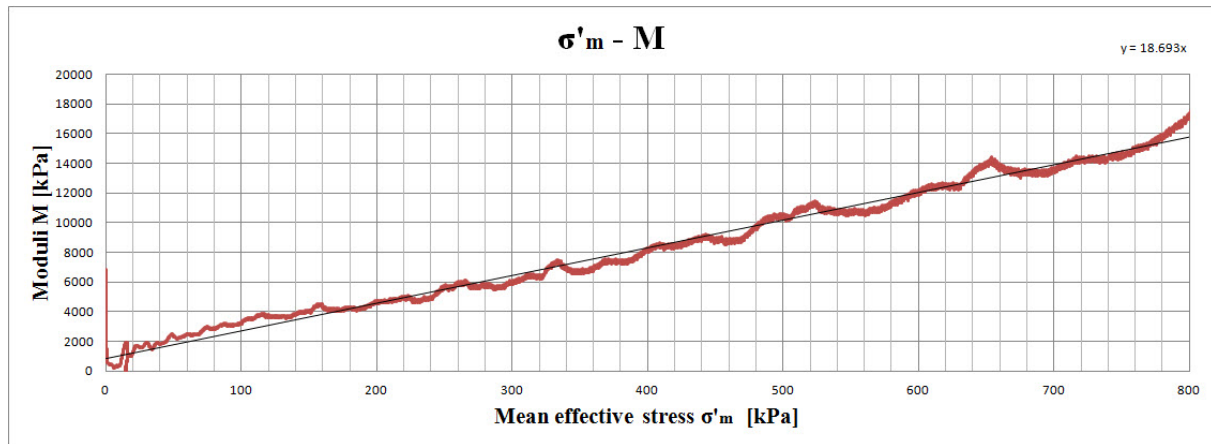


Figure 4.7.13: Sample S3-H1: Stress vs. oedometer modulus from CRS oedometer test on specimen pre-strained to $\gamma_s = 18\%$.

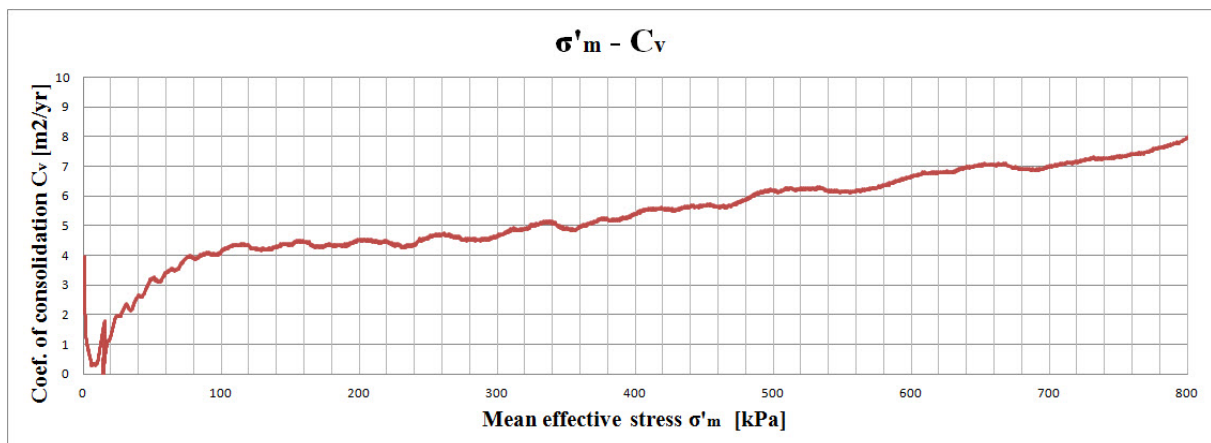


Figure 4.7.14: Sample S3-H1: Stress vs. coefficient of consolidation from CRS oedometer test on specimen pre-strained to $\gamma_s = 18\%$.

4.7.16 CRS Oedometer Test on Remoulded Clay

Calculation of water content for the test specimen is given in Table 4.7.20.

As follows from Table 4.7.20, there is close agreement between the value of water content for remoulded clay specimen and the value calculated for the whole sample S3-H1 (refer to Chapter 4.7.3). Additional control measurement showed water content $w = 43.17\%$.

Table 4.7.20: Sample S3-H1: Calculation of water content for remoulded specimen subjected to CRS oedometer test.

Parameter	Parameter value	Units
Mass, oedometer ring with specimen	109.54	gr.
Mass of oedometer ring	38.79	gr.
Mass of wet specimen (m_s+m_w)	70.75	gr.
Mass of dry specimen (m_s)	49.40	gr.
Mass of water (m_w)	21.35	gr.
Water content (w)	43.22	%

Figures 4.7.15-4.7.18 show the results of CRS oedometer test on totally remoulded clay sample S3-H1. The presented results consist of:

- Stress vs. strain plot ($\sigma'_m - \varepsilon$), Figure 4.7.15.
- Stress vs. pore pressure at sample base ($\sigma'_m - u_b$), Figure 4.7.16.
- Stress vs. modulus plot ($\sigma'_m - M$), Figure 4.7.17.
- Stress vs. coefficient of consolidation ($\sigma'_m - c_v$), Figure 4.7.18.

As follows from the results presented in Figures 4.7.15-4.7.18, the modulus number (m) for the remoulded specimen is constant and equal to 25.4. Coefficient of consolidation (c_v) is increasing with the stress level and is reaching its maximum of 5.1 m²/yr. at 800 kPa.

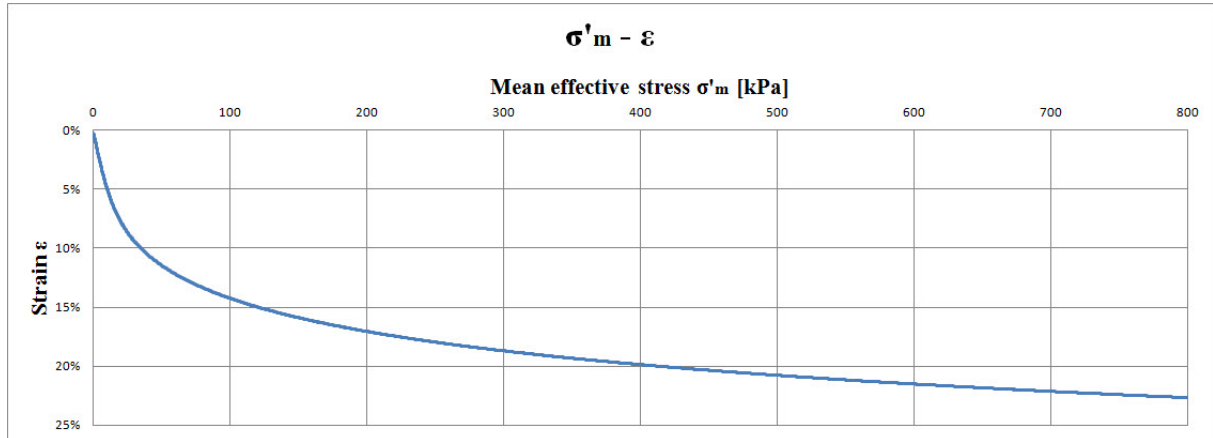


Figure 4.7.15: Sample S3-H1: Stress vs. strain from CRS oedometer test on remoulded specimen.

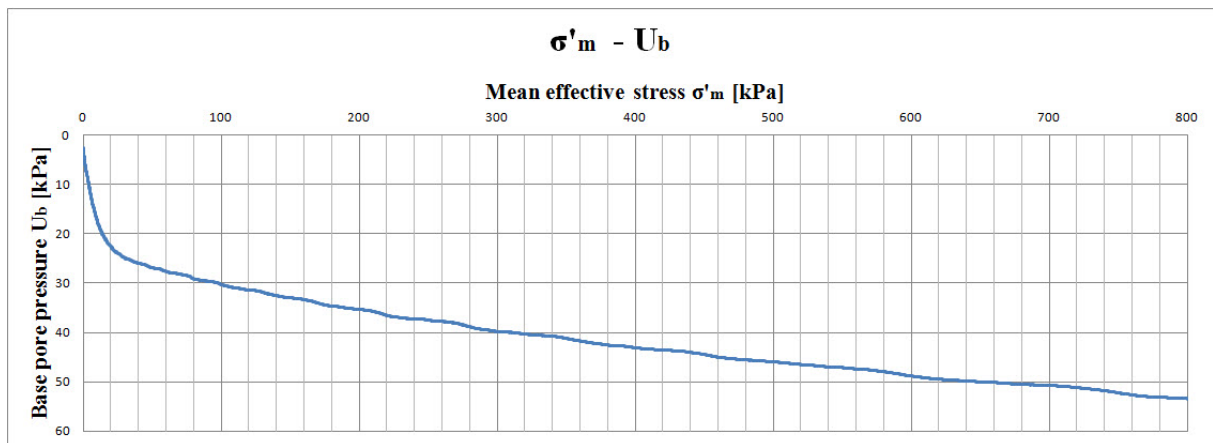


Figure 4.7.16: Sample S3-H1: Stress vs. pore pressure from CRS oedometer test on remoulded specimen.

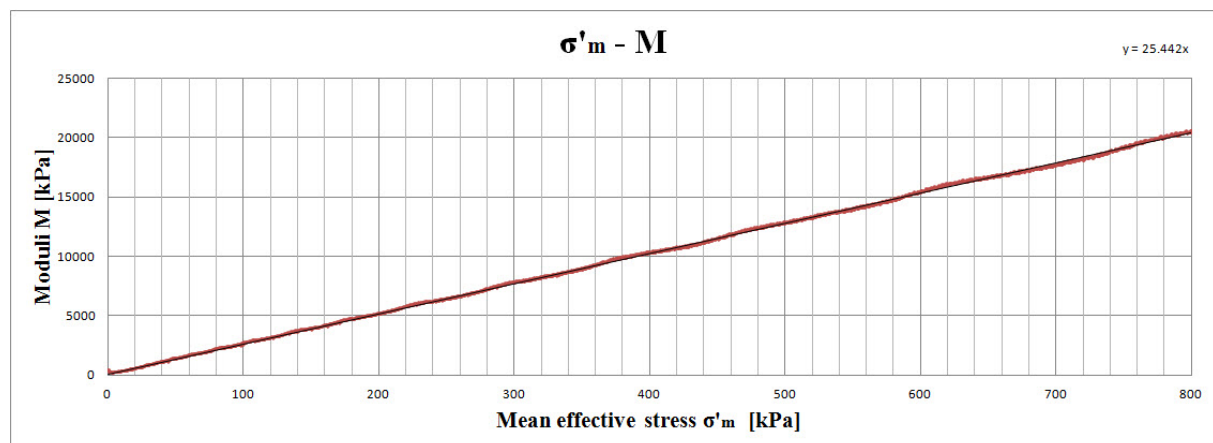


Figure 4.7.17: Sample S3-H1: Stress vs. oedometer modulus from CRS oedometer test on remoulded specimen.

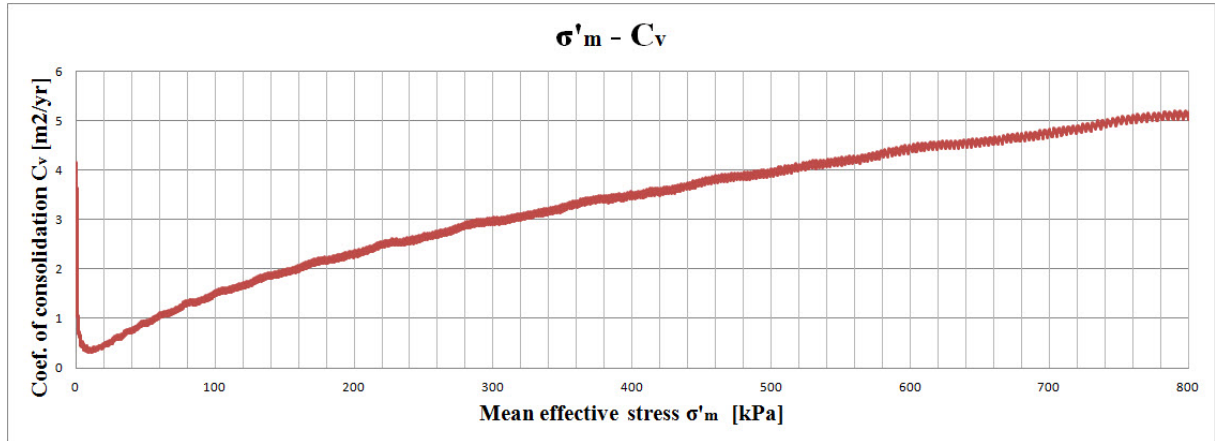


Figure 4.7.18: Sample S3-H1: Stress vs. coefficient of consolidation from CRS oedometer test on remoulded specimen.

CHAPTER 5 Evaluation of Results. Discussion

5.1 Introduction

The chapter is aimed to provide a coherent arrangement of the laboratory test results so that the general trends may be observed and the conclusions may be drawn. The test results and parameters for each sample may be found in respective subchapters of Chapter 4. Where the source of data or parameter value is not clear, reference is given to the relevant subchapter or equation.

Based on the laboratory test results, the chapter first gives a systematic review of the key parameters and classification of the soils involved in the study. Following the brief review of key soil parameters, there is a discussion on the impact of pre-straining and reconsolidation on stress-strain and strength properties of clay. Where applicable, the results of laboratory test programme are also briefly compared to the observations and data from past academic publications.

5.2 Key Soil Parameters

5.2.1 Tiller Clay

The test samples from Tiller originate from depths 3.043-3.800 m, 3.052-3.800 m and 4.045-4.800 m. After guidelines of NGF (1982), the material is classified as clay (depth 4.045-4.800 m, uniformity coefficients d_{60}/d_{10} and d_{75}/d_{25} are not available) and medium-graded silty clay (depth 3.043-3.800 m, ratio d_{75}/d_{25} is 12.6 and 13.7 depending on the sample, uniformity coefficient d_{60}/d_{10} is not available). Maximum grain size d_{\max} for all Tiller samples is 0.125 mm. Average grain size d_{50} ranges from 0.00537 to 0.01051 mm.

Depending on the sample, silt fraction is in range 60-70 % and clay fraction is in range 26-35 % (determined by weight). Silt content tends to decrease and clay content tends to increase with increasing depth. Figure 5.2.1 shows percentage of clay particles (determined by weight) and ratio d_{75}/d_{25} (where available) vs. depth.

There is a good agreement between calculated values of average unit weight and unit weight determined from small ring density. The soil's average unit weight $\bar{\gamma}$ varies between 18.66 and

19.42 kN/m³. The small ring densities suggest unit weights in range 18.25-19.42 kN/m³. Pycnometer test results show consistent values of densities of solids, ranging from 2.78 to 2.86 gr./cm³. The samples' average unit weights, small ring densities and densities of solids are shown in Figure 5.2.2.

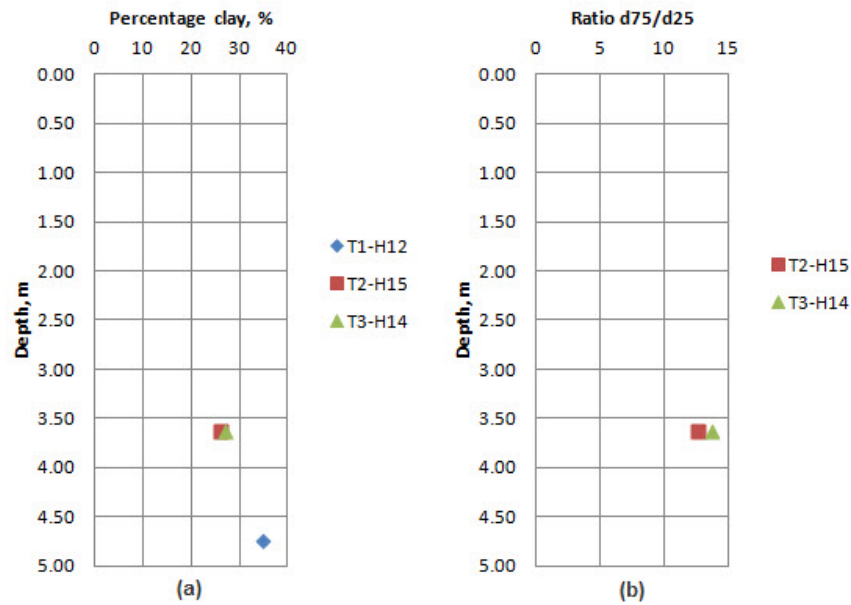


Figure 5.2.1: Tiller clay: (a) Percentage of clay particles (measured by weight), (b) Ratio d_{75}/d_{50} .

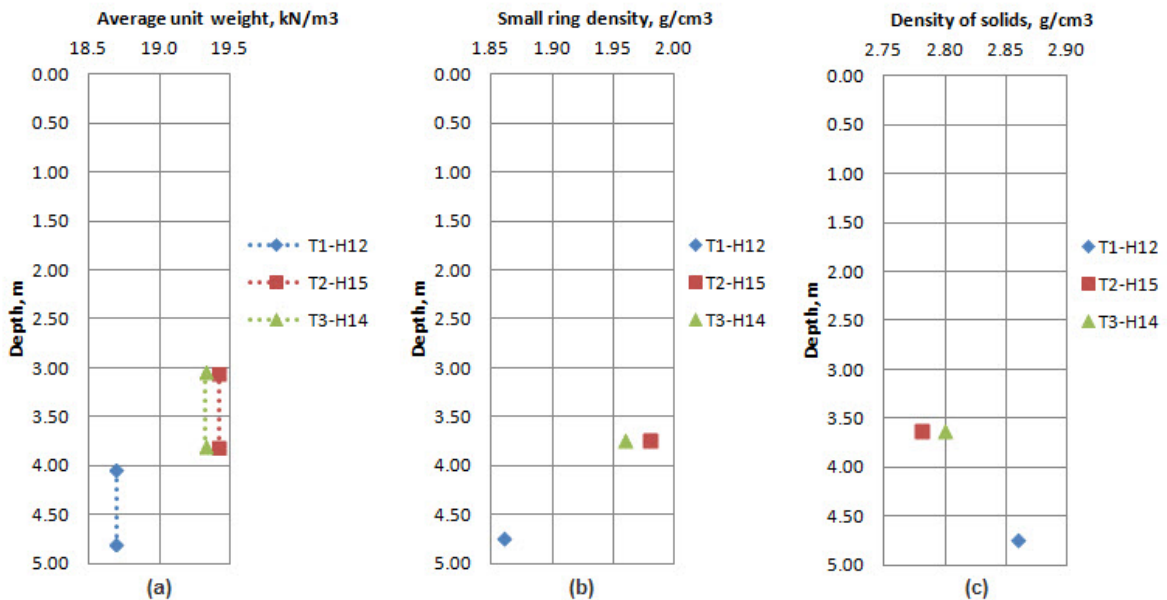


Figure 5.2.2: Tiller clay: (a) Average unit weight, (b) Small ring density, (c) Density of solids.

All samples at Tiller are obtained from the depth below groundwater table. Due to the lack of own measurements, groundwater table is assumed to be located at depth of 0.5 m in

accordance with Gylland et al. (2013). Laboratory tests and calculations show that the material is nearly fully saturated, with degree of saturation S_r between 0.92 and 0.98.

Natural water content has been calculated at three different locations for each cylinder. Because the measurements were taken immediately after the pre-straining, undrained conditions apply and the water content in pre-strained specimens is assumed to be equal to the natural water content. For each sample cylinder, mean value of three water content measurements is used in the calculations of liquidity and plasticity indices. Figure 5.2.3 shows measurements of water content together with calculated values of liquidity and plasticity indices.

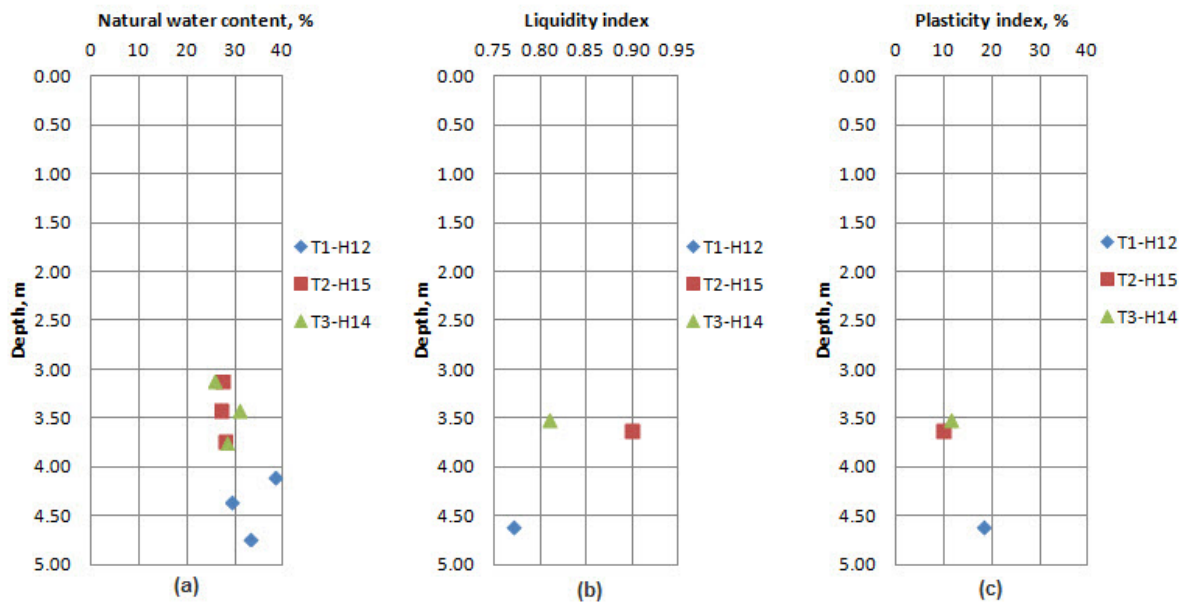


Figure 5.2.3: Tiller clay: (a) Natural water content, (b) Liquidity index, (c) Plasticity index.

The natural water content measurements are consistent for depth 3.043-3.800 m but shows considerable deviations at depth 4.045-4.800 m. Overall, natural water content is varying from 26 to 38 %. A general trend is that natural water content is increasing with depth. The scatter in data may indicate that the material is somewhat inhomogeneous, and that the material at depth 3.043-3.800 m may be affected by the presence of dry crust. Figures 5.2.1, 5.2.2 and 5.2.3(c) support this hypothesis, since the typical values of measured content of clay fraction, unit weights and densities are different for the depths 3.043-3.800 m and 4.045-4.800 m.

Furthermore, the observations of natural water content in sample T1-H12 show some scatter. The scatter cannot be explained by migration of pore water during storage of the cylinder, since the smallest value of natural water content has been measured at the mid-part of cylinder and not at the end of cylinder. The deviations indicate a possible local inhomogeneity in the material at depth 4.045-4.800 m.

Depending on the sample, plasticity index for Tiller clay varies from 9.9 to 18.1 %. According to NGF (1982), the clay is classified as low plastic (sample T2-H15, depth 3.052-3.800 m) to medium plastic (samples T1-H12 and T3-H14, depth 4.045-4.800 m and 3.043-3.800 m). A general trend is increase of the plasticity index with depth.

The shear strength measurements of Tiller clay demonstrate considerable scatter even for material extracted from the same depths from different holes. The deviations may be caused by inhomogeneity of the material and presence of the dry crust. The scatter is largest at depths of 3.043-3.800 m where the undrained shear strength determined by fall cone is 46 and 71 kPa. UCT on the same samples suggest undrained shear strength of 89 and 87 kPa. Due to the apparent variations in sample composition, the quality of UCT test results should be regarded as questionable. Apart from the sample composition, the samples from depths 3.043-3.800 m demonstrate failure strains larger than 5 %, which is an indication of disturbed material. At depth 4.045-4.800 m, however, there is a good agreement between shear strength values determined by fall cone and UCT, which are 24 and 25 kPa, respectively. All Tiller samples demonstrate similar values of fall cone sensitivity, which is in range of 10.3-11.0. Figure 5.2.4 shows the results of falling cone test and unconfined compression test.

According to NGF (1982) and based on fall cone test results, Tiller samples are classified after their undrained shear strength and sensitivity:

- Sample T1-H12 (depth 4.045-4.800 m): medium sensitive and soft clay.
- Sample T2-H15 (depth 3.052-3.800 m): medium sensitive and stiff clay.
- Sample T3-H14 (depth 3.043-3.800 m): medium sensitive and medium stiff clay.

CRS oedometer test results on undisturbed material show that Tiller clay is slightly overconsolidated, with OCR in range 3.3-4.3. The preconsolidation stress is 120 kPa at depth 3.5 m and 180 kPa at depth 4.5 m. Figure 5.2.5 shows the values of OCR and preconsolidation stress.

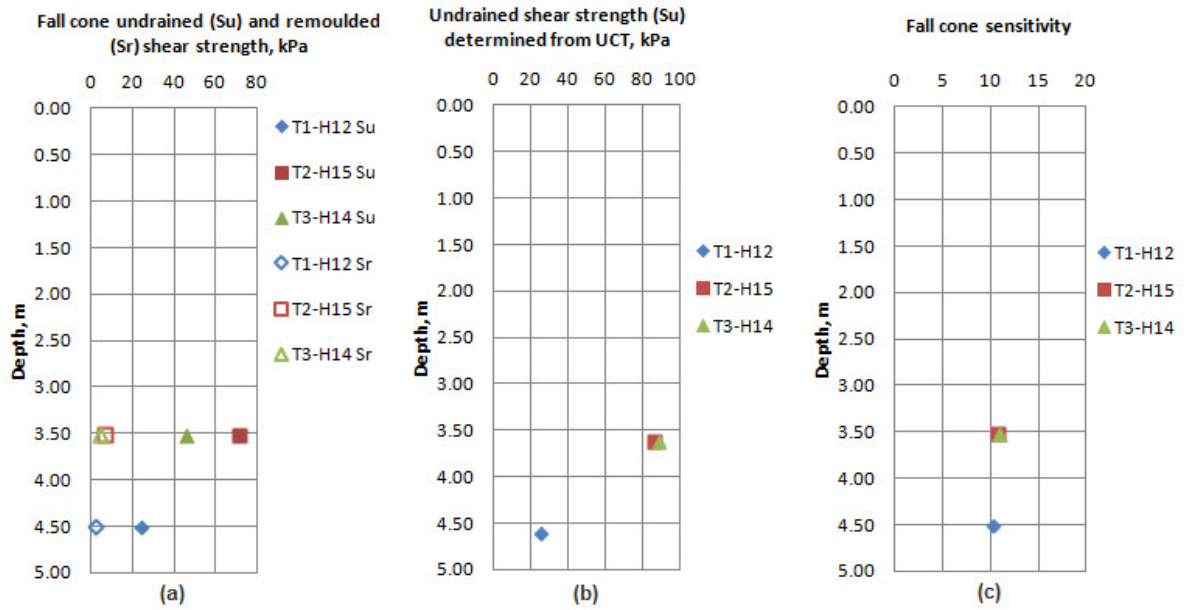


Figure 5.2.4: Tiller clay: (a) Fall cone undrained and remoulded shear strength, (b) UCT undrained shear strength, (c) Fall cone sensitivity.

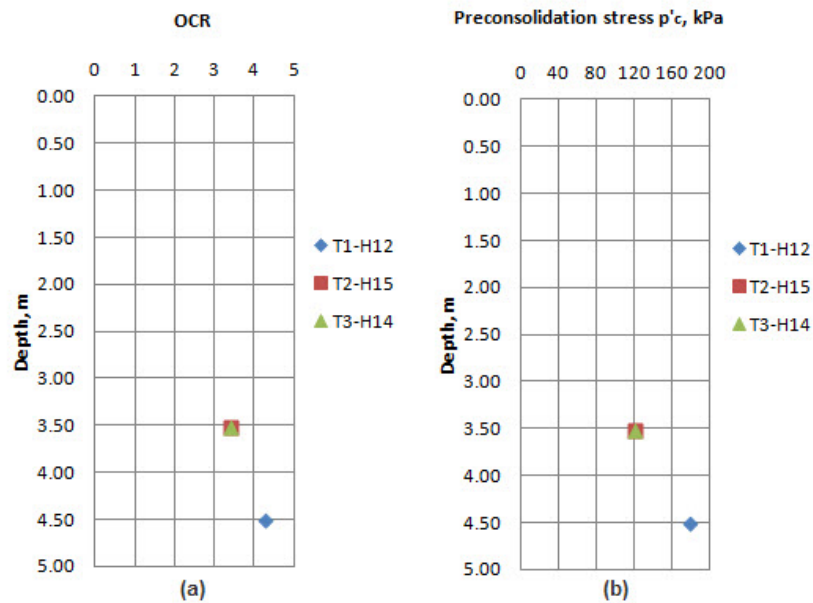


Figure 5.2.5: Tiller clay: (a) OCR, (b) Preconsolidation stress.

The values of constrained modulus in the overconsolidated range (M_o) and at the preconsolidation stress (M_n) are consistent and in range of 3-5 MPa and 2-4 MPa, respectively. In the normally consolidated stress range, all Tiller samples demonstrate similar values of modulus number, which are varying from 22.2 to 23.5. Based on the modulus

number, all Tiller samples are classified as stiff after Janbu (1970). Figure 5.2.6 shows constrained moduli and modulus numbers for Tiller clay samples. For the explanation of terms, refer to the inset in Figure 2.2.6.

The values of coefficient of consolidation in the overconsolidated range (c_{vo}) and at the preconsolidation stress (c_{vn}) are shown in Figure 5.2.7. The values should be treated with caution since there is considerable scatter in the data. All values of c_v except for the sample T1-H12 are within the range which can be expected for Norwegian clays ($5\text{-}25\text{ m}^2/\text{yr.}$).

For sample T1-H12, the values of coefficient of consolidation in the overconsolidated zone (c_{vo}) and at about p'_c (c_{vn}) are $200\text{ m}^2/\text{yr.}$ and $50\text{ m}^2/\text{yr.}$, respectively. The values are higher than what should be expected. One possible explanation of unusually high values of c_v for sample T1-H12 is high content of silt particles (according to NGF, 1982, the values of c_v may be hundreds or thousands times larger for silt and sand than for clay). However, this possible explanation contradicts with other test results since other Tiller samples demonstrate even higher silt content but lower values of c_v .

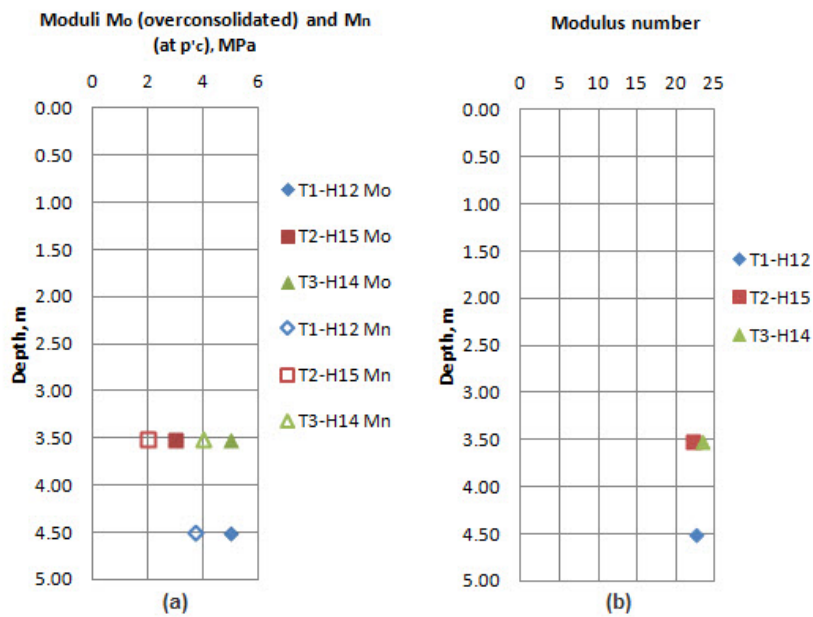


Figure 5.2.6: Tiller clay: (a) Constrained modulus in the overconsolidated range (M_o) and at the preconsolidation stress (M_n), (b) Modulus number (m).

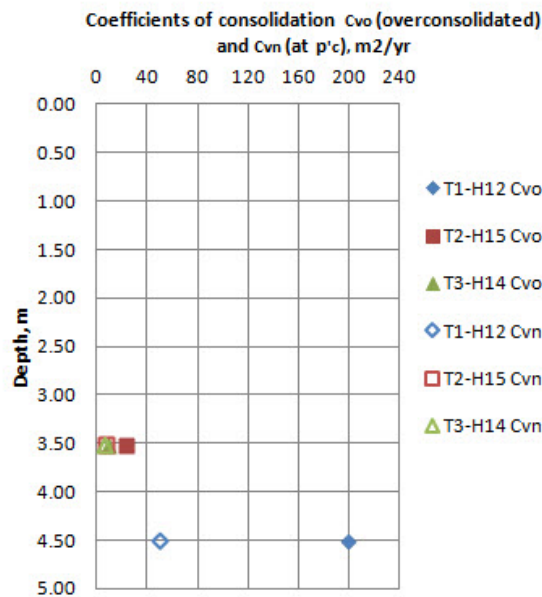


Figure 5.2.7: Tiller clay: Coefficient of consolidation in the overconsolidated range (c_{vo}) and at the preconsolidation stress (c_{vn}).

5.2.2 Stjørdal Clay

The test samples from Stjørdal originate from depths 6.041-6.800 m, 7.040-7.800 m and 8.043-8.800 m. All samples contain high percentage of fines, and are classified as clay in accordance with NGF (1982). Sample from the depth 6.041-6.800 m contains larger quantity of particles from silt fraction than other samples. For all samples, uniformity coefficients d_{60}/d_{10} and d_{75}/d_{25} are not available for practical reasons. Maximum grain size d_{max} for Stjørdal clay varies from 0.074 mm to 0.125 mm, depending on the sample. Average grain size d_{50} is 0.00292 mm and was possible to determine only for one of the samples.

From 7 m depth and below, percentage of clay and silt particles appears to be fairly constant and equal to 63-65 % and 34-35 %, respectively (determined by weight). At depth 6.041-6.800 m, the percentage of clay is 45 % and percentage of silt particles is 53 % (determined by weight). It is clear that the material at depth 6.041-6.800 m is affected by the presence of sand layer above the clay. Figure 5.2.8 shows percentage of clay particles vs. depth.

For depths below 7.0 m, calculations of unit weights and densities show consistent data. At these depths, the soil's average unit weight $\bar{\gamma}$ is in range 17.85-18.15 kN/m³ while the small ring densities suggest unit weights in range 17.66-18.15 kN/m³. Average unit weight and

small ring density at depth 6.041-6.800 m are 19.13 kN/m³ and 1.87 gr./cm³, respectively. The deviations in density values agree closely with the conclusions drawn from hydrometer analysis, namely that the clay at depth 6.041-6.800 m has a distinct material composition and probably distinct material properties. Pycnometer test results show similar values for all samples, with density of solids ranging from 2.78 to 2.81 gr./cm³. The samples' average unit weights, small ring densities and densities of solids are shown in Figure 5.2.9.

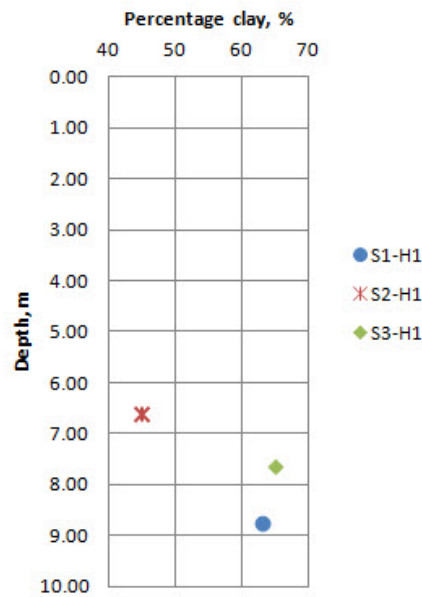


Figure 5.2.8: Stjørdal clay: Percentage of clay particles (measured by weight).

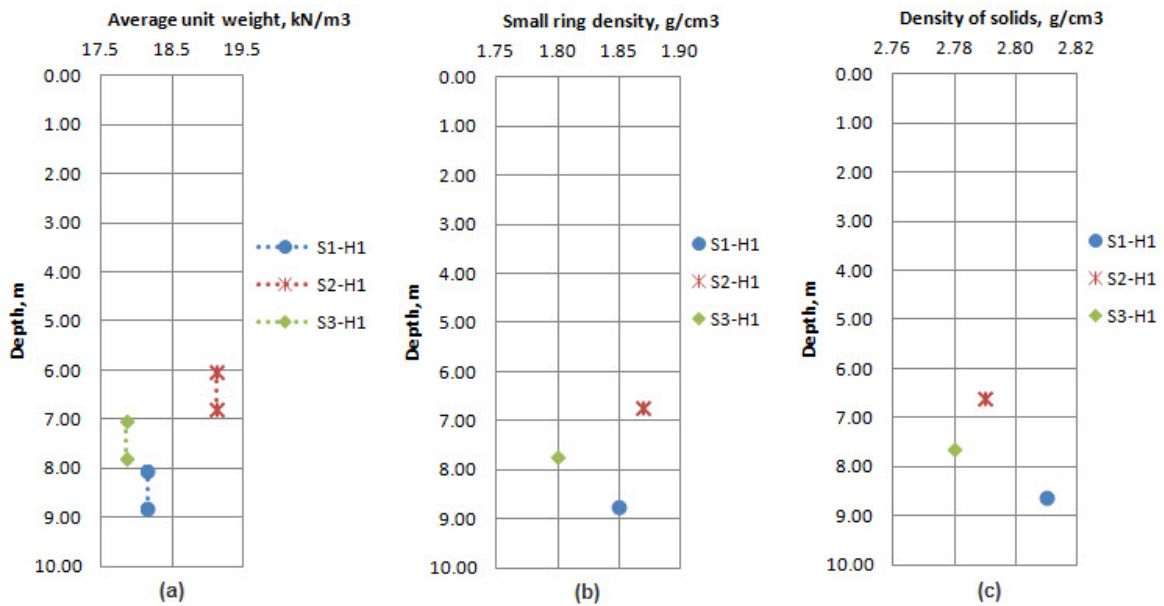


Figure 5.2.9: Stjørdal clay: (a) Average unit weight, (b) Small ring density, (c) Density of solids.

Previous field investigations carried out during one of the courses run by NTNU suggest that groundwater table is located at depth of 2.25 m. Laboratory tests and calculations show that the degree of saturation (S_r) is 0.93 for the depth 6.041-6.800 m and 1.00 for the depths 7.040-7.800 m and 8.043-8.800 m.

Measurements of natural water content and calculations of liquidity and plasticity indices for Stjørdal samples are carried out in similar manner as for Tiller samples. Figure 5.2.10 shows values of natural water content, liquidity index and plasticity index.

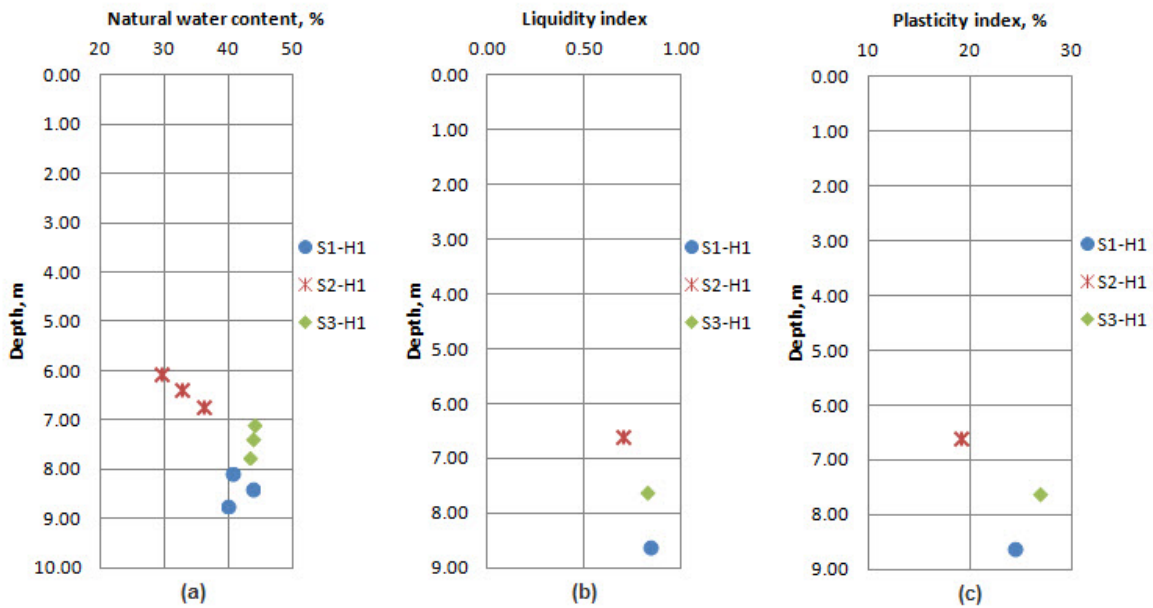


Figure 5.2.10: Stjørdal clay: (a) Natural water content, (b) Liquidity index, (c) Plasticity index.

The measurements of natural water content show uniform values of 40-44 % at depths 7.040-7.800 m and 8.043-8.800 m. The values are considerably lower at the depth of 6.041-6.800 m (29-36 %), indicating a distinct clay layer. These observations agree well with the conclusions drawn from hydrometer and density test results.

Plasticity and liquidity indices follow the same trend as the natural water content values. At depths 7.040-7.800 m and 8.043-8.800 m, plasticity and liquidity indices are in range of 24-27 % and 0.82-0.84. At depth 6.041-6.800 m, the indices are respectively 19 % and 0.70. According to NGF (1982), the clay is classified as medium plastic at depth 6.041-6.800 m and highly plastic at depth 7.0 m and below.

Figure 5.2.11 shows shear strength and sensitivity data for Stjørdal clay. There is lack of agreement between shear strength values obtained from UCT and fall cone tests. Samples from depths 6.041-6.800 m and 7.040-7.800 m subjected to UCT might have contained disturbed material since the recorded axial strain at failure was larger than 5 %. Undrained shear strength values from fall cone tests are consistent and in range of 39-41 kPa at depth 7.040-7.800 m and 8.043-8.800 m. Fall cone test on the material from depth 6.041-6.800 m suggests considerably higher undrained shear strength (73 kPa) at this depth, which is in good agreement with other tests' indications of layering. All Stjørdal samples demonstrate similar values of remoulded shear strength (5.1-7.5 kPa). Sensitivity values are 7.4-8.0 for depth 7.040-8.800 m and 9.7 for depth 6.041-6.800 m. According to NGF (1982) and based on fall cone test results, the clay is classified as medium sensitive and stiff at depth 6.041-6.800 m, and low to medium sensitive and medium stiff at depths below 7.0 m.

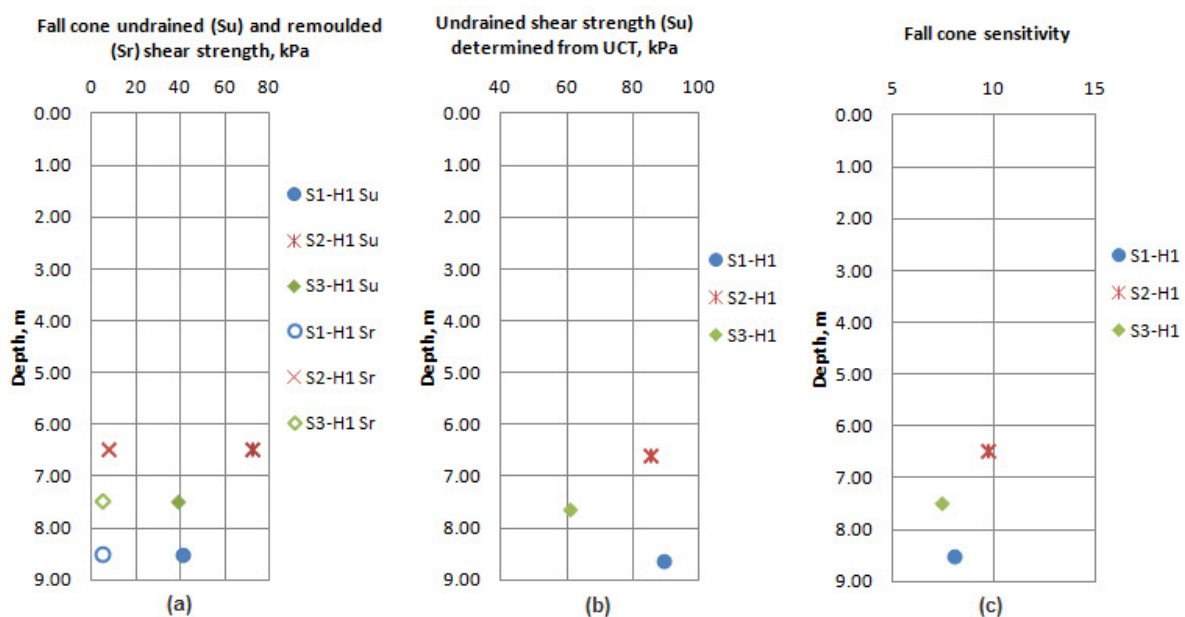


Figure 5.2.11: Stjørdal clay: (a) Fall cone undrained and remoulded shear strength, (b) UCT undrained shear strength, (c) Fall cone sensitivity.

CRS oedometer test results on undisturbed material show that Stjørdal clay samples are slightly overconsolidated, with OCR in range 3.0-3.3. The preconsolidation stress varies from 240 to 270 kPa. Figure 5.2.12 shows values of OCR and preconsolidation stress.

The range of values of the constrained modulus in the overconsolidated range (M_o) and at the preconsolidation stress (M_n) is 5.5-6.9 MPa and 2.4-6.1 MPa, respectively. In the normally consolidated stress range, all values of modulus number agree closely, ranging from 19.3 to

20.5. Based on the modulus number, the clay is classified as medium stiff (depth 7.040-8.800 m) to stiff (depth 6.041-6.800 m) after Janbu (1970). Figure 5.2.13 shows constrained moduli and modulus numbers for Stjørdal clay. For the explanation of terms, refer to the inset in Figure 2.2.6.

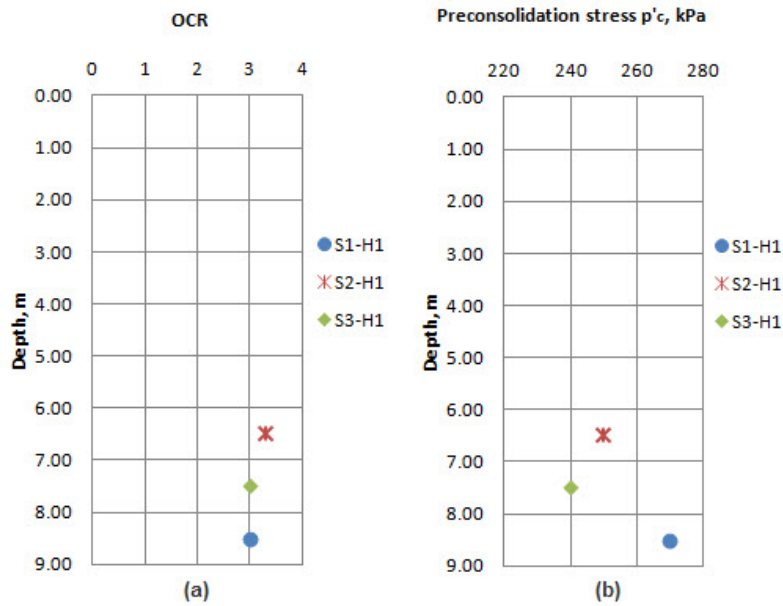


Figure 5.2.12: Stjørdal clay: (a) OCR, (b) Preconsolidation stress.

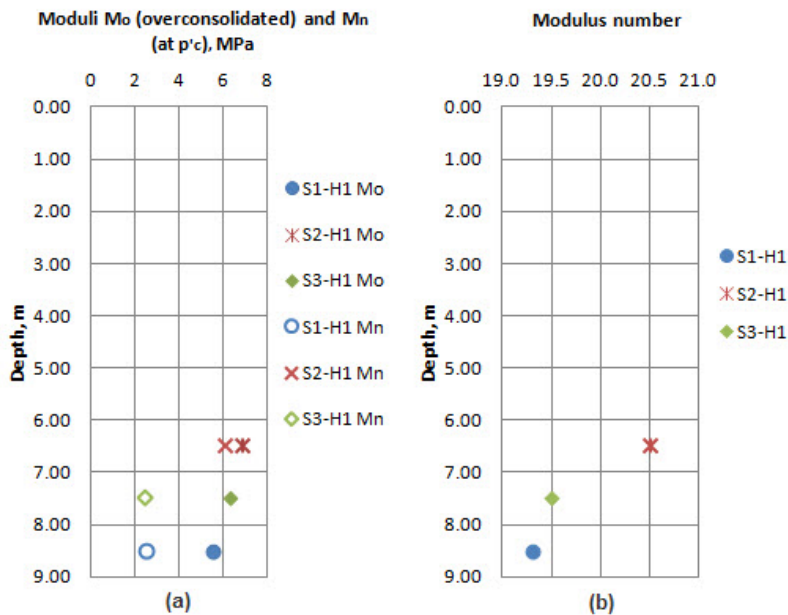


Figure 5.2.13: Stjørdal clay: (a) Constrained modulus in the overconsolidated range (M_o) and at the preconsolidation stress (M_n), (b) Modulus number (m).

The values of coefficient of consolidation in the overconsolidated range (c_{vo}) and at the preconsolidation stress (c_{vn}) are shown in Figure 5.2.14. The values indicate once again a distinct layer at the depth 6.041-6.800 m. All values of c_v are within or close to the range which can be expected for Norwegian clays ($5\text{-}25\text{ m}^2/\text{yr}$).

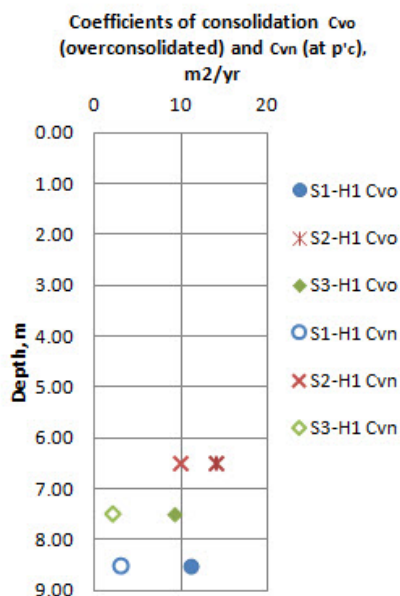


Figure 5.2.14: Stjørdal clay: Coefficient of consolidation in the overconsolidated range (c_{vo}) and at the preconsolidation stress (c_{vn}).

5.3 Pre-Straining Through Extrusion

Uniform strain distribution in the extruded material was expected prior to the execution of the test programme. However, both visual observations and calculations of the displacement ratios have shown that the strain profile was varying in the cross-sections of pre-strained clay samples. While the exact degree of strain variation in the pre-strained mass is challenging to estimate (thus, strain variation remains unknown), several visual observations indicate that highly plastic clay with high water content (Stjørdal) experiences less strain variation than what has been observed in low and medium plastic clay (Tiller).

Although the strain profile does not correspond exactly to the theoretically calculated strain values, the exact value of shear strain (and hence also a minor variation of strain profile) is not significant. This is due to the fact that the study is aimed to simulate the processes around a pile during installation phase. In a real problem, the shear strain magnitude in the soil around a pile is often well above 100 % and quickly drops below 20 % within a limited radial

distance from the pile wall. The variation of strains over radial distance is so large that the exact values of strains are of minor interest. It is rather important to distinguish between different levels of the strains. Karlsrud (2012) recommends a study of straining at three different levels: completely remoulded clay (shear strain above 100 %), severely strained clay (shear strain 20-100 %) and moderately strained clay (shear strain less than 20 %). Even with the variations of strain profiles in the pre-strained cross-sections, the accuracy of the pre-straining is good enough to be grouped in these three categories.

5.4 Impact of Pre-Straining on Shear Strength

Table 5.4.1 provides summary of undrained strength (s_u) determined by falling cone, residual shear strength for pre-strained non-reconsolidated material (s) determined by falling cone, and normalised residual shear strength immediately after the pre-straining (s/s_u), for each sample. The table also includes normalised remoulded shear strength (s_r/s_u) which is given by the inverse of sensitivity (S_t).

The data in Table 5.4.1 are presented graphically in following figures:

- Figure 5.4.1: Undrained, residual and remoulded shear strength (s_u , s and s_r , respectively), Tiller clay.
- Figure 5.4.2: Undrained, residual and remoulded shear strength (s_u , s and s_r , respectively), Stjørdal clay.
- Figure 5.4.3: Normalised undrained, residual and remoulded shear strength (s_u/s_u , s/s_u and s_r/s_u , respectively), Tiller clay.
- Figure 5.4.4: Normalised undrained, residual and remoulded shear strength (s_u/s_u , s/s_u and s_r/s_u , respectively), Stjørdal clay.

A well-defined trend which follows from Figures 5.4.1-5.4.2 is that the increase in shear strain induces non-linear decrease in shear strength of the material. An exception from this general trend is the shear strength of pre-strained sample S2-H1, which is likely to be a result of distinct material composition. As data show, the shear strength of material remoulded by pre-straining ($\gamma_s = 117\%$) approaches the shear strength of material remoulded manually. The latter defines the lowest limit for shear strength. The trend is less visible from normalised values in Figures 5.4.3-5.4.4.

It should be noted that the impact of pre-straining on strength characteristics of non-reconsolidated material can possibly not be captured only by studying the correlation between shear strain and shear strength. An additional attempt should be done on studying the correlation between shear strength after the pre-straining, and applied work (force and displacement) through the pre-straining process. Investigation of such correlation was originally an objective of the thesis, but had to be excluded due to the lack of appropriate equipment.

Table 5.4.1: Impact of pre-straining on strength properties, all samples.

Sample ID	Applied shear strain γ_s , %	Undrained shear strength s_u , kPa	Residual shear strength of pre-strained non-re-consolidated specimen s , kPa	Remoulded shear strength s_r , kPa	Normalised residual shear strength after the pre-straining s/s_u	Normalised remoulded shear strength s_r/s_u
T1-H12	117	23.7	8.7	2.3	0.37	0.10
T2-H15	66	71.0	20.4	6.6	0.29	0.09
T3-H14	18	46.1	30.6	4.2	0.66	0.09
S1-H1	117	40.7	9.3	5.1	0.23	0.13
S2-H1	66	72.6	37.1	7.5	0.51	0.10
S3-H1	18	39.0	19.9	5.3	0.51	0.14

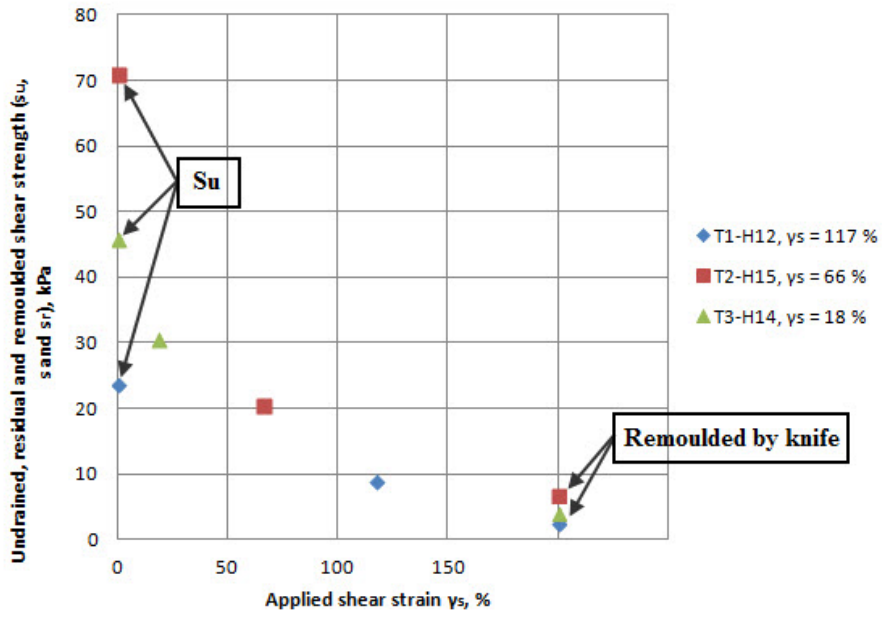


Figure 5.4.1: Tiller clay: Undrained, residual and remoulded shear strength.

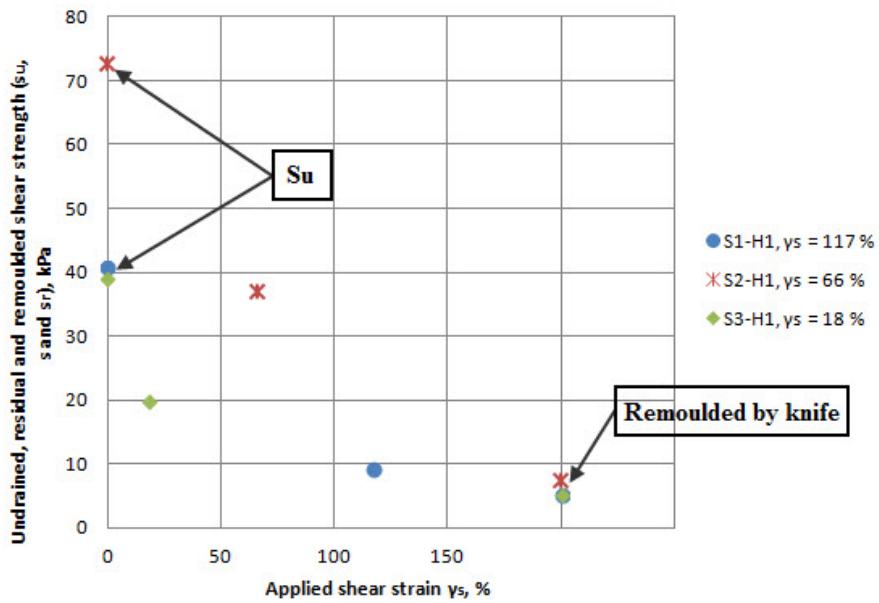


Figure 5.4.2: Stjørdal clay: Undrained, residual and remoulded shear strength.

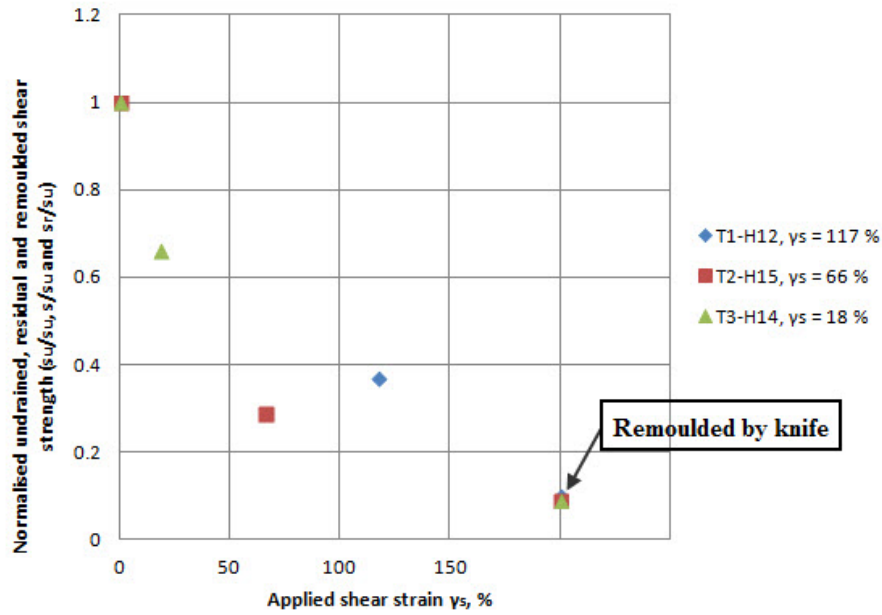


Figure 5.4.3: Tiller clay: Normalised undrained, residual and remoulded shear strength.

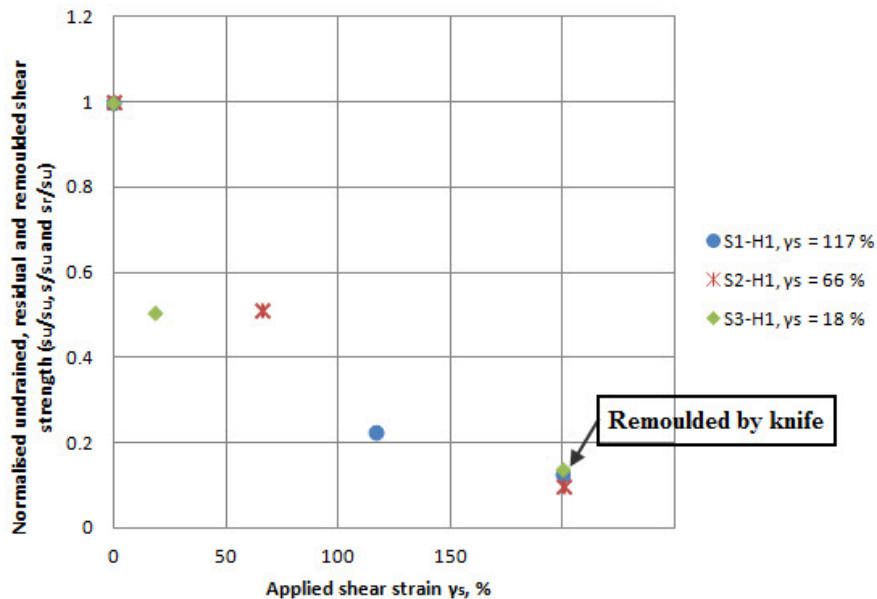


Figure 5.4.4: Stjørdal clay: Normalised undrained, residual and remoulded shear strength.

5.5 Impact of Pre-Straining and Reconsolidation on Shear Strength

Fall cone test results for pre-strained and reconsolidated Tiller and Stjørdal clay specimens are respectively shown in Table 5.5.1 and Table 5.5.2. For more details, refer to the respective chapters dealing with reconsolidation of each sample in the oedometer. The normalised

change in shear strength after pre-straining and reconsolidation ($\Delta s/s_u$) is determined after Eq. 3.28.

Table 5.5.1: Tiller clay: Impact of pre-straining and reconsolidation on strength properties.

Sample ID	Applied shear strain γ_s , %	Undrained shear strength s_u , kPa	Re-consolidation stress p'_{re} , kPa	Shear strength of pre-strained specimen after re-consolidation s_{re} , kPa	Normalised change in shear strength after pre-straining and re-consolidation of the specimen $\Delta s/s_u$	Normalised shear strength after pre-straining and re-consolidation s_{re}/p'_{re}
T1-H12	117	23.7	42.2	47.4	1.00	1.12
			100	73.6	2.11	0.74
			150	85.5	2.61	0.57
			200	80.9	2.41	0.40
T2-H15	66	71.0	35.6	35.8	-0.50	1.01
			100	103.3	0.45	1.03
			150	120.7	0.70	0.80
			200	81.6	0.15	0.41
T3-H14	18	46.1	36.1	42.0	-0.09	1.16
			100	75.2	0.63	0.75
			150	102.6	1.23	0.68
			200	102.3	1.22	0.51

Table 5.5.2: Stjørdal clay: Impact of pre-straining and reconsolidation on strength properties.

Sample ID	Applied shear strain γ_s , %	Undrained shear strength s_u , kPa	Re-consolidation stress p'_{re} , kPa	Shear strength of pre-strained specimen after re-consolidation s_{re} , kPa	Normalised change in shear strength after pre-straining and re-consolidation of the specimen $\Delta s/s_u$	Normalised shear strength after pre-straining and re-consolidation s_{re}/p'_{re}
S1-H1	117	40.7	89.5	69.2	0.70	0.77
			100	75.9	0.86	0.76
			150	74.2	0.82	0.49
			200	86.5	1.13	0.43
S2-H1	66	72.6	75.1	71.1	-0.02	0.95
			100	86.5	0.19	0.87
			150	102.3	0.41	0.68
			200	105.0	0.45	0.53
S3-H1	18	39.0	79.2	30.3	-0.22	0.38
			100	50.4	0.29	0.50
			150	67.7	0.74	0.45
			200	71.6	0.84	0.36

Figures 5.5.1 and 5.5.2 show graphical presentation of normalised changes in shear strength from Tables 5.5.1-5.5.2. The test results for Tiller and Stjørdal clay are separated in two different figures to make the data readable. The manner of presentation implies that the reference point (undrained shear strength for undisturbed material, e.g. zero change in shear strength) is located in origo of the coordinate system.

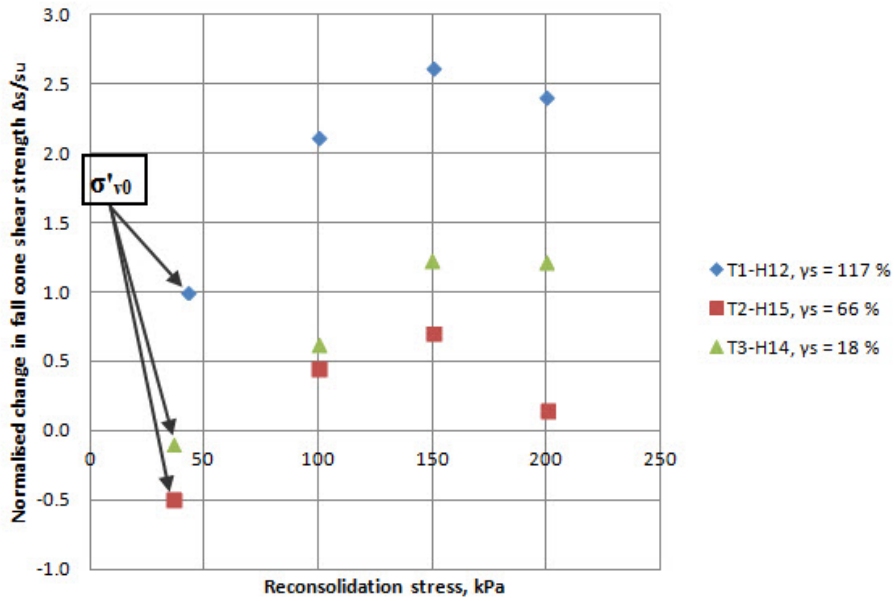


Figure 5.5.1: Tiller clay: Normalised change in shear strength vs. reconsolidation stress.

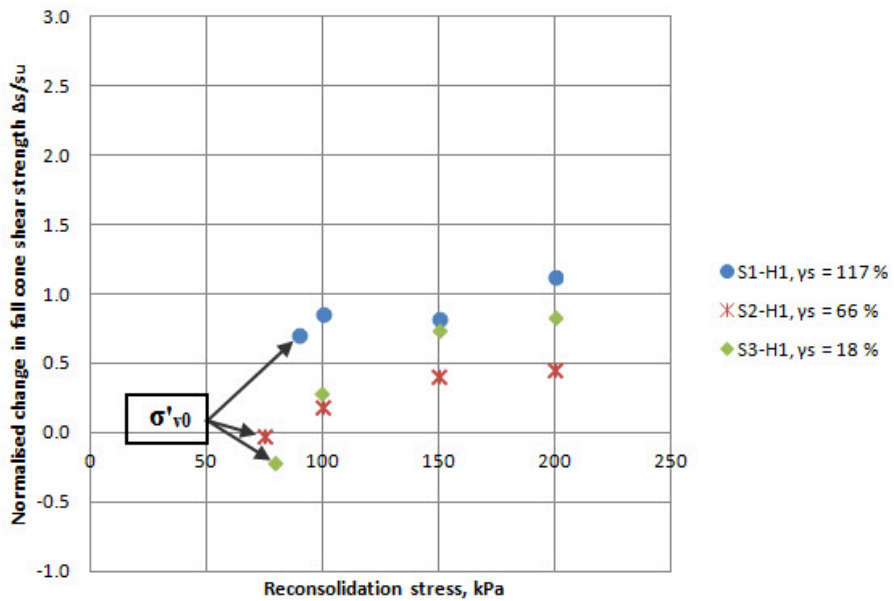


Figure 5.5.2: Stjørdal clay: Normalised change in shear strength vs. reconsolidation stress.

Apart from grain size distribution, the main difference between Tiller and Stjørdal clays are sensitivity values, natural water content and plasticity index (refer to Chapter 5.2 for more details). Compared to material from Stjørdal, Tiller clay has higher silt content, higher sensitivity (S_t in range 10-11), lower natural water content (w in range 26-38 %) and lower

plasticity index (I_p in range 10-18 %). A comparison of data in Figure 5.5.1 and Figure 5.5.2 leads to observation of following trends which are distinct for pre-strained Tiller clay:

- Peak shear strength of pre-strained Tiller clay is reached at approximate reconsolidation stress of 150 kPa. At higher level of reconsolidation stress (200 kPa), a softening seems to occur for all levels of pre-straining. Contrary to this behaviour, a general trend for Stjørdal clay is that shear strength of reconsolidated material is close to its maximum value and becomes nearly constant at reconsolidation stress of 150 kPa or higher, for all levels of pre-straining.
- The effect of shear strength recovery after reconsolidation is largest for Tiller clay.

It is unclear, however, whether the observed behaviour is correlated with high silt content, medium sensitivity, water content or plasticity index. To establish a more coherent understanding of correlation between these variables, more empirical data are required.

In addition to the observations above, data in Figure 5.5.1 and Figure 5.5.2 show following trends which apply for both clay types:

- Completely remoulded ($\gamma_s = 117\%$) and reconsolidated clay demonstrates an increase in shear strength for all levels of reconsolidation stresses in range 42-200 kPa. The normalised change in shear strength $\Delta s/s_u$ for completely remoulded Tiller and Stjørdal clay varies from 0.70 to 2.60, depending on the magnitude of reconsolidation stress.
- Moderately pre-strained ($\gamma_s = 18\%$) and reconsolidated clay demonstrates larger gain in shear strength than what is common for severely pre-strained ($\gamma_s = 66\%$) and reconsolidated clay.
- Material pre-strained to shear strain of 66 % and 18 % (severe and moderate pre-straining) experiences shear strength below s_u (softening) when reconsolidated to a stress level below 80 kPa (only approximate value, obtained from available empirical data).

The latter fact requires special attention. The consequence of this reduction in shear strength for a pile problem is illustrated in Figure 5.5.3. The sketch of strain changes due to the pile installation is based on Cavity Expansion Method (CEM). A review of CEM is omitted in this report since the method has been extensively described in previous academic publications (refer, for instance, to Hill, 1950; Soderberg, 1962 or Ladanyi, 1963). At some radial distance from the pile shaft, radial strain will drop to severe or moderate level, and reconsolidation

stress (either in passive or active stress state) will drop below the approximate magnitude of 80 kPa. In this zone, a reduction of shear strength is likely to occur as it has been observed for severely and moderately pre-strained Tiller and Stjørdal clays reconsolidated at in-situ vertical effective stress. The extent of the zone characterized by reduced shear strength will vary, depending on a number of parameters. As a rough estimate, assuming the soil's unit weight γ in range 16-21 kN/m³ (typical values for most Norwegian saturated clays) and reconsolidation in active stress state, the depth of this zone will vary between 4 m and 14 m depending on the location of groundwater table.

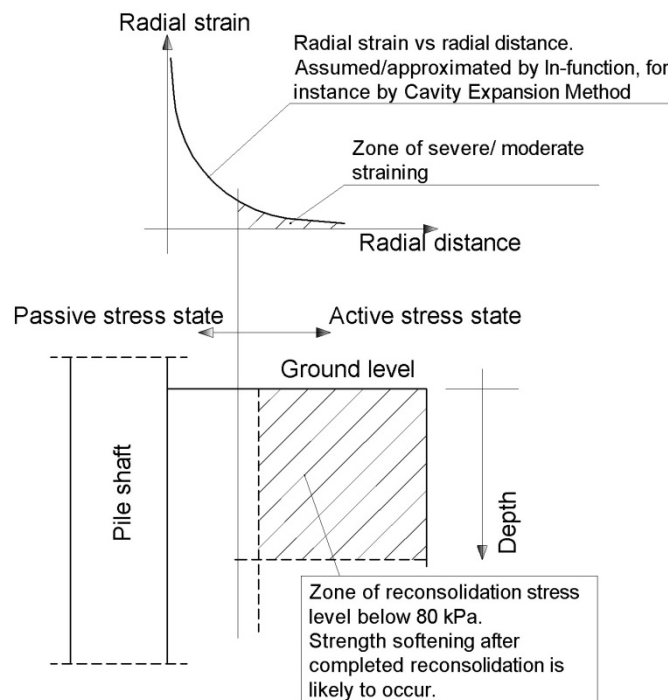


Figure 5.5.3: Softening of pre-strained reconsolidated soil around pile shaft.

The loss of shear strength documented above agrees well with the field observations described in the past publications. Figure 5.5.4 illustrates the observations from one large instrumented pile test programme at Haga test site. The observations in Figure 5.5.4 are based on excavation, trimming and testing of soil blocks around the test piles, carried out by NGI. Most of the test piles at Haga test programme were closed-ended, with or without instrumentation. All piles had an outer diameter 153 mm, wall thickness 4.5 mm and length 5.15 m. The piles were jacked into the ground. For detailed overview of the test site and results of the test programme, refer to Karlsrud and Haugen (1984) and Karlsrud (2012).

Beside of fall cone testing and water content testing, NGI has used microscope to study the clay microfabric at different zones of the soil around Haga test piles. Shear strain variation has been back-calculated from the shape of distorted layers observed from x-ray photography. Following distinct zones have been identified:

- Zone A (RR-clay): approximately 1.5 cm thick zone of clay which has been completely remoulded. The clay in this zone has lost all traces of its original fabric structure. It has been reconsolidated to water content approximately 13 % less than in its undisturbed state, which is a significant value for clay with natural water content of 40-45 %. The reduction of water content after reconsolidation resulted in a volume change of 16 -17 % and doubling of fall cone strength.
- Zone B (disturbed clay): the clay in this zone has gone through a more uniform shear distortion. A back-calculation based on distorted shape of layers has shown a non-linear and asymptotic distribution of shear strains, decreasing from more than 100 % close to zone A, to almost zero at around 12 cm from the pile wall. The distortion has caused changes both in water content and in shear strength.
- Zone C (undisturbed clay): no apparent installation effects were visible in this zone, starting at approximately 15-20 cm from the pile wall.

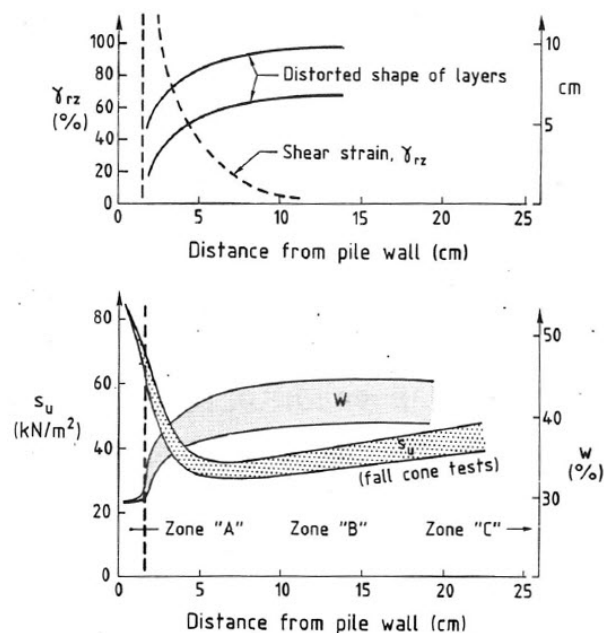


Figure 5.5.4: Haga test site: Shear distortion, water content and fall cone strength vs. radial distance from the pile wall (after Karlsrud and Haugen, 1984)

As seen from Figure 5.5.4, the increase of shear strength in zone A and loss of shear strength in zone B both show good agreement with the test results presented in Figures 5.5.1 and 5.5.2. The behaviour of sample T1-H12 and S1-H1 pre-strained to $\gamma_s = 117\%$ and reconsolidated at high stress levels is corresponding to Haga clay in zone A. The behaviour of other samples (T2-H15, T3-H14, S2-H1, S3-H1) pre-strained to $\gamma_s = 66\%$ and $\gamma_s = 18\%$ and reconsolidated at in-situ vertical effective stress is corresponding to Haga clay in zone B, where similar loss of shear strength is observed.

Figures 5.5.5 and 5.5.6 show data for normalised shear strength after reconsolidation from Tables 5.5.1 and 5.5.2.

As follows from Figures 5.5.5 and 5.5.6, general trend for all pre-strained samples is that the ratio s_{re}/p'_{re} decreases when the reconsolidation stress is increasing within the range of 35-200 kPa. The exception from this trend is moderately pre-strained sample S3-H1 reconsolidated at in-situ vertical effective stress of 79.2 kPa. The values of ratio s_{re}/p'_{re} tend to be larger for Tiller clay than for Stjørdal clay.

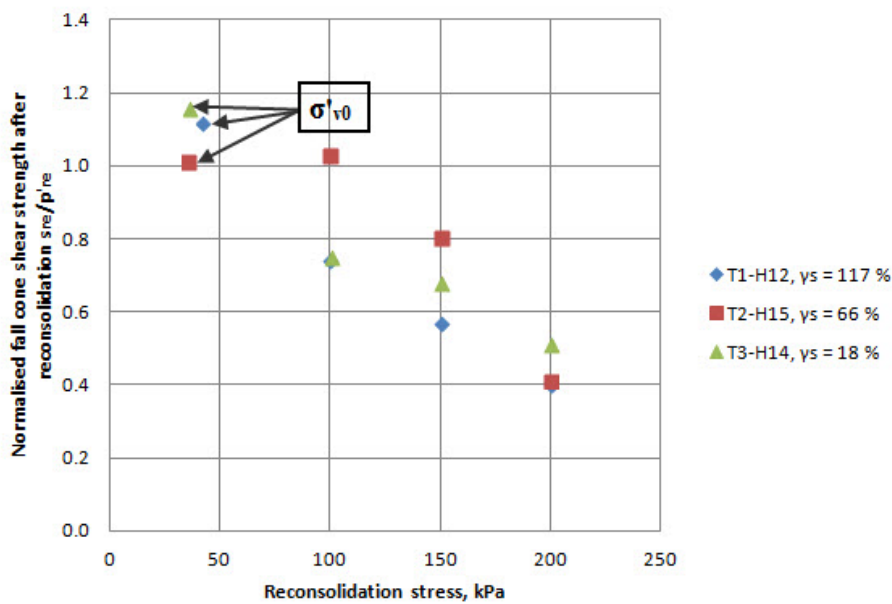


Figure 5.5.5: Tiller clay: Normalised shear strength vs. reconsolidation stress.

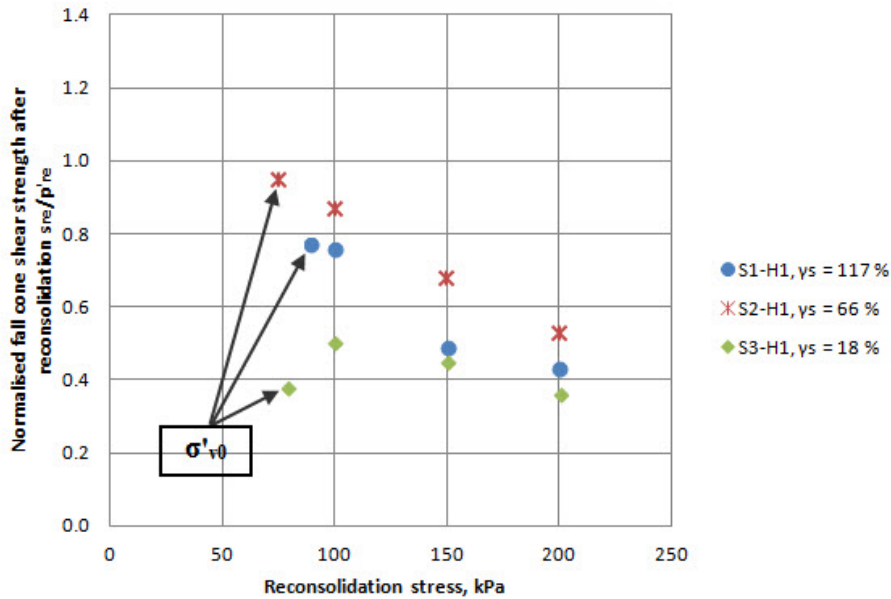


Figure 5.5.6: Stjørdal clay: Normalised shear strength vs. reconsolidation stress.

5.6 Impact of Pre-Straining and Reconsolidation on Water Content and Volume

Table 5.6.1 and 5.6.2 show changes in water content and volume for Tiller and Stjørdal clay after the pre-straining and subsequent reconsolidation in the oedometer. For detailed calculation of presented values, refer to the relevant chapters dealing with reconsolidation of each pre-strained specimen. The decrease in water content due to the reconsolidation (Δw) is calculated from Eq. 3.29. The decrease in volume is given by vertical strain in the end of reconsolidation (equals to volumetric strain in the oedometer).

Changes in water content are illustrated in Figures 5.6.1 and 5.6.2, while the changes in volume are shown in Figures 5.6.3 and 5.6.4. The results for Tiller and Stjørdal clay are separated in different figures to make the data readable.

As follows from Figure 5.6.1 and 5.6.2, there is some scatter in the data for moderately and severely pre-strained clay from Stjørdal and Tiller. For these levels of pre-straining, no clear trend may be identified with respect to changes in water content due to the reconsolidation. One apparent trend, however, is that remoulded Stjørdal and Tiller clays demonstrate similar decrease in water content at the same levels of reconsolidation stresses. Overall, the water content is decreasing evenly with increasing reconsolidation stress level.

Table 5.6.1: Tiller clay: Impact of pre-straining and reconsolidation on water content and volume.

Sample ID	Applied shear strain γ_s , %	Re-consolidation stress p'_{re} , kPa	Water content prior to re-consolidation w , %	Water content after re-consolidation w_{re} , %	Decrease in water content due to the re-consolidation Δw , %	Volumetric strain due to the re-consolidation ϵ_{vol} , %
T1-H12	117	42.2	37.46	31.28	-6.18	8.48
		100	33.99	26.40	-7.59	11.49
		150	34.21	26.23	-7.98	13.91
		200	35.96	26.54	-9.42	16.61
T2-H15	66	35.6	34.61	31.29	-3.32	6.67
		100	26.61	22.20	-4.41	7.17
		150	31.67	26.61	-5.06	8.14
		200	33.14	27.36	-5.78	11.37
T3-H14	18	36.1	35.82	34.21	-1.61	5.04
		100	28.91	25.62	-3.29	8.85
		150	28.60	24.77	-3.83	9.45
		200	34.15	28.11	-7.03	13.24

Table 5.6.2: Stjørdal clay: Impact of pre-straining and reconsolidation on water content and volume.

Sample ID	Applied shear strain γ_s , %	Re-consolidation stress p'_{re} , kPa	Water content prior to re-consolidation w , %	Water content after re-consolidation w_{re} , %	Decrease in water content due to the re-consolidation Δw , %	Volumetric strain due to the re-consolidation ϵ_{vol} , %
S1-H1	117	89.5	38.16	32.91	-5.25	9.59
		100	42.47	35.70	-6.77	11.46
		150	41.31	33.57	-7.74	13.16
		200	40.82	32.68	-8.14	14.39
S2-H1	66	75.1	30.74	27.53	-3.21	7.94
		100	30.01	26.39	-3.62	8.31
		150	30.47	25.97	-4.50	9.85
		200	32.56	26.22	-6.34	11.17
S3-H1	18	79.2	45.06	42.69	-2.37	6.61
		100	43.69	38.48	-5.21	8.92
		150	42.16	36.78	-5.38	8.66
		200	46.26	38.48	-7.78	11.32

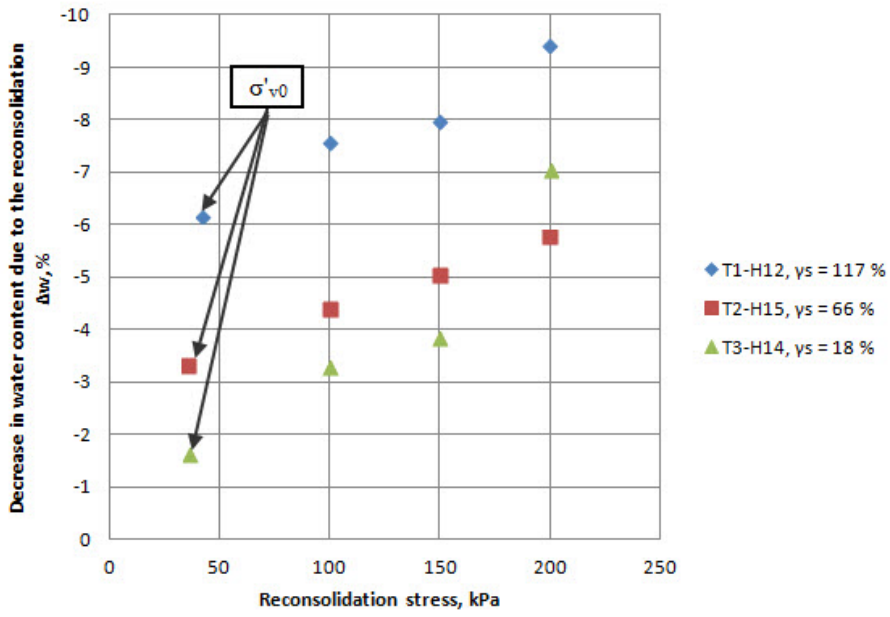


Figure 5.6.1: Tiller clay: Change in water content vs. reconsolidation stress.

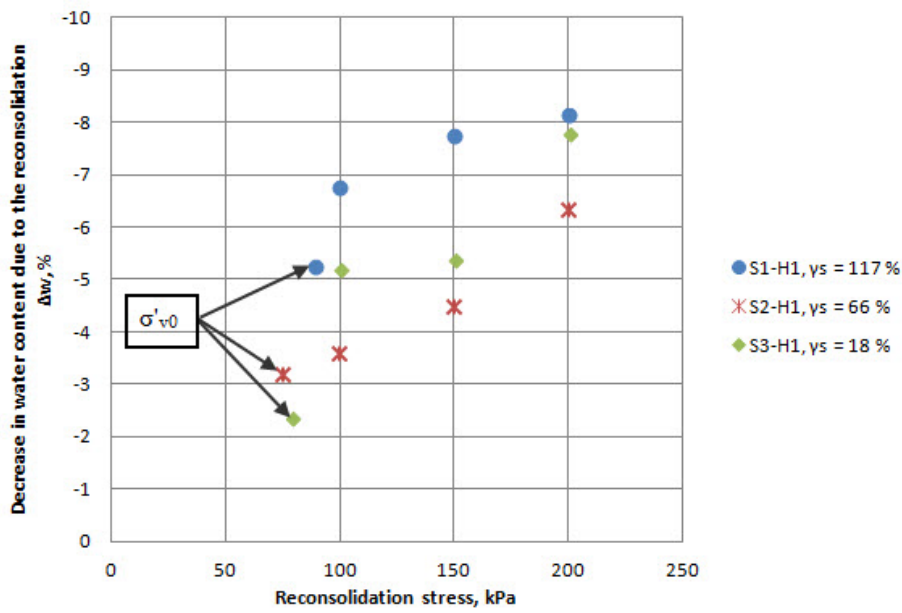


Figure 5.6.2: Stjørdal clay: Change in water content vs. reconsolidation stress.

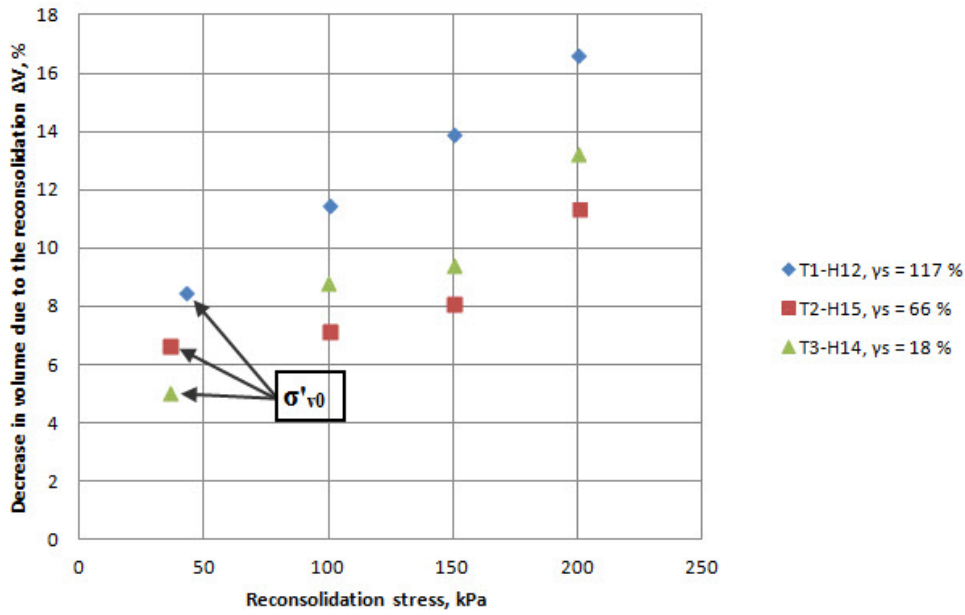


Figure 5.6.3: Tiller clay: Volume change vs. reconsolidation stress.

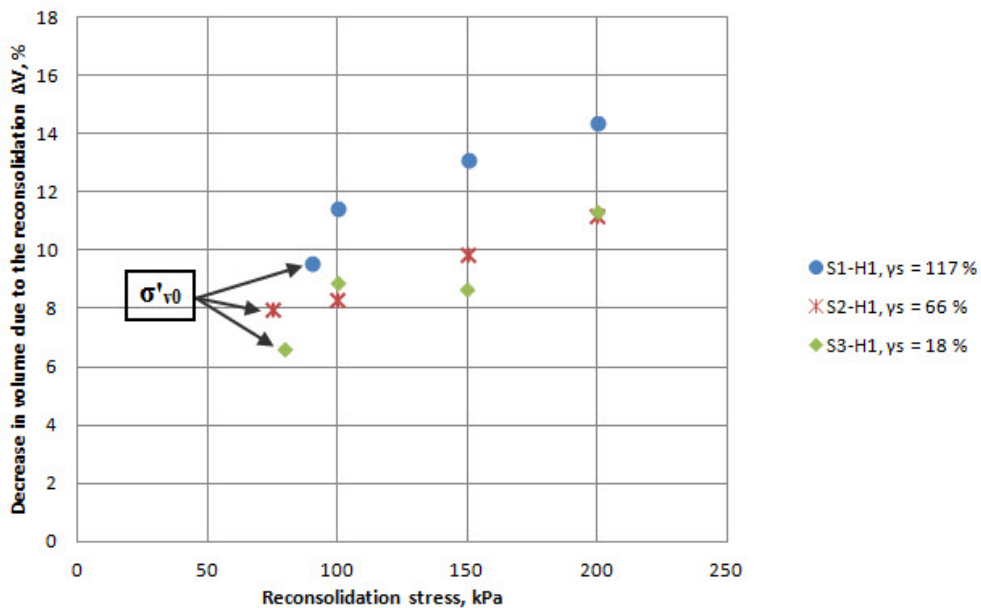


Figure 5.6.4: Stjørdal clay: Volume change vs. reconsolidation stress.

Comparison of Figures 5.6.3 and 5.6.4 reveals following trends:

- Volumetric strain due to the pre-straining and reconsolidation increases almost linearly with the increasing reconsolidation stress level up to 200 kPa. The trend applies for all levels of pre-straining.
- Volumetric strain due to the pre-straining and reconsolidation is largest for the specimens remoulded by pre-straining, regardless of the site of origin. Depending on

the clay type and reconsolidation stress level, the remoulded material ($\gamma_s = 117\%$) demonstrates a volume loss ranging from 8.48 % (reconsolidated at in-situ vertical effective stress 42.2 kPa) to 16.61 % (reconsolidated at 200 kPa). Changes in volume of remoulded and reconsolidated Tiller and Stjørdal clay appear to have approximately same values at the same reconsolidation stress levels up to 200 kPa.

- There is no well-defined trend with respect to whether moderate or severe pre-straining leads to the largest volumetric strain due to the reconsolidation. In fact, the volume changes during reconsolidation are fairly similar for moderately and severely strained specimens. Although these volume changes are below the values which apply for the remoulded material, they are still significant. Depending on the clay type and reconsolidation stress level, the volumetric strain for severely and moderately pre-strained specimens varies from 5.04 % (reconsolidated at in-situ vertical effective stress 36.1 kPa) to 13.24 % (reconsolidated at 200 kPa). (In comparison, CRS oedometer test results show that almost all undisturbed specimens demonstrate volumetric strains in range of 4-6 % at the effective mean stress of 200 kPa).

With respect to the background of the thesis, the latter observation is particularly interesting as it partly explains the settlements encountered around long bored shafts with large cross-sections. The large decrease in volume of severely and moderately strained specimens implies that large settlements will not be limited to the plasticized zone adjacent to the pile shaft. Indeed, significant settlements will extend further radially where severely and moderately strained soft soil will be found. As the large cross-sections (size of the problem) will involve moderate pre-straining at substantial radial distance from the pile shaft, the soil in this area will reconsolidate in active stress state where in-situ vertical effective stress will act as major principal stress (reconsolidation stress). Considering data in Figure 5.6.3 and Figure 5.6.4, the settlements in this zone will become especially notable at the depths where in-situ vertical effective stress will approach a value of 100 kPa or larger. Assuming the soil's unit weight γ in range 16-21 kN/m³ (the values typical for most Norwegian saturated clays), this roughly corresponds to the depths in range of 4-16 m and below, depending on the location of groundwater table.

The significant loss of volume encountered by moderately and severely pre-strained OC clays reconsolidated at the stress level below p'_c provides a new perspective on the installation effects of bored piles. According to this perspective, the main variables involved in an

analysis of settlements arising from bored pile installation will not be limited to strain and stress changes in the surrounding soil. In addition to these two parameters, in-situ vertical effective stress in active stress state acting as reconsolidation stress on moderately and severely pre-strained soil has to be treated as an additional main variable.

5.7 Behaviour in the Oedometer

A comparison of CRS oedometer test results is presented below in the following figures, where the samples are grouped after the clay types and water content:

- Figure 5.7.1: Linear presentation of stress-strain curves for all undisturbed, pre-strained and remoulded specimens from Tiller site (samples T1-H12, T2-H15 and T3-H14). Water content $w = 30-35\%$.
- Figure 5.7.2: Semi-log presentation of stress-strain curves for all undisturbed, pre-strained and remoulded specimens from Tiller site (samples T1-H12, T2-H15 and T3-H14). Water content $w = 30-35\%$.
- Figure 5.7.3: Stress-moduli curves for all undisturbed, pre-strained and remoulded specimens from Tiller site (samples T1-H12, T2-H15 and T3-H14). Water content $w = 30-35\%$.
- Figure 5.7.4: Stress-coefficient of consolidation curves for undisturbed, pre-strained and remoulded specimens (sample T2-H15 and T3-H14) from Tiller site. Water content $w = 30-35\%$.
- Figure 5.7.5: Stress-coefficient of consolidation curves for undisturbed, pre-strained and remoulded specimens (sample T1-H12) from Tiller site. Water content $31-34\%$
- Figure 5.7.6: Linear presentation of stress-strain curves for undisturbed, pre-strained and remoulded specimens from Stjørdal site (samples S1-H1 and S3-H1). Water content $w = 42-46\%$.
- Figure 5.7.7: Semi-log presentation of stress-strain curves for undisturbed, pre-strained and remoulded specimens from Stjørdal site (samples S1-H1 and S3-H1). Water content $w = 42-46\%$.
- Figure 5.7.8: Stress-moduli curves for undisturbed, pre-strained and remoulded specimens from Stjørdal site (samples S1-H1 and S3-H1). Water content $w = 42-46\%$

- Figure 5.7.9: Stress-coefficient of consolidation curves for undisturbed, pre-strained and remoulded specimens (samples S1-H1 and S3-H1) from Stjørdal site. Water content 42-46 %.
- Figure 5.7.10: Linear presentation of stress-strain curves for undisturbed, pre-strained and remoulded specimens from Stjørdal site (sample S2-H1). Water content $w = 30-33$ %.
- Figure 5.7.11: Semi-log presentation of stress-strain curves for undisturbed, pre-strained and remoulded specimens from Stjørdal site (sample S2-H1). Water content $w = 30-33$ %.
- Figure 5.7.12: Stress-moduli curves for undisturbed, pre-strained and remoulded specimens from Stjørdal site (sample S2-H1). Water content $w = 30-33$ %.
- Figure 5.7.13: Stress-coefficient of consolidation curves for undisturbed, pre-strained and remoulded specimens (sample S2-H1) from Stjørdal site. Water content 30-33 %.

The water content values in the figures are obtained from weight measurements of wet and dry oedometer test specimens, carried out prior to and after the test. For more details, refer to the chapters dealing with oedometer test results for each specimen.

The stress-strain and stress-modulus curves for Tiller clay contain test results for all samples. This is due to the fact that all samples from Tiller site have similar water content and more or less similar material composition (although natural variations in the test material do occur). For stress-coefficient of consolidation curves, presentation of test results of sample T1-H12 is separated from other samples to provide the correct scaling since the coefficient of consolidation of undisturbed specimen T1-H12 show unusually high values.

Stress-modulus and stress-coefficient of consolidation curves for pre-strained specimen T1-H12 are only presented for the stress range 0-600 kPa due to an inconsistency in the end of the test. For more details, refer to the chapter dealing with CRS oedometer test results for this specimen.

As the water content of sample S2-H1 is significantly lower than other Stjørdal clay samples, comparison of results for sample S2-H1 is carried out in separate plots.

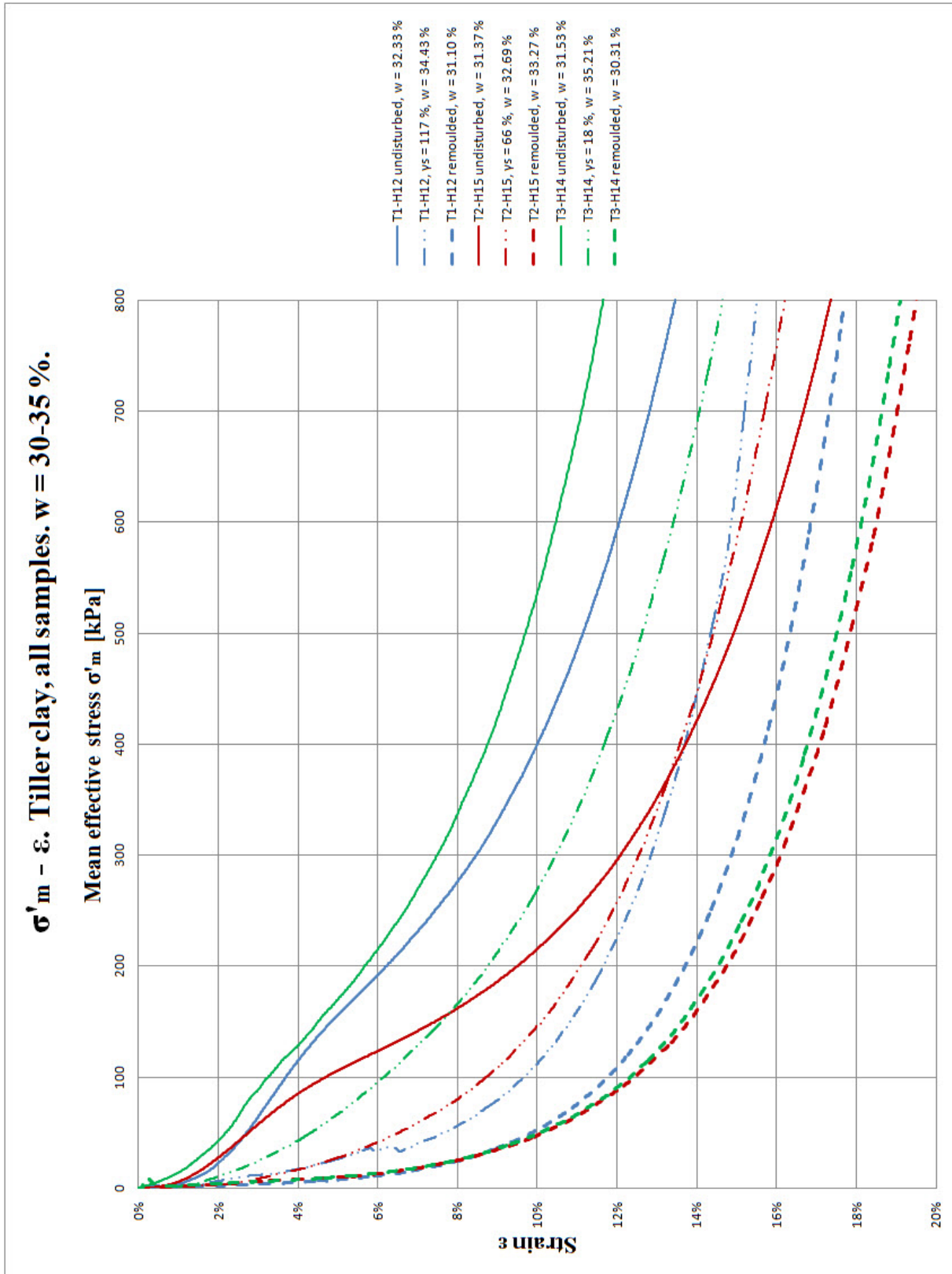


Figure 5.7.1: Stress-strain plot for all Tiller clay samples, water content 30-35 %. Linear scale.

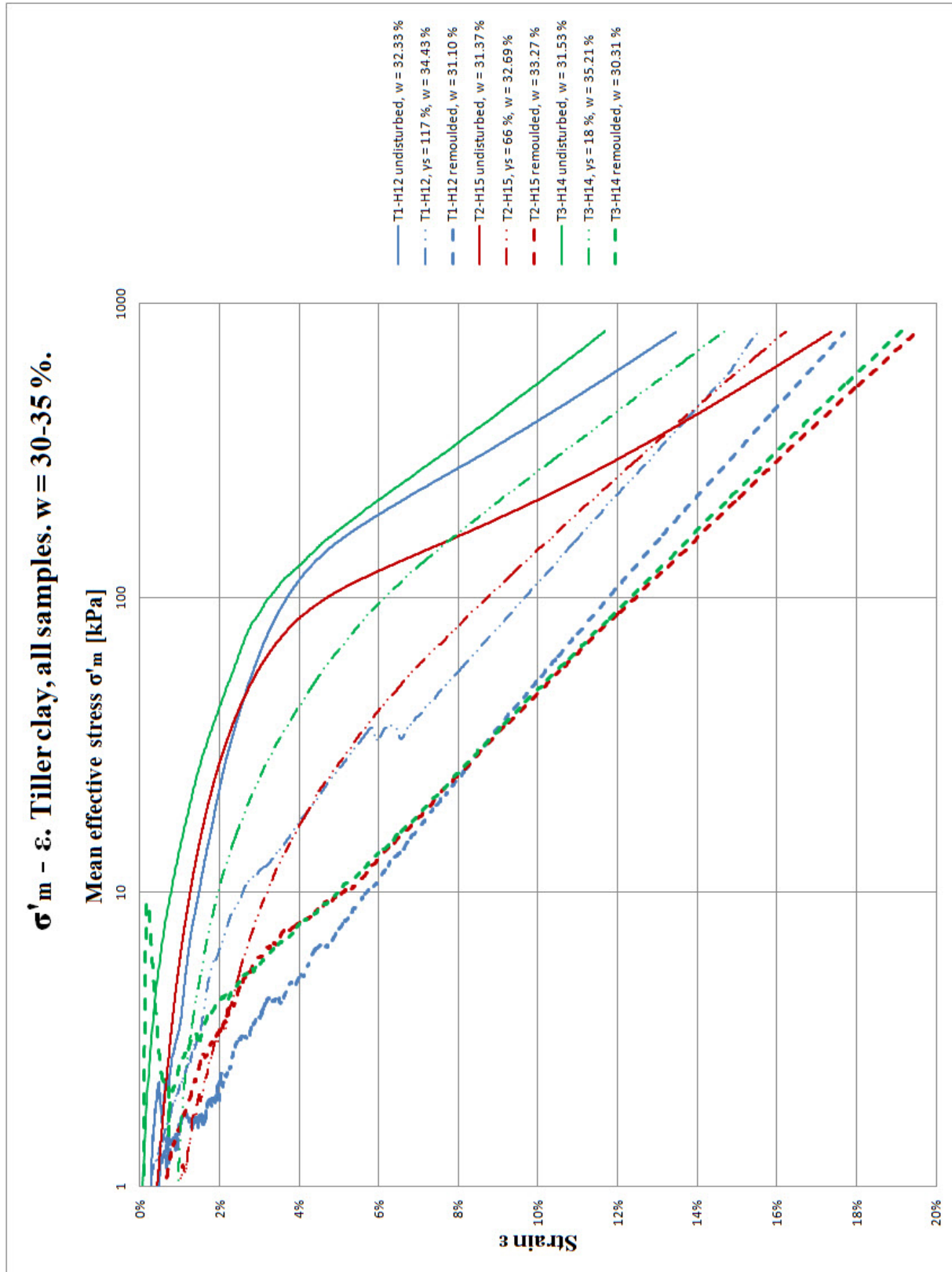


Figure 5.7.2: Stress-strain plot for all Tiller clay samples, water content 30-35 %. Semi-log scale.

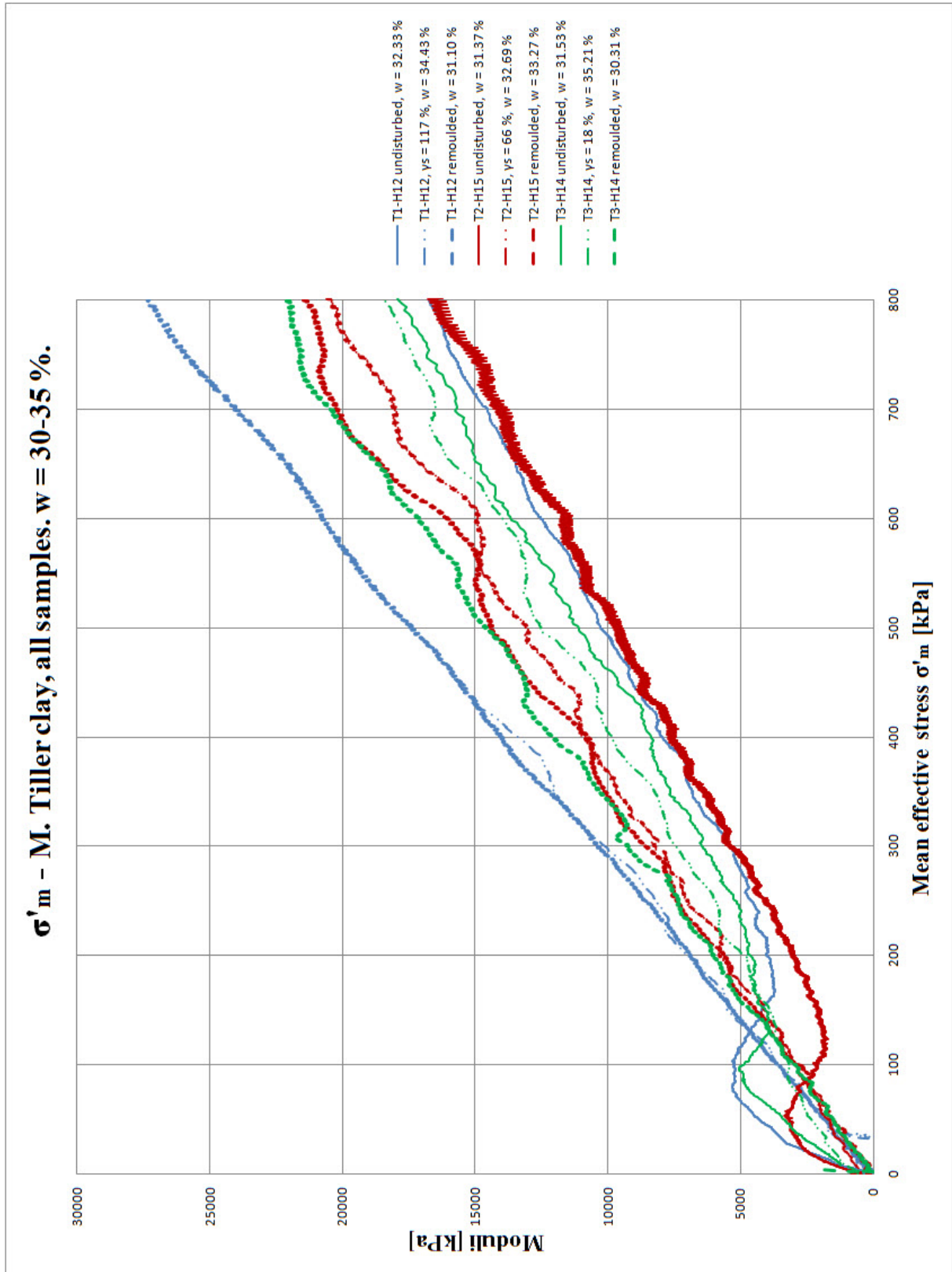


Figure 5.7.3: Stress-moduli plot for all Tiller clay samples, water content 30-35 %.

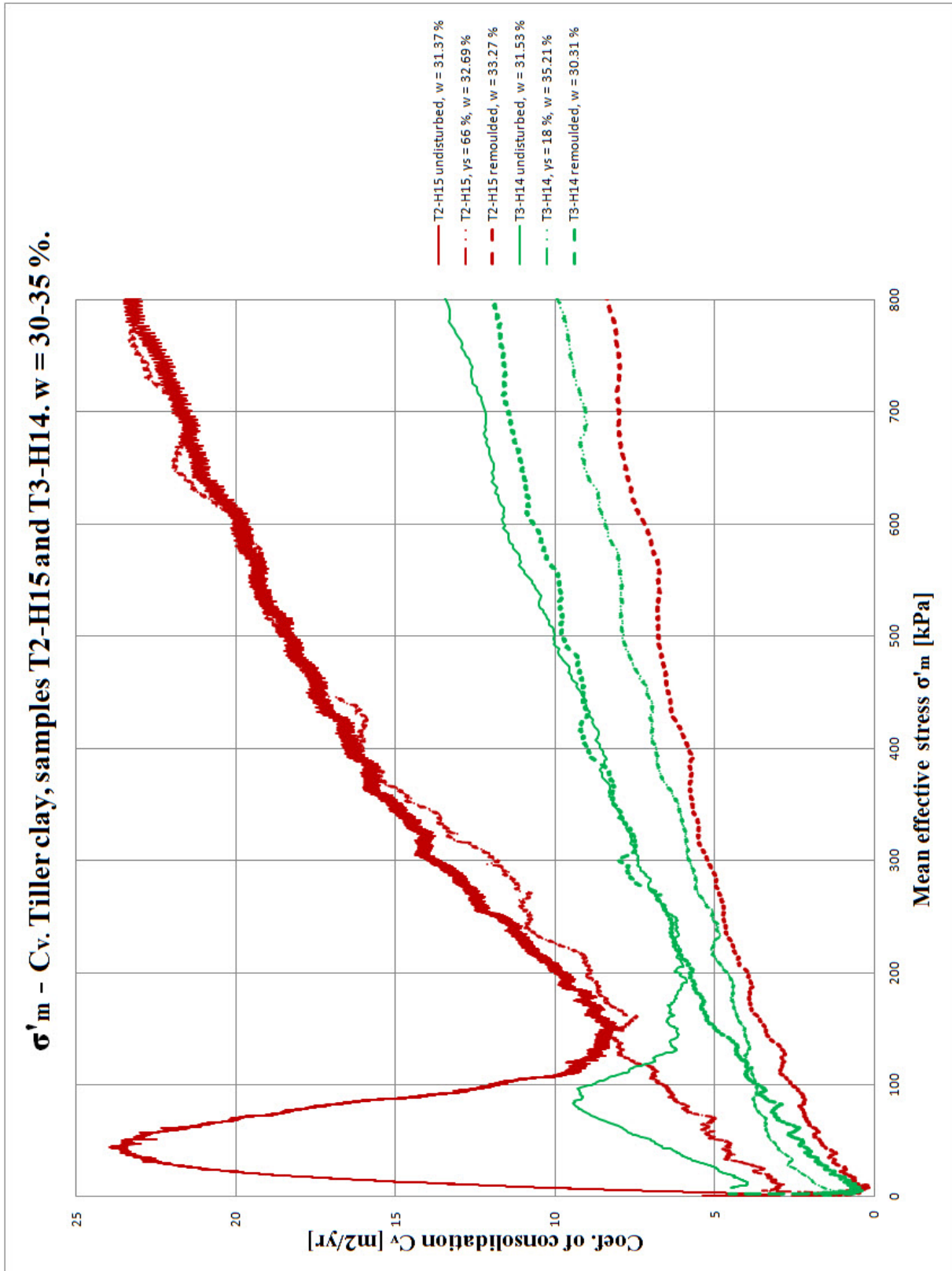


Figure 5.7.4: Stress-coefficient of consolidation plot for Tiller clay samples T2-H15 and T3-H14, water content 30-35 %.

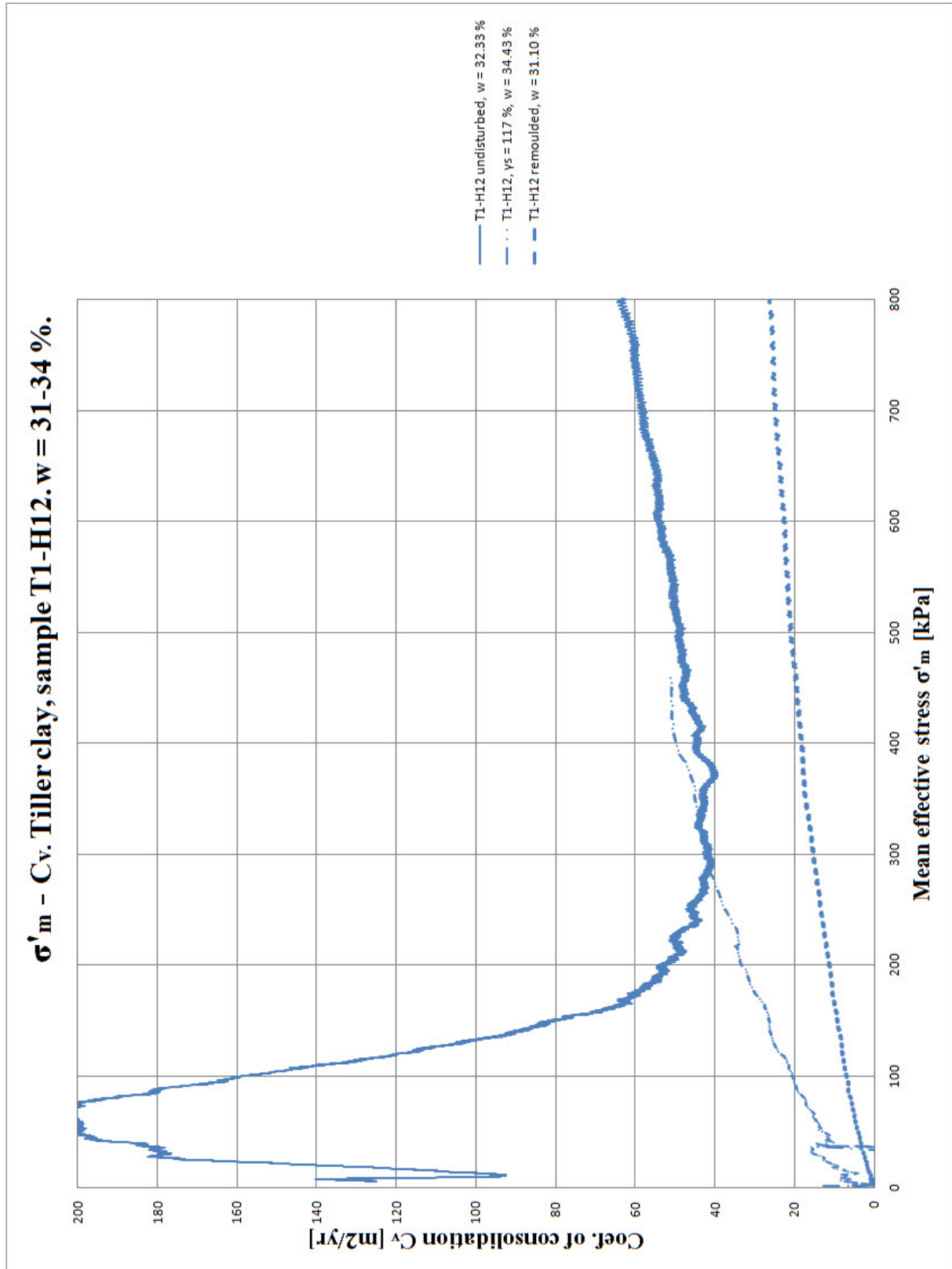


Figure 5.7.5: Stress-coefficient of consolidation plot for Tiller clay sample T1-H12, water content 31-34 %.

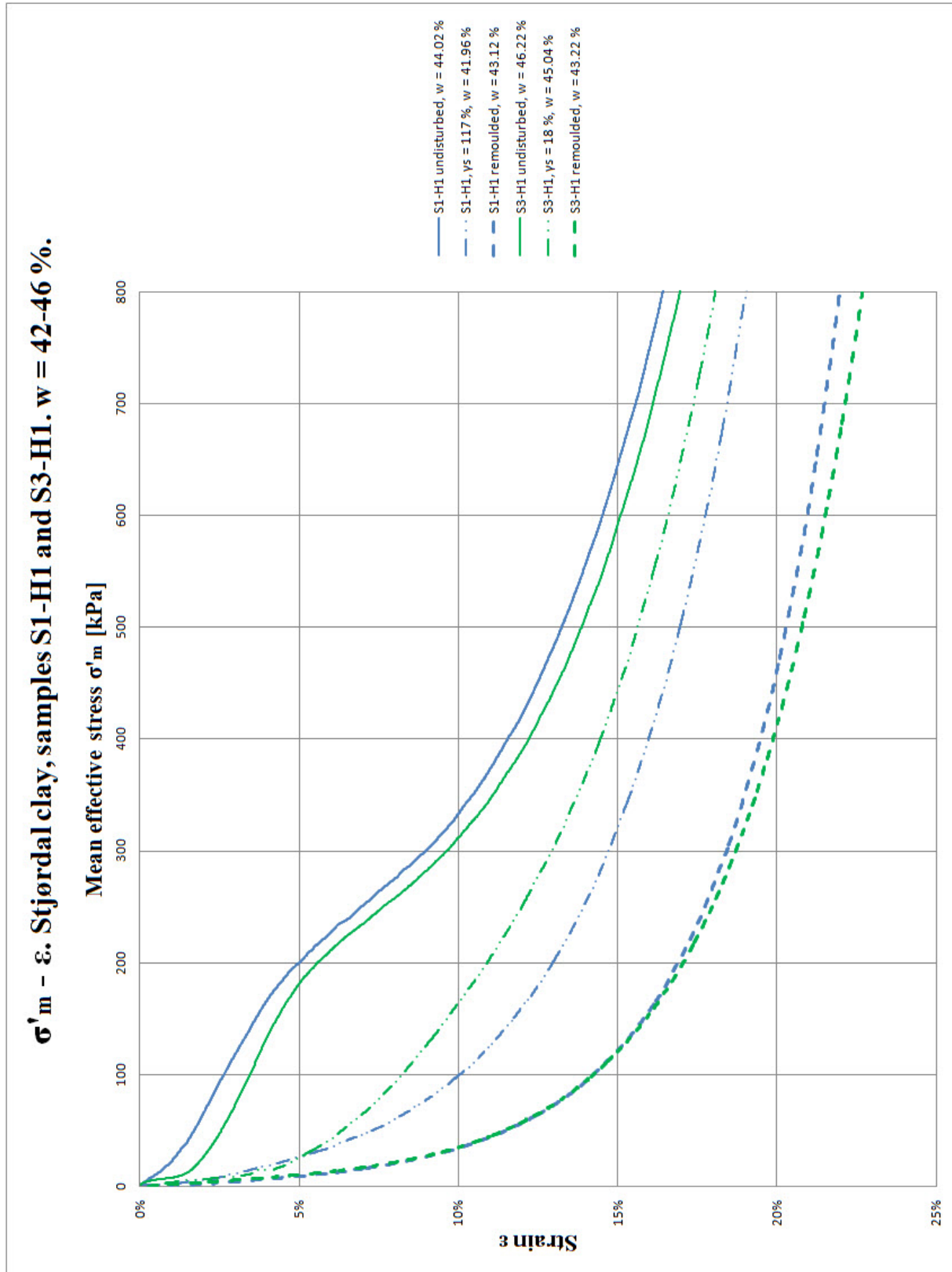


Figure 5.7.6: Stress-strain plot for Stjørdal clay samples S1-H1 and S3-H1, water content 42-46 %. Linear scale.

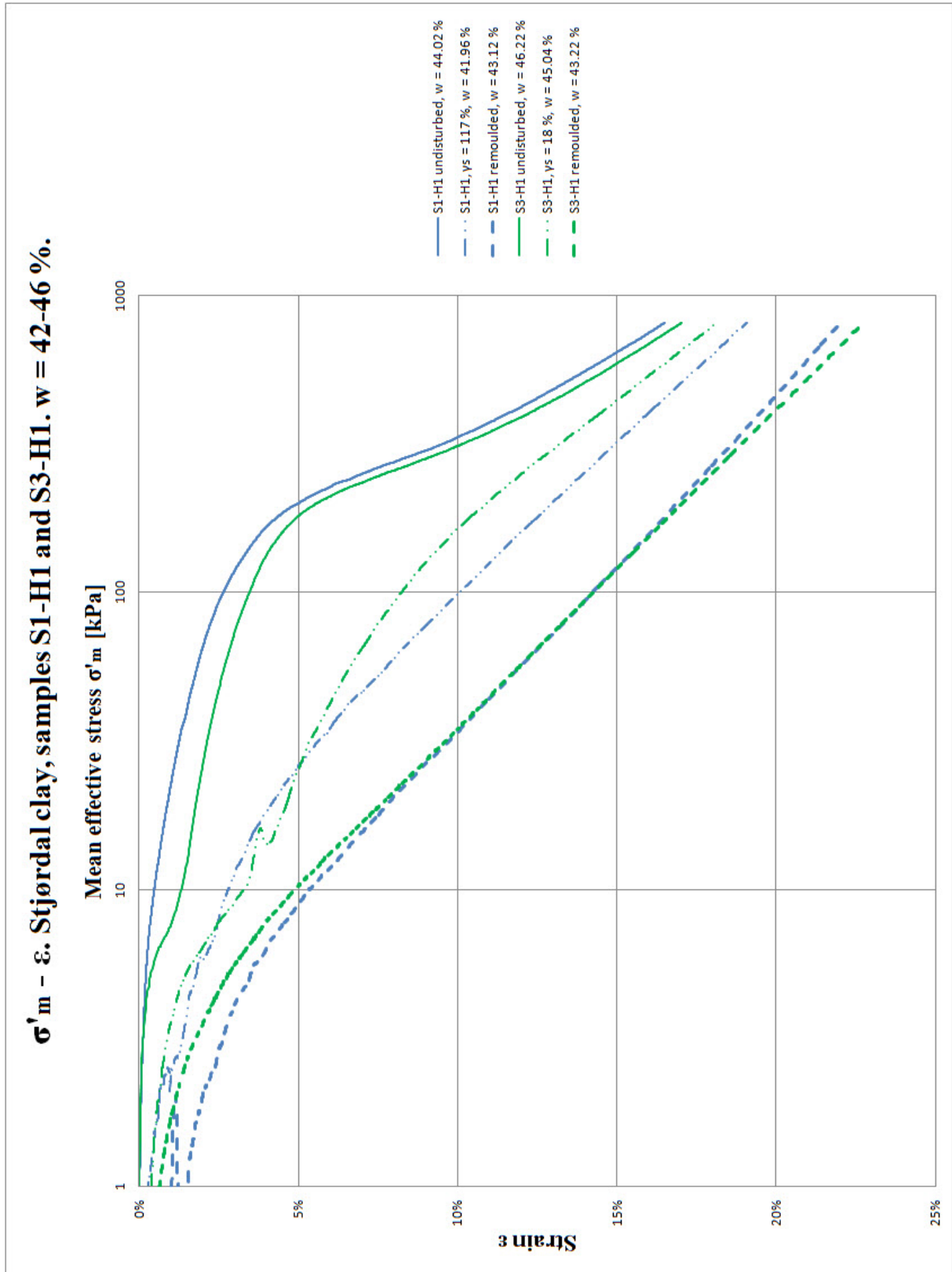


Figure 5.7.7: Stress-strain plot for Stjørdal clay samples S1-H1 and S3-H1, water content 42-46 %. Semi-log scale.

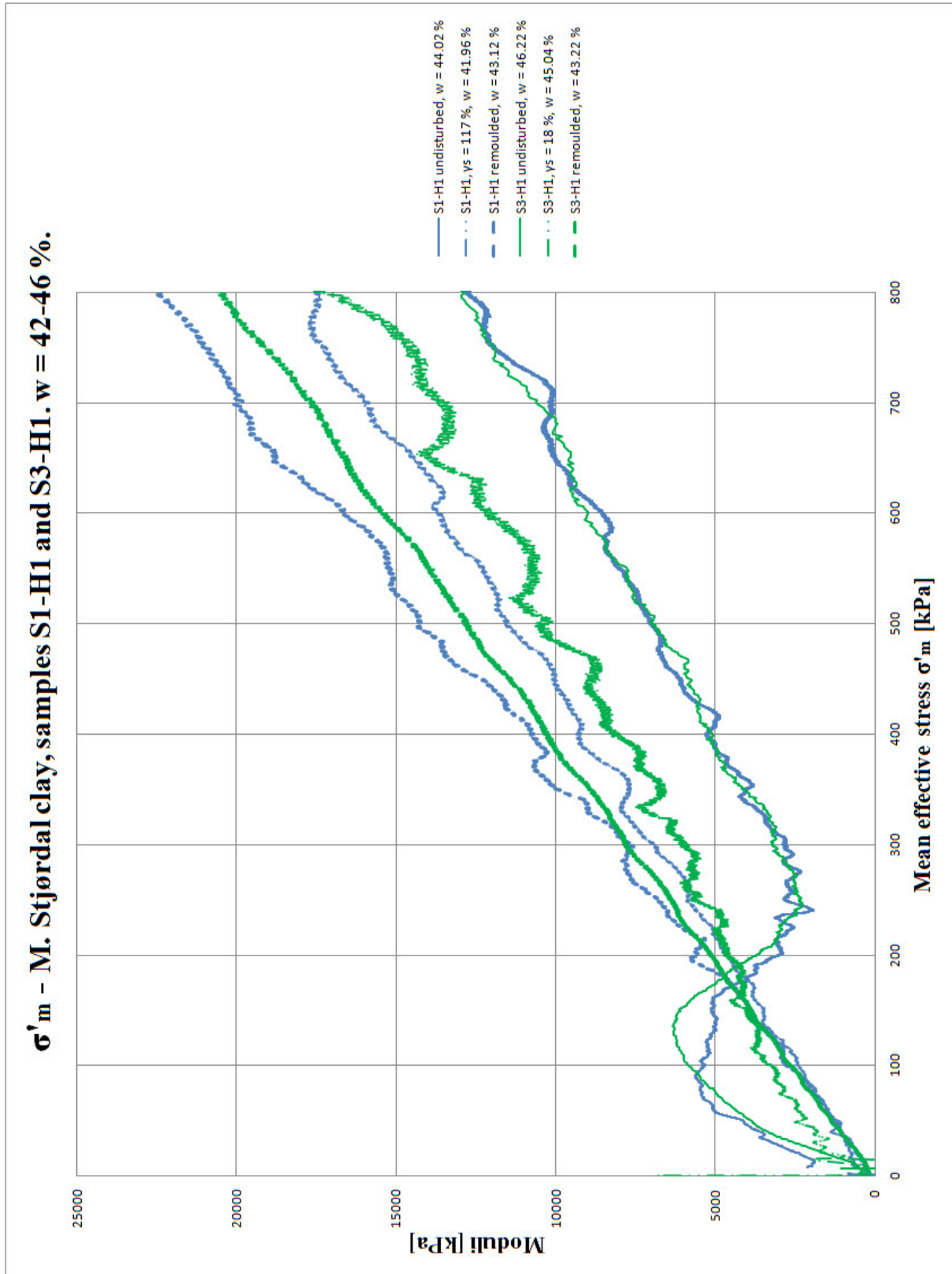


Figure 5.7.8: Stress-moduli plot for Stjørdal clay samples S1-H1 and S3-H1, water content 42-46 %.

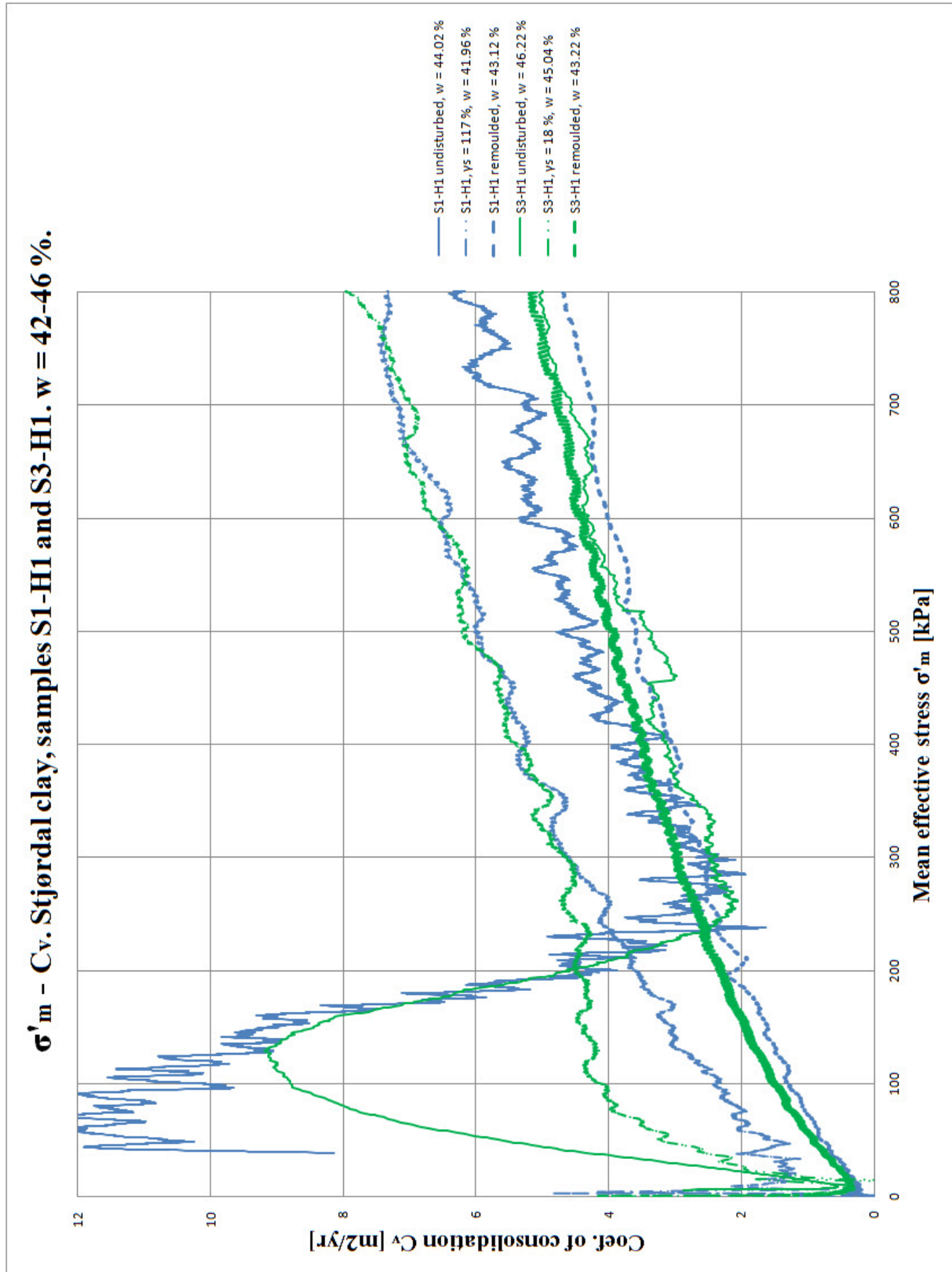


Figure 5.7.9: Stress-coefficient of consolidation plot for Stjørdal clay samples S1-H1 and S3-H1, water content 42-46 %.

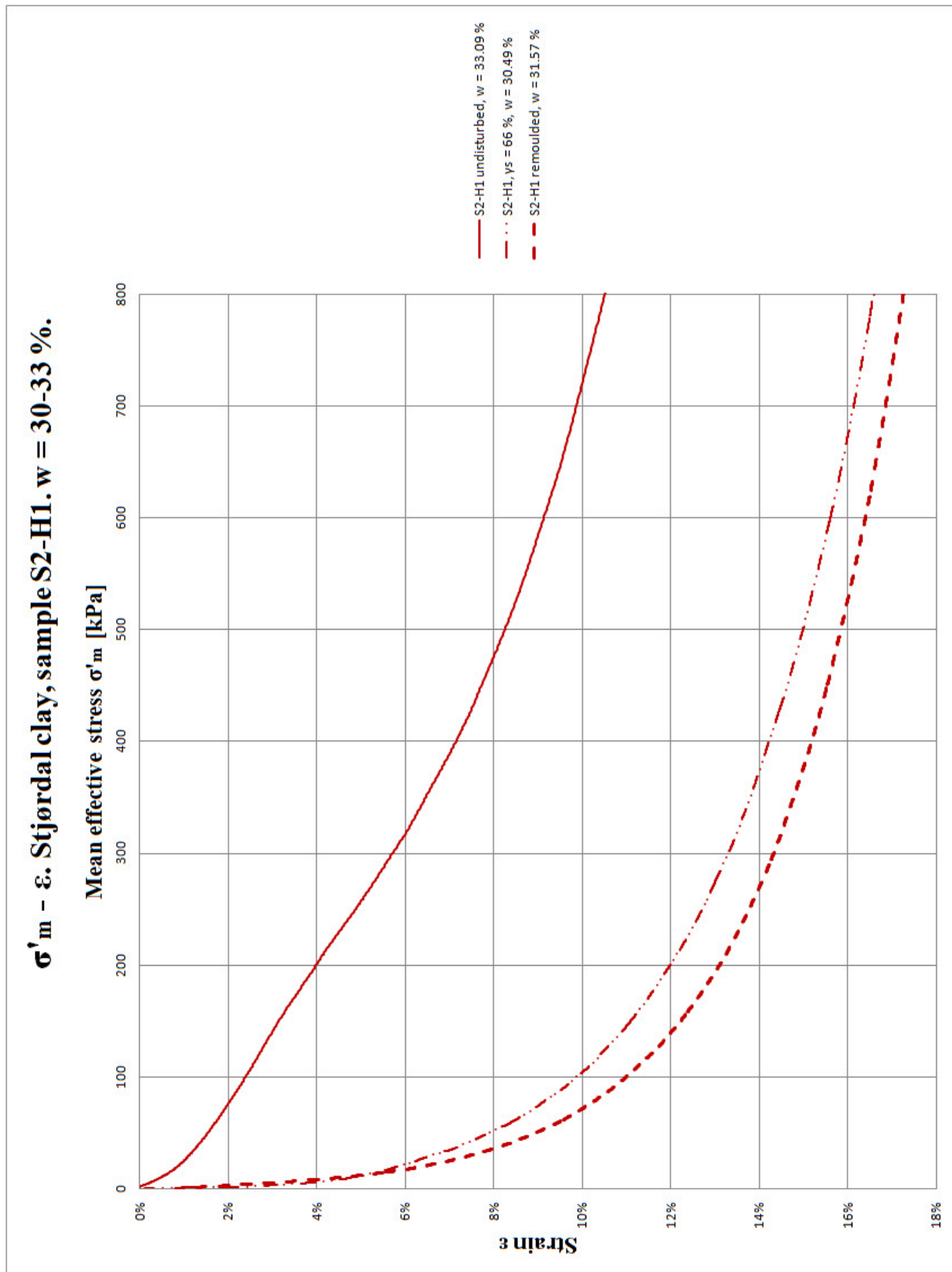


Figure 5.7.10: Stress-strain plot for Stjørdal clay sample S2-H1, water content 30-33 %. Linear scale.

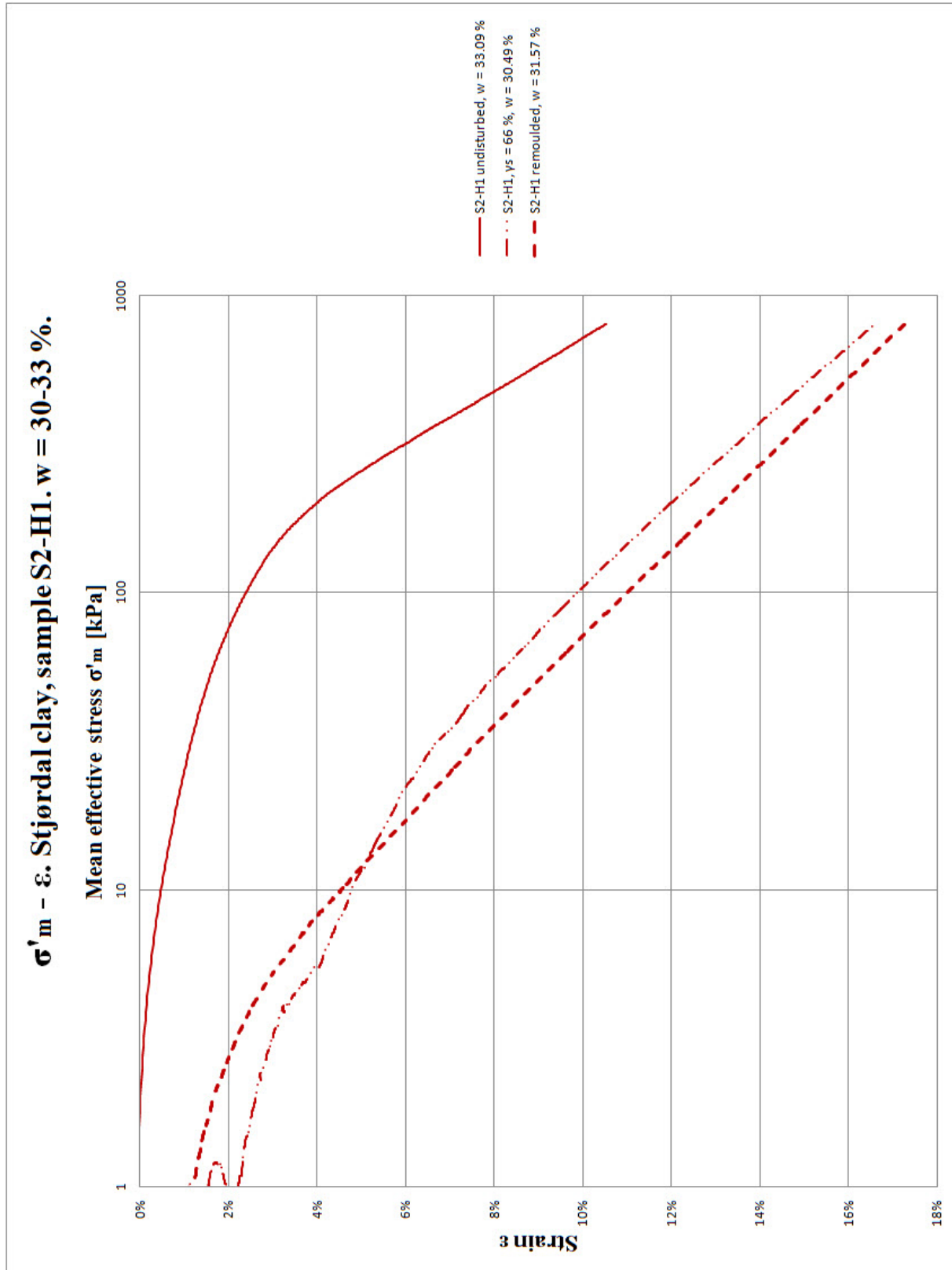


Figure 5.7.11: Stress-strain plot for Stjørdal clay sample S2-H1, water content 30-33 %. Semi-log scale.

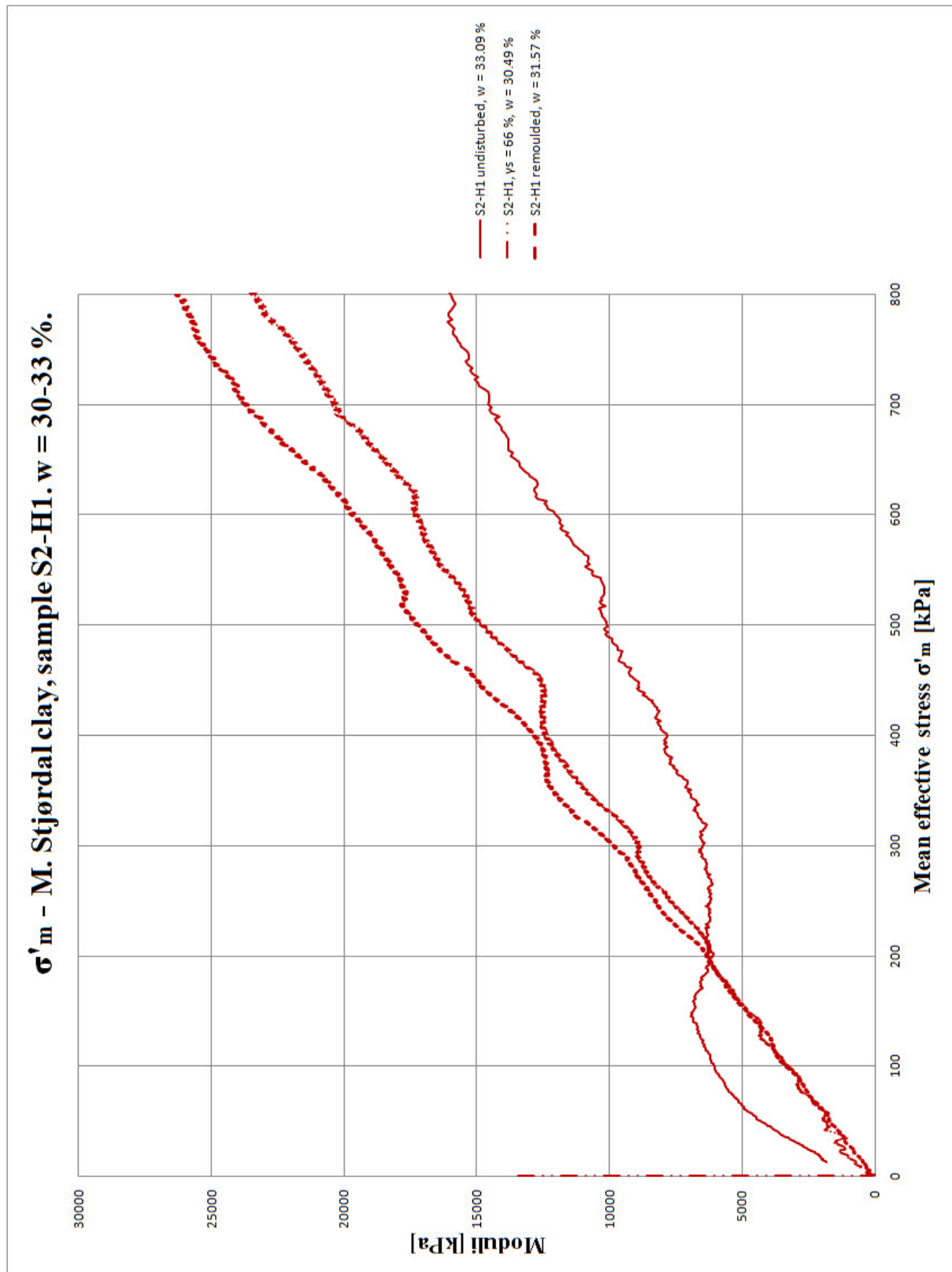


Figure 5.7.12: Stress-moduli plot for Stjørdal clay sample S2-H1, water content 30-33 %.

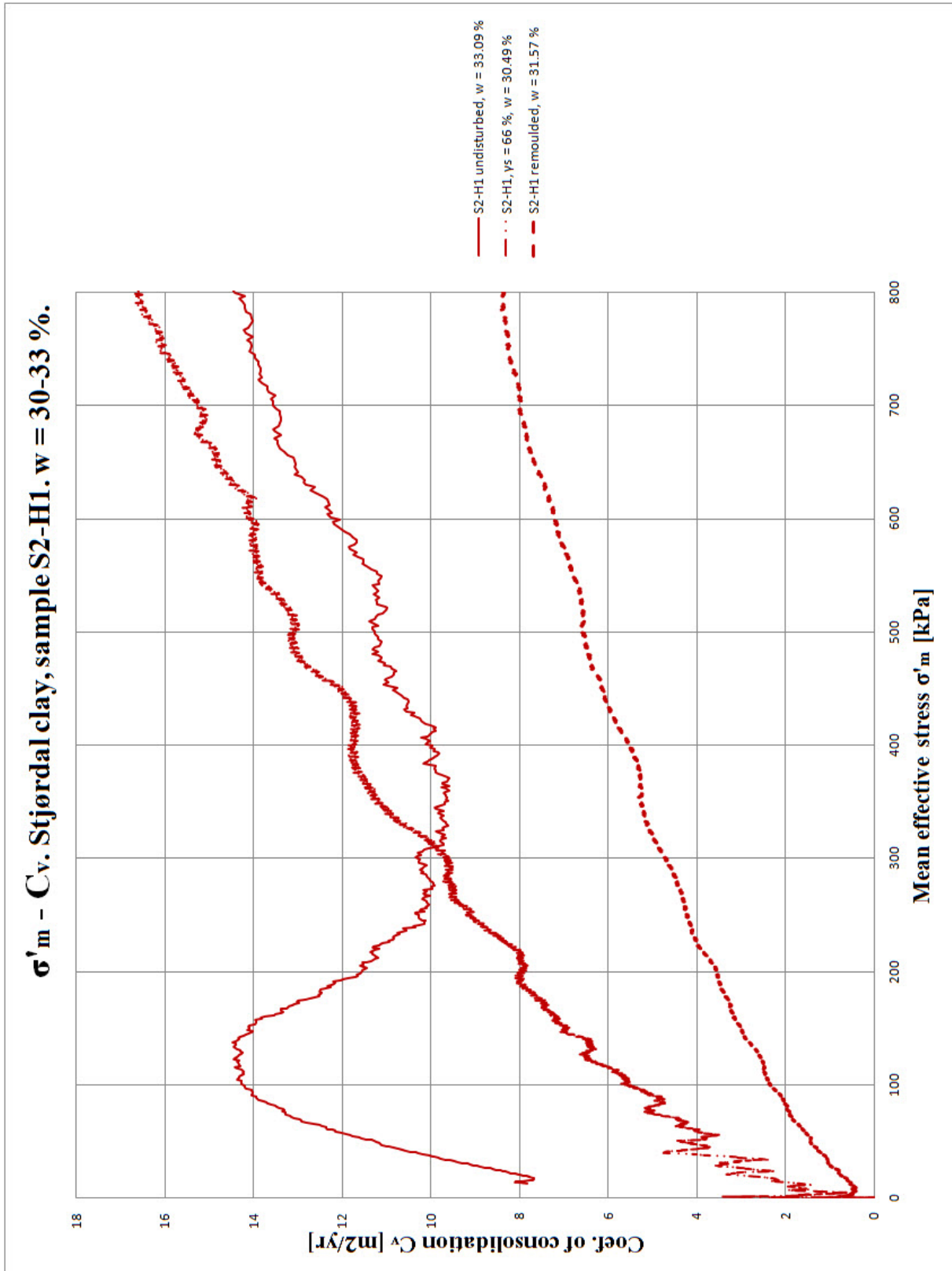


Figure 5.7.13: Stress-coefficient of consolidation plot for Stjørdal clay sample S2-H1, water content 30-33 %.

Following general trends may be noted from stress-strain plots (Figures 5.7.1, 5.7.2, 5.7.6, 5.7.7, 5.7.10 and 5.7.11):

- Remoulded material demonstrates a reduction of volume in range 17-23 % under CRS tests up to 800 kPa
- For the clays with the same water content, the deformation and loss of volume due to the loading is increasing with the increasing degree of pre-straining. Remoulded material defines the absolute limit value for volume reduction due to the straining and subsequent loading.
- Stress-strain curves for material remoulded by pre-straining and material remoulded manually deviate largely. Even the material pre-strained to $\gamma_s = 117\%$ is not able to capture loss of volume and deformations encountered by the manually remoulded clay. The stress-strain curves for pre-strained clay specimens are located in between the curves for undisturbed and remoulded specimens, in the order defined by increasing degree of pre-straining.
- The stress-strain curves for undisturbed and pre-strained material are just about to meet when the vertical strain in the oedometer is becoming sufficiently large.

The latter observation agrees well with past publications. As proposed by Schmertmann (1955), the stress-strain curves for intact and disturbed clay of the same type will meet when the void ratio (e) is approximately 0.35 to 0.45 of the void ratio at zero volume change (e_0). Refer also to Mod. Cam Clay model and intrinsic oedometer curve for re-constituted samples (Cam Clay model and critical state soil mechanics are treated for instance in Schofield et al., 1968). Assuming that the intact and disturbed stress-strain curves meet at $0.4 \cdot e_0$, the corresponding volumetric strain is:

$$\varepsilon_{vol} = \frac{\Delta e}{1+e_0} = \frac{e_0 - 0.4 \cdot e_0}{1+e_0} = \frac{0.6 \cdot e_0}{1+e_0} \quad (\text{Eq. 5.1})$$

where

ε_{vol} = volumetric strain

Δe = change in void ratio

e_0 = void ratio at zero volume change

Based on Eq. 5.1, Table 5.7.1 summarises the expected volume reductions (vertical strains of the oedometer specimens) at which the intact and pre-strained oedometer curves of each

sample will meet. The values of initial void ratios in Table 5.7.1 have been obtained from the chapters dealing with oedometer tests on undisturbed specimens.

Table 5.7.1: Volume reduction corresponding to void ratio $0.4 \cdot e_0$ for intact and disturbed oedometer curves.

Sample ID	Void ratio of undisturbed oedometer test specimen at zero volume change e_0	Volumetric strain at which the undisturbed and pre-strained oedometer curves are expected to meet ε_{vol} , %
T1-H12	0.96	29.39
T2-H15	0.87	27.91
T3-H14	0.89	28.25
S1-H1	1.22	32.97
S2-H1	0.91	28.59
S3-H1	1.27	33.57

The values of volume reduction in Table 5.7.1 agree reasonably well with the data presented in Figures 5.7.1, 5.7.2, 5.7.6, 5.7.7, 5.7.10 and 5.7.11. Although the calculated values of volume reduction corresponding to $0.4 \cdot e_0$ are outside of the plot area in stress-strain plots, the intact and disturbed stress-strain curves clearly approach each other at sufficiently large volumetric strains.

Comparison of stress-moduli curves (Figures 5.7.3, 5.7.8 and 5.7.12) shows that:

- Pre-straining or remoulding leads to decreasing oedometer modulus under the stresses corresponding to OC range and to increasing oedometer modulus under the stresses corresponding to NC range of undisturbed material. As a consequence, pre-strained or remoulded clays are becoming stiffer when loaded beyond p'_c , compared to what the undisturbed clay's properties would suggest. The increasing modulus in NC range is caused by significant reduction in volume of the pre-strained material, since such volume reduction is considerably larger than what may be expected for intact clay structure. This is a well-known effect of sample disturbance, treated for instance by Karlsrud and Hernandez-Martinez (2010).

- The differences between moduli of pre-strained and remoulded clay are insignificant for the stresses corresponding to OC range of undisturbed material. For increasing stress levels beyond p'_c , the difference is becoming more and more notable. In this stress range, the remoulded clay demonstrates largest modulus in the most cases.

Stress vs. coefficient of consolidation plots (Figures 5.7.4, 5.7.5, 5.7.9 and 5.7.13) show that:

- Pre-straining and remoulding significantly reduce the coefficient of consolidation at the stress levels corresponding to OC stress range of intact material. In this stress range, the pre-strained and remoulded clays need more time to complete primary consolidation than what the properties of undisturbed material would suggest.
- At the stress levels corresponding to NC range of undisturbed material, the coefficients of consolidation for remoulded clays demonstrate contradictory trends. In this stress range, c_v -curve for remoulded material either follows the intact c_v -curve or drops considerably below the latter. Thus, for the stress levels beyond p'_c , the primary consolidation time for the remoulded clay remains the same or becomes larger than what the properties of undisturbed material should suggest.
- Also the pre-strained materials show contradictory behaviour at the stress levels corresponding to NC range of intact clay. In this stress range, c_v -curves for pre-strained materials either follow the intact c_v -curves, or rise above the latter. Furthermore, one sample (T3-H14) demonstrates that the pre-strained c_v -curve may drop below the intact c_v -curve.

The two latter contradictory trends may be explained by the fact that the coefficient of consolidation depends both on constrained modulus and permeability, e.g.:

$$c_v = \frac{k \cdot M}{\gamma_w} \quad (\text{Eq. 5.2})$$

where

M = oedometer modulus

k = coefficient of permeability, hydraulic conductivity

γ_w = unit weight of water

During the volume changes, the coefficient of permeability (k) will differ from the coefficient of permeability at zero volume change (k_0). Thus, during volumetric strains, the development

of c_v will be governed by two variables which altogether may lead to contradictory behaviour of pre-strained and remoulded clays in NC stress range. Karlsrud and Hernandez (2010) present the data for changes in permeability due to the volume changes, which might be relevant to use for further evaluation of the test results presented in this thesis. Unfortunately, the longitudinal limitations in the study have prevented such evaluation.

CHAPTER 6 Summary, Conclusions and Recommendations

6.1 Summary of Work Undertaken

The presented work is a master's thesis by research. The thesis is a part of MSc programme "Geotechnics and Geohazards" taught at NTNU from 2013 to 2015.

The study deals with reconsolidation of clay pre-strained in shear mode. The background for the research work are unexpectedly large settlements and structural damages on the existing structures which have been observed during several construction projects as a result of geotechnical site works, and especially, due to the boring and installation of steel core piles.

The effects related to the installation of driven piles are well-researched and well-documented. There are also several analytical methods dealing with prediction of strains and stresses around the shaft of a driven pile. However, little is known with respect to the effects of remoulding and shear straining of the soft soil surrounding the shaft of a bored pile.

Through an extensive laboratory test programme, the thesis investigates the effect of pre-straining on shear strength and compressibility characteristics of soft soils. Furthermore, an effort is made to study the correlation between different levels of reconsolidation stresses, and corresponding increase in shear strength and decrease in volume and water content. The study is carried out by altering the values of two main variables:

- Different magnitudes of shear strain, γ_s .
- Different clay types with respect to overconsolidation ratio (OCR), natural water content (w) and sensitivity (S_t).

The clay types involved in the study are Norwegian clays obtained from Tiller and Stjørdal site. Both sites are located in proximity to Trondheim city in central Norway.

Tiller clay is slightly overconsolidated, medium sensitive. Depending on the sample considered, the clay is classified as soft, medium stiff and stiff. The values of overconsolidation ratio (OCR), natural water content (w) and sensitivity (S_t) are in range of 3.3-4.3, 26-38 % and 10.3-11.0, respectively.

Stjørdal clay is slightly overconsolidated, classified as low to medium sensitive and medium stiff to stiff. The values of overconsolidation ratio (OCR), natural water content (w) and sensitivity (S_t) are in range of 3.0-3.3, 29-44 % and 7.4-9.7, respectively.

The laboratory test programme included the tests on undisturbed, pre-strained and manually remoulded material from each sample cylinder. Undisturbed clay samples were subjected to following tests:

- Density measurements (average density, density by small ring, grain density).
- Determination of water content, plastic and liquid limits.
- Determination of degree of saturation, void ratio and porosity.
- Determination of grain size distribution.
- Unconfined compression test.
- Falling cone test.
- CRS oedometer test up to 800 kPa.

The clay samples were pre-strained to remoulding, severe straining and moderate straining (shear strains 117 %, 66 % and 18 %, respectively). The pre-strained samples were subjected to following tests:

- Measurement of piston displacement during the pre-straining.
- Water content measurements.
- Falling cone test prior to reconsolidation.
- Reconsolidation in the oedometer at four different stress levels (in-situ vertical effective stresses σ'_{v0} , 100 kPa, 150 kPa and 200 kPa), for 24 hr.
- Falling cone tests on specimens reconsolidated in the oedometer at the stress levels stated above.
- Water content measurements after reconsolidation at the stress levels stated above.
- CRS oedometer test up to 800 kPa.

The intact clay samples were also remoulded manually by knife. Manually remoulded samples were subjected to following tests:

- Falling cone test.
- CRS oedometer test up to 800 kPa.
- Water content measurements on the samples built in the oedometer.

The results from laboratory test programme described above were post-processed and discussed in systematical manner. Where applicable, the achieved results were compared to the data from past academic publications.

6.2 Overall Conclusions

Summary of the main conclusions of the study is given below. More detailed discussion of the findings may be found in the respective chapters.

6.2.1 Pre-Straining Through Extrusion

- Calculations on displacement ratios from pre-straining process indicate that the strain profile is varying in the cross-section of the pre-strained clay samples.
- Visual inspection of the pre-strained cross-sections confirms the variation in the strain profile. The strain variations appear to be largest for the clay with lowest water content and lowest plasticity index (Tiller clay).
- Despite the presence of some strain variations in the cross-sections of pre-strained samples, these variations are of minor importance as the study is aimed to research the effect of different levels of pre-straining. Even with varying strain profile, each pre-strained sample may be grouped unambiguously into one of three categories: completely remoulded clay (shear strain above 100 %), severely strained clay (shear strain 20-100 %) and moderately strained clay (shear strain less than 20 %). The falling cone and oedometer test results confirm that each pre-strained sample uniquely demonstrates the behaviour typical to its respective level of pre-straining.

6.2.2 Impact of Pre-Straining on Strength Properties

- With respect to the strength properties of pre-strained non-reconsolidated clay, the conclusion is that increasing pre-straining in shear mode leads to decreasing residual shear strength of the material. When plotted against applied shear strain, the residual shear strength decreases non-linearly to the minimum value given by remoulded shear strength.

- The normalised residual shear strength after the pre-straining is given by the ratio s/s_u , where s is residual shear strength and s_u is undrained shear strength. For Tiller clay pre-strained to remoulding, severe straining and moderate straining, the values of ratio s/s_u are 0.37, 0.29 and 0.66, respectively. The normalised remoulded shear strength (s_r/s_u) of this clay is in range 0.09-0.10.
- For Stjørdal clay pre-strained to remoulding, severe straining and moderate straining, the normalised residual shear strength is 0.23, 0.51 and 0.51, respectively. Normalised remoulded shear strength of Stjørdal clay varies from 0.10 to 0.14.

6.2.3 Impact of Pre-Straining and Reconsolidation on Strength Properties

- After reconsolidation at any stress level in range 42.2-200 kPa, all clay samples remoulded by pre-straining (shear strain 117 %) demonstrate significant increase in shear strength compared to the undrained shear strength of intact material. However, the changes in strength properties due to the reconsolidation proceed differently for Tiller and Stjørdal clay. The effect of shear strength recovery appears to be largest for Tiller clay. Depending on the magnitude of reconsolidation stress, the shear strength of remoulded Tiller clay after reconsolidation varies from 2.0 to 3.6 times undrained shear strength of intact material. The peak shear strength (3.6 times s_u) of remoulded reconsolidated Tiller clay is reached at reconsolidation stress of 150 kPa. When reconsolidated at higher stress level (200 kPa), the shear strength of remoulded reconsolidated Tiller clay sample slightly decreases to a value of 3.4 times s_u . The shear strength of remoulded and reconsolidated Stjørdal clay increases monotonously with reconsolidation stress, from 1.7 times s_u (at reconsolidation stress 89.5 kPa) to 2.1 times s_u (at reconsolidation stress 200 kPa).
- All moderately and severely pre-strained clay specimens show shear strength below s_u after reconsolidation at in-situ vertical effective stress σ'_{v0} , the latter typically less than 80 kPa for the samples involved in the study. The in-situ vertical effective stresses σ'_{v0} are 36.1 kPa for moderately pre-strained Tiller clay, 35.6 kPa for severely pre-strained Tiller clay, 79.2 kPa for moderately pre-strained Stjørdal clay and 75.1 kPa for severely pre-strained Stjørdal clay. The shear strength values of the latter test specimens reconsolidated at σ'_{v0} are $0.9 \cdot s_u$ for moderately pre-strained Tiller clay, $0.5 \cdot s_u$ for severely pre-strained Tiller clay, $0.8 \cdot s_u$ for moderately pre-strained Stjørdal clay and nearly $1.0 \cdot s_u$ for severely pre-strained Stjørdal clay. Considering the

background of the thesis, the observation indicates that the zone of moderately and severely strained soft soil around a pile shaft may encounter reduced strength properties at shallow depths, where the soil reconsolidates anisotropically and in-situ vertical effective stress is acting as major principal stress (active stress state). This observation is in accordance with field observations described in past publications.

- All moderately and severely pre-strained clay specimens regain and increase their shear strength when reconsolidated at stresses in range 100-200 kPa. The moderately pre-strained ($\gamma_s = 18\%$) and reconsolidated clay demonstrates larger increase in shear strength than what is common for severely pre-strained ($\gamma_s = 66\%$) and reconsolidated clay.
- For moderately pre-strained Tiller clay reconsolidated at stresses in range 100-200 kPa, the shear strength after reconsolidation is in range of 1.6 to 2.2 times s_u . Severely pre-strained Tiller clay specimens reconsolidated at the same stress levels demonstrate shear strength values in range of 1.2 to 1.7 times s_u . For the latter test specimens, the peak shear strength of 1.7 times s_u is observed at reconsolidation stress level of 150 kPa, while further increase of reconsolidation stress up to 200 kPa forces the shear strength to drop down to 1.2 times s_u .
- After reconsolidation at stress levels 100-200 kPa, moderately pre-strained Stjørdal clay shows shear strength in range of 1.3 to 1.8 times s_u . Severely pre-strained Stjørdal clay reconsolidated at the same stress levels demonstrates shear strength in range of 1.2 to 1.5 times s_u . For both degrees of pre-straining, the shear strength of pre-strained reconsolidated Stjørdal clay appears to increase uniformly and almost linearly with increasing reconsolidation stress.
- Normalised shear strength after pre-straining and reconsolidation is given by the ratio s_{re}/p'_{re} , where s_{re} is shear strength of pre-strained reconsolidated material and p'_{re} is reconsolidation stress. For all pre-strained samples except moderately strained Stjørdal clay reconsolidated at σ'_{v0} , the ratio s_{re}/p'_{re} appears to decrease uniformly and almost linearly with increasing reconsolidation stress up to 200 kPa.

6.2.4 Impact of Pre-Straining and Reconsolidation on Water Content and Volume

- For Tiller clay subjected to remoulding by pre-straining and subsequent reconsolidation, the difference between water content values after and prior to the reconsolidation is ranging from -6.2 % (when reconsolidated at in-situ vertical effective stress $\sigma'_{v0} = 42.2$ kPa) to -9.4 % (for reconsolidation at 200 kPa). The corresponding volumetric strain is ranging from 8.5 % (for reconsolidation at $\sigma'_{v0} = 42.2$ kPa) to 16.6 % (for reconsolidation at 200 kPa). The volumetric strain appears to increase linearly with increasing reconsolidation stress.
- For Stjørdal clay subjected to remoulding by pre-straining and subsequent reconsolidation, the difference in water content values after and prior to the reconsolidation is ranging from -5.3 % (for reconsolidation at in-situ vertical effective stress $\sigma'_{v0} = 89.5$ kPa) to -8.1 % (for reconsolidation at 200 kPa). The corresponding volumetric strain is ranging from 9.6 % (reconsolidated at $\sigma'_{v0} = 89.5$ kPa) to 14.4 % (reconsolidated at 200 kPa). The values of volumetric strains and changes in water content are similar to those observed for Tiller clay remoulded by the pre-straining and reconsolidated subsequently. The volumetric strains for remoulded and reconsolidated Stjørdal clay appear to increase linearly with increasing reconsolidation stress. The exception from this trend is remoulded Stjørdal clay specimen reconsolidated at 89.5 kPa.
- Moderately and severely pre-strained specimens demonstrate similar volumetric strains at the same levels of reconsolidation stresses. At reconsolidation stresses ranging from 35.6 kPa to 200 kPa, the volumetric strains of moderately and severely pre-strained Tiller clay specimens are in range of 5.0-13.2 % and 6.7-11.4 %, respectively. Reconsolidation of Stjørdal clay in stress range 75.1-200 kPa results in volumetric strains from 6.6 % to 11.3 % for moderately pre-strained material, and from 7.9 % to 11.2 % for severely pre-strained material. For moderately and severely pre-strained samples reconsolidated at stress levels up to 200 kPa, the general trend is that the volumetric strain increases almost linearly with increasing reconsolidation stress.
- The volumetric strains for moderately and severely pre-strained clays reconsolidated at stress levels up to 200 kPa are significant, and not far below the volume changes of remoulded material reconsolidated at the same stress levels. For the former degrees of

pre-straining, the effects of volume changes become especially notable when the reconsolidation stresses exceed 100 kPa. With respect to the background of the thesis, this implies that the zone of moderately and severely pre-strained soft soil around pile shaft will undergo large settlements at moderate and large depths where in-situ vertical effective stress is acting as major principal stress (active stress state) and exceeds 100 kPa. Thus, analysis of the settlements around a pile shaft should not only be limited to prediction of strains and stresses induced by the pile installation, but should also involve in-situ vertical effective stress as an additional main variable.

- The difference in water content values after and prior to the reconsolidation of moderately and severely pre-strained clays show considerable scatter, so that no apparent trend may be recognized. In general, reconsolidation of moderately and severely pre-strained Tiller and Stjørdal clays at stress levels 35.6-200 kPa leads to water content 1.6-7.8 % less than water content of the respective clay prior to the reconsolidation. The exact values depend on the type of clay and the reconsolidation stress level (refer to the relevant chapter for full transcript of data). Overall, the water content is decreasing evenly with increasing reconsolidation stress level.

6.2.5 Behaviour in the Oedometer

- Stress-strain plots for undisturbed, pre-strained and manually remoulded specimens clearly illustrate the effects of pre-straining or sample disturbance. For the same clay type, the stress-strain curve for pre-strained specimen is unambiguously located between the curves for undisturbed and manually remoulded test specimens. The arrangement of stress-strain curves for pre-strained specimens shows that increasing level of pre-straining is perfectly correlated with increasing volumetric strain at the same stress levels. For the same type of clay, maximum volumetric strain is defined by stress-strain curve of manually remoulded material. In the end of CRS oedometer test (stress level 800 kPa), the reduction of volume for remoulded clay specimens is typically in range of 17-23 %.
- The observations from CRS oedometer tests reveal that even the material pre-strained to remoulding (shear strain of 117 %) is not capable of capturing the volumetric strains encountered by manually remoulded specimens.

- The stress-strain curves for undisturbed and pre-strained material are just about to meet when the vertical strain in the oedometer is becoming sufficiently large, apparently corresponding to the void ratio 0.4 of void ratio at zero volume change.
- Stress-moduli curves show that pre-straining and remoulding lead to decreasing oedometer modulus at the stresses within OC range of intact material. At the stress levels corresponding to NC stress range of undisturbed clay, the pre-straining and remoulding lead to increasing oedometer modulus so that the clay becomes stiffer. The increasing modulus in NC stress range is a well-known effect of sample disturbance. This effect is caused by significant reduction in volume of the pre-strained or remoulded material subjected to loading.
- Within the same clay type, pre-strained and manually remoulded clay specimens show similar values of oedometer moduli within OC stress range of undisturbed material. For the stresses beyond p'_c , the difference between moduli of pre-strained and manually remoulded material is becoming more and more notable. In this stress range, the remoulded clay demonstrates largest modulus.
- Stress- c_v curves show that pre-straining and remoulding considerably reduce coefficient of consolidation at the stress levels corresponding to OC range of intact material.
- At the stress levels corresponding to NC range of undisturbed material, the coefficients of consolidation for remoulded clays either follow the intact c_v -curves or drop considerably below the latter. For the pre-strained material, it is observed that c_v -curves in NC stress range may either follow the intact c_v -curves, or rise above the intact curves, or drop below these curves. These contradictory trends may be explained by the fact that the coefficient of consolidation is depending on both oedometer modulus and coefficient of permeability. As coefficient of permeability changes with volumetric strains, so does coefficient of consolidation.

6.3 Needs for Improvement and Recommendations for Further Research

Although the laboratory test programme presented above has collected some empirical data which explain the behaviour of pre-strained and remoulded clay, the study is by no means complete. To achieve further understanding of the effects of pre-straining and remoulding, more empirical data are required.

In short term, author recommends execution of additional laboratory test programmes on pre-strained and remoulded clays, so that the new empirical data may be generated and collected. Planning of such additional laboratory test programmes should extend beyond the limitations of this thesis. The new laboratory test programmes should involve a broad range of clay types, both NC and heavily OC clays with different water content and sensitivity.

Due to the lack of appropriate equipment, the correlation between applied work (force-displacement) during the pre-straining and shear strength of non-reconsolidated material has not been studied. Although an attempt has been made to find the correlation between applied shear strain and shear strength of non-reconsolidated material, it is logical to expect that force-displacement ratio is correlated with applied shear strain and thus, also with the shear strength of pre-strained material. Further studies on the behaviour of pre-strained clays should include measurements of force-displacement during the pre-straining process, since it may provide more accurate information about the correlation between applied work and shear strength of pre-strained material.

It is essential that further laboratory test programmes include an assessment of permeability of pre-strained and remoulded material during post-processing of oedometer test results, since such evaluation has not been included in this study due to the longitudinal limitations. As it has been shown in this thesis, changes in coefficient of permeability during volumetric strains in pre-strained and remoulded material largely affect the development of coefficient of consolidation of such material. Therefore, further study on this issue is vital to identify general trends for prediction of reconsolidation times for pre-strained and remoulded soft soil around a pile shaft. Based on such empirical data, new methods for prediction of time for pile set-up may be developed.

Another relevant aspect which should be included in the further research is the study on ageing effects. These effects may lead to significant gain in shear strength of pre-strained material after the reconsolidation, and will have large impact on design of piled foundations.

Traditional analytical methods for prediction of strain and stress changes in the soil due to the pile installation are based on un-coupled two-staged calculation. Currently, the most common methods for prediction of strains imposed by driven pile installation are Cavity Expansion Method (CEM) and Strain Path Method (SPM). The solution for stress changes in the soil surrounding the driven pile shaft is obtained by coupling these methods with various soil

models. None of such approaches are known to provide a true and correct picture of the effects of pile installation and reconsolidation. Especially with respect to the installation of bored shafts, the solutions obtained by these prediction methods are uncertain and should be treated with caution.

With respect to the background of the thesis, author recommends that further research in mid- and long term perspective should be aimed to develop completely new methods dealing with prediction of strain and stress changes in the soft soils around the bored shafts. Development of such semi-empirical methods would make it possible to avoid use of CEM and SPM and secure more coherent solutions for the problems related to bored piles.

Development of new semi-empirical methods may, for instance, be based on large scale field test programmes on bored shafts. The field test programmes should include piezometer measurements to monitor the stress changes induced by pile installation. The programmes should also include excavation, trimming and sampling of the soil surrounding the installed piles. The excavated and trimmed samples may then be tested in the laboratory to identify general trends. To find the radial extent of the zones of remoulded and pre-strained soil and their correlation with pile diameter and shape, the sample microfabrics should be studied in the microscope. The distribution of shear strains around the pile shaft may be back-calculated from distorted shape of layers by studying the soil samples with x-ray photography. Finally, a new method for prediction of bored shaft installation effects may be developed by assembling the data from these field investigations with the empirical results from laboratory test programmes presented in this thesis and similar studies.

Appendix A: References

- Bihs, A., Nordal, S., Boylan, N., Long, M. (2012). "Interpretation of Consolidation Parameters from CPTU Results in Sensitive Clays". In: Mayne, P.W., Coutinho, R.Q. (Eds.), Proceedings 4th International Conference on Geotechnical and Geophysical Site Characterisation (ISC'4). Recife, Brazil, September 2012, pp227-234.
- Gylland, A.S. (2012). "Material and Slope Failure in Sensitive Clays". PhD Thesis. Geotechnical Division, Department of Civil and Transport Engineering, Norwegian University of Science and Technology (NTNU), Trondheim.
- Gylland, A., Long, M., Emdal, A., Sandven, R. (2013). "Characterisation and Engineering Properties of Tiller Clay". Engineering Geology 164 (2013) 86-100, 2013.
- Hill, R. (1950). "The Mathematical Theory of Plasticity". Oxford University Press, London, 356p.
- Holsdal, I.R. (2012). "Prøveforstyrrelse ved Bruk av NGI 54 mm Sylinderprøvetakerleire (Sample Disturbance Using the NGI 54 mm Piston Sampler in Clay)". MSc Thesis, Geotechnical Division, Department of Civil and Transport Engineering, Norwegian University of Science and Technology (NTNU), Trondheim.
- Janbu, N. (1970). "Grunnlag i Geoteknikk". Trondheim (available in Norwegian only).
- Karlsrud, K. (2012). "Prediction of Load-Displacement Behavior and Capacity of Axially Loaded Piles in Clay Based on Analyses and Interpretation of Pile Load Test Results". Ph.D. Thesis, Norwegian University of Science and Technology (NTNU), Trondheim.
- Karlsrud, K., Haugen, T. (1984). "Cyclic Loading of Piles and Pile Anchors - Field Model Tests - Phase II". Final Report. Summary and Evaluation of Test Results Computational Models. Norwegian Geotechnical Institute, Oslo. Report 40018-11.
- Karlsrud, K., Hernandez-Martinez, F.G. (2010). "Strength and Deformation Properties of Norwegian Clays from Laboratory Tests on High Quality Block Samples". Paper based on Bjerrum Lecture No. 23 presented to the Norwegian Geotechnical Society in Oslo on 26 November 2010.
- Kummeneje, O. (1981). "Sutterøleiret, Stjørdal. Soil Profile Boring 4. Project 3794". Drawing 06, June 1981.

- Kummeneje, O. (2003). "Bygg-element Stjørdal. Hulldekkefabrikk, Sutterøleiret. Borprofil Hull: 7. Oppdrag 630334A". Drawing nr. 105, September 2003 (Available in Norwegian only).
- Ladanyi, B. (1967). "Deep Punching of Sensitive Clays". Presented at the 3. Panamerican Conf. on Soil Mech. and Found. Eng., Caracas, 1967.
- Lande, E.J., Karlsrud, K. (2015). "BegrensSkade. Begrensning av Skader som Følge av Grunnarbeider. Delprosjekt nr.: 4". Preliminary report. Expected to be released during 2015. Norwegian Geotechnical Institute, Oslo.
- NGF (1982). "Veiledning for Symboler og Definisjoner i Geoteknikk - Presentasjon av Geotekniske Undersøkelser". Norwegian Geotechnical Society (Norsk Geoteknisk Forening), Oslo (Available in Norwegian only), 1982 (Revised 2011).
- Norwegian Geotechnical Institute (1985). "In-situ Site Investigation Techniques and Interpretation. Laboratory Tests on Onsøy Clay". NGI Report 40019-17, December 1985.
- Norwegian Geotechnical Institute (1989^a). "Pile load tests West Delta - Review and Assessment of Reliability of Test Data". NGI Report 882016-1, Revision 1, 1989.
- Norwegian Geotechnical Institute (1989^b). "Pile load tests West Delta - Review of Analytical Models". NGI Report 882016-2, 1989.
- Norwegian Geotechnical Institute (1989^c). "Pile load tests West Delta - Supplementary Laboratory Tests and Interpretation of Soil Data". NGI Report 882016-3, 1989.
- Norwegian Geotechnical Institute (1989^d). "Pile load tests West Delta - Analyses and Comparisons to Other Test Results". NGI Report 882016-2, 1989.
- NS 8000:1982. "Geotechnical Testing - Laboratory Methods - Consistency Limits - Terms and Symbols". Norges Byggstandardiseringsråd (NBR), 1st Edition, November 1982.
- NS 8001:1982. "Geotechnical Testing - Laboratory Methods - Percussion Liquid Limit". Norges Byggstandardiseringsråd (NBR), 1st Edition, November 1982.
- NS 8003:1982. "Geotechnical Testing - Laboratory Methods - Plastic Limit". Norges Byggstandardiseringsråd (NBR), 1st Edition, November 1982.
- NS 8005:1990. "Geotechnical Testing - Laboratory Methods - Grain-size Analysis of Soil Samples". Norges Byggstandardiseringsråd (NBR), 1st Edition, December 1990.

- NS 8011:1982. "Geotechnical Testing - Laboratory Methods - Density". Norges Byggstandardiseringsråd (NBR), 1st Edition, November 1982.
- NS 8013:1982. "Geotechnical Testing - Laboratory Methods - Water Content". Norges Byggstandardiseringsråd (NBR), 1st Edition, November 1982.
- NS 8015:1988. "Geotechnical Testing - Laboratory Methods - Determination of Undrained Shear Strength by Fall-Cone Testing". Norges Byggstandardiseringsråd (NBR), 1st Edition, February 1988.
- NS 8016:1988. "Geotechnical Testing - Laboratory Methods - Determination of Undrained Shear Strength by Unconfined Pressure Testing". Norges Byggstandardiseringsråd (NBR), 1st Edition, February 1988.
- NS-EN ISO 14688-2:2004/A1:2013. "Geotechnical Investigation and Testing - Identification and Classification of Soil - Part 2: Principles for a Classification". European Committee for Standardization, 1st Edition, October 2004 (Revised December 2013).
- NS-EN ISO 17892-1:2014. "Geotechnical Investigation and Testing - Laboratory Testing of Soil - Part 1: Determination of Water Content". European Committee for Standardization, 1st Edition, December 2014.
- NS-EN ISO 17892-2:2014. "Geotechnical Investigation and Testing - Laboratory Testing of Soil - Part 2: Determination of Bulk Density". European Committee for Standardization, 1st Edition, December 2014.
- Sandene, T. (2010). "Effekt av Grunnvannstandøkning på Kort og Lang Tidsstyrkeegenskaper i Kvikkleire". Norwegian University of Science and Technology (NTNU), Trondheim (available in Norwegian only).
- Sandven, R. (1990). "Strength and Deformation Properties of Fine Grained Soils Obtained from Piezocone Tests". Norges Tekniske Høgskole (NTH, currently NTNU), Trondheim.
- Schmertmann, J. (1955). "The Undisturbed Consolidation of Clay". Transactions ASCE Vol. 120.
- Schofield, A.N and Wroth, C.P. (1968). "Critical State Soil Mechanics". McGraw-Hill, London.

Seierstad, H.H. (2000). "Prøveforstyrrelse i Leire - Vurdering av ø75 mm Stempelprøvetaker". Norwegian University of Science and Technology (NTNU), Trondheim (available in Norwegian only).

Sodenberg, L.O. (1962). "Consolidation Theory Applied to Foundation Pile Time Effects". *Geotechnique*, Vol. 12, No. 3, pp217-225.

Yesuf, G.Y. (2008). "Behaviour of Norwegian Quick Clays under Varying Strain Rates". Norwegian University of Science and Technology (NTNU), Trondheim.

Appendix B: Nomenclature Used in the Text

ENGLISH

A_1	=	Cross-sectional area of undisturbed sample
A_2	=	Cross-sectional area of pre-strained sample
c_v	=	Coefficient of consolidation
c_{v0}	=	Coefficient of consolidation in the overconsolidated range
c_{vh}	=	Coefficient of consolidation obtained from piezocone (CPTU) dissipation tests
c_{vn}	=	Coefficient of consolidation at the preconsolidation stress
d	=	Displacement of piston during pre-straining of clay
D_1	=	Diameter of undisturbed sample
D_2	=	Opening diameter of the extruder cone (tapered cylinder)
e	=	Void ratio
e_0	=	Void ratio at zero volume change
g	=	Gravitational acceleration, 9.81 m/s^2
H	=	Drainage distance
I_L	=	Liquidity index
I_p	=	Plasticity index
K	=	Coefficient of earth pressure = σ'_h/σ'_v
K_0	=	Coefficient of earth pressure at rest = $\sigma'_{h0}/\sigma'_{v0}$
k	=	Coefficient of permeability, hydraulic conductivity
k_0	=	Coefficient of permeability at zero volume change
L_{ext}	=	Length of extruded clay material
L_1	=	Length of undisturbed sample
L_2	=	Length of extruder cone (tapered cylinder)

m	=	Modulus number
m_s	=	Mass of solid particles
m_w	=	Mass of water, mass of water before reconsolidation
$m_{w, re}$	=	Mass of water after reconsolidation
n	=	Porosity
M	=	Constrained (oedometer) modulus
M_o	=	Constrained modulus in the overconsolidated range
M_n	=	Constrained modulus at the preconsolidation stress
P	=	Applied pressure during sample extrusion
P_f	=	Failure load during unconfined compression test
p'_c	=	Preconsolidation stress
p'_{re}	=	Reconsolidation stress
S_t	=	Sensitivity
S_r	=	Degree of saturation
s	=	Residual shear strength (pre-strained, non-reconsolidated specimen)
s_u	=	Undrained shear strength
s_r	=	Remoulded shear strength
s_{re}	=	Shear strength of pre-strained sample after reconsolidation
u	=	Pore pressure
u_b	=	Pore pressure at sample base, CRS oedometer test
W	=	Work
w	=	(Natural) water content, water content before reconsolidation
w_{re}	=	Water content after reconsolidation
w_L	=	Liquid limit
w_p	=	Plastic limit
V	=	Volume
V_{ext}	=	Volume of pre-strained/extruded material

V_p	=	Volume of voids
V_s	=	Volume of solid particles
V_{und}	=	Volume of undisturbed material subjected to pre-straining
V_w	=	Volume of water
z	=	Depth
z_w	=	Depth to ground water table

GREEK

γ	=	Unit weight of soil
γ_s	=	Shear strain
γ_{solid}	=	Unit weight of solids
γ_w	=	Unit weight of water, 9.81 kN/m ³
Δ	=	Change in value of parameter/variable
δ_r	=	Displacement ratio during pre-straining of clay
ϵ_a	=	Axial strain
ϵ_{vol}	=	Volumetric strain
ρ	=	Density
$\bar{\rho}$	=	Mean density
ρ_d	=	Dry density
ρ_s	=	Grain density
σ_h, σ'_h	=	Horizontal stress (total, effective)
$\sigma_{h0}, \sigma'_{h0}$	=	Initial horizontal stress (total, effective)
σ_v, σ'_v	=	Vertical stress (total, effective)
$\sigma_{v0}, \sigma'_{v0}$	=	Overburden stress (total, effective)
ϕ'	=	Internal angle of friction

NOTE: Nomenclature used above may differ from the diagrams extracted from reference sources.

Appendix C: Abbreviations

ASCE	=	American Society of Civil Engineers
CAUC	=	Anisotropically consolidated undrained triaxial test sheared in compression
CEM	=	Cavity Expansion Method
CIUC	=	Isotropically consolidated undrained triaxial test sheared in compression
CRS	=	Constant rate of strain oedometer test
GWT	=	Ground water table
IL	=	Incremental loading oedometer test
NC	=	Normally consolidated
NTNU	=	Norwegian University of Science and Technology
NGI	=	Norwegian Geotechnical Institute
OC	=	Overconsolidated
OCR	=	Overconsolidation ratio
SPM	=	Strain Path Method
UCT	=	Unconfined compression test